Novel Diagnostic and Analytical Applications of Benchtop Time-Domain NMR

By

Michelle Denise Robinson

March, 2015

Director of Dissertation: Dr. David P. Cistola

Major Department: Interdisciplinary Program of Biological Sciences

Biochemistry and Molecular Biology

ABSTRACT

High-resolution nuclear magnetic resonance (NMR) spectroscopy is a powerful technique, yet practical application outside of the research laboratory has been limited due to the high cost and complexity of the instrumentation. Recently, miniaturized low-field benchtop time-domain NMR (TD-NMR) instruments have been developed to solve practical problems within the industrial setting. While the low-field instruments sacrifice some degree of sensitivity and resolution, they are capable of powerful relaxation time analysis and have gained popularity due to their simplicity and cost effectiveness. Currently these instruments are utilized primarily in the food, agricultural and pharmaceutical industry. This project was initiated to investigate the utility of benchtop TD-NMR in clinical diagnostics and health assessment. Using TD-NMR relaxometry, we analyzed a variety of complex biological liquids, which included oil-phase lipids, purified proteins and lipoproteins, and whole human serum and plasma. For oil-phase non-esterified fatty acids, we demonstrated that the NMR T_2 relaxation times were sensitive to

hydrocarbon chain structure, particularly the number of *cis*-double bonds, which impact chain packing and fluidity. Triglyceride mixtures displayed the same sensitivity to double bond content and fluidity. Therefore, we developed a practical method for using benchtop-TD NMR to determine the omega-3 fatty acid content of nutritional supplements. Analysis of aqueous biological samples suffered initially from radiation damping and hardware artifacts. Therefore, we developed new methods to optimize TD-NMR analysis of water-rich samples such as human blood serum. The T_2 profile of whole human serum or plasma displayed four resolved T_2 peaks. One was the intense water peak, which correlated with biomarkers of insulin resistance, dyslipidemia, oxidative stress and inflammation. The other three peaks monitor the molecular motions of the lipid and protein components in serum and plasma. In an apparently healthy population of human subjects, the lipid-protein T_2 values correlated with insulin resistance biomarkers by detecting metabolic changes in proteins and lipoproteins. The analysis of human serum and plasma using TD-NMR shows promise as a front-line health screening tool for identifying individuals at risk for developing diabetes, cardiovascular disease and Alzheimer's disease.

Novel Diagnostic and Analytical Applications of Benchtop Time-Domain NMR

A Dissertation Presented to the Faculty of Interdisciplinary Program of Biological Sciences- Biochemistry and Molecular Biology

East Carolina University

In Partial Fulfillment of the Requirements for the Degree of Doctor of Philosophy in Biochemistry and Molecular Biology

by

Michelle Denise Robinson

March, 2015

Signature page

Novel Diagnostic and Analytical Applications of Benchtop Time-Domain NMR

By

Michelle Denise Robinson

APPROVED BY:
DIRECTOR OF DISSERTATION: _____.
DAVID CISTOLA, MD, PhD

COMMITTEE MEMBER : _____.
JOSEPH CHALOVICH, PhD

COMMITTEE MEMBER : _____.
ART RODREIGUEZ, PhD

COMMITTEE MEMBER : _____.
SAAME RAZA SHAIKH, PhD

COMMITTEE MEMBER : _____.
TONYA ZECZYCKI, PhD

CHAIR OF THE DEPARTMENT OF BIOCHEMISTRY:

_____.
JOSEPH CHALOVICH, PhD

CHAIR OF THE INTERDISCIPLINARY PROGRAM OF BIOLOGICAL SCIENCES:

_____.
TERRY WEST, PhD

DEAN OF THE GRADUATE SCHOOL:

_____.
PAUL J. GEMPERLINE, PhD

Acknowledgements

Dr. Cistola, I am forever indebted to your mentorship and contributions through this process. You have sacrificed your weekends and evenings to properly train me as a graduate student. You intellect, creativity and positive attitude has made the lab the success it is today. Thank you for allowing me to join your lab, and teaching me all you know. You've encouraged me to become the best scientist I could be and have always treated me with the upmost respect. I am so proud of what we've accomplished together through these years as a team. The other lab members have also been invaluable; Sneha, Ina, Vipul and Stephen. I could not have successfully accomplished the work on this project without your input, direction and continuing support.

My thesis committee, Dr. Chalovich, Dr. Rodreiguez, Dr. Shaikh , Dr. Zeczycki and Dr. Pekala. Thank you for your help and support during these past years. You have encouraged me to push my limits and develop during each meeting. You all have been extremely patient when an issue arose concerning the distance and for that I am very grateful. Without you all I would not be here today.

I'd like to thank my mom and dad, Jill and Michael Robinson for all of their support during these past six years. You guys helped me move across the country twice and have been a crucial support system when I needed it the most. The loving and encouraging home you guys have provided me has helped to develop me in to the strong independent woman I am today. I have acquired so many wonderful traits and habits from both of you that have helped me successfully get to this point. Mom, you have taught me to see the positive in every scenario, to follow my dreams, not to be too hard on myself when I encounter a bump in my path, and to have faith in the things that are to come. Dad, you are my inspiration. I've always wanted to be just like you, which meant working hard and persevering no matter the task, and that anything

worth doing is worth doing the right way. I remember watching you write your dissertation while I was growing up, which inspired me to pursue mine. I am forever grateful for you both and could not ask for a better support system.

I'd like to thank my fiancé and soon to be husband Steven Little. You have selflessly sacrificed so much for me while I peruse my dreams. You build me up when I am down, know how to make me smile when I'm having a bad day and support me with all of your heart. I cannot imagine this journey without you. You have taught me so much about myself, and I can't wait to spend the rest of my life with you. I also would like to thank Arlene and Arnie Little, who have taken me in as their own and treated me like nothing less than a daughter. Your support, encouragement and understanding are invaluable and I am so happy to have you in my life.

Finally, I'd like to thank my friends at ECU who have been a shoulder to cry on, listened to my rants and have provided non-stop encouragement through graduate school. You were my family away from home and your friendship is irreplaceable. Heather Teague and Rylee Petrole, Andrew Friday, Kaitlin Morrison, Whitney and Kelsey Crosson, Andrew Franklin, Taylor Mattox and Kyle and Charolette Tipton.

TABLE OF CONTENTS

List of Tables

List of Figures

List of Abbreviations

AA	Arachidonic Acid
ALT	Alanine Aminotransferase
AST	Aspartate Aminotransferase
ATP	Adenosine Triphosphate
ATP-III	Adult Treatment Program - III
BMI	Body Mass Index
BUN	Blood Urea Nitrogen
CETP	Cholesteryl Ester Transfer Protein
CHD	Coronary Heart Disease
CL	Cholesterol Linoleate
CO	Cholesterol Oleate
CPMG	Carr-Purcell-Meiboom-Gill
CVD	Cardiovascular Disease
DE	Dummy Echo
DHA	Docosahexaenoic Acid
DOPC	Dioleoylphosphatidylcholine
DMPC	Dimyristolphosphatidylcholine
DLS	Dynamic Light Scattering
EDTA	Ethylene-diamene-tetra-acetic-acid
eGFR	Estimated Glomerular Filtration Rate
EPA	Eicosapentaenoic Acid
FA	Fatty acid
FC	Free Cholesterol
FFA	Free Fatty Acid
FID	Free-Induction Decay
Free T_4	Free Thyroxine to Diagnose Thyroid Disease
FT-NMR	Fourier Transform Nuclear Magnetic Resonance
GGT	Gamma Glutamyl Transpeptidase
HABS	Health and Aging Brain Study at the UNT Health Science Center, Fort Worth
HbA1C	Glycated Hemoglobin
HDL	High-Density Lipoprotein
HDL-C	High-Density Lipoprotein Cholesterol Concentration
HDL-P	High-Density Lipoprotein Particle Number Concentration
HNE	4-hydroxynonenal
HOMA2-%B	Homeostatic Model Assessment Version 2, % Beta Cell Function
HOMA2-%S	Homeostatic Model Assessment Version 2, % Insulin Sensitivity
HOMA2-IR	Homeostatic Model Assessment Version 2, Insulin Resistance Index
HPLC	High-Pressure Liquid Chromatograpy
hs-CRP	High-sensitivity C-reactive Protein

HSA	Human Serum Albumin
HTC	Hematocrit
I-309	Member of the CC Subfamily of Chemokines
IDL	Intermediate Density Lipoprotein
ILT	Inverse Laplace Transform
KBr	Potassium Bromide
IR	Inversion Recovery
IR Score	Insulin Resistance Score (from NMR Lipoprofile, Liposcience)
LDL	Low-Density Lipoproten
LDL-C	Low-Density Lipoprotein Cholesterol Concentration
Lp(a)	Lipoprotein (a) Cholesterol Concentration
MCH	Mean Corpuscular Hemoglobin
MCHC	Mean Corpuscular Hemoglobin Concentration
MCV	Mean Corpuscular Volume
MDA	Malondialdehyde
MetS	Metabolic Syndrome
MHz	Mega Hertz
MRI	Magnetic Resonance Imaging
MUFA	Monounsaturated Fatty Acid
NMR	Nuclear Magnetic Resonance
Non-HDL C	Non High Density Lipoprotein cholesterol concentration
NP	Number of Points
NS	Number of Scans
PBS	Phosphate Buffer Saline
PL	Phospholipid
PUFA	Polyunsaturated Fatty Acid
RBC	Red Blood Cell Count
SAFA	Saturated Fatty Acid
r	Pearson Correlation Coefficient
r_s	Spearman Correlation Coefficient, Non-Parametric
R^2	Square of the Pearson Correlation Coefficient
RD	Recycle Delay
RDW	Red Cell Distribution Width
rf	Radio Frequency
sICAM	Soluble Intercellular Adhesion Molecule
T_1	Spin-Lattice Relaxation or Longitudinal Relaxation
T_2	Spin-Spin Relaxation or Transverse Relaxation
T_{2A}	Regression Residuals From a Linear Fit of Plasma or Serum T_2 *vs*. Serum Albumin
T_{2C}	Regression Residuals From a Linear Fit of Plasma or Serum T_2 *vs*. Serum Cholesterol
T_{2G}	Regression Residuals From a Linear Fit of Plasma or Serum T_2 *vs*. Serum Globulins
T_{2O3}	Regression Residuals From a Linear Fit of Plasma or Serum T_2 *vs*. Omega-3 Index

T_{2P}	Regression Residuals From a Linear Fit of Plasma or Serum T_2 *vs*. Serum Proteins
T_{2TG}	Regression Residuals From a Linear Fit of Plasma or Serum T_2 *vs*. Serum Triglycerides
T_{2V}	Regression Residuals From a Linear Fit of Plasma or Serum T_2 *vs*. Serum Viscosity
T-DHA	Tridocosahexaenoin
T-EPA	Trieicosapentanoin
TD-NMR	Time-Domain Nuclear Magnetic Resonance
TG	Serum Triglyceride Concentration
TNF alpha	Tumor Necrosis Factor Alpha
TO	Triolein
TL	Trilinolein
TSH	Thyroid Stimulating Hormone
[UA]	Unmeasured Anion Concentration, in meq/L
[UC]	Unmeasured Cation Concentration, in meq/L
UNTHSC	University of North Texas Health Science Center
VLDL	Very-Low Density Lipoprotein Cholesterol Concentration
ω-3	Omega-3
WEFT	Water-Exclusion Fourier Transform
WBC	White Blood Cell

Chapter 1: Introduction

Nuclear magnetic resonance (NMR) is a physical phenomenon that exploits the magnetic properties of certain nuclei to provide detailed structural, dynamic and energetic information of molecular compounds. Physicists and chemists have conventionally used NMR as a highly specialized research laboratory tool. Advancements in hardware and data processing have broadened the applications across a wide range of industries. Some of the most successful and unique applications include: magnetic resonance imaging (MRI) as a non-destructive diagnosis tool in clinical medicine[1-4], petrophysical applications in oil and gas companies [5-11], food processing and quality[12-20] and the conservation and characterization of building materials in chemical engineering [12,21-25].

Top of the line high-resolution NMR instruments contain superconducting magnets that require cryogenics and occupy a large space, making them a highly expensive piece of equipment. In addition the specialized NMR techniques require an extensive skill set and training. Miniaturized benchtop instruments with permanent magnets that operate at lower field strengths have been developed which overcome the limitations from high-field NMR[26]. While they sacrifice sensitivity, the low price, small size and simplified user interface has increased the appeal of NMR for many scientists previously deterred by the specialized technique.

Benchtop time-domain NMR (TD-NMR), also known as relaxometry, is a relatively new low-field instrument that probes molecular motions by measuring T_1 and T_2 relaxation times. While specialized techniques have been developed for pharmaceutical and industrial settings[9,27,28], these instruments have yet to reach their full potential. Therefore, we have set out to expand the current benchtop TD-NMR methods into clinical diagnostic laboratories.

Theory and Fundamentals

The NMR Phenomenon and Behavior of Nuclei

Certain nuclei possess spin (angular momentum), which is an intrinsic fundamental property similar to mass and charge. Spin angular momentum is characterized by the spin quantum number I. Nuclei with a non-zero I have magnetic resonance properties (Table 1).

Isotope	Atomic Weight	Spin (I)	Gyromagnetic Ratio (γ) [10^7rad/(Ts)]
^{1}H	1	½	26.75196
^{2}H	2	1	4.106625
^{13}C	13	½	6.72828
^{14}N	14	1	1.933
^{15}N	15	½	-2.71262
^{19}F	19	½	25.18147
^{31}P	31	½	10.8394

Table 1.1: Nuclear Properties of Selected Isotopes. *Modified from The 64th CRC Handbook of Chemistry and Physics, CRC Press, 1984*

When a nucleus possesses both a charge and spin it generates a magnetic moment (μ_m,**).** This occurs because when a charged particle has angular momentum (motion/spin) it generates a magnetic field (magnetic moment). The magnitude of μ_m can be calculated using equation 1.1 where I is the spin number, h is planks constant and **γ** is the gyromagnetic ratio.

Equation 1.

$$\boldsymbol{\mu_m = \gamma I \left(\frac{h}{2\pi}\right)}$$

The most common isotopes utilized in an NMR experiment have a spin number of ½ (i.e.: ^{1}H, ^{13}C and ^{15}N). Nuclei with spin ½ can be visualized as a tiny bar magnet possessing a north and south pole (directionality). In the absence of a magnetic field, the nuclei are randomly oriented and are of equal energy (Figure 1A). In the presence of an external magnetic field, B_0,

the magnetic moments are quantized into 2I+1 energy levels (for spin I = ½ → 2(½) + 1 = 2 energy levels). Each level is given a magnetic quantum number, m. The nuclei can occupy one of two energy levels m +½ (also known as α) and m –½ (also known as β); m +½ is of lower energy and aligned parallel to the external magnetic field while m –½ of higher energy and is aligned anti-parallel to the external magnetic field . The energy difference between the two states is described in Figure 1B, and is proportional to the strength of B_0 [29].

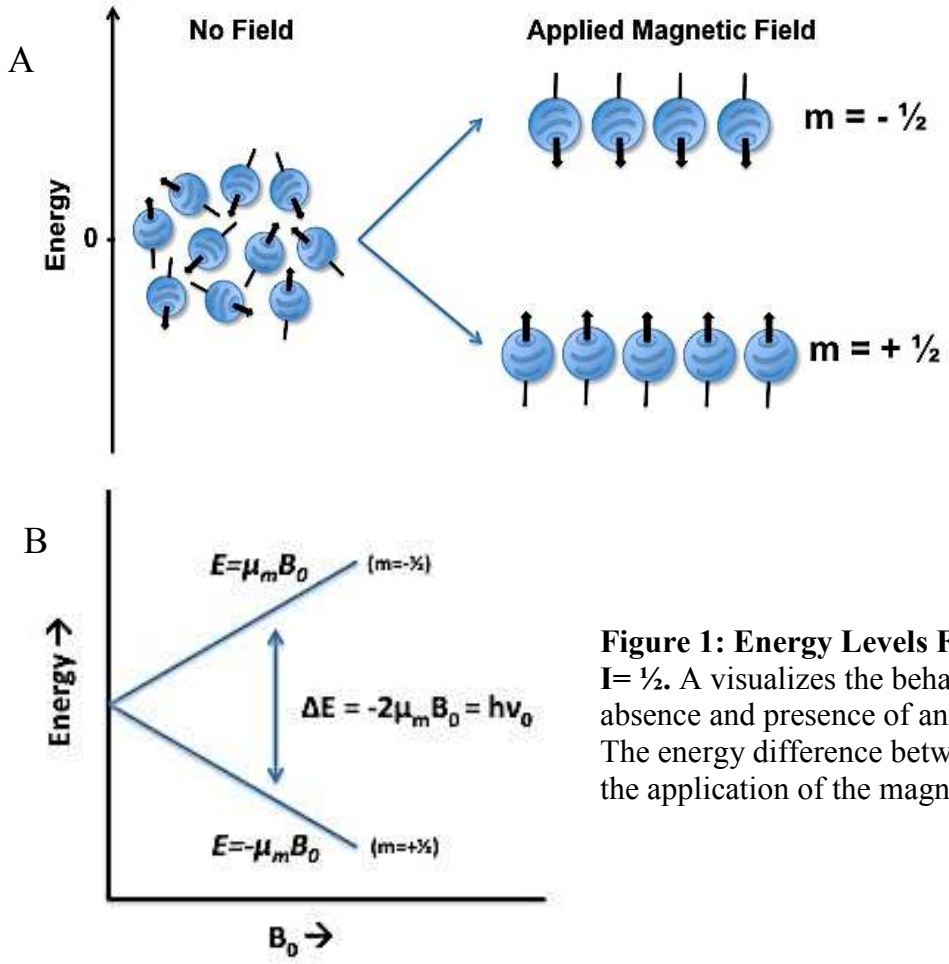

Figure 1: Energy Levels For a Nucleus with Spin I= ½. A visualizes the behavior of nuclei in the absence and presence of an external magnetic field. The energy difference between the two states upon the application of the magnetic field is shown in B.

The distribution of nuclei between the energy levels is not equal; the m +½ state, is more favorable and thus slightly more populated. The distribution ratio between states is given by the

Boltzmann equation in equation 2. The small abundance of nuclei occupying the lower energy state is aligned parallel with B_0, which leads to a net macroscopic magnetic moment, $\mathbf{M_z}$[30,31].

Equation 2.

$$\frac{N_\beta}{N_\alpha} = e^{-\Delta E/\, k_B T}$$

Nuclei are not perfectly parallel to the external magnetic field but precess in the direction of the static magnetic field (Figure 2), similar to that of a gyroscope in a gravitation field[32]. Precessional frequency, also known as the Larmor frequency, is dependent on the gyromagnetic ratio, which is constant for a given nuclei (Table 1), and the strength of B_0. As shown in equation 3 the Larmour frequency is designated ω_0 in radians per second or ν_0 in Hertz (Hz).

Equation 3.

$$\omega_0 = \gamma B_0$$

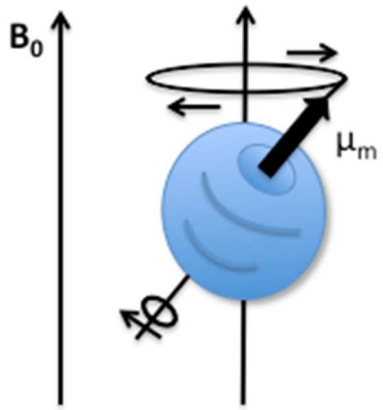

Figure 2: Larmor or precessional frequency. Once placed in an external magnetic field, nuclei will precess along the path of the applied field.

The NMR Experiment: Detection of Resonance

After a sample is placed in a magnet the nuclei begin precessing around to the axis of the external magnetic field (B_o) producing a net magnetization vector, **M** (sum of individual nuclear magnetic moments) aligned along the Z-axis in a coordinate system (Figure 3). At this state, which is known as thermal equilibrium, the population of nuclei is defined by the Boltzman distribution, and there is no coherence between the nuclear spins [29,33]. These conditions may be

broken when a radiofrequency pulse, B_1, is applied on resonance (Larmor frequency) perpendicular to B_o. The application of a RF pulse perturbs, or tips, the orientation of **M** away from B_o (Z axis) and the magnitude depends on the strength and duration of that RF pulse (Equation 4: α- the angle of tipping, γ- gyromagnetic ratio, B_1- applied magnetic field, t_p- duration of the pulse).

Equation 4.

$$\boldsymbol{\alpha = \gamma B_0 t_p}$$

Imagine a scenario where a RF pulse is applied just long enough to tip the **M** vector 90° away from Z (longitudinal) into the X-Y (transverse) plane (this is known as a 90° pulse). Immediately after the pulse has been turned off the nuclei will undergo Larmor precession about B_0 in coherence (Figure 3B). The precessing magnetization vector produces an oscillating voltage detected by a receiver coil located in the transverse plane[34]. As the nuclei return back to their thermal equilibrium (described below in more detail) a multiexponential signal is generated, known as a free induction decay (FID)[30]. The time-domain signal can be converted into the frequency domain by computing the Fourier transform of the FID.

Relaxation: Introduction to T_1 and T_2

The process through which equilibrium is regained after a RF pulse is known as relaxation, which is monitored by two time constants; T_1 (spin-lattice relaxation) and T_2 (spin-spin relaxation). The study of nuclear spin relaxation provides important information about the motional processes in molecules[35]. Immediately after a RF pulse has been turned off, nuclei in the X-Y plane are precessing in coherence, meaning they have the same exact precessional frequency. Over time, small perturbations and inhomogeneities in the respective local magnetic

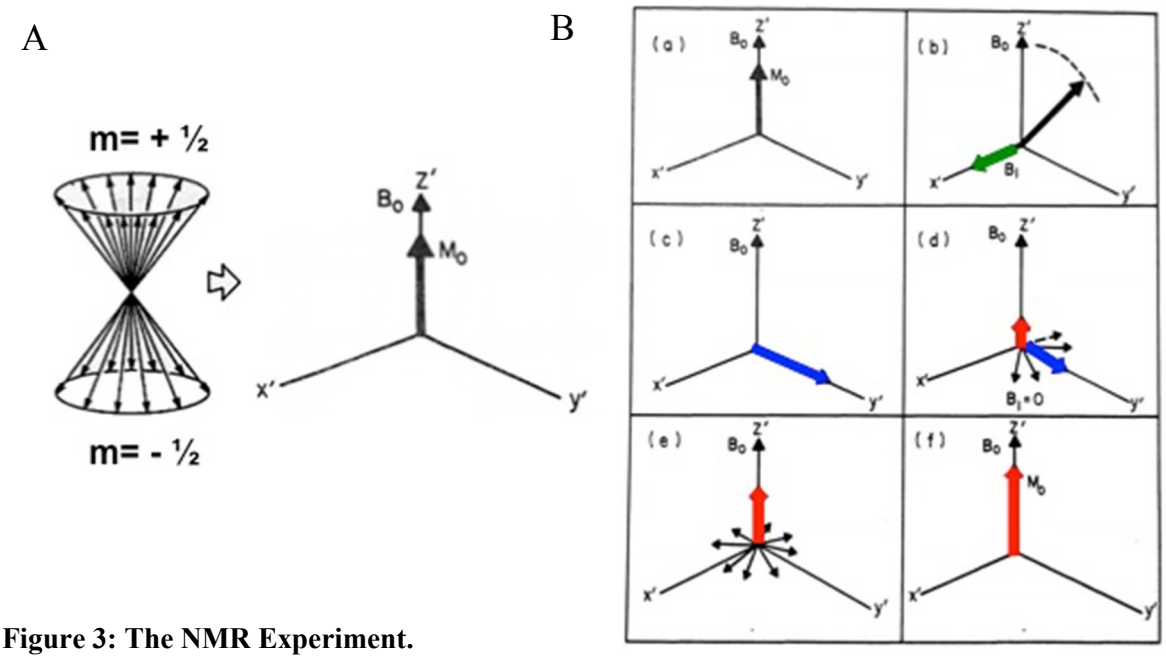

Figure 3: The NMR Experiment.
(A) According to the Boltzman distribution, a small excess of nuclei populate the lower energy state, which is aligned parallel to B_o. By taking the sum of the individual nuclei vectors we obtain a net magnetization vector, **M**. (B) Visualization of **M** after the application of a RF pulse. In panel b, the application of B_1 (green arrow) tips **M** into the XY-plane. After the RF pulse has been turned off the nuclei precess in coherence in the transverse plane as shown by the blue arrow. Over time the nuclei lose coherence and the transverse signal decays (3B:b-d). Notice in panel e, that in addition to a loss of the transverse signal (absence of blue arrow), the longitudinal component begins its recovery back to thermal equilibrium (red arrow), until eventually all of the nuclei have returned back along B_o (panel f).

fields cause the nuclei to lose their coherence in the X-Y plane; this is monitored by **T_2, also known as transverse relaxation**. The recovery of magnetization along the Z-axis back to thermal equilibrium is characterized by **T_1, also known as longitudinal relaxation**. The equations for T_1 and T_2 are shown in Equation 5.

Equation 5

$$M_z(t) = M_Z(1 - 2e^{-\tau/T_1})$$
$$M_{xy}(t) = M_{xy}(0)(e^{-\tau/T_2})$$

Spin-lattice relaxation: T_1

T_1 monitors the restoration of the Boltzman distribution as the excited spins transfer their magnetic energy back to their surrounding environment (lattice) around the nucleus of interest[30,35,36], which results in the recovery of **M** along the z-axis. This exchange occurs through indirect mechanisms such as dipole-dipole interactions, chemical shift anisotropy and spin-rotation interactions. The primary mechanism of relaxation is dipole-dipole interactions, where the nucleus experiences a fluctuating field due to the motion of neighboring dipoles (nuclei)[30]. **Brownian motions such as rotational diffusion, translation diffusion, vibrations and conformational changes cause these fluctuating magnetic fields** [35].

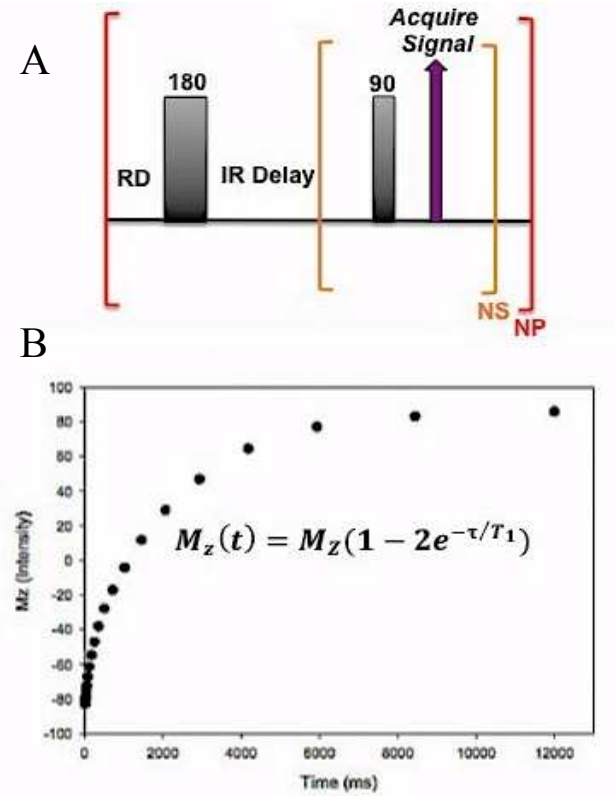

Figure 4. T_1 Inversion Recovery Experiment. Panel A displays the IR pulse sequences utilized in our lab. A recycle delay (RD) is inserted at the start to ensure all nuclei have reached their thermal equilibrium along the Z-axis. A 180 pulse inverts the magnetization vector from +Z to –Z. During the time delay (IR) the nuclei begin to relax back towards +Z. After the time delay a 90 pulse is applied, which monitors the progress of recovery back to +Z during at that moment in time. The length of the time delay is arrayed (increases with each data point) until the system has fully relaxed (~5*T_1). An example of a T_1 recovery curve is shown in panel B.

These fluctuations induce transitions between spin states, which restores the Boltzman distribution. Our lab uses an inverse recovery pulse sequence to measure T_1 [37]. The pulse sequence and an example of a T_1 recovery curve are shown in Figure 4.

Spin-spin relaxation: T_2

T_2 is also known as transverse relaxation because it monitors the irreversible decay of **M**, or coherence, in the XY-plane. The transverse magnetization decays overtime because it is impossible to keep synchrony between the precessing nuclear vectors due to local magnetic field fluctuations [35,36]. In addition to the relaxation mechanism described for T_1 (dipole-dipole interactions, chemical shift anisotropy and spin-rotation interactions), chemical exchange is a major contributor to T_2 relaxation.

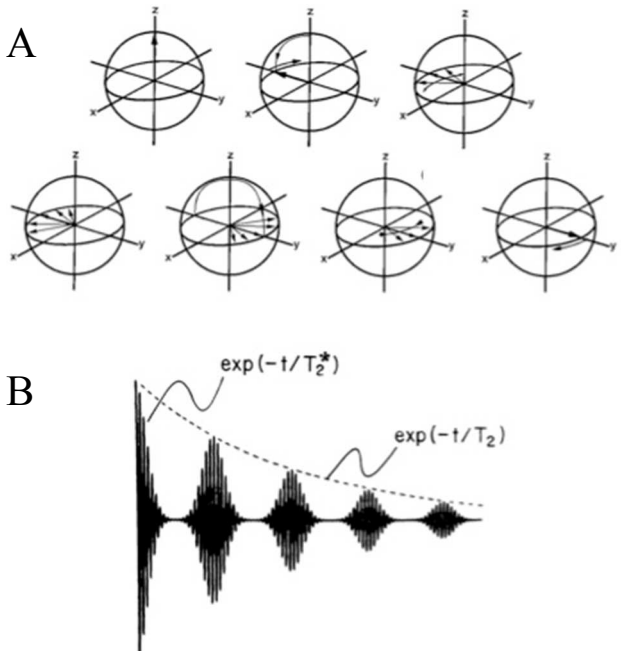

Figure 5: Loss of Coherence Due to an Inhomogenous Magnetic Field Corrected With a Spin-Echo Pulse Sequence. (A) Vector diagram illustrating the refocusing of nuclear vectors in a spin echo experiment. (B) A train of spin echo's demonstrating the rapid decay due to an inhomogeneous magnetic field, also known as T_2*. The real T_2 relaxation time (dotted line) can be determined by implementing a spin-echo pulse sequence. Modified from Handbook of Nuclear Magnetic Resonance, Freeman, R., 1987, 2nd Edition.

A reversible dephasing effect exists in the presence of an inhomogeneous magnetic field known as T_2* [38]. T_2* relaxation time is usually much less than T_2 and can be reversed using a spin-echo pulse sequence (Figure 5A). This sequence refocuses the spins that have loss coherence due to an inhomogeneous magnetic field with a string of **τ**-180°-**τ.** The Carr-Purcell-Meiboom-Gill (CPMG) experiment shown in Figure 6 utilizes the spin-echo pulse sequence to measure T_2 relaxation time [39,40].

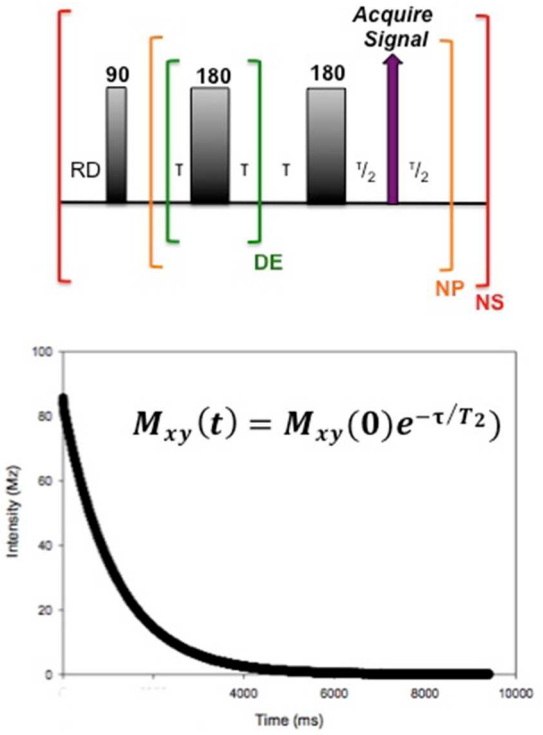

Figure 6: T_2 Carr-Purcell-Meiboom-Gill (CPMG) experiment. (A) The pulse sequence pulse sequence to measure T_2. Upon the application of a 90 degree pulse the magnetization vector is tipped into the X-Y plane. Afterwards a series of **τ**-180°-**τ** are applied to correct for any field homogeneity. (B) An example of a T_2 decay curve.

Bloch Equations

Felix Bloch developed a semi-classical set of equations to describe the macroscopic behavior of nuclear spins in a static magnetic field under the influence of a RF pulse [31,41,42]. The equations are all solutions of the net magnetization vector (sum of individual nuclear magnetic moments) as a function of time (dM(t)/dt). They are used to explain T_1 and T_2 relaxation, effect of a single RF pulse, chemical shifts, precession in static field and isolated spin behaviors (Equation 6).

Equation 6.

$$\frac{dM_z(t)}{dt} = -\frac{M_z(t) - M_0}{T_1}$$

$$\frac{dM_x(t)}{dt} = -\omega M_y(t) - \frac{M_x(t)}{T_2}$$

$$\frac{dM_y(t)}{dt} = \omega M_x(t) - \frac{M_y(t)}{T_2}$$

Molecular Motions

Brownian molecular motions such as rotational, vibrational and translational motions generate fluctuating magnetic fields that induce an NMR transition, resulting in relaxation. NMR can probe molecular motions over a wide range of timescales, ranging from picoseconds to several seconds depending on the experiment utilized (Figure 7)[43,44].

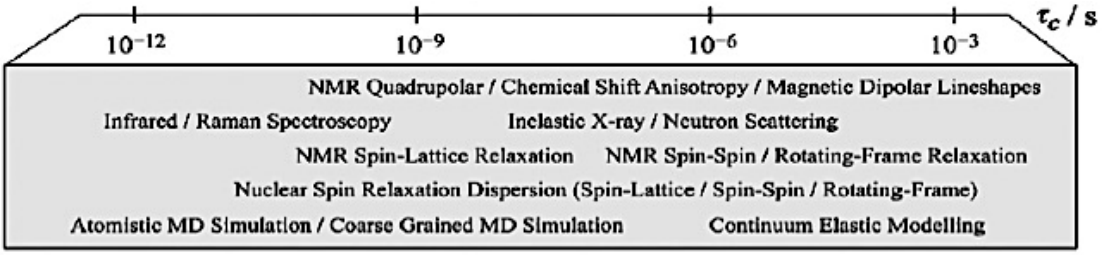

Figure 7: Types of motions NMR can monitor and their timescales Modified from *An NMR database for simulation of membrane dynamics. Leftin, A.,2010.Biochim Biophys Acta.*

Molecular motion frequencies that match the Lamor precessional frequency promote efficient exchange of energies to induce an NMR transition. Slow rotational motions are the most closely matched to Larmor frequencies. Rotational motions can be described by the rotational correlation time, τ_c, which on average is the time it takes for a molecule to rotate one radian. Motions that are greater than or less than the Lamor frequency will not exchange as efficiently, affecting the T_1 or T_2 relaxation time.

A spectral density plot (also known as a motional frequency spectrum) is useful for determining the probability of observing various motions as a given angular frequency. Figure 8 shows a spectral density plot for slow, intermediate and fast motions. Notice at the Larmor frequency (ω_0), the majority of motions are intermediate and approximately equal to $1/\tau_c$. As the

frequency increases and the τ_c becomes shorter, one is more likely to observe faster motions whereas at lower frequencies one is more likely to find slower motions with longer τ_c.

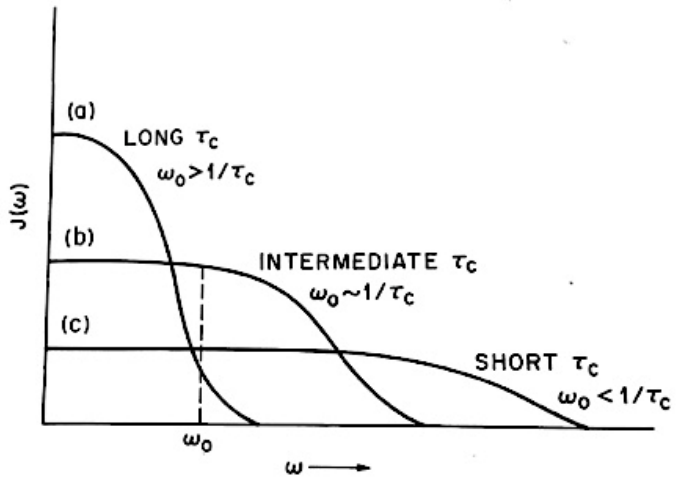

Figure 8: Spectral Density Plot for slow, intermediate and fast molecular motions. Modified from Handbook of Nuclear Magnetic Resonance, Freeman, R., 1987, 2nd Edition.

The nature and rate of the molecular motions affect both the T_1 and T_2 relaxation times [45-48]. Figure 9 demonstrates how T_1 and T_2 time constants vary with motional correlation times. An almost linear correlation exists between T_2 and molecular motions; as the frequency of motional correlation times increase so does the T_2. When the molecular motions are fast $T_1 \approx T_2$. Unlike T_2, a minimum is reached at the Larmor frequency when energy exchange is most efficient, and further slowing of the molecular motions increases the T_1.

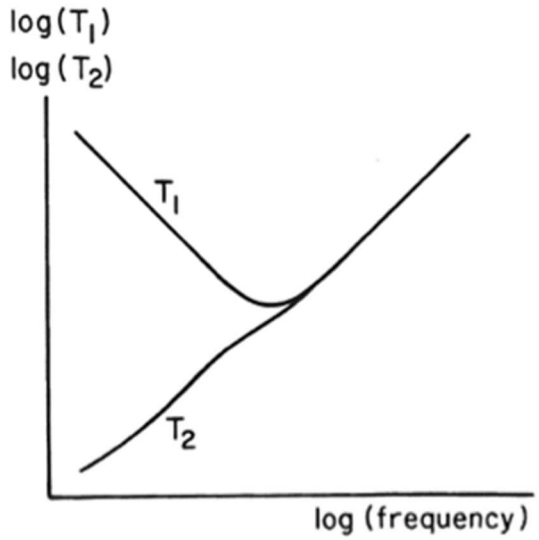

Figure 9: Behavior of T_1 and T_2 in response to molecular motions. Modified from Handbook of Nuclear Magnetic Resonance, Freeman, R., 1987, 2nd Edition.

Applications of NMR

In 1946 two groups of scientists at Stanford[49] and Harvard[50] applied known physical concepts of nuclear spin and magnetic moments to generate the first detectable NMR signal[51]. After its discovery, NMR was utilized primarily by physicist and chemists to elucidate structural and physical properties of small molecules. NMR has come a long way since then and is now capable of solving 3 or 4-dimensional structures of 30kDa macromolecules, observe complex dynamic processes and *in vivo* imaging of humans and animals. While an extensive overview of all the applications of NMR is beyond the scope of this thesis, a few of the most popular and novel utilizations of NMR are detailed below.

High-resolution Fourier Transform NMR

The inherent poor sensitivity from NMR remains one of the major limiting factors for this technique. To demonstrate this, two signal-to-noise proportionality equations are shown in Equation 6, where n is the number of nuclear spins, γ_e is the gyromagnetic ratio being excited, γ_d is the gyromagnetic ratio being detected, B_o is the magnetic field strength and t is the experiment acquisition time.

Equation 6.

$$S/N \propto n\gamma_e \sqrt{\gamma_d^3 B_0^3 t}$$

$$S/N \propto \sqrt{\#\ of\ scans}$$

Throughout the lifetime of NMR many techniques have been developed to overcome this lack of sensitivity. One of the first improvements was the introduction of larger, more powerful magnets (increase B_0), which enhance spectroscopic resolution and shorten the acquisition time.

Modern day NMR instruments not only operate at high magnetic fields, they employ superconducting magnets and cryogenics to increase the magnetic field strength and ensure a highly homogenous magnetic field. While the most common field strengths utilized range from 400-600mHz, instruments can be purchased with magnetic fields up to 1000MHz (23.5 Tesla). Additional developments that have markedly improved the signal-to-noise include the discovery of Fourier transformation, nuclear labeling techniques, solvent suppression, multidimensional analyses, and the generation of complex, specialized pulse sequences[52].

Together, these advancements have propelled high-resolution NMR outside of basic research. Some of the most unique applications include metabolomics analysis of biological fluids, [53,54] LDL particle counting available through Liposcience[55-58], forensic detection and identification of unknown chemical agents[59] and quantitative detection of nucleic acids in a complex mixture[60]. Nuclear magnetic resonance imaging (MRI) has been by far the most successful implementation of NMR outside of basic research and is used to non-invasively develop high special-resolution specialized imagines of bodily tissues and organs [61].

As NMR improvements continue, the complexity and costs of these instruments also rise. Superconducting instruments cost on average around $500,000.00[9]. A constant supply of liquid helium and nitrogen also add to the cost. Modern day high-resolution instruments are capable of multiple measurements (spectroscopy, relaxation time analysis, diffusion, imaging), which require a highly skilled operator limiting its commercialization and commercial appeal to non-specialists. New low-field instruments have been developed to overcome these limitations and are proving to be just as powerful as high-resolution NMR, while compromising in sensitivity.

Low-field NMR and Applications: Imaging, Spectroscopy and Relaxometry

State of the art low-field instruments are currently on the market operating between 50mT-1T for ^{1}H (corresponds to Larmor frequencies of 425 kHz- 42.5MHz). The superconducting magnets and cryogenics are replaced with permanent magnets, which significantly cuts down on cost (on average about $100,000.00 for a benchtop instrument[9]) and miniaturizes the console. In fact some instruments are now portable or even handheld allowing scientist to access remote or extreme environmental conditions previously inaccessible to convention NMR systems. An example of various instruments, experiments and their applications is shown in Figure 10. Common low-field NMR measurements, (imaging, spectroscopy and relaxometry) their instrumentation, and applications are described below.

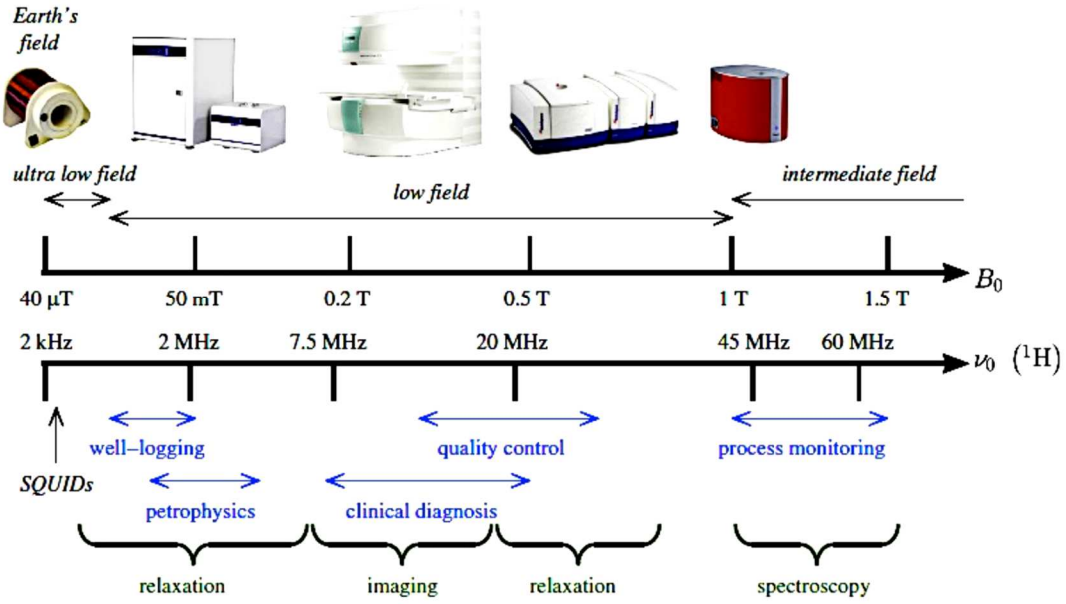

Figure 10: Various NMR instruments, applications and experiments that operate at low-field strengths. Adapted from Mitchell, L. et al. *Low field permanent magnets for industrial process and quality control.* Prog Nucl Magn Reson Spectrosc. 2014 Jan;76:1-60

Low-field Imaging

Most molecular imaging is performed using high-magnetic fields (> 1.0T). While there is no doubt high magnetic fields provide better quality images, low (<0.5 T) and medium field (0.5-1.0T) strength systems have gained popularity due to their small size, low cost, faster patient diagnosis and data quality[62]. The low-field MRI systems are used to image bodily tissue and organs to search for tumors, cysts, tissue tears/strains and other physiological abnormalities [63]. Whole body imaging with permanent magnets have been designed with open access improving the patient experience and allowing for simultaneous treatment [64], while intermediate sized systems monitor extremities such as arms, legs, fingers and shoulders.

Low-field Benchtop Spectroscopy and Relaxometery

Benchtop low-field NMR spectroscopy and relaxometry systems have developed a niche in industry where robustness, applicability and the industrial environment become important factors [65]. Benchtop spectroscopy computes a Fourier Transform of the FID signal, which creates a frequency domain chemical spectrum. Variations in the chemical peaks, known as chemical shifts, occur because nuclei experience small variations in the local magnetic field due to their local electronic environment. Spectroscopy needs excellent field homogeneity and thermal stability. Benchtop relaxometry on the other hand operates in the time-domain to monitor relaxation processes T_1 and T_2. Unlike spectroscopy, the magnetic field for data acquisition can be inhomogeneous using echo techniques [26].

Both techniques provide valuable information and are capable of an array of measurements. Chemical shifts can be recorded to provide structural content whereas T_1 and T_2 relaxation times are used to characterize and probe the motions aqueous samples. Pulse field gradients can be applied to extract coefficients of self-diffusion restricted diffusion and flow [66-69].

Multi-dimensional correlations (2D-NMR) can be used to provide robust chemical identification when the necessary spectroscopy resolution is not available. Types of 2-D correlations include relaxation time correlations (T_1 vs T_2) [12,70-72], diffusion-relaxation correlations (d*iffusion coefficient* vs T_1 or T_2) [73-75], and exchange rate measurements (T_2 vs T_2) [76-78].

These benchtop NMR instruments can be found across a wide range of industries. The food and agriculture industry commonly utilize low-field systems for quality and process control. For example, it has been used to determine the water holding capacity and quality of meat, albumin quality in hen eggs [79], crystal formation in ice cream[80] and as a non-invasive tool for the determination of oyster mass and phenotype [18,22]. Civil engineers and construction sites employ low-field NMR for the characterization of construction materials like cement and wood. Oil and gas companies also utilize these instruments for fluid and rock characterization[81], and development of oil-recovery methods[8,10]. Finally, pharmaceutical companies have developed methods for identifying drugs, their isomers, decomposition rates and for counterfeit analysis [82].

Handheld and portable low-field MRI's have gained popularity for their ability to access remote or extreme environmental conditions previously inaccessible to convention NMR systems. They are usually one-sided and allows the operator to see short distance into the sample and have been developed for specialty purposes such as analyzing car tires, characterizing building materials, monitoring moisture transport in skin, oil-well logging, and water transport in trees [83,84]. The NMR MOUSE and Surface GARField are two types commonly used [21,85-87]

These analytical methods only begin to demonstrate the versatility and capabilities of low-field benchtop-NMR. As improvements in the hardware, experimentation and data analysis continue, the opportunity to develop and commercialize novel NMR methods arises. Applications within pharmaceutical and industrial process and quality control are large and

continually growing. Clinical applications on the other hand remain limited. **Therefore our laboratory has sought out to develop benchtop TD-NMR (relaxometry) for clinical applications to assess human health status in biological fluids.**

SIGNIFICANCE, HYPOTHESIS AND SPECIFIC AIMS

Overview

One defining feature of lipoprotein particles is their size, and the dynamic range between lipoprotein classes. HDL for example on average is about 12nm whereas the largest lipoprotein, chylomicrons (CM), can reach up to 1000nm[88]. Initial attempts were aimed at developing an alternative to the current particle sizing methods such as the Vertical Auto Profile (Atherotech Diagnostics,[89,90]), Gradient Gel Electrophoresis [91-94] and the NMR Lipoprofile (Liposcience [95-97]). It was hypothesized that benchtop-TD NMR relaxation times could distinguish variations in lipoprotein size based on differences in their overall tumbling correlation time. Instead it was determined that the NMR T_2 values were sensitive to the internal lipoprotein lipid motions, generating the new hypothesis that NMR T_2 values in whole human serum were reporting on lipoprotein fluidity.

Two primary mechanisms impact lipoprotein fluidity; hydrocarbon chain composition and the choesteryl-esters to triglycerides ratio found in the non-polar lipid core. It is well known that metabolic dysfunction manifests itself through abnormal lipoprotein structure and composition early during disease progression [98-103]. Insulin-resistant patients for example generate larger than normal VLDL particles, which leads to modified LDL and HDL non-polar lipid core composition through CETP action [104-108]. Hydrocarbon chain composition is impacted primarily via the diet. Consumption of polyunsaturated fatty acids has been shown to increase lipoprotein fluidity, by disrupting hydrocarbon chain packing [109-114]. Therefore the ability to

directly monitor lipoprotein fluidity and thus lipoprotein lipid composition may have implications for clinical utility.

Aim 1: Configure benchtop TD-NMR for the analysis of aqueous biological fluids such as whole human serum and plasma.

Low-field benchtop NMR instruments are relatively new with limited literature resources. Therefore, we must parameterize the instrument for the robust analysis of aqueous samples. Unmodified serum and plasma gives rise to a radiation damping artifact which interferes with the relaxation analysis. Hence, we will develop a simple solvent suppression technique to overcome the intense water signal. Next we will optimize the CPMG pulse sequence to minimize hardware artifacts during data collection. Then we will concentrate on finding the appropriate ILT algorithm for the relaxation decay data analysis. Given the complexity of human serum, selecting the right algorithm is crucial to obtain run-to-run reproducibility.

Aim 2: Resolve and characterize the T_2 values in whole human serum.

Once the instrument and data collection has been optimized we will begin collecting data for whole human serum and plasma. To elucidate the mechanism riving these T_2 values, a series of controls will subsequently be analyzed. First we will study a mixture of the most abundant serum proteins, HSA and IgG. These two proteins constitute 80% of the total proteins found in human serum. Next we will generate protein-depleted serum, then compare the results to whole human serum. Doing so will unveil the contributions from serum proteins and small molecules to human serum T_2 values. Finally, a detailed study of lipoproteins and lipids will be performed. We will begin by observing how various lipids that differ in their hydrocarbon chain composition compare to one another, and how they impact NMR T_2. Next we will investigate how variation

in triglyceride and cholesteryl ester mixtures affects the NMR T_2, to mimic the lipoprotein lipid core. Phospholipid surface models will be constructed to mimic the lipoprotein surface. Finally, fractionated lipoproteins will be collected and analyzed by benchtop TD-NMR. A comprehensive list of the control samples and their purpose is shown in Table 1.2. Together these experiments will help us determine the main contributors to the human serum T_2 peaks

Control Category	Samples Prepared	Purpose
Protein	• HSA • γ- globulin fraction • HSA and γ- globulin mixtures	• Analyze T_2 values of proteins • Study concentration dependence of protein and T_2 value
Protein Depleted Serum	• HSA and γ- globulin depleted • Most proteins and small molecules removed	• Observe changes on T_2 profile after removing proteins and/or small molecules • Enhance lipoprotein signals
Lipids	• Free fatty acids that vary in chain length, degrees of saturation and stereochemistry • Triglycerides that vary in omega-3 content • Dilution series of triglyceride and cholesterol mixtures • Phospholipid multilamellar sheets and emulsions • Reconstituted lipoproteins • Fractionated lipoproteins from all classes (CM, VLDL, IDL, LDL, HDL)	• Analyze T_2 values of lipid and lipoproteins • Study impact on NMR values as fatty acid or triglyceride hydrocarbon chains vary • Mimic non-polar lipid core of lipoproteins • Study impact on NMR values as CE:TAG ratio varies • Mimic lipoprotein phospholipid surface

Table 1.2: List of control samples and their purpose for analysis.

Aim 3: Plan and execute an observational clinical study across a healthy population, and correlate NMR findings with known clinical biomarkers.

This aim will determine the feasibility of using benchtop TD-NMR as a clinical analytical tool. We will collect a human serum and plasma from a range of participants through two approved IRB protocols. NMR T_2 values among the cohort of participants will be correlated with over 70 conventional clinical biomarkers. Correlation statistics will be used to interpret the results and identify significant correlations between the NMR measurements and other blood biomarkers. In addition, results from the control samples prepared in aim 2 will help us narrow in on the molecular motion mechanism TD-NMR is monitoring in whole human serum. This will complete Phase I of our clinical study and multi-biomarker development using benchtop TD-NMR.

Significance

Completion of this proposal will lead to a novel configuration of benchtop TD-NMR that can be applied to other research, manufacturing, and diagnostic methods. We will have successfully analyzed one of the most complex biological mixtures, human serum, using benchtop TD-NMR. Finally, we will have successfully correlated the human serum NMR T_2 values with clinical biomarkers to assess the future potential of this instrument for clinical diagnostic use. Together these findings will open the door for future development of this instrument for the analysis of biological aqueous and lipid samples.

Chapter 2: Nanofluidity of Fatty Acid Hydrocarbon Chains as Monitored by Benchtop Time-Domain Nuclear Magnetic Resonance.

Introduction and Background

Lipids in biological systems display a remarkable variability in hydrocarbon chain composition, particularly in chain length and in the number, position and stereochemistry of double bonds. That compositional variability underlies a considerable diversity in physical properties and biological functions [115-119]. For example, low density lipoprotein or LDL, which functions as the primary cholesterol-carrying particle in the blood, undergoes a liquid-crystalline-to-liquid phase transition near body temperature [120-125]. Below this transition, the cholesteryl ester molecules in LDL pack in an ordered smectic liquid-crystalline phase, which makes LDL less fluid and more susceptible to oxidation, altered metabolism and clearance from the circulation [126-129]. The temperature at which this phase transition occurs depends on the fatty acyl composition of cholesteryl esters and triglycerides, which, in turn, is influenced by the dietary intake of saturated, mono- and polyunsaturated fatty acids [130-136]. Similarly, the hydrocarbon chain fluidity of biological membranes and membrane domains is thought to be a key determinant of cell surface receptor function [137-148]. For example, B-cell membrane lipid fluidity is altered through *n-3* polyunsaturated fatty acid supplementation, which disrupts the major histocompatibility complex class II lateral translocation into lipid rafts and suppresses T-cell activation[149].

A variety of methods have been used to probe the fluidity of lipid-rich biological assemblies such as cell membranes, lipid droplets and serum lipoproteins. Fluorescence and electron spin resonance methods have excellent sensitivity and have been used to characterize

the rotational and lateral motions of a variety of lipid probes [150-155]. With the exception of parinaric acid found in exotic plants, biologically native fatty acids lack intrinsic fluorescence. Therefore, fluorescent probes such as DPH (1,6-diphenyl-1,3,5-hexatriene), NBD (nitrobenzoxadiazole), bis-pyrene and BODIPY (4,4-difluoro-4-bora-3a,4a-diaza-s-indacene) have been synthetically incorporated into the fatty acid hydrocarbon chains of phospholipids and other lipids [154,156]. For electron spin-resonance, fatty acid analogues incorporating a variety of spin labels such as TEMPO [(2,2,6,6-tetramethylpiperidin-1-yl)oxyl] and doxyl moieties have been utilized [151,157-160]. While fatty acid analogues offer powerful tools for measuring probe dynamics, it is not clear what impact their non-native structures have on hydrocarbon chain packing in the vicinity of the probe. This potential complication can be avoided using NMR spectroscopy, where ^{1}H, ^{2}H, or ^{13}C have been used to monitor hydrocarbon chain motions, order parameters and/or fluidity [44,161-166]. Deuterium NMR is particularly well suited for studies of membranes, as it can be used to derive order parameters for hydrocarbon chains from quadrupolar splittings. However, it may not always be feasible or practical to incorporate ^{2}H into the biological system of interest; also, sensitivity can be a limiting factor. High-resolution ^{1}H and ^{13}C NMR is well suited for smaller assemblies such as serum lipoproteins and model membranes, including micelles, bicelles and small unilamellar vesicles. However, the spectra of larger lipid assemblies like liposomes and cell membranes suffer from line broadening and poor chemical shift resolution.

Another source of uncertainty in studies of lipid fluidity is the ill-defined relationship between the properties of the spectroscopic probe and the actual fluidity of the lipid hydrocarbon chain environment. In strict terms, fluidity is defined as the inverse of viscosity that, in turn, is a measure of a fluids resistance to flow [167]. There may be an implicit assumption that the

spectroscopic or motional properties of a molecular probe are monitoring the fluidity of the lipid microenvironment. However, for that assumption to be rigorously validated, the spectroscopic or motional parameters should be calibrated against independent measures of fluidity.

Here we present a new approach for monitoring the nanofluidity of fatty acyl hydrocarbon chains using benchtop time-domain ^{1}H NMR (TD-NMR). In contrast to conventional Fourier-transform NMR spectroscopy, which emphasizes analysis via the frequency domain, TD-NMR focuses on the exponential analysis of the time-domain signal. This type of NMR relaxometry (as opposed to spectroscopy) circumvents the requirement for superconducting magnets with high magnetic field strength and field homogeneity. As a result, time-domain NMR can be performed on simpler, smaller and less expensive benchtop instruments equipped with low-field permanent magnets. Thus, TD-NMR is more practical for use in non-NMR research labs, as well as in non-research settings, such as clinical diagnostic laboratories, manufacturing/quality control and field-testing sites. Moreover, it is better suited for the study of larger lipid membrane assemblies, as it does not rely on chemical shift resolution. While TD-NMR sacrifices chemical shifts, it retains the information content of the T_1 and T_2 relaxation time constants, which possess significant resolving power on their own. In this study, we utilized benchtop TD-NMR to resolve T_2 domains in a series of oil-phase fatty acids and biologically relevant fatty acid mixtures of varying hydrocarbon chain structure. The use of single-phase fatty acid oils afforded us the opportunity to correlate the TD-NMR values for hydrocarbon chain T_2 domains with independent measurements of sample fluidity. The results demonstrate the exquisite influence of hydrocarbon chain structure on T_2 and fluidity. The findings from this study illustrate the potential of employing benchtop TD-NMR as a nanofluidity meter for analyzing a variety of biologically significant lipid, lipoprotein and

membrane assemblies. Moreover, this approach could help inform strategies for acquiring and interpreting T_2-weighted and –corrected MRI images of lipid-rich tissues [168,169], as well as *in vivo* MRS analyses of hepatic lipid content in fatty liver disease [170,171].

Experimental Procedures

Sample preparation

Individual neat fatty acids (>99% purity) were purchased from Nu-Chek Prep (Elysian, Minnesota, USA); for several of these samples, the purity was cross-checked and verified by ^{1}H and ^{13}C NMR spectroscopy. Free fatty acid-based fish oil extracts were kindly provided as a gift by Originates (Aventura, Florida), a global supplier of omega-3 fish oil concentrates; they also provided a certificate of analysis for sample composition and physical characteristics. The 7.5 mm diameter NMR tubes used for TD-NMR were filled to a sample volume of approximately 350 µL, corresponding to a sample height of 0.7 mm. The NMR tubes were evacuated with dry nitrogen gas before and after sample filling to minimize lipid oxidation during experiments. Most of the fatty acid samples used in this study showed no susceptibility to oxidation during multiple repeat experiments at 37°C or higher, the highly unsaturated α-linolenic (18:3), arachidonic (20:4), eicosapentaeneoic (20:5; EPA) and docosahexaeneoic (22:6; DHA) were more susceptible. For these fatty acids, each NMR experiment was performed within 2 hours using a fresh sample.

Viscosity/fluidity measurements

The absolute viscosity values for single-phase fatty acid oil samples were measured using a VISCOlab 3000 instrument (Petroleum Analyzer Company or PAC, L.P., Houston, Texas, USA). This laboratory viscometer utilizes a piston-style electromagnetic sensor, a Peltier-type temperature controller and an integrated temperature sensor. In this study, two different pistons

were employed, suitable for the absolute viscosity ranges of 0.5-10 cP and 10-200 cP. Each measurement utilized approximately 0.7 mL of fatty acid. Sample fluidity, reported here in units of centiPoise^{-1} or cP^{-1}, was obtained by simply taking the inverse of the absolute viscosity.

Benchtop time-domain NMR relaxometry

Measurements were acquired using a Bruker mq40 Minispec NMR instrument equipped with a permanent magnet and operating at 0.94 Tesla, corresponding to a resonance frequency of 40 MHz for ^{1}H. The magnet temperature on this particular instrument is controlled at 37°C. This mq40 is equipped with a 7.5 mm ^{1}H probe with variable sample temperature capability (Bruker probe model H40-7.5-15BAV) and a circulating water bath (Julabo, Model F32-MA). To ensure sample temperature equilibration, the NMR samples were incubated in the instrument probe compartment at the experimental sample temperature at least 30 minutes before final NMR data acquisition was initiated.

Time-domain spin-spin relaxation exponential decay curves were acquired using a CPMG pulse sequence (Figure 1S) with a 2τ delay of 380 μs between 180° pulses – kept short to eliminate the potential impact of diffusion on T_2 values [172,173]. The 90° and 180° pulses were calibrated for each sample at each temperature prior to CPMG acquisition. The NMR intensities were acquired during the middle of the 2τ delays, and 4000-8000 data points were acquired for each decay curve, depending on the T_2. The recycle delay was set to 8*T_1 to ensure that the spins were fully relaxed at the beginning of the pulse sequence, and the data acquisition time was set to 8-9*T_2 so that the exponential decay curve reached baseline. We observed that acquisition times significantly less than 8*T_2 resulted in poor resolution of the CONTIN-derived peaks in the T_2 profile. For signal averaging, 512 scans were acquired for each experiment, corresponding to a total experiment time of ~2 hours.

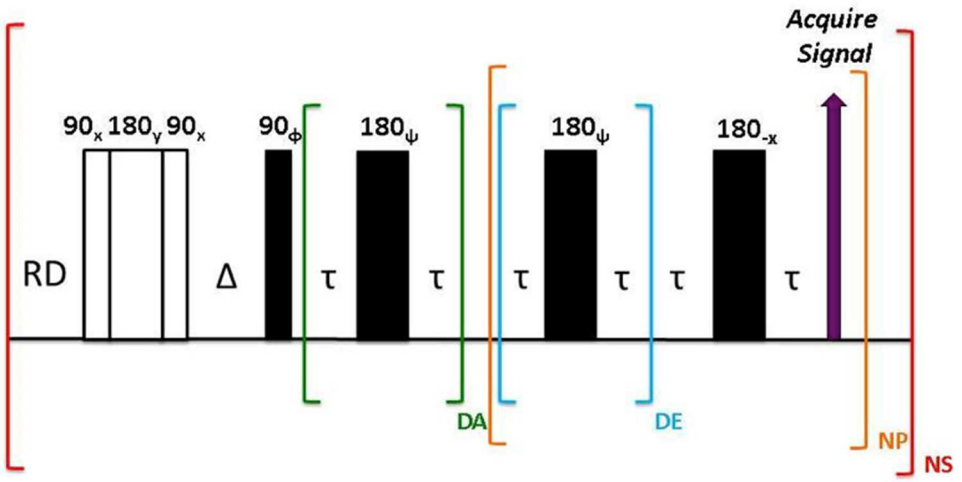

Figure 1S: Modified CPMG pulse sequence for measuring T_2 in benchtop time-domain NMR. In contrast to NMR spectroscopy, the time points for the exponential decay curve are acquired directly during the CPMG pulse scheme. For the current study, the first 180˚ pulse and Δ delay were set to zero. RD, relaxation delay; DE, dummy echoes; NP, number of points; NS, number of scans.

The multi-exponential T_2 decay curves were analyzed using an inverse Laplace transform algorithm as implemented in CONTIN [174] (see also s-provencher.com). For oil-phase fatty acids, this analysis yielded two-to-four resolved T_2 exponential terms and the amplitudes associated with each term. The high signal-to-noise obtained for oil-phase fatty acid samples provided sufficient information content in the data to ensure that the inverse Laplace calculations were stable and reproducible. The data are represented as T_2 profiles: intensity vs. T_2. While these T_2 profiles superficially resemble NMR spectra (intensity vs. chemical shift), the two should not be confused since they have a fundamentally different x-axis.

This Bruker mq40 instrument is also equipped with a 10 mm ^{1}H probe that ultimately was not used in this study. We observed that T_2 decay curves acquired with the larger diameter probe for concentrated neat oil-phase fatty acid samples led to radiation damping. That phenomenon manifested itself as an oscillatory component in the residuals for the fit of the experimental data with the calculated CONTIN exponential decay curves. No such oscillations

were observed when the smaller 7.5 mm probe was used, which has a sample volume about half that of the 10 mm probe.

NMR spectroscopy

In this study, frequency-domain NMR spectroscopy was used for two purposes: (1) as an independent check of the T_2 domain assignments inferred from the time-domain NMR results, and (2) as an independent check of the purity of the fatty acid samples obtained from Nu-Chek Prep. NMR spectra were acquired with a Magritek SpinsolveCarbon benchtop NMR spectrometer operating at 1 Tesla, corresponding to a resonance frequency of 42.5 MHz for ^{1}H and 10.8 MHz for ^{13}C. One-dimensional ^{1}H and ^{13}C spectra were acquired, and CPMG-based frequency-domain T_2 experiments were accumulated. Unlike TD-NMR, the T_2 curves in this case were generated by measuring the areas of resolved NMR resonances after Fourier transformation. In some cases, individual decay curves fit well to single exponentials, whereas in other cases, a bi-exponential fit was required, as analyzed on GraphPad Prism.

Results

Fatty acid T_2 profiles and T_2 assignments

The T_2 profiles for five different 18-carbon *cis*-unsaturated fatty acids, varying in the position and numbers of double bonds, are shown in Figure 1. Although T_2 profiles displayed in this manner (intensity vs. T_2) bear a superficial resemblance to NMR spectra (intensity vs. chemical shift), the two types of NMR data should not be confused with one another since they have a different x-axis and a fundamentally different meaning. The profiles displayed in this manuscript are inverse Laplace transforms of the multi-exponential T_2 decay curves.

The first three T_2 profiles in Figure 1 correspond to fatty acids with a single *cis* double bond in the Δ6, Δ9 and Δ11 positions – panels A, B and C, respectively. Petroselenic acid

displays only two T_2 peaks, whereas oleic and vaccenic acids reveal three. As the position of the double bond moves away from the carboxyl group and closer to the methyl terminus, the peak at lowest T_2 value increases in intensity (area under peak). However, the T_2 values for the peaks are comparable for these three mono-unsaturated 18-carbon fatty acids. By contrast, the presence of a second and third *cis* double bond results in a large increase in T_2 values, resulting in a dramatic right shift in the T_2 profiles for linoleic and α-linolenic acids, panels D and E, respectively.

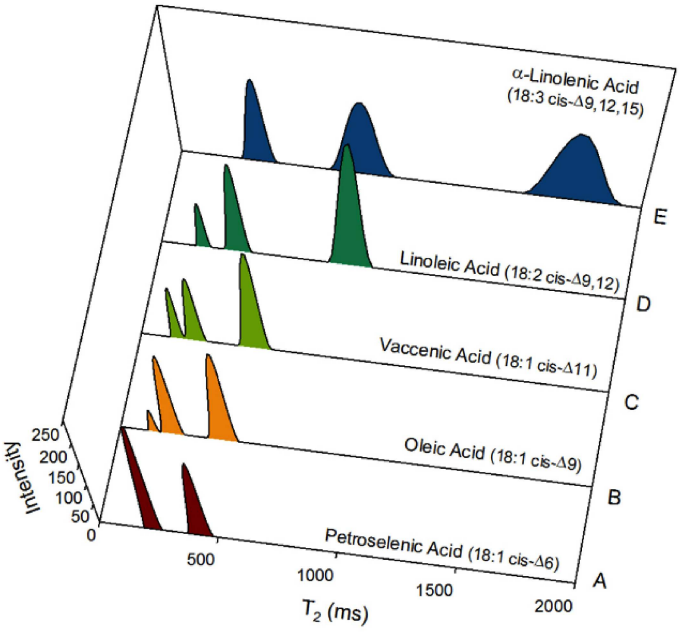

<u>Figure 1</u>: T_2 profiles for 18-carbon *cis*-unsaturated fatty acids at 37°C: Effect of double bond position and number. (A) Petroselenic acid, 18:1 *cis*-Δ^6; (B) Oleic acid, 18:1 *cis*-Δ^9; (C) Vaccenic acid, 18:1 *cis*-Δ^{11}; (D) Linoleic acid, 18:2 *cis*-$\Delta^{9,12}$; (E) α-Linolenic acid**,** 18:3 *cis*-$\Delta^{9,12,15}$

The center of each resolved peak represents the average T_2 value for a domain or cluster of hydrogen atoms in the fatty acid molecule. The number of hydrogen atoms contributing to each domain, *i.e.*, to each resolved T_2 peak, can be inferred from the relative amplitudes of the peaks derived from the inverse Laplace analysis. Oleic acid has a total of 34 hydrogen atoms and displayed a relative intensity ratio of ~3:18:13. Reasoning that the carboxyl proton is the least mobile because of inter-molecular hydrogen bonding with the carboxyl group of an adjacent molecule [117], we tentatively assigned the lowest T_2 domain to the 3 hydrogen's at the carboxyl end, including the carboxyl proton and the C-2 methylene protons. The middle T_2

domain was assigned to the 18 hydrogen atoms in the middle of the hydrocarbon chain, spanning the double bond. The highest T_2 domain was assigned to the distal 13 hydrogen atoms including the methyl terminus. These tentative assignments of the T_2 profile of oleic acid (Table 1 and Figure 2S) were subsequently confirmed using T_2 data from frequency-domain NMR spectroscopy (Figure 3S).

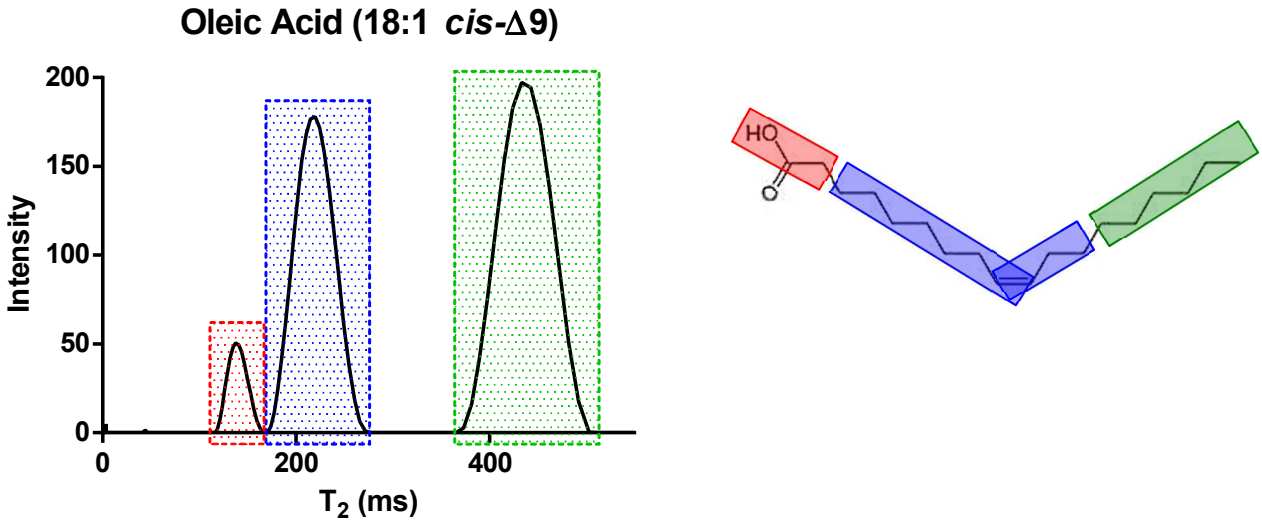

Figure 2S: **T_2 profile for oleic acid**, showing the assignment of the three T_2 domains to hydrogen atoms in the molecule.

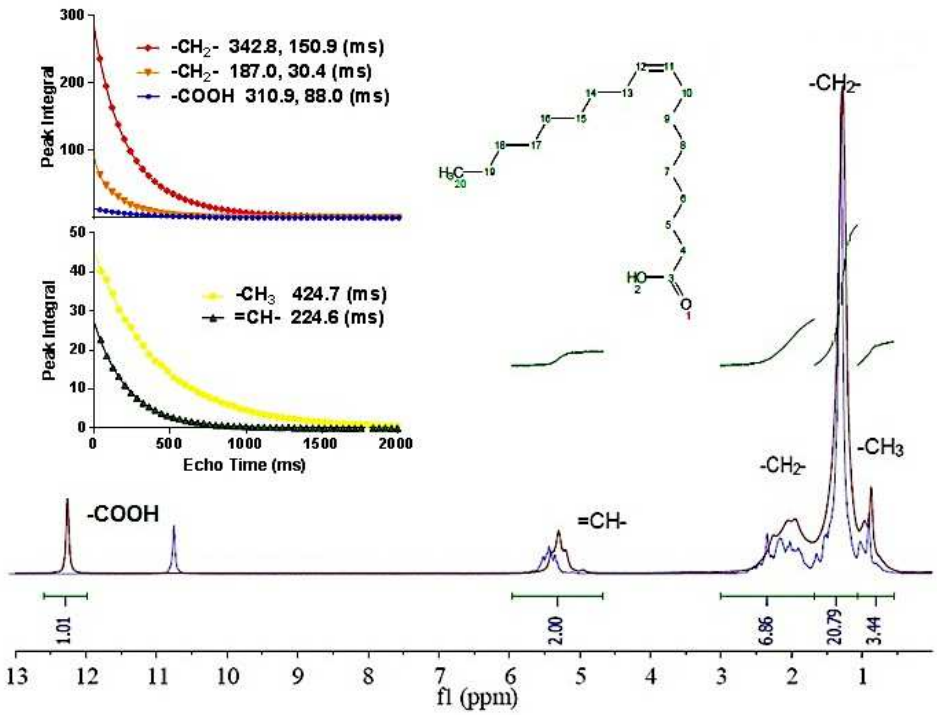

Figure 3S: **Proton FT-NMR spectra and T_2 exponential decay curves for oleic acid**, obtained using a Magritek Spinsolve benchtop NMR spectrometer operating at 43MHz. The NMR trace shown in red is the experimental spectrum, whereas the trace in blue is a simulated spectrum. The exponential decay curves were obtained by measuring the areas under the peaks designated by the integrals.

Effect of hydrocarbon chain length on T_2 profile

Figure 2A-C displays T_2 profiles for three saturated fatty acids of increasing chain length: lauric (12:0), myristic (14:0) and palmitic acids (16:0), respectively. These data were acquired at 65°C to ensure that all three fatty acids were above their crystalline-to-liquid phase transition and in the oil phase. Each of the saturated fatty acids displayed only two resolved T_2 domains. As hydrocarbon chain length increased, the T_2 values decreased, and the profile shifted to the left (Figure 2A-C). Moreover, the number of hydrogens in the lowest T_2 domain increased with increasing hydrocarbon chain length, while the protons in the higher T_2 domain remained constant (Table 1).

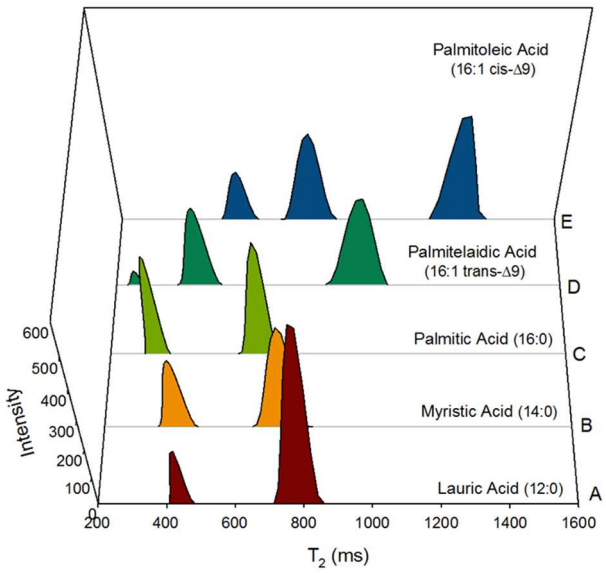

<u>Figure 2</u>: T_2 profiles for saturated and unsaturated fatty acids at 65°C: Effect of hydrocarbon chain length, saturation and stereochemistry. (A) Lauric acid**,** 12:0 (B) Myristic acid**,** 14:0; (C) Palmitic acid**,** 16:0; (D) Palmitelaidic acid**,** 16:1 *trans*-Δ^9; (E) Palmitoleic acid**,** 16:1 *cis*-Δ^9

Comparison of T_2 profiles for saturated and monounsaturated fatty acids

Figure 2, Panels C-E, compares palmitic acid with two of its monounsaturated counterparts, palmitoleic (16:1 *cis*- Δ9) and palmitelaidic (16:1 *trans*- Δ9) acids, respectively. The addition of a double bond, regardless of the stereochemistry, increased the number of resolved T_2 domains from two to three. In addition, the T_2 values for 16-carbon fatty acids containing one double bond (Figs. 2D and E) were both higher compared with the 16-carbon saturated fatty acid (Fig 2C).

Effect of double bond stereochemistry

Two matched sets of monounsaturated fatty acids in their *cis* and *trans* configuration were compared: 16:1-*cis* and *trans* at 65°C (Table 1 and Figure 2, D-E), and 18:1 *cis* and *trans* at 55°C (Table 1). Each monounsaturated fatty acid displayed three T_2 domains, although those with *cis* double bonds had much higher T_2 values than those with *trans*. Note that the T_2 value

Table 1: Fluidity and TD-NMR Parameters for Pure Oil-phase Fatty Acids at Several Temperatures

Fatty Acid	Fluidity (cP^{-1})	Melting Point (°C)	Domain 1		Domain 2		Domain 3		Domain 4	
			T_2 (ms)	# of ^1H	T_2 (ms)	# of ^1H	T_2 (ms)	# of ^1H	T_2 (ms)	# of ^1H
37°C										
Myristoleic Acid (14:1 *cis*-Δ^9)	0.078	-4.0	732.5 ± 4.5	10	353.0 ± 2.1	12	217.0 ± 1.2	4		
Palmitoleic Acid (16:1 *cis*-Δ^9)	0.068	0.5	536.0 ± 6.7	14	256.8 ± 8.5	15	160.0 ± 8.0	4		
Palmitelaidic Acid (16:1 *trans*-Δ^9)	0.056	31.0	453 ± 1.4	12	204 ± 0	16	111 ± 0	2		
Petroselenic Acid (18:1 *cis*-Δ^6)	0.057	30.0	416.3 ± 4.3	12	219.0 ± 1.5	22				
Oleic Acid (18:1 *cis*-Δ^9)	0.056	13.4	433 ± 1.2	13	211.3 ± 3.2	18	124.2 ± 7.2	3		
Vaccenic Acid (18:1 *cis*-Δ^{11})	0.055	15.0	493.0 ± 2.5	12	243.4 ± 4.2	12	152.3 ± 0.8	10		
Linoleic Acid (18:2 *cis*-$\Delta^{9,12}$)	0.080	-5.0	831.7 ± 7.9	11	396.8 ± 13.2	9	218.3 ± 7.9	11	81±	1
α-Linolenic Acid (18:3 *cis*-$\Delta^{9,12,15}$)	0.108	-11.3	1692.8 ± 3.2	6	779.0 ± 0.0	10	336.2 ± 0.2	14		
Arachidonic Acid (20:4 *cis*-$\Delta^{5,8,11,14}$)	0.128	-49.5	1241.5 ± 6.4	14	665.8 ± 4.2	15	347.8 ± 1.8	3		
Eicosapentaenoic Acid (20:5 *cis*-$\Delta^{5,8,11,14,17}$)	0.152	-54.0	2133.0 ± 9.9	8	1045.0 ± 12.7	16	507.5 ± 6.3	9		
Docosahexaenoic Acid (22:6 *cis*-$\Delta^{4,7,10,13,16,19}$)	0.151	-44.0	2211.0 ± 4.2	8	1078.0 ± 2.8	18	575.0 ± 4.2	6		
55°C										
Oleic Acid (18:1 *cis*-Δ^9)	0.099	13.4	636.5 ± 1.8	11	325.0 ± 0	16	194.0 ± 1.5	7		
Elaidic Acid (18:1 *trans*-Δ^9)	0.077	44.0	539.0 ± 1.5	10	263.3 ± 2.7	17	162.0 ± 2.5	7		
60°C										
Myristic Acid (14:0)	0.145	54.4	635.7 ± 1.3	14	356.7 ± 2.0	13	166.7 ± 5.9	1		
Myristoleic Acid (14:1 *cis*-Δ^9)		-4.0	1317.3 ±9.3	9	644.7 ± 8.7	12	366.0 ± 8.0	5		
65°C										
Lauric Acid (12:0)	0.226	43.5	789 ± 13.4	18	437 ± 6.4	6				
Myristic Acid (14:0)	0.167	54.4	728 ± 0.4	15	415 ± 0.7	13				
Palmitic Acid (16:0)	0.123	62.9	658 ± 0.1	15	341 ± 0.7	17				
Palmitoleic Acid (16:1 *cis*-Δ^9)	0.166	0.5	1126 ± 2.5	13	513 ± 3.3	15	247 ± 2.6	2		
Palmitelaidic Acid (16:1 *trans*-Δ^9)	0.132	31	969 ± 7.1	12	461 ± 2.1	16	260 ± 1.4	2		

for fatty acids with a *trans* double bond were in between those for *cis*-unsaturated and saturated fatty acids. The number of hydrogen atoms corresponding to each T_2 domain was only minimally affected by double bond stereochemistry (Table 1).

Correlation of T_2 from TD-NMR with sample fluidity

Figure 3A displays the T_2 values for oleic acid measured across the temperature range of 25-55°C. The results reveal a positive correlation of T_2 with temperature and with sample fluidity, as measured using a viscometer. All three resolved T_2 domains in oleic acid showed this positive correlation with fluidity. Similar positive correlations between NMR T_2 and sample fluidity were obtained for all three domains in palmitoleic acid (Figure 3B) and linoleic acid (Fig. 3C).

To determine how hydrocarbon chain structure impacted the correlation between NMR T_2 and fluidity measurements, we compared values for a wide range of fatty acids that varied in hydrocarbon chain length, number of double bounds and double bond stereochemistry, all at 37°C. As shown in Figure 4, a positive correlation between TD-NMR T_2 and sample fluidity is apparent for each of the three resolved T_2 domains.

Overall, the highest T_2 and fluidity values were observed for the fatty acids with the largest number of double bonds. We reasoned that the deviation from linearity for α-linolenic and arachidonic acids might be explained, in part, by the variations in hydrogen domain size (and hence average T_2) seen with different fatty acids. Note that the number of protons in domain 1 for α-linolenic acid is relatively low, in contrast to arachidonic acid, which is relatively high (Table 1).

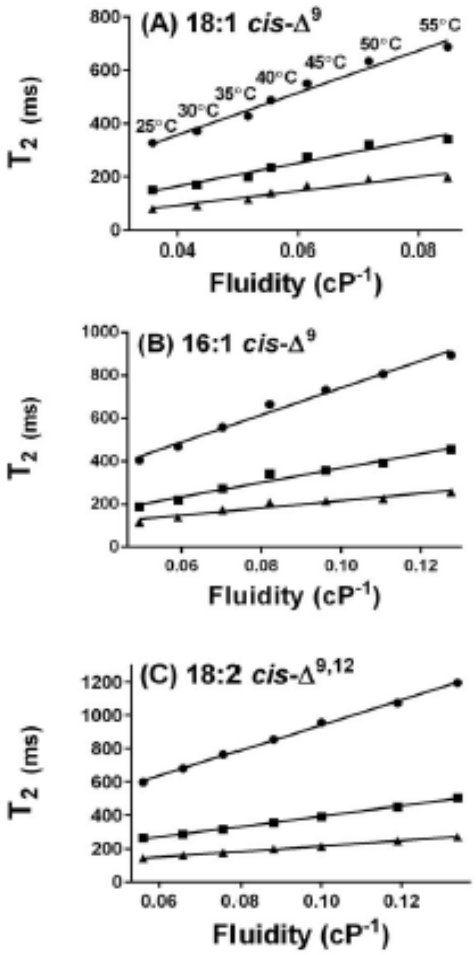

Figure 3: Temperature dependence of T_2 and fluidity for oleic acid (A), palmitoleic acid (B) and linoleic acid (C). The temperatures shown above the points in panel A also pertain to the points shown in panel B and C; domain 1 (circles), domain 2 (squares), domain 3 (triangles). For oleic acid, the R^2 correlation coefficients for the plots are 0.99, 0.99 and 0.96 for domains 1, 2 and 3, respectively. For palmitoleic, they are 0.99, 0.97 and 0.94, respectively. For linoleic, all three domains exhibit a R^2 value of 0.99.

T_2 profiles for fatty acid mixtures

Binary mixtures of oleic and linoleic acids were prepared with varying percentages of the two components. As the volume percent of linoleic acid increased, so did the T_2 values and the fluidity for each domain at 37°C (not shown).

To mimic the diversity of fatty acyl hydrocarbon chain structures seen in biological samples, we prepared oil-phase fatty acid mixtures with compositions similar to those seen in the human blood serum lipid profiles from individuals on a diet rich in saturated fats (SAFA), mono-unsaturated fats (MUFA), or polyunsaturated fats (PUFA)[134,135]. The composition of these three mixtures is specified in Table 1S. The T_2 profiles are shown in Figure 5. Like pure linoleic acid, the mixtures showed four resolved T_2 components: three intense peaks and a very small peak at low T_2 value. The PUFA mixture had the highest T_2 and fluidity

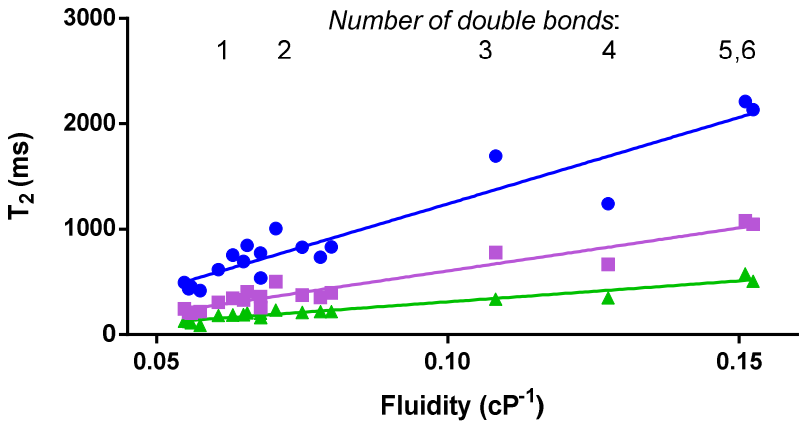

Figure 4: T_2 correlation with fluidity for a range of structurally distinct fatty acids and fatty acid mixtures at 37°C. The blue curve represents domain 1 and the purple and green curves, domains 2 and 3 respectively. The R^2 correlation coefficients for the plots of domains 1, 2 and 3 were 0.90, 0.93 and 0.94, respectively.

values, whereas the SAFA mixtures yielded the lowest. These results demonstrate that TD-NMR is able to detect differences in T_2 and fluidity in complex mixtures that mimic biological variations in hydrocarbon chain composition.

To assess the ability of benchtop TD-NMR to detect fluidity differences in nutritional oils, we compared two different free fatty acid-based fish oil samples highly enriched in *n-3* (ω-3) fatty acids. These two samples varied only slightly in the total percentage of *n-3* fatty acids (74.8% vs. 73.6%). The T_2 and fluidity values for the 74.8% *n-3* sample were significantly higher (Figure 4S), consistent with the observation that *n-3* fatty acids have the highest T_2 values (Figure 4). These results suggest that TD-NMR may be sensitive to small differences in hydrocarbon chain composition in nutritional oils.

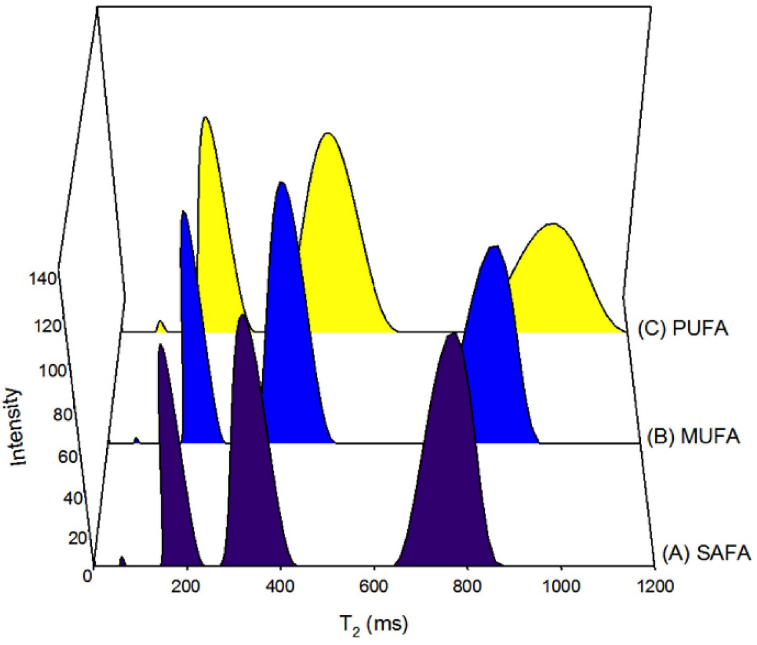

Figure 5: T_2 profiles at 37°C for fatty acid mixtures that mimic serum lipid profiles for subjects on a saturated fatty acid diet (A), monounsaturated fatty acid diet (B) and a polyunsaturated fatty acid diet (C). [134,135] The composition of each fatty acid mixture is listed in Table 1S.

Saturated Fat Diet		Monounsaturated Fat Diet		Polyunsaturated Fat Diet	
Fatty Acid	**% Volume**	**Fatty Acid**	**% Volume**	**Fatty Acid**	**% Volume**
14:0	1.05	14:0	0.63	14:0	0.73
16:0	23.71	16:0	21.94	16:0	20.81
16:1	2.53	16:1	1.73	16:1	1.87
18:0	7.27	18:0	6.24	18:0	7.39
18:1	22.34	18:1	25.44	18:1	23.41
18:2	34.67	18:2	32.55	18:2	28.72
18:3	0.32	18:3	0.31	18:3	0.42
20:4	7.06	20:4	6.84	20:4	6.56
20:5	0.42	20:5	0.95	20:5	6.35
22:6	0.63	22:6	3.37	22:6	3.75

Table 1S: Composition of fatty acid mixtures designed to mimic human blood serum fatty acid profiles of individuals consuming a saturated fatty acid diet (left), monounsaturated fatty acid diet (middle) and polyunsaturated fatty acid diet (right).

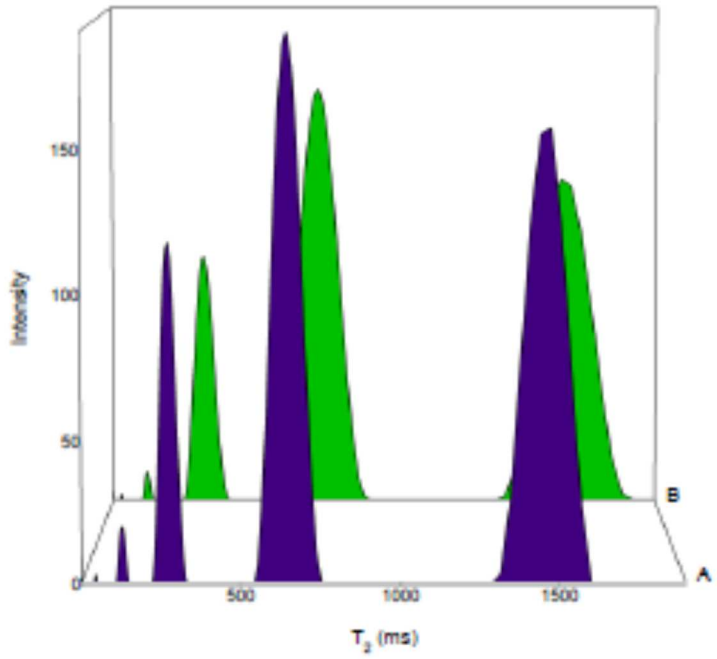

Sample A			Sample B		
% ω-3	Fluidity(cP^{-1})	T_2 values	% ω-3	Fluidity(cP^{-1})	T_2 values
73.6	0.086	1478, 660, 275,122	74.8	0.106	1628, 738, 322, 125

Figure 4S: T_2 profiles for two different free fatty acid-based fish-oil samples that vary slightly in total *n-3* fatty acid content.

Molecular origins of T_2 and fluidity differences

In principle, spin-spin or transverse relaxation time constants are able to probe molecular motions over a wide range of timescales [29]. Fast motions on the nanosecond-to-picosecond time scale include small amplitude, high frequency fluctuations such as segmental bond rotations bonds or small-amplitude translational displacements [32]. Slow motions on the millisecond-to-second timescale involve high amplitude fluctuations such as global conformational exchange or oligomerization in macromolecules. For the fatty

acid systems studied here, we observed that T_2 is approximately equal to T_1 (extreme narrowing limit), implying that T_2 relaxation was driven primarily by fast motions with lifetimes < < 25 nsec.

Upon comparison of T_2 values for domains within a given fatty acid molecule, the domain at the methyl end had average T_2 values higher than those of the middle and carboxyl domains. Thus, the hydrocarbon chain becomes progressively more mobile from the carboxyl end toward the methyl end, consistent with the notion that the carboxyl end is anchored by intermolecular hydrogen bonding. However, increasing the number of double bonds, which reduced the number of degrees of freedom for intramolecular bond rotations, had the effect of *increasing* the T_2 value, the opposite of what would be expected if intramolecular carbon–carbon bond rotations were the dominant contributors to fast Brownian motions. Instead, we propose that the dominant source of variation in the ^{1}H T_2 values measured in this study is variation in the interactions that occur between adjacent hydrocarbon chains.

Neat oil phase fatty acids do not form ideal fluids, but consist of small domains of hydrogen-bonded bilayers somewhat similar to the molecular organization seen in their x-ray crystal structures [117,175]. For saturated oil-phase fatty acids, the hydrocarbon chains pack quite tightly with low mean volumes per methylene group, especially near the carboxyl end. As demonstrated by J. A. Hamilton and D. M. Small, the ^{13}C T_1 values for oil-phase undecanoic acid, an 11-carbon saturated fatty acid, increase progressively from the carboxyl to the methyl end (Figs. 8-26 through 8-28 in ref. 3). For unsaturated fatty acids, the addition of a *cis*-double bond introduces a 120-degree kink into the chain, which is only partially overcome by trans-gauche isomerization in adjacent methylene

groups. Hydrocarbon chain packing is disrupted, with a corresponding decrease in melting temperature. The increased volume per methylene group provides greater freedom for adjacent hydrocarbon chains to undergo molecular fluctuations. As those fluctuations increase well above the Larmour frequency (here 40 MHz, corresponding to a 25 msec lifetime), T_2 and T_1 relaxation becomes less efficient and the relaxation time constants increase.

Molecular packing considerations may help explain the correlation between T_2 and fluidity as observed in this study. Viscosity, the inverse of fluidity, can be described as liquid friction. Such friction is increased by intermolecular interactions between molecules. For oil-phase saturated fatty acids, those interactions include hydrogen bonding between opposing carboxyl groups and van der Waals interactions between adjacent hydrocarbon chains. As double bonds are introduced into the chain, van der Waals interactions are weakened, resulting in less liquid friction and an increase in fluidity. Thus, the variations in T_2 and fluidity measurements appear to be monitoring the same fundamental phenomenon, variations in hydrocarbon chain packing.

The relationship between T_2 and fluidity can be explained using the generalized Stokes-Einstein-Debye relationship for rotational diffusion [176]

$$\boldsymbol{\tau}_c^i = 1/D_{\boldsymbol{\tau}} = \boldsymbol{\eta} \mathrm{V} f_i / k_B T$$

where τ_c^i is the rotational correlation time about the *i*th axis of a molecule in solution, D_r is the rotational diffusion constant, η is the absolute viscosity, V is the molecular volume, k_B is Boltzmann's constant, and T is the absolute temperature. The friction coefficient, f_i, is a dimensionless quantity that depends on the shape of the molecule and the boundary conditions imposed by the molecule and surrounding fluid. As fatty acid hydrocarbon

chains have a dense network of spin-1/2 nuclei, the dominant relaxation mechanism is through dipole–dipole interactions [29]. The relationship between τ_c and T_2 for dipole–dipole relaxation is $\boldsymbol{\gamma}$

$$1/T_2 = \boldsymbol{\gamma^2\langle B^2\rangle\{\tau_c + \tau_c/1 + (2\pi\nu_0\tau_c)^2\}}$$

where γ is the gyromagnetic ratio for ^{1}H, $\langle B^2 \rangle$ is the mean square fluctuating field (the magnitude of the fluctuating field resulting from Brownian motion), and ν_o is the Larmor frequency [32]. In the extreme narrowing limit, where $T_2 = T_1$ and $(2\pi\nu_o\tau_c)^2 \ll 1$, eq 2 simplifies to

$$1/T_2 = \boldsymbol{\gamma^2\langle B^2\rangle 2\tau_c}$$

Considering eqs 1–3 together leads to the following proportionality

$$T_2 \propto 1/\boldsymbol{\tau_c} \propto D_r \propto 1/\boldsymbol{\eta}$$

which predicts that T_2 should be inversely proportional to viscosity and directly proportional to fluidity. A similar proportionality holds for the Stokes–Einstein equation, which describes translational diffusion. Thus, the experimental observation of a linear relationship between T_2 and fluidity in this study provides evidence that these theoretical constructs are valid for the analysis of fatty acid hydrocarbon chains, at least for the systems studied here.

Measuring Nanofluidity in Other Biological Systems

The use of single-phase fatty acid oil samples permitted us to validate the correlation between ^{1}H T_2 and fluidity measurements and to establish T_2 from TD-NMR as a "nanofluidity meter". Similar T_2 measurements from benchtop TD-NMR could be used to measure nanofluidity in multi-phase biological samples such as hydrated

phospholipid bilayers, biological membranes, cell suspensions or serum lipoproteins. All of these complex assemblies are bathed in an aqueous milieu, where measurements of bulk sample fluidity may not be relevant to the fluidity of the lipid nanoenvironment inside the membrane or lipoprotein assembly. In such complex samples, TD-NMR may be able to probe what a viscometer cannot.

While ^{1}H T_2 measurements can be performed using conventional Fourier transform NMR spectroscopy, the benchtop TD-NMR relaxometry approach has several advantages. First, the time decay points are recorded directly during the delays embedded into the CPMG pulse scheme (Figure S1). Therefore, the T_2 decay curve can be heavily sampled, enabling a more robust multi-exponential analysis using inverse Laplace transforms. By contrast, in NMR spectroscopy, the T_2 decay is assessed indirectly through the intensities obtained from a series of Fourier-transformed spectra. In practice, the T_2 decay curves from TD-NMR have 4000-8000 time points, whereas the corresponding curves from NMR spectroscopy typically have about 10-50 points. A second advantage is that TD-NMR does not suffer from "line-broadening" as seen in high-resolution ^{1}H or ^{13}C NMR spectroscopy of large membrane assemblies. It can be used to measure systems with short T_2 values, as it does not rely on resolving NMR resonances in the frequency domain. Like ^{2}H NMR, benchtop TD-NMR is particularly well suited for studying membranes. A third advantage of benchtop TD-NMR is the relative simplicity and low cost of the instrumentation. It can be deployed in environments outside of the typical NMR research lab, and may be more accessible to non-NMR specialists.

Finally, TD-NMR detects the properties of the ubiquitous hydrogen atom. Therefore, there is no need to enrich molecules with ^{2}H or ^{13}C or to synthetically incorporate fluorescent or ESR probes into biological lipids. For all these reasons, benchtop TD-NMR shows promise to become a versatile tool for investigating lipid and membrane fluidity in a variety of samples of biological interest. Current efforts in our lab are focused on the application of TD-NMR to characterize lipoproteins in whole human serum from subjects with different metabolic disorders.

Chapter 3: Omega-3 Content of Fish-Oil Supplements as Monitored by Benchtop Time-Domain NMR

Introduction

Increased media coverage, scientific research and recommendations made through the American Heart Association regarding the health benefits of long chain polyunsaturated fatty acids [177-179] has led to a substantial rise in the use of omega-3 (ω-3) dietary supplements. Research suggests increased consumption of ω-3 fatty acids may lead to improvements in fetal development, cognitive well-being, inflammation and immune response [178,180-184] The most compelling evidence though, has been observed in the prevention and management of cardiovascular disease through a number of clinical trials including GISSI-Prevenzion, JELIS, GISSI-HR, COMBOS, and ESPRIT[181]. These studies showed a significant inverse correlation between dietary ω-3 fatty acids, coronary heart disease mortality rates and circulating triglyceride levels [181,182,185-189]. However, not all clinical trials support these claims; the Omega, Alpha Omega, ORIGIN and Su.Fol.Om3 trials found no significant impact on human health with increased ω-3 consumption [186]. While some trials have been criticized for poor trial design quality (*i.e.*, ω-3 dosage and duration, baseline ω -3 levels, population heterogeneity and additional medication interactions [181]), their negative findings have led to mixed perceptions in the community. Nonetheless, ω-3 supplement sales remains strong, and it is estimated that sales in the U.S. will rise from $25.4 billion in 2011, to $34.7 billion by 2016 [178].

The ω-3 fatty acids of particular interest are eicosapentaenoic (EPA), docosahexaenoic acid (DHA) and alpha-linolenic acid (ALA). All are essential fatty

acids, meaning they must be obtained through the diet. For example, EPA and DHA are found primarily in fish such as albacore tuna, salmon, mackerel and herring [190,191], whereas ALA is plant based and found in walnuts, flaxseed and canola oil. Routine intake of EPA, DHA and ALA is highly recommended, but the dose (g/day) varies based on an individual's metabolic state. For example, those with average CVD risk are recommended to consume at least 250mg/day of EPA+DHA [192,193]; those with documented coronary heart disease are recommended to consume 1g/day of EPA and/or DHA [186]; and those with severely elevated triglycerides (>500mg/dL) may be prescribed as much as 2-4 g/day of EPA and/or DHA [186]. Achieving these doses through fish consumption alone can be quite difficult, and many people have turned to fish-oil ω-3 dietary supplements available at local retailors [194] . The FDA has recently approved three highly pure and concentrated ω-3 pharmaceuticals to treat severe hypertriglyceridemia: Lovaza (GlaxoSmithKline, DHA and EPA ethyl esters) Vascepa (Amarin, EPA ethyl ester) and Epanova (AstraZeneca, DHA and EPA free fatty acids), but these are only available through a prescription.

Regulation of dietary supplements by the FDA is not as strict as over the counter or prescribed mediation, therefore many of the commercially available fish-oil supplements are not as pure or concentrated as their labels claim [177,183,195,196]. In fact, a recent study from 2014 showed that out of 31 supplements, 74% contained less than 100% of the stated label amount of EPA and DHA [180]. Consequently, the consumer may inadvertently be ingesting a significantly lower concentration of ω-3's, thereby not taking full advantage of potential health benefits.

Gas-liquid chromatography (GLC) is the gold-standard method used to determine

the fatty acid composition and fish-oil supplement purity [197-200] . Not only is GLC expensive, the lipids must be extracted using organic solvents, which is time consuming, generates organic waste and can potentially lead to sample loss and contamination [197].

Here we present a new approach for non-invasively measuring total ω-3 concentration in oil-phase samples using benchtop time-domain ^{1}H NMR (TD-NMR) relaxometry. In contrast to Fourier-transform high-resolution NMR spectroscopy, TD-NMR operates in the time domain, bypassing the requirement for superconducting magnets with high magnetic field strength and field homogeneity. As a result TD-NMR can be performed on simpler, smaller and less expensive benchtop instrument equipped with low-field permanent magnets. While TD-NMR sacrifices the measurement of chemical shifts, it retains the ability to measure T_1 and T_2 relaxation time constants, which possess significant information content and resolving power on their own. Previously we demonstrated that benchtop TD-NMR was capable of monitoring hydrocarbon chain fluidity in oil-phase fatty acid samples; the fluidity was highly dependent upon the content of cis-double bonds [201] . In this study, we apply this approach to triglyceride based fish-oil supplements and tested the hypothesis that TD-NMR-derived T_2 values are a sensitive indicator of ω-3 content.

Experimental Procedure:

Sample preparation

Individual neat triglycerides (>99% Purity) were purchased from Nu-Chek Prep (Elysain, Minnesota, USA). Five commercial fish-oil supplements (Nordic Naturals) that varied in composition and purity were purchased from a local retailor. Oil was removed from the capsules using a needle syringe, placed into and NMR tube and analyzed

immediately. Fatty acid composition of the fish-oil supplements was determined by Omega-Quant (Sioux Falls, SD, USA). Approximately 350ul of sample was necessary to fill a 7.5mm diameter NMR tube to reach the optimal sample height of 0.7 mm. The NMR tubes were evacuated with dry nitrogen gas and sealed after sample filling to minimize lipid oxidation during experiments. The triglyceride samples did no show signs of oxidation during multiple repeat experiments at 37°C.

Viscosity/fluidity measurements

Absolute viscosity for single-phase triglyceride oil samples was measured using a VISCOlab 3000. Each measurement required approximately 0.7ml of triglyceride. Sample fluidity, reported here in units of centipoise^{-1} or cP^{-1} was obtained by taking the inverse of the absolute viscosity.

Benchtop time-domain NMR relaxometry

Benchtop TD-NMR methods used were described in detail in *Robinson 14*[201]. Briefly, data was collected using a Bruker mq40 Minispec NMR equipped with a permanent magnet, operating at 0.94 Tesla (40 MHz for ^{1}H). All experiments were run at 37°C. Time-domain spin-spin relaxation exponential decay curves were acquired using a CPMG pulse sequence [50,202-205] . The multi-exponential T_2 decay curves were analyzed using and inverse Laplace transform algorithm as implemented in CONTIN [206] (see also s-provencher.com). For oil-phase triglycerides this analysis provided three-to-four resolved T_2 exponential terms and amplitudes associated with each term. The data are represented as T_2 profiles: intensity vs. T_2.

Results

Triglyceride T_2 profiles

The T_2 profiles of five pure oil-phase triglycerides commonly found in fish-oil supplements are shown in Figure 1. All of the profiles display at least four resolvable T_2 peaks or mobile domains. The center for each peak represents the average T_2 values for a cluster of ^1H nuclei in the triglyceride (Table S1). For a single triglyceride, the lowest T_2 value is assigned to the least mobile region, the glycerol backbone; the middle peak is assigned to the middle of the hydrocarbon chain and the highest T_2 represents the most mobile region of the triglyceride, the distal end of the methyl chain.

The primary structural variation between the triglycerides shown in Figure 1 are the number of *cis*-double bonds: 1, 2, 3, 5 or 6 – panels A, B, C, D and E, respectively. As the content of *cis*-double bonds for a given triglyceride increases, the T_2 value for each mobile domain shifts to the right, with the most dramatic shift observed for T-DHA.

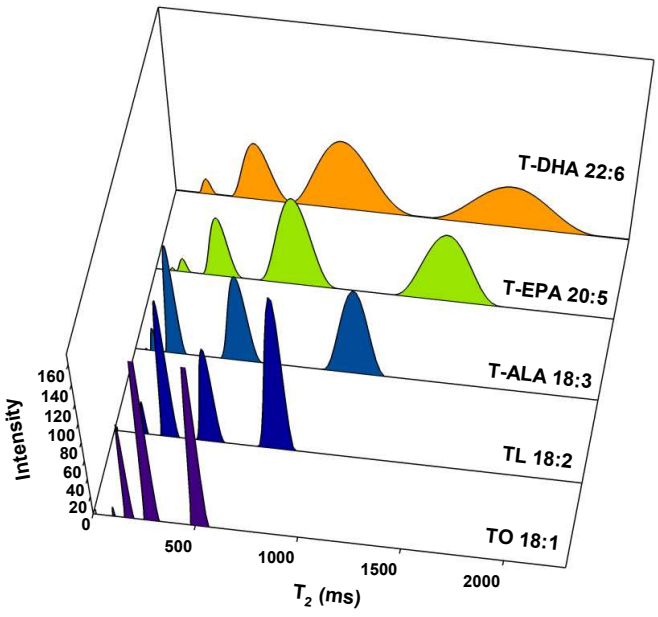

Figure 1: T_2 profiles for triglycerides that vary in number of double bonds.
(A) Triolein, 18:1 *cis*-Δ^9
(B)Trilinolein, 18:2 *cis*-$\Delta^{9,12}$ (C) Trilinolenin, 18:3 *cis*-$\Delta^{9,12,15}$ (D) Trieicosapentaenoin, 20:5 *cis*-$\Delta^{5,8,11,14,17}$
(E) Tridocosahexaenoin, 22:6 *cis*-$\Delta^{4,7,10,13,16,19}$

Tables 1S: Fluidity and TD-NMR Values for Pure Oil-phase Triglycerides at 37˚C

Triglyceride	Fluidity (cP^{-1})	Domain 1		Domain 2		Domain 3		Domain 4	
		T_2 (ms)	# of ^1H	T_2 (ms)	# of ^1H	T_2 (ms)	# of ^1H	T_2 (ms)	# of ^1H
Tripalmitolein (16:1 *cis*-Δ^9)	0.036	562.4±2.3	9	298.9±1.9	36	126.8±1.9	42	57.5±2.6	5
Tripalmitelaidin Acid (16:1 *trans*Δ^9)	0.024	305.8±5.1	29	124.4±2.1	46	63.2±1.3	17		
Triolein (18:1 *cis*-Δ^9)	0.026	330.7±7.4	30	154.3±2.9	51	80.4±4.3	22	41.3±3.6	1
Trilinolein (18:2 *cis*-$\Delta^{9,12}$)	0.037	580.2±2.7	29	294.5±5.4	23	148.3±2.2	39	70.6±1.5	7
Trilinolenin (18:3 *cis*-$\Delta^{9,12,15}$)	0.054	1093.5±4.9	17	528.3±8.7	24	199.3±1.6	42	96.5±3.3	9
Triarachidonin (20:4 *cis*-$\Delta^{5,8,11,14}$)	0.065	949.5±0.7	24	522.5±0.1	45	247.8±1.7	24	100.1±1.8	5
Trieicosapentaenoin (20:5 *cis*-$\Delta^{5,8,11,14,17}$)	0.056	1453.5±6.3	26	695.6±8.7	40	319.9±9.6	25	129.9±13.1	1
Tridocosahexaenoin (22:6 *cis*-$\Delta^{4,7,10,13,16,19}$)	0.080	1673.6±38.7	18	825.6±47.2	43	409.5±11.5	30	154.1±7.1	7

T_2 profile behavior of binary triglyceride mixtures

Figure 2 displays 1:1 binary mixtures of trilinolein (TL, 18:2 *cis*-$\Delta^{9,12}$) and various other triglycerides that differ in the number of *cis*-double bonds. As shown in panel A, the addition of triolein (TO), which contains one less *cis*-double bond than TL, decreases the T_2 values for each mobile domain versus TL alone (Figure 1, panel B). Panels B-D of Figure 2 demonstrate that the addition of a triglyceride that contains more *cis*-doubles bond than TL (more than two) increases the T_2 values for each domain. The most dramatic shifts were observed for the highly unsaturated triglycerides, T-EPA and T-DHA. To demonstrate the concentration dependence of ω-3 triglycerides in binary mixtures, a dilution series of TL and various polyunsaturated triglycerides (T-ALA, T-EPA or T- DHA) were prepared, as shown in Figure 2B. A linear dependence was observed between % ω-3 content and TD-NMR T_2 values.

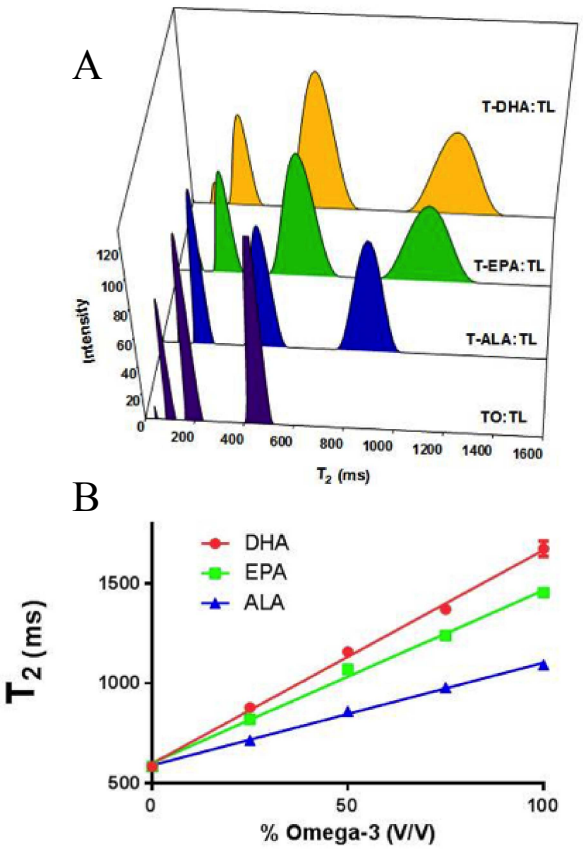

Figure 2: (A.) T_2 profiles for 1:1 binary triglyceride mixtures with TL(18:2 *cis*-$\Delta^{9,12}$) and one other triglyceride. Triglycerides that contain less cis-double bonds than TL shift the T_2 profile to the left, whereas additional cis-double bonds increase T_2 and shift the profile to the right. (A)TO,18:1 *cis*-Δ^9 (B)T-ALA, 18:3 *cis*-$\Delta^{9,12,15}$ (C)T-EPA, 20:5 *cis*-$\Delta^{5,8,11,14,17}$ (D)T-DHA, 22:6 *cis*-$\Delta^{4,7,10,13,16,19}$ **(B.) T_2 correlated with ω-3 content for binary mixtures of triglycerides.** (●) TL and T-DHA (▲) TL and T-EPA (■) TL and T-ALA

Correlation of ω-3 concentration with TD-NMR T_2 values in complex mixtures

Defined mixtures of triglycerides mimicking fish-oil supplements were prepared and analyzed (Figure 3). As the total concentration of ω-3 triglycerides increased, so did the NMR T_2 values for each mobile domain. In addition, five commercial fish-oil supplements from the same manufacturer that varied in purity and ω-3 concentration were analyzed using benchtop TD-NMR.

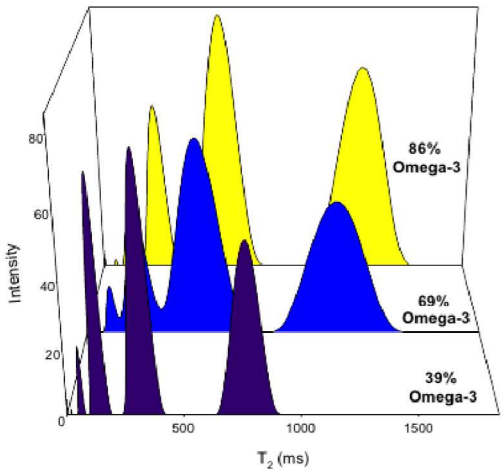

	% Volume Triglyceride						
Sample	**16:00**	**18:01**	**18:02**	**18:03**	**20:04**	**20:05**	**22:06**
A	30.6	24.2	4.6	1.1	1.1	21.7	16.8
B	8.2	12.7	2.1	0.6	3.1	15.6	57.7
C	2.8	5.4	1.2	0.7	4.2	85.7	0

Figure 3: T_2 profile for complex triglyceride mixtures that vary in ω-3 fatty acid content. Defined triglyceride mixtures that mimic the composition of fish-oil supplements were prepared. As the volume percent of total ω-3 triglyceride increases, the T_2 value for each mobile domain increases. The composition of each mixture is detail in the table below.

As shown in Figure 4 the supplements containing the highest ω-3 concentration had the highest T_2 values, whereas the supplements with the lowest ω-3 concentration have the lowest T_2 values. These results demonstrate that TD-NMR is highly sensitive to variations in ω-3 concentration in oil-phase lipid samples.

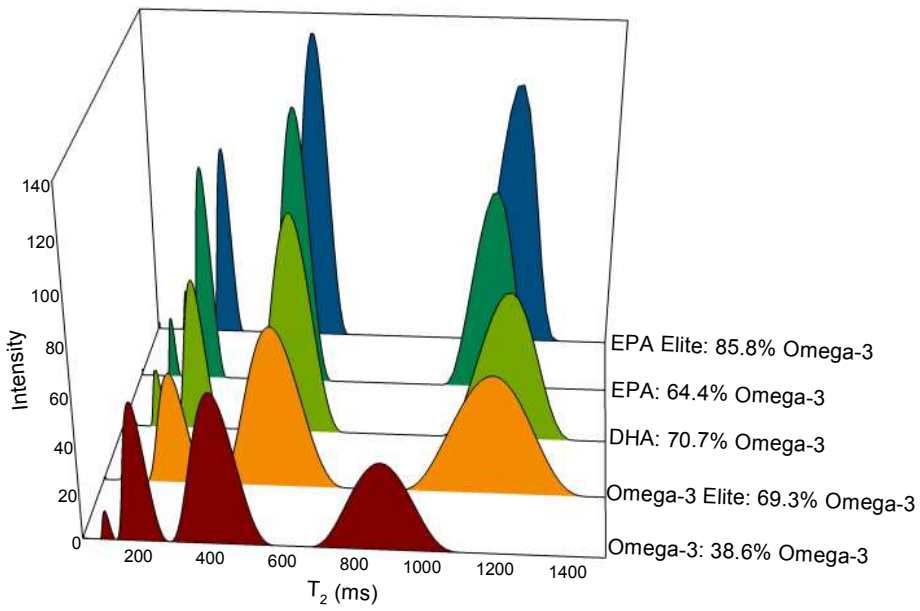

Figure 4: T_2 profiles of store bought Omega-3 neutraceutical supplements that vary in composition and Omega-3 content. Commercial source: Nordic Naturals, Inc. (Watsonville, CA). The fatty acid content of each product was analyzed by an independent laboratory: OmegaQuant (Sioux Falls, SD)

Correlation of T_2 from TD-NMR with % ω-3 and fluidity

Figure 5A displays the correlation between NMR T_2 values and % ω-3 in defined and commercially available oil-phase lipid mixtures. A positive correlation is observed for all three mobile domains regardless of the type or origin of the triglyceride mixture. Overall, the highest T_2 values were observed for samples that contained the highest ω-3 concentration. In addition, a positive correlation was observed between fluidity and % ω-3 content for the same set of lipid mixtures, demonstrating that the T_2 values in oil-phase lipids are sensitive to sample fluidity. This result is consistent with our previously published work using pure oil-phase non-esterified fatty acids [201]. These results indicate that TD-NMR is sensitive to small variations in ω-3 concentration in nutritional oils.

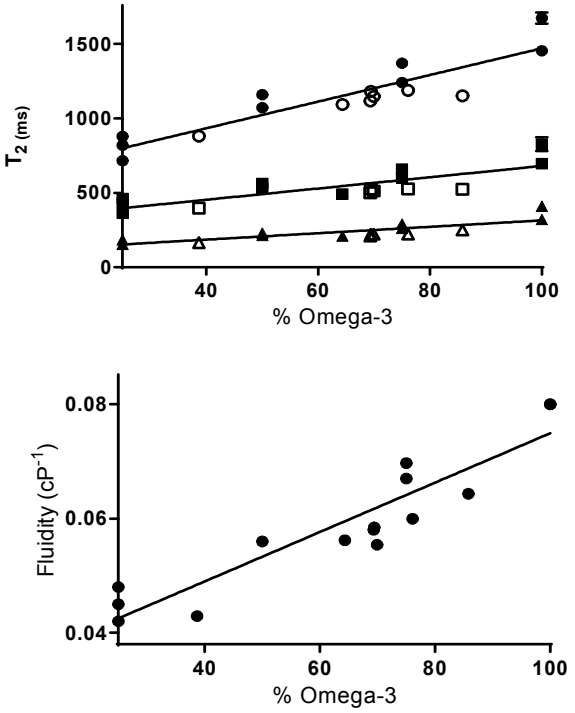

Figure 5: (A) T_2 correlation with % Omega-3 (V/V) in triglyceride mixtures. The highest three T_2 domains resolved by TD-NMR for each sample are plotted, and each domain correlates linearly with ω -3 content (vol %); R= 0.94, 0.80 and 0.82 for T_2 domains 1, 2 and 3, respectively. ● Defined triglyceride mixtures ○ Commercial triglyceride mixtures

(B) Fluidity correlation with % ω-3 (V/V) in defined and commercial triglyceride mixtures (R=0.92). T_2 from TD-NMR monitors the nanofluidity of hydrocarbon chains

Discussion and Conclusion

This study yielded three key observations. First, the T_2 profiles of pure triglycerides and triglyceride mixtures, including fish-oil supplements, revealed three-to-four resolved T_2 domains. Each of these domains represents a cluster of ^1H atoms in a structurally distinct region of the triglyceride. The T_2 profiles are similar to those for non-esterified fatty acids, with the exception of an additional T_2 domain that corresponds to the glycerol backbone. The number of cis-double bonds in the hydrocarbon chain heavily impacts triglyceride T_2 values. As the number of double bonds increase, the T_2 values for each mobile domain and the sample fluidity also increase. Finally, the T_2 values are positively correlated with ω-3 content in compositionally diverse set of samples including pure triglycerides, binary and complex triglyceride mixtures, and commercial fish oil-supplements.

Triglyceride T_2 value is governed by molecular packing.

Triglycerides consist of three hydrocarbon chains covalently linked through a glycerol. The physical and structural properties of triglycerides are determined by the number, position and orientation of hydrocarbon double bonds [116,207,208] . Saturated acyl chains promote tight and efficient molecular interactions, whereas the introduction of a cis-double bond creates a kink that disrupts molecular packing [209] . Highly unsaturated hydrocarbon chains, such as those found in fish-oil, have a highly kinked, almost circular conformation. This molecular shape prevents the close molecular packing characteristic of saturated or mono-unsaturated chains and promotes a fluid environment with increased molecular motions [207]. Previously we demonstrated TD-NMR was capable of probing the fluidity and thus, hydrocarbon chain packing of non-esterified fatty acids [201]. Also similar to fatty acids, triglyceride T_2 displays a linear correlation with fluidity, where the most *cis*-unsaturated hydrocarbon chains are the most fluid.

Application to Fish Oil Analysis

The linear correlation between T_2 and omega-3 concentration provides a basis for developing a TD-NMR method for the analysis of fish-oil supplements for manufacturing and quality control purposes. The experiments in this study provide proof-of-concept and demonstrate the capability and resolving power of TD-NMR for oil-phase triglycerides. However, an even simpler, quicker version of the analysis can be envisioned for practical real-world applications. For example, it may not be necessary to resolve all four domains to quantify omega-3 content. Instead of collecting 512 scans (~2 hours) to achieve sufficient signal-to-noise for the inverse Laplace transform, it should be possible to

collect only 8 scans (1 CPMG phase cycle, approximately 2 minutes) and analyze the data with a single exponential decay function. In addition, 2-3 runs were collected per sample to assess precision. The calculated error values were sufficiently small such that one run should be sufficient for routine analysis.

Applications to plant-derived omega-3 oils

This method has implications for the quantification of omega-3 content in plant-derived dietary supplements. Unlike fish-oil supplements whose primary polyunsaturated fatty acids are EPA and DHA, plant based omega-3 supplements contain ALA. This hydrocarbon chain contains approximately half of the number cis-double bonds rendering it less fluid than the major fish-oil components. Therefore, the analysis of plant-based supplements containing ALA will require a different calibration curve as compared with fish oil supplements. However, the same principles and processes hold, with T_2 being proportional to overall ALA content.

Advantages of TD-NMR over other methods

While GLC remains the gold standard for quantifying omega-3 content, additional methods exist which overcome the disadvantages associated with this conventional analysis. Liquid chromatography-tandem mass spectrometry (LCMS) is a chromatographic alternative with exquisite sensitivity [210-212] and is commonly used to provide a detailed analysis of lipid systems. One particular novel application determines the hydrocarbon composition of red blood cell membranes, which details a patient's omega-3 index [213-215]. LCMS is an expensive technique and therefore impractical for

manufacturing and process control environments [216]. A range of spectroscopic techniques are also commonly employed which include Fourier transform infrared [217], near-infrared [179], visible and short-wave near infra-red, mid-infra-red, and Raman spectroscopy [218]. These methods monitor vibrational motions combined with a chemometric analysis to determine total ω-3 concentration in fish oil supplements. While spectroscopic methods show promise, the instruments require an extensive skill set, and the analyses demand a complex partial least squares regression algorithm to make their prediction. The chemometric database requires continual revision. The efficiency and prediction accuracy of these algorithms is largely dependent upon spectral quality [217].

Benchtop TD-NMR possesses several advantages over both conventional GLC and the newer spectroscopic techniques for quantifying ω-3 content in fish-oil supplements. First, the TD-NMR technique is non-destructive and non-perturbing. It does not require any sample manipulation, chemical reactions or organic reagents, rendering it cost effective and environmentally friendly. While the proof-of-concept approach presented here generates a result in about 2 hours, simpler routine protocols may be developed with shorter acquisition times to generate a report in under two minutes. Finally, the data analysis does not require a complex chemometric algorithm, which may interfere with the prediction accuracy if the spectral quality is poor.

Benchtop TD-NMR is already utilized in the food industry for quality control. Typical applications include the compositional analysis of total water, fat and protein content, the observation of microstructural changes in food products under different processing or storage conditions [9,22,219], the freezing behavior of food products [80], production quality [13] and food authentication. However, to our knowledge, this is the first

report that details the application of benchtop TD-NMR for the determination of ω-3 content in oil-phase dietary supplements.

Chapter 4: Lipid-Protein Profiling of Human Serum Using Benchtop Time-Domain NMR: Toward an Early Indicator of Insulin Resistance and Metabolic Syndrome

Introduction

Metabolic syndrome (MetS) is a cluster of physical and diagnostic findings associated with an elevated risk of type 2 diabetes mellitus (T2DM) and cardiovascular disease (CVD).[220-226] The NIH/Adult Treatment Panel III designation of metabolic syndrome requires three out of the following five: abdominal obesity (increased waist circumference), decreased high-density cholesterol (HDL), elevated blood pressure, fasting plasma glucose and/or fasting triglycerides.[223,226] At the point that an individual meets MetS criteria, some of the underlying metabolic abnormalities such as insulin resistance may have been in place for some time. In addition, some individuals may not meet the strict definition of MetS, but still have significant metabolic abnormalities that place them at higher risk for T2DM and/or CVD. Therefore, significant effort has gone into identifying MetS biomarkers that identify high-risk individuals at an earlier stage. Examples include adipokines such as adiponectin and leptin,[226] fatty acid omega-3 composition of serum lipids,[213-215,227,228] inflammatory cytokines such as TNF-α and C-reactive protein,[229,230] oxidative stress markers,[231-233] and lipoprotein abnormalities.[98,222]

Advancements in high-throughput technologies, such as genomics, transcriptomics, proteomics and metabolomics have propelled the discovery of novel biomarkers for metabolic syndrome.[234,235] However, most biomarkers do not make it into the clinical laboratory because they lack the appropriate specificity and sensitivity.[236]

One potential solution is to develop of an assay or tool that combines the power of multiple biomarkers to more accurately assess human health.

Our laboratory has been evaluating a relatively simple and practical application of nuclear magnetic resonance, benchtop time-domain relaxometry (TD-NMR), for analyzing blood samples and assessing health status and disease risk. The TD-NMR relaxation time T_2 non-invasively monitors the molecular motions of many of the abundant biomolecules (including water) in whole human serum, and has the potential to broadly sense an individual's metabolic state. The appeal of the technique also stems from the ease and low cost of measurement, which is a necessity for translation into the clinic[234]. Thus, TD-NMR may provide a practical health assessment tool that can help prevent the development and progression of diseases that arise from metabolic abnormalities, such as diabetes, atherosclerosis and Alzheimer's disease.

Here we present a benchtop TD-NMR analysis of blood serum samples from a population of apparently healthy human subjects. The TD-NMR measurables consist of four T_2 values: one peak arising from the intense water signal and three small peaks that directly monitor the lipid and protein components in serum. The results for the water T_2 values are reported in Chapter 5, so the focus of the current chapter is on the three smaller lipid/protein T_2 peaks. The results show that two of the peaks report on insulin sensitivity/resistance by monitoring the most mobile (peak 2) and a less mobile (peak 3) lipid domain within a population of lipoprotein particles. The fourth peak does not correlate with any of the diagnostic biomarkers monitored in this study.

Experimental Procedure

Subject recruitment

Human subject volunteers were recruited with informed consent through two protocols approved by the Institutional Review Board of the University of North Texas Health Science Center (UNTHSC). One protocol recruited seemingly healthy subjects from the student and staff population at UNTHSC. The second protocol recruited members enrolled in the Health and Aging Brain Study at UNTHSC. Patient exclusion criteria included clinically diagnosed with diabetes (HbA1c > 6.4) or had elevated C-reactive protein levels (>10), which is indicative of acute/chronic infection or illness.

Serum and plasma preparation

Blood samples were collected in the morning after an overnight fast. Plasma was collected into lavender-top tubes containing EDTA as the anticoagulant. Serum was collected into plain glass red-top tubes, which lack a clot activator and gel separator (BD model 366441). Blood obtained for the LipoProfile (LabCorp/LipoScience) analysis was drawn into a specialized black-top tube. In a few circumstances, the sample volume was not enough to perform all 70+ biomarkers measurements, which accounts for the variable sample size (n) in the statistical analyses. A list of the biomarkers measured in this study is displayed in Table S1.

Protein depleted serum was made using low-pressure chromatography hydroxyapatite column described in detail elsewhere [237,238] . Two fresh 450ul aliquots of whole serum were applied to the column and the proteins were eluted with potassium phosphate buffer. The samples were then desalted and concentrated using a pressure dialysis amicon cell with a 100KDa filter. Given the size of the filter the only remaining

elements are residual's proteins and lipoproteins; small molecules would have passed through the filter during the concentration process. Afterwards the sample was analyzed using DLS for protein content.

Blood sample analysis

Serum and plasma samples were processed immediately after each blood draw. The samples were centrifuged to remove blood cells, followed by a second low speed spin of the supernatant to remove any residual blood cells. Four TD-NMR measurements were collected immediately after sample processing. Likewise viscosity measurements were made on the same day using a VISCOLab3000 described elsewhere [201]. Aliquots of serum and plasma were immediately frozen and stored at -80°C for in-house analyses. These tests include apolipoprotein E concentration (Abcam, ab108813), ORAC antioxidant capacity (Cell Biolabs, STA-345), protein carbonyl content (Cell Biolabs STA-307), HNE (Cell Biolabs, STA-838) and free fatty acid concentration (BioAssay Systems, EFFA-100). Aliquots of fresh serum or plasma were shipped to outside laboratories for all other testing, which include Atherotech Inc, Labcorp, Quest Diagnostics, Liposcience and OmegaQuant.

Lipoprotein fractionation and purification

Lipoprotein classes were fractionated by density gradient ultracentrifugation described elsewhere [91,239-242]. In brief, three milliliters of fresh plasma was added to 1.21grams of KBr and gently vortexed in an ultracentrifugation tube. Various density gradient solutions are carefully layered in the following order; 1 mL 1.22 g/ml, 4 ml of 1.063 g/ml, 3 ml of 1.019 g/ml and lastly at least 1 ml of HPLC grade water to top it off. The sample is centrifuged at 4°C, 36,000rpm for at least 12 hours. Afterwards, 1ml

Category	Correlated with T_2†	Did not correlate with T_2†
Water T_1 and T_2	T_2, T_{2V}, T_{2P}, T_{2A}, T_{2G}, T_{2TG}, T_{2O3}, T_{2H}	T_{2C}
Protein, viscosity, liver function markers	Serum viscosity, plasma viscosity, α1-antitrypsin	Total serum protein, serum albumin, serum globulins, AST, ALT, GGT
Inflammation, blood cell & oxidative stress markers	WBC, neutrophils, RBC, hematocrit, MCHC, eosinophils, basophils, TNFα	hs-CRP, Lp-Pla2, hemoglobin, MCV, MCH, RDW, platelets, monocytes, lymphocytes, HNE, total antioxidant capacity, protein carbonyl, anion gap
Cholesterol-rich lipoprotein markers	Total cholesterol, non-HDL-C, LDL-C	LDL-P, LDL size, small LDL-P, Lp(a), apoE, apoB, phospholipids
Omega 3 and 6 lipids	Omega-3 index, DHA, EPA, AA	
Triglyceride-rich lipoprotein markers & insulin resistance	Total triglycerides, VLDL-C, TG/TC, Glucose, HOMA2-%B, IR Score (LipoScience)	Free fatty acids, BMI, insulin, C-peptide, HbA_{1c}, apoAI,. HDL-C, HDL-P, remnant-C, VLDL-P
Electrolyte markers		Sodium, potassium, calcium, chloride, bicarbonate, anion gap
Kidney function markers	Blood urea nitrogen (BUN)*, creatinine*	Estimated glomerular filtration rate (eGFR)*
Thyroid function markers		Free T4, Thyroid stimulating hormone (TSH)
Nutritional markers	B12*, Folate*	
Amino acids	Alanine, Alpha-amino butyric acid, beta-alanine, hydroxyproline, homocystine, Isoleucine, 1-methyl histidine, phenylalanine, sarcosine	Anserine, arginine, asparagine, beta-proline, butyric acid, citruline, cystathionine, ethanolamine, glycine, glutamine, leucine, methionine, ornithine, taurine, threonine, tryptophan, tyrosine, serine, valine

Table S1. Biomarkers measured in this study. †In this table, a correlation is defined as one where $p<0.05$ for the Pearson correlation, non-parametric Spearman correlation or both for at least one variant of serum T_2. The null hypothesis is that there is no correlation between a given serum T_2 measure and a particular biomarker. The individual correlation coefficients and statistics are provided in Tables 3-5 and Tables S2-7. *These particular biomarkers were measured for only five-to-ten subjects; although they met the p-value threshold, the correlations are considered preliminary.

aliquots are carefully removed and collected from the ultracentrifuge tube each corresponding to a particular lipoprotein class or subclass.

The lipoprotein fractions were stored at 4°C and used within a month. Before analyzed on TD-NMR, the lipoprotein fractions were desalted and concentrated using a pressure dialysis amicon cell, with a 10, 100 or 300KDa filter depending on the fraction. The homogeneity and purity of the individual lipoprotein classes was determined using dynamic light scattering (DLS). Fractions were not used for TD-NMR analysis unless there were more than ~95% pure.

Reconstituted HDL was generated using cholate dialysis [88,208,243-248]. Particles were prepared using DOPC or DPMC, free cholesterol and ApoA1 at a molar ratio of 80:10:1. Phospholipids and free cholesterol were fully dissolved in chloroform, and subsequently dried under a nitrogen stream generating a film of lipids at the bottom of the flask. 140ul of sodium cholate (100mg/ml stock, pH 7.4, PBS) was added to the flaks and gently mixed until the film was dissolved. Purified ApoA1, the major apolipoprotein in HDL, was added to the solution and incubated for 12 hours at 4°C. Over the next 2 days the sample was dialyzed against 2L of PBS undergoing three buffer exchanges. The final product analyzed using DLS for purity and homogeneity.

Benchtop time-domain NMR relaxometry

Measurements of T_2 and T_1 were performed at 37°C using a Bruker mq20 Minispec benchtop time-domain NMR instrument equipped with a 10 mm variable temperature probe (Model H20-10-25-AVGX). The 10 mm NMR tube was filled to a sample height of 1 cm, corresponding to a sample volume of ~680 uL. Three runs were collected at 256 scans (~2 hours), which was the minimum number of scans to achieve

optimal signal-to-noise. An additional overnight run with 2048 scans was collected to utilize the instrument time efficiently. The final T_2 was an average between the three 256 and one 2048 scan run.

T_2 was measured using a modified CPMG pulse sequence [40,173,202], shown in Figure 1. The modified pulse sequence allows us to suppress the intense water signal to avoid radiation damping, which readily manifests itself by a non-random oscillatory artifact observed in the residuals of the fit after an inverse Laplace transform [30]. By suppressing the solvent signal we also enhance the signal of our peaks of interest, the smaller lipid and protein peaks. We determined empirically that a delta delay of $0.95*T_1$ (leading to a water signal that is ~23% of its full intensity) provides a level of suppression of the water sufficient to avoid radiation damping, while still maximizing the overall signal intensity of the water and the other lipid/protein peaks for analysis. Another unique aspect to this TD-NMR pulse scheme was the delayed acquisition of the data points, which began 19 ms after the beginning of the CPMG scheme. This strategy de-emphasizes the very fast processes at the beginning of the decay curve in order to emphasize the slower processes such as the lipids and proteins. This delayed acquisition scheme reduces the number of exponential terms; simplifying the inverse Laplace transforms calculation. If attempts are made to fit the data using too many exponential terms, the calculation can become unstable, and becomes a mathematically ill-posed problem and leads to poor run-to-run precision.

T_2 values were quantitated using an inverse Laplace transform implemented in the discrete components analysis of XPFit (http://www.softscientific.com/science/xpfit.html). A key to obtaining stable, reproducible calculations is to restrain the number of

exponential terms to a consistent number; the data obtained with 256 or 2048 scans were fit to four terms. XPFit has the advantage of being able to constrain the number of exponentials and employs a non-negative truncated single value decomposition algorithm, which stabilizes the calculation. For illustrative purposes, the T_2 profile distributions shown in Figure 1 were generated using CONTIN (s-provencher.com), even though the T_2 values were quantified using XPFit as described above. CONTIN is a robust algorithm for samples that have plenty of signal-to-noise (water signal), which was not the case for our analyses of lipid and protein components in whole human serum.

Statistical analysis

The correlation, linear regression and statistical analyses were performed using GraphPad Prism v. 6.05 (GraphPad Software, Inc.). The principles for the statistical analyses were derived from the book by Motulsky [249]. The null hypothesis states that there is no correlation between the variables being compared. The two-tailed p value defines the probability of observing a correlation as strong or stronger if the null hypothesis were true. For example, for $r = -0.6$ and $p < 0.01$, there is less than 1% probability of observing a correlation this strong or stronger by random chance; thus, the null hypothesis is rejected. For each correlation that met p-value thresholds, we inspected the plot to ensure that the correlation was not heavily influenced by one or two outliers.

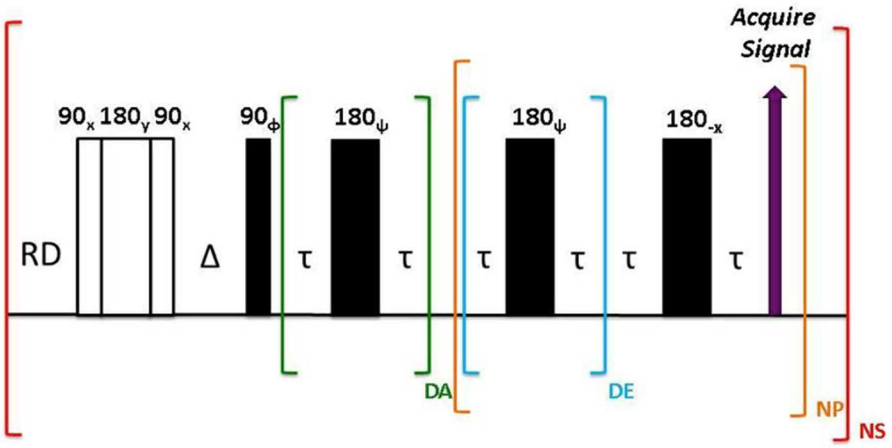

Figure 1: Modified Carr-Purcell-Meiboom-Gill (CPMG) pulse sequence for measuring T_2 values in human serum using benchtop time-domain NMR. The data were recorded at 37°C using a Bruker mq20 minispec NMR instrument equipped with a 10 mm variable temperature probe, model H20-10-25-AVGX. The composite 180˚ pulse ($90_x180_y90_x$) and Δ delay were introduced prior to the CPMG scheme to achieve partial water suppression and eliminate radiation damping. The Δ delay was tuned to $0.95*T_1$, which corresponds to suppression of the water to 23% of its full intensity. The τ delay was kept short (0.19 ms) to minimize the possible impact of translational diffusion on T_2 in an inhomogeneous B_o field. The green loop with DA=42 was added to achieve delayed acquisition of the first data point until after the first 19 ms of intensity decay; this suppresses very fast decay components in order to reduce the number of exponential terms and simplify the analysis of the slower components of the exponential decay curve. Water has the slowest decay rate and the longest T_2. The DE loop generates dummy echos without recording intensity data; with DE=5, the signal intensity of one in every six echoes was recorded during the NP loop. For all experiments, the relaxation delay RD was set to $5* T_1$, corresponding to ~ 8 sec for serum or plasma; NP=5600, NS=256 or 2048. Phase cycles for the pulses: $\varphi = (x)_2, (-x)_2, (y)_2, (-y)_2$; $\psi = x,-x$. Phase cycle of the receiver: same as φ.

Materials

All samples were prepared with phosphate-buffered saline, pH 7.4, with 0.05% sodium azide. Reagents obtained from Sigma Aldrich include human serum albumin (A8763), human γ-globulin (G4386) apolipoprotein A-1 (A0722), KBr (60089), HPLC grade water (270733). All triglycerides and cholesterol esters were purchased from NuChek Prep. Phospholipids were purchased from Avanti Polar Lipids. Chloroform was purchased from Ricca Chemical Company (RSOC0020-1C). Ultracentrifuge tubes were

purchased from Beckman Coulter (344059). 10 (13612), 100 (14412) and 300KDa filters (PBMK02510) were purchased from Millipore.

Results

Human study population

The characteristics of the human subjects analyzed in this study are presented in Table 1. Overall, this is a healthy group of adults spanning a wide age range. The exclusion criteria are diabetes (HbA_{1c} >6.4) or acute/chronic illness (C-reactive protein >10). The mean values for various blood biomarkers fall within the normal reference ranges, although the values for some individuals are outside of those ranges. Time-domain NMR relaxometry directly analyzes the multi-exponential decay curve to extract the relaxation time constants (Figure 2A).

T_2 profile of whole human serum

The T_2 profile for whole human serum contains one intense peak >650ms (Figure 2B), corresponding to the water T_2, and the three smaller peaks shown in Figure 2C. The three less intense peaks arise from the abundant components of human serum such as lipoprotein lipids, proteins and small molecules. Across a population of 28 human subjects, we observed significant variability in the T_2 values of each peak: peak 2 ranges from 573-172 ms, peak 3, from 77-58 ms and peak 4, 18-11ms (Table 1).

Parameter	Mean ± SD	Range, This Study	Reference Values[1]
Age	43 ± 18	24 - 80	n/a
Peak 2 (ms)	411.6 ± 22.1	171.9 – 573.2	n.d.
Peak 3 (ms)	66.3 ± 1.9	57.6 - 76.5	n.d.
Peak 4 (ms)	14.5 ± 0.3	10.9 – 17.5	n.d.
Total serum protein (g/dL)	7.2 ± 0.4	6.2 - 7.9	6.1 - 8.1
Serum albumin (g/dL)	4.5 ± 0.3	4.0 - 5.0	3.6 - 5.1
α_1-antitrypsin (mg/dL)	130 ± 19	102 - 177	90 - 200
Serum viscosity (cP)	1.17 ± 0.10	1.04 - 1.54[2]	1.27 ± 0.06
WBC count (x 10^3/µL)	6.3 ± 1.5	3.9 - 10.2	3.4 - 10.8
Neutrophil count (x 10^3/µL)	3.6 ± 1.4	1.8 - 7.3	1.4 - 7.0
***hs*-CRP (mg/L)**	1.9 ± 1.6	0.1 - 5.1	< 1.0 (low risk) 1.0 – 3.0 (average risk) > 3.0 (high risk)
Glucose (mg/dL)	91 ± 8	78 - 115	<100 non-diabetic 100-125 (pre-diabetic)
HbA_{1c} (%)	5.5 ± 0.3	4.9 - 6.2	<5.7 (non-diabetic) 5.7-6.4 (pre-diabetic)
Insulin C-peptide (ng/mL)	2.4 ± 0.8	1.1 - 4.3	1.1 - 4.4
Triglycerides (mg/dL)	111 ± 57	42 - 245	< 150 mg/dL
HDL-C (mg/dL)	55 ± 12	32 - 85	> 40 mg/dL
Total cholesterol (mg/dL)	196 ± 44	111 - 329[2]	< 200 mg/dL
LDL-C (mg/dL)	119 ± 43	42 - 257[2]	< 130 mg/dL
TSH (µIU/mL)	2.2 ± 1.1	0.6 - 5.3	0.5 - 4.5
Free T4, direct (ng/dL)	1.2 ± 0.2	0.9 - 1.5	1.0 - 1.5

Table 1 Characteristics of the human study group (n=29). This sample size provided sufficient statistical power to identify correlations using conventional p-value thresholds. There were 15 females and 14 males, with an ethnic/racial distribution of 15 white, 6 Asian/Indian, 5 Hispanic and 3 African American/Caribbean. The mean BMI is 25.6 ± 4.2. [1]Reference values are from Quest, Labcorp and Atherotech; viscosity reference values were obtained from the literature; use of a different method may explain why the measured viscosity range is approximately 0.1 cP lower than the reference range. [2]One subject had a serum viscosity of 1.54 cP, a statistical outlier; the next highest was 1.30. This subject had the highest total cholesterol (329 mg/dL) and LDL-C (257 mg/dL), as well as a family history of type II hypercholesterolemia (father).

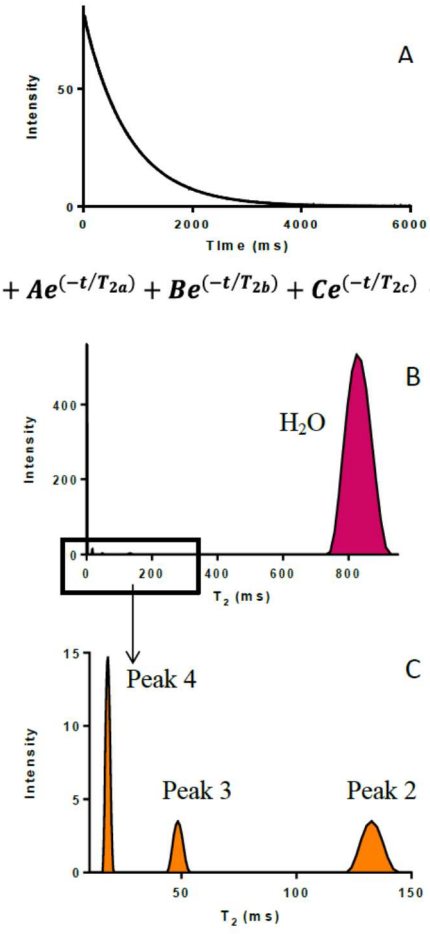

Figure 2: Time-domain NMR relaxometry analysis of whole human serum. (A) Raw T_2 multi-exponential decay curve for whole human serum, (B) T_2 profile of whole human serum derived from an inverse Laplace transform (CONTIN) of the multi-exponentail decay curve. The intense water peak is shown in pink. (C) An expansion of the T_2 profile reveals three small peaks arising from lipid and protein components in serum.

Statistical analysis

The correlation, linear regression and statistical analyses were performed using GraphPad Prism v. 6.05 (GraphPad Software, Inc.). The principles for the statistical analyses were derived from the book by Motulsky [249]. The null hypothesis states that there is no correlation between the variables being compared. The two-tailed p value defines the probability of observing a correlation as strong or stronger if the null hypothesis were true. For example, for r = -0.6 and p

<0.01, there is less than 1% probability of observing a correlation this strong or stronger by random chance; thus, the null hypothesis is rejected. For each correlation that met p-value thresholds, we inspected the plot to ensure that the correlation was not heavily influenced by one or two outliers.

Human serum controls for peak assignment

Assignments for the three non-water T_2 peaks in whole human serum to particular motional domains of biomolecules were made using isolated control samples. Individual samples contained either a mixture of the most abundant proteins in serum, one of the three individual fractionated lipoprotein classes (LDL, HDL and VLDL+IDL, also known as the triglyceride rich lipoproteins), reconstituted lipoproteins and phospholipid vesicles which mimic the lipoprotein phospholipid surface, and finally oil-phase lipid mixtures designed to mimic the lipid mixtures found in the non-polar lipid core of serum lipoprotein particles.

Table 2 shows the results from the control samples. The top line displays the range of T_2 values for each peak in whole human serum observed across the human study population. Some of the control samples contained T_2 peaks that were not observed in human serum and were given a separate column and peak description. As expected, all of the aqueous samples had a water T_2 peak; the exact location differed due to the variations of water binding (determined mainly by protein concentration). All of the lipoprotein related control samples (protein depleted serum, fractionated lipoprotein subclasses, and reconstituted lipoproteins) contained a peak between 2000 and 1200 ms (Peak A). We hypothesize that Peak A monitors the most mobile components on the outermost surface of the lipoproteins, either water tightly bound to the surface or the rapid motions of phospholipid head groups in the lipoprotein surface monolayer.

Peak A is not resolved in samples of whole human serum, presumably because it is masked by the intense water peak. The identity and nature of Peak A will be explored in future studies.

Peak 2 in human serum aligns with many of the lipoprotein controls including protein depleted serum, all three of the lipoprotein classes, phospholipid surface models and the triglyceride-rich lipoprotein core models. Noticeably missing are the cholesterol-rich lipoprotein non-polar core models. Peak 3 in human serum seems to have contributions from all of the controls we examined. Finally, peak 4 in human serum aligns with the protein control and several of the non-polar core lipid mimics. Interestingly, protein depleted serum, fractionated lipoproteins and reconstituted lipoproteins do not display any peaks in this range. Overall, the assignment of T_2 peaks in the profiles of whole human serum was not straightforward -- not surprising given the compositional complexity of this biological sample.

Correlations with metabolic biomarkers

Peak 2

The T_2 values from TD-NMR vary considerably across the study population (Table 1). To identify the factors governing the variation, we measured over 70 established diagnostic biomarkers and correlated them with the T_2 values for each peak. Only the statistically significant ($p<0.05$) correlations are displayed. An example of statistically significant correlation plots for both peaks 2 and 3 are shown in Figure 3.

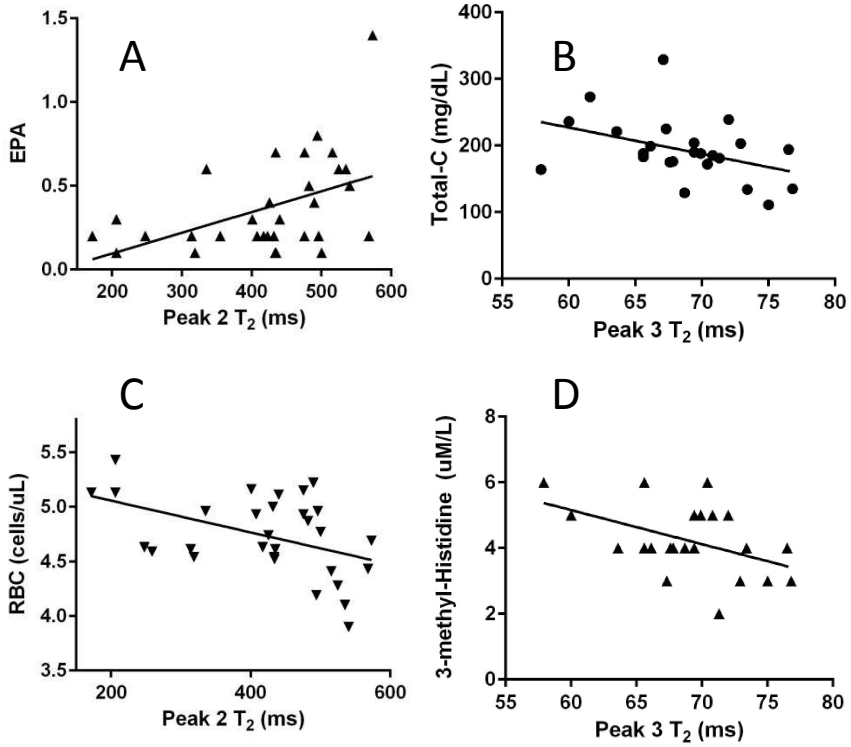

Figure 3. Correlation plots between T_2 and selected clinical diagnostic biomarkers. A and C demonstrate selected correlation plots for peak 2, while panels B and D show selected plots for peak 3. The correlation statistics are presented in the Tables 3 and 4.

	Peak 1 (H_2O)	Peak A	Peak 2	Peak B	Peak 3	Peak C	Peak 4
Whole Human Serum	**915 - 692.1**		**573.1 - 171.9**		**76.5 – 57.6**		**17.5 - 10.9**
Protein Depleted Serum	2414.5 ± 6.3	1289.5 ± 263.7	474.3 ± 43.3		43.2 ± 5.5		
60% HSA 40% γ-Globulin	876.6 ± 3.4		345.9 ± 62.6		94.3 ± 50		13.0 ± 2.3
LDL	3481.3 ± 49.5	1793 ± 369.1	314.1 ± 7.9		55.8 ± 4.8		
HDL	2760.5 ± 16.2	1271.5 ± 66.4	451.7 ± 4.5			36.1 ± 0.3	
VLDL + IDL	4099.5 ± 6.3	2981 ± 231	533.3 ± 45		83.2 ± 3.5		
30% DOPC	1262 ± 0		568.3 ± 1.5		110.8 ± 18		15.8 ± 5
24% DOPC 6 % FC	584.2 ± 16.8		312.0 ± 22.1		57.4 ± 83		21.3 ± 2.7
DOPC FC & ApoA1	3474.3 ± 30.5	1598.1 ± 108	412.2 ± 104			30.2 ± 9.7	
DMPC FC & ApoA1	3490.5 ± 3.5	1563.5 ± 115.2	358.4 ± 26.5			41.0 ± 20.3	
84% CL 5% FC 11%TO				112.7 ± 0.1	27.9 ± 9.2	18.2 ± 0.6	8.0 ± 0.3
75% CL 5% FC 20%TO				134.1 ± 1.5	62.6 ± 0.8	24.7 ± 0.2	8.9 ± 0.2
89% CL 11% TO				137.1 ± 2.1	61.6 ± 1.4	22.8 ± 1.1	8.7 ± 0.14
80% CL 20% TO				144.3 ± 0.83	66.7 ± 1.3	28.9 ± 1.67	10.7 ± 0.2
60% CL 40 % TO			221.5 ± 2.3	101.2 ± 1.4	47.1 ± 0.8		15.8 ± 0.2
40% CL 60% TO			257.7 ± 4.1	117.7 ± 2.7	57 ± 2		20.3 ± 0.3
20% CL 80% TO			271.1 ± 1.2	122.3 ± 2.4	62.1 ± 2.6		24.8 ± 0.4
100% TO			331.7 ± 3.7	152.7 ± 2.9	81.0 ± 2.3		42.1 ± 2.1

Table 2: TD-NMR T_2 results for isolated human serum components and control samples. The top line displays the range of T_2 values observed in whole human serum across a population of healthy subjects. To assign these peaks, controls samples of fractionated lipoproteins, a protein mixture containing the most abundant proteins found in serum, phospholipids, and oil-phase lipid mixtures were analyzed. Some of the control samples contained T_2 peaks that were not observed in human serum and were given a separate column which are assigned to peaks A, B and C. Unlike NMR spectroscopy, the TD-NMR method has a practical upper limit of resolving 4 peaks per profile. Thus, some peaks are not observed in a given type of sample due to coalescence and overlap.

Table 3 shows the correlations between peak 2 and the diagnostic biomarkers. The strongest correlations were observed with alpha-1 antitrypsin, omega-3 index, EPA, insulin resistance score (LipoScience), red blood cell count, hematocrit and mean corpuscular hemoglobin concentration (MCHC). Additional correlations were observed with several amino acids, serum and plasma water T_1 and turbidity (O.D. at 550 nm). To gain additional insight into these correlations, a series of statistical regression residual analyses were performed. This analysis eliminates the influence of one variable, emphasizing the correlation with those that remain. Variables removed were chosen to assess the influence of a given variable or to remove a known influence on relaxation mechanisms (i.e., viscosity and protein concentration).

Removing the influence of protein concentration from peak 2 did not impact the significance or number of correlations, indicating that protein concentration provides minimal influence on the variation of peak 2 in whole human serum (Table S3). On the other hand, removing the influence of viscosity revealed additional correlations with Peak 2, such as glucose, total triglycerides, triglyceride-to-total cholesterol ratio and triglyceride-to non-HDL cholesterol ratio. The reaming correlations remain unchanged for the most part with the exception of RBC and HCT, which lost their significance (Table S2). Interestingly, removing the influence of triglycerides led to the loss of a number of correlations and greatly diminished the remaining R and R^2 values (Table S4). Together, these findings suggest that circulating triglycerides, both concentration and composition, heavily influence the T_2 value of peak 2.

Peak 2 T_2 Correlations	N	Pearson		Spearman
		R	R^2	R
Peak 3 T_2	26	0.63***	0.40****	0.46*
Plasma Water T_1	25	0.57**	0.32**	0.44*
Serum Water T_1	26	0.44*	0.19*	0.32
Alpha-1 Anti Trypsin	24	0.38	0.14	0.44*
0.1 um Filtered Serum OD 550	23	-0.44*	0.20*	-0.19
IR Score (LipoProfile)	15	-0.57*	0.32*	-0.34
Omega-3 Index	26	0.41*	0.17*	0.33
EPA	26	0.46*	0.21*	0.43*
RBC	25	-0.48*	0.23*	-0.42*
HCT	25	-0.38	0.14	-0.44*
MCHC	25	0.25	0.07	0.41*
Homocysteine	25	-0.45*	0.20*	-0.50*
Aspartic Acid	24	-0.49*	0.24*	-0.52**
Sarcosine	24	-0.38	0.14	-0.42*
Beta-Alanine	24	-0.50*	0.25*	-0.45*
Alpha Amino Butyric Acid	24	-0.48*	0.23*	-0.41*
Isoleucine	24	-0.42*	0.18*	-0.35

***p<0.05 **p<0.01 ***p<0.001**

Table 3. Correlation statistics for peak 2 T_2 value with serum and T_1 (blue), proteins and viscosity (yellow), blood cell markers (red), insulin resistance (green), omega-3 lipids (orange) and amino acids (unshaded). Biomarkers were included in the table if they demonstrated at least one correlation coefficient with a p value < 0.05. The null hypothesis is defined as no correlation between serum peak 2 T_2 and a particular biomarker in the overall population. A p value < 0.05 is the threshold for rejecting the null hypothesis.

Peak 2 - T_{2V} Correlations	N	Pearson		Spearman
		R	R^2	R
Peak 3 T_2	25	0.62**	0.38**	0.44*
Plasma Water T_1	25	0.52**	0.27**	0.35
Viscosity (cP)	*25*	*0.00*	*0.00*	*-0.20*
Serum OD 550	22	-0.43*	0.18*	-0.37
0.45 um Filtered Serum OD 550	22	-0.55**	0.30**	-0.36
0.1 um Filtered Serum OD 550	22	-0.56**	0.32**	-0.32
IR Score (LipoProfile)	15	-0.57*	0.33*	-0.28
Glucose	25	-0.47*	0.22*	-0.44*
TG (Quest/Labcorp)	25	-0.49*	0.24*	-0.38
TG/TC (Quest/Labcorp)	25	-0.44*	0.20*	-0.37
TG/non-HDL-C (Quest/Labcorp)	25	-0.41*	0.17*	-0.39
VLDL-C (VAP)	24	-0.43*	0.18*	-0.27
TG (VAP)	24	-0.48*	0.23*	-0.34
TG/TC (VAP)	24	-0.43*	0.18*	-0.31
TG/non-HDL-C (VAP)	24	-0.40*	0.16*	-0.32
Omega-3 Index	25	0.43*	0.18*	0.32
EPA	25	0.49*	0.24*	0.42*
MCHC	24	0.19	0.04	0.48*
Homocysteine	24	-0.41*	0.17*	-0.44*
Aspartic Acid	23	-0.46*	0.21*	-0.46*
Beta- alanine	23	-0.51*	0.26*	-0.45*
α-Amino Butyric Acid	23	-0.46*	0.22*	-0.38
Isoleucine	23	-0.43*	0.18*	-0.33

***p<0.05 **p<0.01 ***p<0.001**

Table S2. Correlation coefficients for peak 2 T_{2V} with biomarkers for water T_1 and T_2, (blue), protein concentration and viscosity (yellow), triglyceride-rich lipoproteins and insulin resistance (green), omega-3 lipids (orange), blood cell counts (red), and amino acids (unshaded). Peak 2 T_{2v} values represent the regression residuals obtained from a linear fit of peak 2 T_2 *vs*. serum viscosity. This analysis removes the influence of serum viscosity on peak 2 T_2 and emphasizes the influence of other variables.

Peak 2 T_{2P} Correlations	N	Pearson		Spearman
		R	R^2	R
Peak 3	26	0.59**	0.35**	0.44*
Plasma T_1 Water	25	0.50*	0.25*	0.41*
Serum Protein	*26*	*0.00*	*0.00*	*0.03*
Alpha-1 anti trypsin	24	0.45*	0.21*	0.47*
0.1 um Filtered Serum OD 550	23	-0.46*	0.21*	-0.26
IR Score	15	-0.57*	0.32*	-0.31
Omega-3 Index	26	0.46*	0.21*	0.30
EPA	26	0.53**	0.29**	0.49*
DHA	26	0.40*	0.16*	0.26
RBC	25	-0.44*	0.19*	-0.36
MCHC	25	0.25	0.06	0.43*
Homocysteine	26	-0.40*	0.16*	-0.49*
Aspartic Acid	24	-0.45*	0.20*	-0.42*
Sarcosine	24	-0.47*	0.22*	-0.51*
Beta-Alanine	24	-0.54**	0.29**	-0.54**
α-Amino Butyric Acid	24	-0.51*	0.26*	-0.44*
Isoleucine	24	-0.45*	0.20*	-0.37

***p<0.05 **p<0.01 ***p<0.001**

Table S3. Correlation coefficients for peak 2 T_{2P} with biomarkers for Water T_1 and T_2, (blue), protein concentration and viscosity (yellow), insulin resistance (green), omega-3 lipids (orange), blood cell counts (red), and other processes (unshaded). Peak 2 T_{2P} values represent the regression residuals obtained from a linear fit of peak 2 T_2 *vs*. serum protein. This analysis removes the influence of serum protein on peak 2 T_2 and emphasizes the influence of serum lipoproteins.

Peak 2 T_{2TG} Correlations	N	Pearson		Spearman
		R	R^2	R
Peak 3	25	0.54***	0.29***	0.54*
Serum Water T_1	25	0.23*	0.05*	0.37
Triglyceride	*25*	*0.00*	*0.00*	*-0.03*
HOMA %B (C-peptide)	25	0.19*	0.04*	0.34
Glucose	25	-0.36	0.13	-0.40*
Omega-3 Index	25	0.23*	0.05*	0.41*
EPA	25	0.23*	0.05*	0.39
DHA	25	0.19*	0.03*	0.41*
AA	25	0.37	0.13	0.53*
MCHC	24	0.26	0.07	0.47*
Beta-alanine	23	0.54**	0.29**	-0.48*
Aspartic Acid	23	-0.35	0.12	-0.44*
Sarcosine	23	-0.30	0.10	-0.45*
α-Amino Butyric Acid	23	-0.38	0.14	-0.44*

***p<0.05 **p<0.01 ***p<0.001**

Table S4. Correlation coefficients for peak 2 T_{2TG} with biomarkers for water T_1 and T_2, (blue), insulin resistance (green), omega-3 lipids (orange), blood cell counts (red), and amino acids (unshaded). Peak 2 T_{2TG} values represent the regression residuals obtained from a linear fit of peak 2 T_2 *vs*. total serum triglycerides. This analysis removes the influence of triglycerides on peak 2 T_2.

Peak 2 $T_{2\text{-}O3}$	N	Pearson		Spearman
		R	R^2	R
Peak 3	26	0.67***	0.45***	0.53**
Serum Water T_2	26	0.48*	0.23*	0.49*
Plasma Water T_2	26	0.41*	0.17*	0.40
Serum Water T_{2V}	26	0.43*	0.18*	0.36
Serum Water T_{2P}	26	0.39*	0.15*	0.38
Serum Water T_{2G}	26	0.43*	0.19*	0.47*
Serum Water T_{2A}	26	0.47*	0.22*	0.44*
Serum Water T_1	26	0.48*	0.23*	0.41*
Plasma Water T_1	25	0.65***	0.42***	0.57**
0.45 um Filtered Serum OD 550	23	-0.35	0.12	-0.42*
0.1 um Filtered Serum OD 550	23	-0.49*	0.24*	-0.41*
IR Score	15	-0.63*	0.39*	-0.48
Omega-3 Index	*26*	*0.00*	*0.00*	*-0.14*
WBC Count	25	-0.41*	0.17*	-0.39
Neutrophils	25	-0.40*	0.16*	0.42*
Basophils	25	-0.41*	0.17*	-0.36
RBC	25	-0.45*	0.20*	-0.38
Homocysteine	26	-0.49	0.24	-0.58**
Hydroxyproline	24	-0.27	0.07	-0.44*
Beta Alanine	24	-0.44*	0.19*	-0.35
Alanine	24	-0.41*	0.17*	-0.26
α-Amino Butyric Acid	24	-0.42*	0.16*	-0.36

***p<0.05 **p<0.01 ***p<0.001**

<u>Table S5</u>. Correlation coefficients for peak 2 $T_{2\text{-}O3}$ with biomarkers for serum and plasma water T_1 and T_2, (blue), insulin resistance (green), omega-3 lipids (orange), blood cell counts (red), and other processes (unshaded). Peak 2 $T_{2\text{-}O3}$ values represent the regression residuals obtained from a linear fit of peak 2 T_2 *vs*. omega-3 index. This analysis removes the influence of omega-3 fatty acid concentration on peak 2 T_2.

Peak 3

Peak 3 T_2 correlates positively with the serum water T_2 and negatively with viscosity, total cholesterol and several amino acids (Table 4).

Peak 3 T_2 Correlations	N	Pearson		Spearman
		R	R^2	R
Peak 2	24	0.40*	0.05*	0.32
Serum Water T_2	24	0.46*	0.21*	0.51*
Serum Water T_{2V}	24	0.46*	0.21*	0.47*
Serum Water T_{2P}	24	0.68***	0.47***	0.71***
Serum Water T_{2G}	24	0.56**	0.31**	0.60**
Serum Water T_{2A}	24	0.42*	0.18*	0.45*
Serum Water T_1	24	0.51*	0.26*	0.56**
Plasma Water T_1	24	0.42*	0.17*	0.35
Plasma Viscosity	9	-0.69*	0.47*	-0.85**
Total-C (VAP)	24	-0.41*	0.16*	-0.37
Hydroxyproline	22	-0.47*	0.22*	-0.41
Alanine	22	-0.39	0.15	-0.50*
1-methyl Histidine	22	-0.46*	0.22*	-0.40
Phenylalanine	22	-0.47*	0.23*	-0.54**
BUN	7	-0.89**	0.79**	-0.87**
Creatinine	7	-0.84*	0.71*	-0.93**

***p<0.05 **p<0.01 ***p<0.001**

Table 4. Correlation coefficients for peak 3 T_2 with serum and plasma water T_1 or T_2 values (blue) proteins and viscosity (yellow), blood cell counts (red), cholesterol markers (purple), and amino acids/other (unshaded). Biomarkers were included in the table if they demonstrated at least one correlation coefficient with a p value < 0.05. The null hypothesis is defined as no correlation between peak 3 T_2 and a particular biomarker in the overall population.

Removing the influence of serum viscosity through a regression residual analysis eliminated the correlation of the peak 3 T_2 value with total cholesterol (Table S6). Previous work has shown that the concentration of lipoproteins has a significant impact on serum viscosity.[250,251] These observations suggest that peak three is heavily influenced by lipoproteins

and their lipid composition. Similarly, removing the influence of cholesterol on peak 3 also removed the correlations with plasma viscosity (Table S7). Interestingly, the amino acids alanine, phenylalanine and hydroxyproline are negatively correlated with the peak 3 T_2 value (Tables 4 and S7). Many of these correlations persist after correcting for viscosity, total cholesterol or total protein (Tables S5-S8). Correlations with BUN and creatinine were observed, but the n is small and this observation warrants further investigation.

Peak 3 T_{2V} Correlations	N	Pearson		Spearman
		R	R^2	R
Peak 4	23	0.56*	0.31*	0.50*
Serum Water T_{2V}	23	0.46*	0.22*	0.41
Serum Water T_{2P}	23	0.68***	0.46***	0.69***
Serum Water T_{2G}	23	0.52*	0.27*	0.53**
Serum Water T_{2A}	23	0.36	0.13	0.42*
Serum Water T_1	23	0.60**	0.36**	0.54**
Plasma Water T_1	23	0.45*	0.21*	0.37
Serum Viscosity	*23*	*0.00*	*0.00*	*-0.27*
Plasma Viscosity	9	-0.64	0.41	-0.80*
Hydroxyproline	21	-0.48*	0.23*	-0.47*
Alanine	21	-0.41	0. 17	-0.57*
1-Methyl Histidine	21	-0.50*	0.25*	-0.45*
Phenylalanine	21	-0.48*	0.23*	-0.56**
BUN	6	-0.90*	-.80*	-0.91***
Creatinine	6	-0.91*	0.84*	-0.94*

***p<0.05 **p<0.01 ***p<0.001**

Table S6. Correlation coefficients for peak 3 T_{2V} with biomarkers for water T_1 and T_2, (blue), protein concentration and viscosity (yellow), blood cell counts (red), and other processes (unshaded). Peak 3 T_{2v} values represent the regression residuals obtained from a linear fit of peak 3 T_2 *vs*. serum viscosity. This analysis removes the influence of serum viscosity on peak 3 T_2.

Peak 3 T_{2C} Correlations	N	Pearson		Spearman
		R	R^2	R
Peak 2	23	0.42*	0.18*	0.36
Peak 4	23	0.41	0.17	0.54**
Serum Water T_{2P}	23	0.57**	0.32**	0.59**
Serum Water T_{2G}	23	0.41	0.17	0.42*
Serum Water T_1	23	0.57**	0.32**	0.46*
Plasma Water T_1	23	0.43*	0.18*	0.31
Total Cholesterol	*23*	*0.00*	*0.00*	*0.0*
Hydroxyproline	21	-0.52*	0.27*	-0.46*
Alanine	21	-0.34	0.12	-0.50*
1-methyl-Histidine	21	-0.46*	0.21*	-0.42
Phenylalanine	21	-0.39	0.15	-0.48*
BUN	6	-0.88*	0.78	-0.97***
Creatinine	6	-0.89*	0.80*	-0.94*

***p<0.05 **p<0.01 ***p<0.001**

Table S7. Correlation coefficients for peak 3 T_{2C} with biomarkers for water T_1 and T_2, (blue) and other processes (unshaded). Peak 3 T_{2C} values represent the regression residuals obtained from a linear fit of peak 3 T_2 *vs*. total cholesterol. This analysis removes the influence of serum cholesterol on peak 3 T_2.

Peak 3 T_P Correlations	N	Pearson		Spearman
		R	R^2	R
Peak 4	23	0.38	0.14	0.49*
Serum Water T_2	23	0.41	0.17	0.46*
Serum Water T_{2V}	23	0.42*	0.17*	0.33
Serum Water T_{2G}	23	0.54**	0.29**	0.61**
Serum Water T_{2P}	23	0.69***	0.47***	0.73***
Serum Water T_{2A}	23	0.37	0.13	0.45*
Serum Water T_1	23	0.59**	0.36**	0.61**
Plasma Water T_1	23	0.44*	0.19*	0.59**
Plasma Viscosity	9	-0.68*	0.47*	-0.85**
Serum Protein	*23*	*0.00*	*0.00*	*0.00*
Hydroxyproline	21	-0.49*	0.24*	-0.44*
Alanine	21	-0.41	0.17	-0.57**
1-methyl-Histidine	21	-0.49*	0.24*	-0.44*
Phenylalanine	21	-0.49*	0.24*	-0.59**
BUN	6	-0.89*	0.79*	-0.97***
Creatinine	6	-0.92*	0.84*	-0.94*

Table S8. Correlation coefficients for peak 3 T_{2P} with biomarkers for water T_1 and T_2, (blue), viscosity and protein (yellow) and other processes (unshaded). Peak 3 T_{2C} values represent the regression residuals obtained from a linear fit of peak 3 T_2 *vs*. serum protein. This analysis removes the influence of serum protein concentration on peak 3 T_2.

Peak 4

Peak 4 did not show any significant correlations with the diagnostic biomarkers analyzed in this study. Based on the analysis of control samples, this peak includes contributions from virtually all of the lipid, lipoprotein and protein components of serum and hence is highly non-specific. This peak also includes contributions from the slower motions of proteins resulting from the delayed acquisition approach used in the CPMG experiment.

Discussion and Conclusions

Benchtop TD-NMR can resolve 3 non-water T_2 domains in whole human serum. The T_2 values for all 3 peaks vary considerably across a population of seemingly healthy individuals. In addition, peaks 2 and 3 each correlate with a different cluster of diagnostic biomarkers. Thus, in a single TD-NMR experiment, we can assess the metabolic state of an individual from several different perspectives. Peak 2 shows the strongest correlations with triglycerides, α1-antitrypsin, omega-3 index, EPA, RBC, HTC and MCHC. Peak 3's strongest correlations are with viscosity, total cholesterol, and several amino acids.

Peak 2 monitors insulin resistance and cardiovascular disease risk.

All of the biomarkers that correlate with peak 2 are associated with the development of insulin resistance and risk for cardiovascular disease. The insulin resistance score generated by LipoScience[98] is based on the number and size of VLDL, LDL and HDL particles in circulation. Early insulin resistance is suggested to occur through abnormal lipid and lipoprotein metabolism, which causes high triglycerides and reduced HDL-cholesterol levels.[252,253] This score is thought to predict insulin resistance before loss of beta-cell function and progression to pre-diabetes.

Complete blood count is a common clinical test used to monitor a wide range of disorders including anemia, leukemia and infections [254]. Red blood cell count, hematocrit and MCHC displayed significant correlations with peak 2, but cannot be directly influencing the T_2 directly since serum is devoid of red blood cells. Rather, these blood cell makers appear to be indirectly linked through insulin resistance and metabolic syndrome.[255] A positive correlation between serum insulin and insulin resistance with RBC and hematocrit has been reported in the literature.[256] Studies have shown that insulin stimulates the proliferation of erythroid

colonies.[257-259] The RBC count is also a strong predictor of cardiovascular events such as stroke and myocardial infarction.[255,260]

Omega-3 index measures the fatty acid composition of red blood cells to determine the concentration of omega-3 fatty acids, particularly DHA and EPA. Increased consumption of omega-3 fatty acids have been linked to a number of health benefits including improved cardiovascular disease risk, improvements in fetal development, cognitive well-being, inflammation and immune response.[178,180,181,183,184] Recently, it has been suggested that an elevated Omega-3 index is associated with higher insulin sensitivity and lower fasting glucose[213-215] through the lowering of circulating free fatty acids and C-reactive protein, an inflammatory marker.

The abundant serum protein α1-antitrypsin is a serine protease inhibitor, which plays an important protective role against the enzymes of inflammatory cells, such as neutrophil elastase. Increased concentrations of α1-antitrypsin in whole serum have also been positively correlated with pancreatic beta cell survival, inversely correlated with obesity, waist-to-hip ratio[261,262] and serum levels of adiponectin, leptin and insulin. While the mechanism is still unclear, it is hypothesized α1-antitrypsin may effect adipocyte proliferation and differentiation.

Direct mechanism driving variations in peak 2

Liposcience IR score and the various blood count markers are negatively correlated with peak 2 T_2, while omega-3, EPA and α1-antitrypsin are positively correlated. Overall, we observe that the higher the peak 2 T_2 value the more likely that subject will be insulin sensitive with an improved cardiovascular disease risk outlook and inflammatory status. By combining the statistical analysis, control samples and clinical biomarker patterns, we can elucidate the direct influences on the observed T_2 values of peak 2.

Removing the influence of serum protein concentration does not significantly impact the strength or number of correlations with peak 2, so that factor can be ruled out. By contrast, removing the influence of triglyceride concentration drastically changes the correlations, indicating their contribution peak 2 T_2. Inspection of the controls reveals that the fractionated lipoproteins have T_2 values that fall within the range of peak 2. A trend is observed between the second T_2 of VLDL+IDL, LDL and HDL vs. lipoprotein composition; the triglyceride-rich lipoproteins have a higher peak 2 T_2 values versus the cholesterol-rich lipoproteins. In addition, the lipoprotein lipid core models that mimic the triglyceride-rich particles have T_2 values with the range of peak 2, but the cholesterol-rich mimics do not.

We propose that the T_2 value of peak 2 likely reflects the average molecular motions of lipids in the core of lipoprotein particles. Previously, we demonstrated that higher numbers of cis-double bonds in a hydrocarbon chain increase T_2 by disrupting molecular packing and increasing fluidity (Chapters 2 and 3)[201]. Thus, the positive correlation between T_2 and omega-3 index/EPA is consistent with the notion that the T_2 is monitoring lipid fluidity in triglyceride-rich lipoproteins. The inverse relationship with the remaining markers can be attributed to the abnormal changes that occur in lipoproteins as patients become increasingly insulin resistant. Abnormal lipoprotein lipid composition is commonly associated with diabetes. Free fatty acids accumulate in circulation resulting in increased production of VLDL-1 particles, which are larger and more triglyceride rich than their normal counterparts[263-267]. As a result lipoproteins begin to accumulate and possess an increased residence time in the blood. The combined action of various modification proteins, in particular cholesterol-ester transfer protein (CETP), leads to heavily processed lipoproteins that are more cholesterol-rich. Therefore, the decrease in T_2 is monitoring an increase in cholesterol content across the whole population of lipoprotein

particles. As a subset of lipoproteins become increasingly cholesterol rich, the average molecular motions of the most mobile lipid domain within the lipoprotein core monitored by peak 2 will decrease due to disruptions in metabolism related to insulin resistance.

Peak 3 monitors insulin resistance risk

Higher T_2 values for peak 3 are associated with lower total cholesterol and viscosity. Interestingly, when the influence of viscosity on peak 3 was removed, the correlation with total cholesterol was eliminated, indicating that the two variables are related. Serum and plasma viscosity has long been associated with metabolic abnormalities such as diabetes mellitus and dyslipidemia.[250,251] The association between metabolic dysfunction and viscosity is attributed to the accumulation of serum proteins, glucose and lipids in circulation. Alterations in the blood protein composition have also been hypothesized to increase the viscosity of serum and plasma.

We propose that the TD-NMR T_2 of peak 3 is significantly influenced by a less-mobile lipid domain within the core of lipoprotein particles. The value likely reflects the average molecular motions of lipids in the core from a range of particles, including LDL, HDL and cholesterol-rich remnants. The remodeling of lipoprotein particles that occurs with insulin resistance and metabolic syndrome results in larger numbers of small LDL and remnant particles. The observed decrease in the T_2 value for peak 3 is consistent with a decrease in core fluidity resulting from this remodeling.

Another indicator that peak 3 is probing the molecular motions of cholesterol-rich lipoproteins is the correlation of peak 3 with various serum water T_2's; T_2, T_{2V}, T_{2P}, T_{2G} and T_{2A} (corrected for viscosity, total protein, globulin concentration and albumin concentration respectively). The only biomarker all of these have in common is cholesterol.

With respect to amino acids, the pattern observed is consistent with the mobilization of amino acids from muscle (1-methyl-histidine) and connective tissue (hydroxyproline). This catabolic process is also consistent with insulin resistance.

Together we have concluded that the NMR T_2 values for peak 2 and 3 are reflective of the lipoprotein lipid core fluidity. In this study we observed lower T_2 values in serum are indicative of increasing degrees of metabolic dysfunction in apparently healthy subjects. We concluded this was due to an increasingly less fluid, cholesterol rich lipoprotein lipid core brought on by the beginning stages of insulin resistance. Hypothetically, it should be possible to detect lipoprotein particle that are *more* fluid than normal, due to frank hypertriglyceridemia and an increased triglyceride component within the non-polar lipid core. This will be explored in future studies.

Benchtop TD-NMR T_2 as a front-line screening tool for insulin resistance and metabolic syndrome

A primary reason for developing biomarkers is to identify metabolic abnormalities in at-risk individuals early on, well before these abnormalities progress to pre-diabetes, diabetes or cardiovascular disease. A biomarker can be defined as "cellular, biochemical or molecular alterations that are measurable in biological media such as human tissues, cells or fluids" and include "tools and technologies that can aid in the understanding and prediction, cause, diagnosis, progression, regression or outcome of treatment of disease".[268] Biomarkers can be classified into two main categories: biomarkers of exposure, which are used to predict risk, and biomarkers of disease, which screen and monitor disease progression.[235] We envision benchtop TD-NMR as a screening tool, but not for disease. Rather, it could serve to screen seemingly healthy individuals for hidden metabolic abnormalities that put them at risk for developing disease. Specifically, it would identify the presence or absence of insulin resistance, a precursor

of disease. Robust clinical tests and diagnostic criteria already exist to diagnose full-blown diabetes as well as pre-diabetes. We envision that TD-NMR would have the greatest value in screening individuals who do not meet the diagnostic criteria for diabetes or pre-diabetes. Some of those individuals may meet the criteria for metabolic syndrome, and the TD-NMR test could be used to screen for insulin resistance. Early identification and elimination of insulin resistance is a key strategy for diabetes and CVD prevention.

According to the National Cancer Institute's Early Detection Network, there are five phases of biomarker development. Phase I is the preclinical exploratory studies, Phase II demonstrates reproducibility, sensitivity and specificity Phase III evaluates sensitivity and specificity for diseases that have not been detected by conventional clinical diagnostics, Phase IV evaluates the sensitivity and specificity on a prospective cohort of patients and finally Phase V evaluates the overall benefits and risks associated with the new biomarker [234]. Currently we have successfully completed Phase I of development. This method holds great promise as it already meets many of the requirements for an ideal biomarker: a safe simple method with relatively low cost. In addition, the measurement is capable of monitoring multiple processes in one simple measurement, enhancing its utility.

Chapter 5: Water as a Universal Biosensor for Inflammation, Insulin Resistance, Oxidative Stress and Dyslipidemia

Introduction

An era can be envisioned, not far in the future, where each individual will be accompanied by a personal data cloud for ongoing health assessment. That data may include the individual's entire genomic sequence as well as proteomic and metabolomic profiles, some monitored in real time. Although the acquisition of big data clouds is becoming feasible, complexity and cost remain significant barriers to widespread use for health screening. Therefore, streamlined approaches are needed. Our laboratory has been evaluating a relatively simple and practical implementation of nuclear magnetic resonance, benchtop time-domain relaxometry (TD-NMR), for analyzing blood samples and assessing health status. The initial focus was on lipid and lipoprotein T_2 values, which non-invasively monitor changes in the fluidity and composition of lipid domains[201].

Time-domain NMR relaxometry, in contrast with conventional frequency-domain NMR spectroscopy, incorporates the direct analysis of the exponentially decaying signal to extract relaxation time constants (Fig. 1A). As acquired with this experimental protocol, the T_2 profiles for human serum are comprised of three tiny lipid/protein peaks with T_2 values <200 ms (Fig. 1B, orange) and an intense water peak with a T_2 value >600 ms (Fig. 1B, blue). In this context, the intense water signal was considered a nuisance, as it can lead to radiation damping and obscure the detection and analysis of the much smaller lipid/protein peaks. Recently we initiated a pilot study to assess the variability of serum and plasma T_2 values in a human subject population. After a few months, it became apparent that the water T_2 value (not just the

lipid/protein T_2) was tracking with a variety of metabolic biomarkers. So we halted the protocol and redesigned it to include fast, six-minute analyses of the water. Collected this way, the water T_2 values for serum and plasma exhibit high precision, with standard errors less than 0.5%.

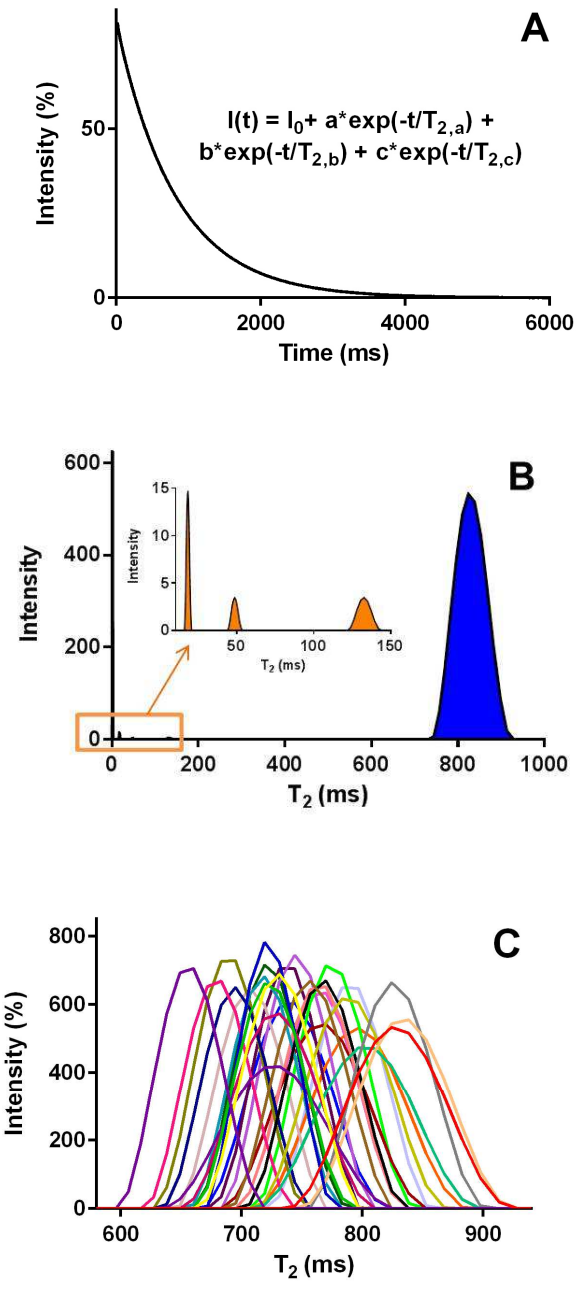

<u>Figure 1</u>. Time-domain NMR relaxometry analysis of water in unmodified blood plasma and serum. (A) Raw TD-NMR data for human serum consisting of a multi-exponential decay curve; (B) T_2 profile for human serum derived from an inverse Laplace transform of the multi-exponential decay curve in (A). This profile is not to be confused with a conventional NMR spectrum where the x-axis is frequency. The T_2 profile reveals an intense water peak (blue) and a few small peaks arising from directly-detected lipid and protein components of serum (orange). (C) Expansions of the water T_2 profiles for individual human subjects illustrating the wide range of T_2 values observed across this study population. Data acquisition and processing details are provided in Fig. S1 and Materials and Methods.

Experimental Procedures

Subject recruitment.

Human subject volunteers were recruited with informed consent into two protocols approved by the Institutional Review Board of the University of North Texas Health Science Center in Fort Worth (UNTHSC). One protocol recruited apparently healthy adult subjects from the student and staff population of UNTHSC, including some spouses and significant others. The second protocol recruited community members enrolled in the Health and Aging Brain Study at UNTHSC[269]. Exclusion criteria for the current study included diabetes ($HbA_{1C} > 6.4$), acute/chronic infection or illness (C-reactive protein > 10), or not fasting for at least 12 hours. Characteristics of the human study group are detailed in Table S1.

Plasma and serum preparation.

Fasting blood samples were drawn in the morning by a trained nurse or phlebotomist. For plasma preparation, blood was drawn into lavender-top tubes containing EDTA as the anticoagulant. For serum, blood was drawn into plain glass red-top tubes lacking any gel separator or clot activators (BD model 366441) in order to avoid potential interference of additives with TD-NMR or viscosity testing. Blood obtained for NMR LipoProfile analysis (LabCorp/LipoScience) was drawn into black-top tubes specialized for that purpose. Every effort was made to collect enough blood from each subject to perform all 70+ planned measurements. However, there were situations where the amount of blood collected from a given subject was not sufficient or samples were rejected by the testing lab. That variability accounts for the test-to-test differences in sample size (n) in the statistical analyses.

Table S1: Human Study Group

Parameter	Mean ± SD	Range, This Study	Reference Values[1]
Age	43 ± 18	24 - 80	n/a
Plasma T_2 (ms)	748.8 ± 57.1	642.8 - 865.9	n.d.
Serum T_2 (ms)	810.5 ± 52.1	692.1 - 915.0	n.d.
Total serum protein (g/dL)	7.2 ± 0.4	6.2 - 7.9	6.1 - 8.1
Serum albumin (g/dL)	4.5 ± 0.3	4.0 - 5.0	3.6 - 5.1
α_1-antitrypsin (mg/dL)	130 ± 19	102 - 177	90 - 200
Serum viscosity (cP)	1.17 ± 0.10	1.04 - 1.54[2]	1.27 ± 0.06
Plasma viscosity (cP)	1.27 ± 0.17	1.07 - 1.46	1.39 ± 0.08
WBC count (x $10^3/\mu L$)	6.3 ± 1.5	3.9 - 10.2	3.4 - 10.8
Neutrophil count (x $10^3/\mu L$)	3.6 ± 1.4	1.8 - 7.3	1.4 - 7.0
hs-CRP (mg/L)	1.9 ± 1.6	0.1 - 5.1	< 1.0 (low risk) 1.0 – 3.0 (average risk) > 3.0 (high risk)
Glucose (mg/dL)	91 ± 8	78 - 115	<100 non-diabetic 100-125 (pre-diabetic)
HbA_{1c} (%)	5.5 ± 0.3	4.9 - 6.2	<5.7 (non-diabetic) 5.7-6.4 (pre-diabetic)
Insulin C-peptide (ng/mL)	2.4 ± 0.8	1.1 - 4.3	1.1 - 4.4
Triglycerides (mg/dL)	111 ± 57	42 - 245	< 150 mg/dL
Total cholesterol (mg/dL)	196 ± 44	111 - 329[2]	< 200 mg/dL
HDL-C (mg/dL)	55 ± 12	32 - 85	> 40 mg/dL
LDL-C (mg/dL)	119 ± 43	42 - 257[2]	< 130 mg/dL
TSH (µIU/mL)	2.2 ± 1.1	0.6 - 5.3	0.5 - 4.5
Free T4, direct (ng/dL)	1.2 ± 0.2	0.9 - 1.5	1.0 - 1.5

Table S1: Characteristics of the human study group (n=29). This sample size provided sufficient statistical power to identify correlations using conventional p-value thresholds. There were 15 females and 14 males, with an ethnic/racial distribution of 15 white, 6 Asian/Indian, 5 Hispanic and 3 African American/Caribbean. The mean BMI is 25.6 ± 4.2. [1]Reference values are from Quest, Labcorp and Atherotech; viscosity reference values were obtained from [270]; use of a different method may explain why the measured viscosity range is approximately 0.1 cP lower than the reference range. [2]One subject had a serum viscosity of 1.54 cP, a statistical outlier; the next highest was 1.30. This subject had the highest total cholesterol (329 mg/dL) and LDL-C (257 mg/dL), as well as a family history of type II hypercholesterolemia (father).

Blood sample analysis and banking.

The plasma and serum samples were processed immediately after each blood draw. The samples were centrifuged to remove pelleted blood cells, followed by a second low speed spin of the supernatant to remove residual blood cells. The TD-NMR water T_2 measurements were performed five times on a sample of fresh plasma followed immediately by five repeats on fresh serum such that all water T_2 measurements were completed within ~2 hours after the blood draw. Likewise, viscosity was measured in house on fresh serum and plasma samples within a few hours of the blood draw using a VISCOLab3000 instrument as described elsewhere [201]. Aliquots of fresh serum were sent on ice to Atherotech, Inc. for Vertical Autoprofile (VAP) advanced lipoprotein testing, as well as to determine LDL-P, hs-CRP, GGT, homocysteine, and Lp(a). Aliquots of plasma and serum were frozen at -80°C prior to in-house analysis using assay kits: apolipoprotein E concentration (Abcam, Ab108813); ORAC antioxidant capacity (Cell Biolabs, STA-345), protein carbonyl content (Cell Biolabs STA-307), and HNE (Cell Biolabs, STA-838); and free fatty acids (BioAssay Systems, EFFA-100). All other testing of serum and plasma samples was performed by LabCorp, Quest Diagnostics and their affiliates including LipoScience (NMR LipoProfile) and OmegaQuant (Omega-3 Index). Plasma aliquots for amino acid analysis were frozen immediately after preparation and stored at -80°C prior to shipment to Quest.

Samples for controlled experiments.

All samples were prepared with phosphate-buffered saline, pH 7.4. Reagents obtained from Sigma-Aldrich included human serum albumin (Catalog No. A8763), human γ-globulin (G4386), uric acid (U2625), DL-lactic acid (69785), malondialdehyde tetrabutylammonium salt (63287) and glyceraldehyde (G5001). Reagents obtained from Fisher Scientific included

adenosine-tri-phosphate (S25123), D-glucose (D15-500), urea (BP169-500) and cupric sulfate (S25285).

Benchtop Time-domain NMR Relaxometry.

Measurements of T_2 and T_1 were performed at 37°C using a Bruker mq20 Minispec benchtop time-domain NMR instrument equipped with a 10 mm variable temperature probe (Model H20-10-25-AVGX). The 10 mm NMR tube was filled to a sample height of 1 cm, corresponding to a sample volume of ~680 µL. Given the abundance of signal, it should be feasible to use a smaller probe diameter and sample volume, although a small-diameter probe was not available to us for this study.

The pulse sequence for T_2 measurement is illustrated in Figure 1S. In our experience, a critical factor in obtaining high quality TD-NMR data with aqueous samples is carefully tuning the delta delay to avoid radiation damping. This artifact occurs when the additional magnetic field created by the intense oscillating water signal distorts the performance of CPMG pulse scheme [30]. Radiation damping manifests itself by a non-random oscillatory artifact observed in the residuals of the fit after inverse Laplace transform. We determined empirically that a delta delay of $0.95*T_1$ (leading to a water signal that is ~23% of its full intensity) provides a level of suppression of the water sufficient to avoid radiation damping, while still maximizing the overall signal intensity of the water and the other lipid/protein peaks for analysis. Even after partial suppression, the intensity of the water signal was still sufficiently intense to measure water T_2 with high precision after only 16 scans. In this regard, the goal of water suppression in TD-NMR is different from that of frequency-domain NMR spectroscopy, as essentially complete suppression of the water is typically desired in the latter.

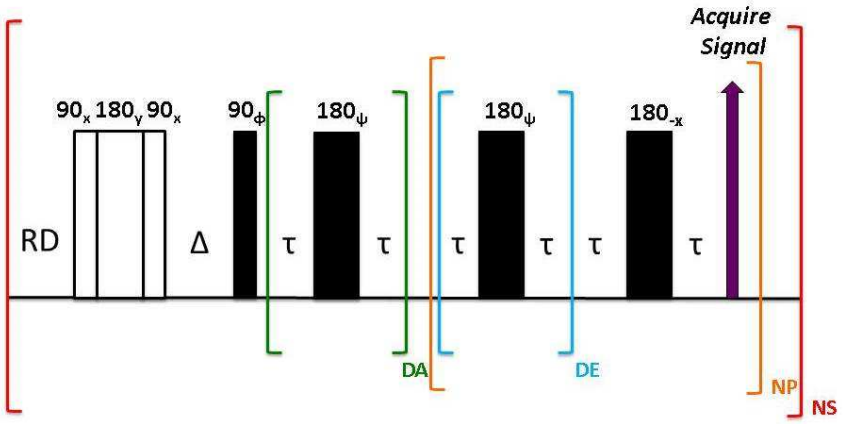

Figure S1: Modified Carr-Purcell-Meiboom-Gill (CPMG) pulse sequence for measuring water T_2 in human serum or plasma using benchtop time-domain NMR. The data were recorded at 37°C using a Bruker mq20 minispec NMR instrument equipped with a 10 mm variable temperature probe, model H20-10-25-AVGX. The composite 180˚ pulse ($90_x180_y90_x$) and Δ delay were introduced prior to the CPMG scheme to achieve partial water suppression and eliminate radiation damping. The Δ delay was tuned to $0.95*T_1$, which corresponds to suppression of the water to 23% of its full intensity. The τ delay was kept short (0.19 ms) to minimize the possible impact of translational diffusion on T_2 in an inhomogeneous B_o field. The green loop with DA=42 was added to achieve delayed acquisition of the first data point until after the first 19 ms of intensity decay; this suppresses very fast decay components in order to reduce the number of exponential terms and simplify the analysis of the slower components of the exponential decay curve. Water has the slowest decay rate and the longest T_2. The DE loop generates dummy echos without recording intensity. For all experiments, the relaxation delay RD was set to $5* T_1$, corresponding to ~ 8 sec for serum or plasma; NP=5600, NS=16. Phase cycles for the pulses: $\varphi = (x)_2, (-x)_2, (y)_2, (-y)_2$; $\psi = x,-x$. Phase cycle of the receiver: same as φ. Total experiment time, 6.4 min.

Another unique aspect to this TD-NMR pulse scheme was the delayed acquisition of the data points, which began 19 ms after the beginning of the CPMG scheme. This strategy de-emphasizes the very fast processes at the beginning of the decay curve in order to emphasize the slower processes such as the water. This delayed acquisition scheme reduces the number of exponential terms, simplifying the inverse Laplace transform calculation. If attempts are made to fit the data using too many exponential terms, the calculation can become unstable, as it

becomes a mathematically ill-posed problem. Such overfitting is evidenced by poor run-to-run precision, which was not observed using the current protocol.

For quantification of serum and plasma water T_2 values, each raw CPMG decay curve was analyzed using an inverse Laplace transform as implemented in the discrete components analysis of XPFit (http://www.softscientific.com/science/xpfit.html). An important consideration for sample-to-sample comparisons is to restrain the number of exponential terms to a consistent number; the data obtained with 16 scans were fit to three terms. Less than three is not adequate to fit the data, as evidenced by poor residuals. Given the high signal-to-noise ratio of the water, it is not difficult to obtain stable fitting solutions for serum or plasma water T_2 data recorded with 16 scans. For illustrative purposes, the T_2 profile distributions shown in Figure 1 were generated using CONTIN (s-provencher.com), even though the T_2 values were quantified using XPFit as described above. The water T_2 values from CONTIN and XPFit are essentially identical. XPFit has the advantage of being able to contrain the number of exponentials and employs a non-negative truncated single value decomposition algorithm, which stabilizes the calculation.

Statistical Analysis.

The correlation, linear regression and statistical analyses were performed using GraphPad Prism v. 6.05 (GraphPad Software, Inc.). The guiding principles for the statistical analyses were derived from the book by Motulsky[249] . The null hypothesis states that there is no correlation between the variables being compared. The two-tailed p value defines the probability of observing a correlation as strong or stronger if the null hypothesis were true. For example, for $r = -0.6$ and $p < 0.01$, there is less than 1% probability of observing a correlation this strong or stronger by random chance; thus, the null hypothesis is rejected. For each correlation that met p-

value thresholds, we inspected the plot to ensure that the correlation was not heavily influenced by one or two outliers. Sample plots are provided in Figs. 2 and 3. Regression residuals were analyzed in GraphPad Prism using the simple strategy outlined in the web link within ref. [271,272].

Results and Discussion

The characteristics of the human subjects analyzed in this study are presented in Table S1. Overall, this is a healthy group of adults spanning a wide age range. The exclusion criteria are diabetes (HbA_{1c} >6.4) or acute/chronic illness (C-reactive protein >10). The mean values for various blood biomarkers fall within the normal reference ranges, although the values for some individuals are outside of those ranges. For example, the mean HbA_{1c} value is 5.5 ± 0.3, and 19 of the 29 subjects are not diabetic or pre-diabetic by that criterion. Of the remaining 10, seven have HbA_{1C} values of 5.7 or 5.8, near the borderline between non-diabetes and pre-diabetes. By fasting glucose criteria, only 3 of the 29 show evidence of pre-diabetes. Similarly, some individual subjects have lipid levels outside the reference ranges, even though the mean values are not. However, for white blood cell counts, insulin C-peptide, total protein and albumin concentrations, all 29 subjects are within normal reference ranges.

Table S2: Biomarkers Measured in this Study

TD-NMR Markers: plasma water T_2, T_{2p}, T_{2a}, T_{2g}, T_{2c}, T_{2v} serum water T_2, T_{2p}, T_{2a}, T_{2g}, T_{2c}, T_{2v}

Category	Correlated with T_2[†]	Did not correlate with T_2[†]
Protein, viscosity, liver function markers	total serum protein, serum albumin, serum globulins (calc), serum viscosity, plasma viscosity	α1-antitrypsin, AST, ALT, GGT
Inflammation, blood cell and oxidative stress markers	hs-CRP, WBC, neutrophils, monocytes, eosinophils, basophils, platelets, RDW, anion gap corrected for albumin concentration, TNFα, sICAM[*], I-309[*], factor VII[*]	RBC, hematocrit, hemoglobin, MCV, MCH, MCHC, lymphocytes, HNE, ORAC antioxidant capacity
Cholesterol/lipid markers	Total cholesterol, HDL-C, non-HDL-C, LDL-C, LDL-P, LDL size, small LDL-P, HDL-P, VLDL-C, remnant-C, apoB, DHA, omega-3 index	Lp(a), EPA, AA, apoAI, phospholipids, apoE
Insulin resistance & diabetes markers	insulin, insulin C-peptide, HbA_{1c}, HOMA2-IR, -%B, -%S, triglycerides, IR Score (LipoScience)	glucose, free fatty acids, body-mass index
Electrolyte markers	chloride, bicarbonate, anion gap	sodium, potassium, calcium
Kidney function markers	blood urea nitrogen (BUN)[*], estimated glomerular filtration rate (eGFR)[*]	creatinine
Thyroid function markers	thyroid stimulating hormone (TSH)	free T4

Table S2. Biomarkers measured in this study. [†]In this table, a correlation is defined as one where $p<0.05$ for the Pearson correlation, non-parametric Spearman correlation or both for at least one variant of serum or plasma water T_2. The null hypothesis states that there is no correlation between a plasma or serum water T_2 measure and a particular biomarker. The individual correlation coefficients and statistics are provided in Tables 1, 2 and S3-S12. [*]These particular biomarkers were measured for only five-to-eight subjects; although they met the p-value threshold, the correlations are considered preliminary. The most compelling of these preliminary correlations was plasma T_{2a} with TNFα: $r = -0.93$, $R^2 = 0.87$, $r_S = -0.97$, with p values <0.05, <0.05 and <0.001, respectively.

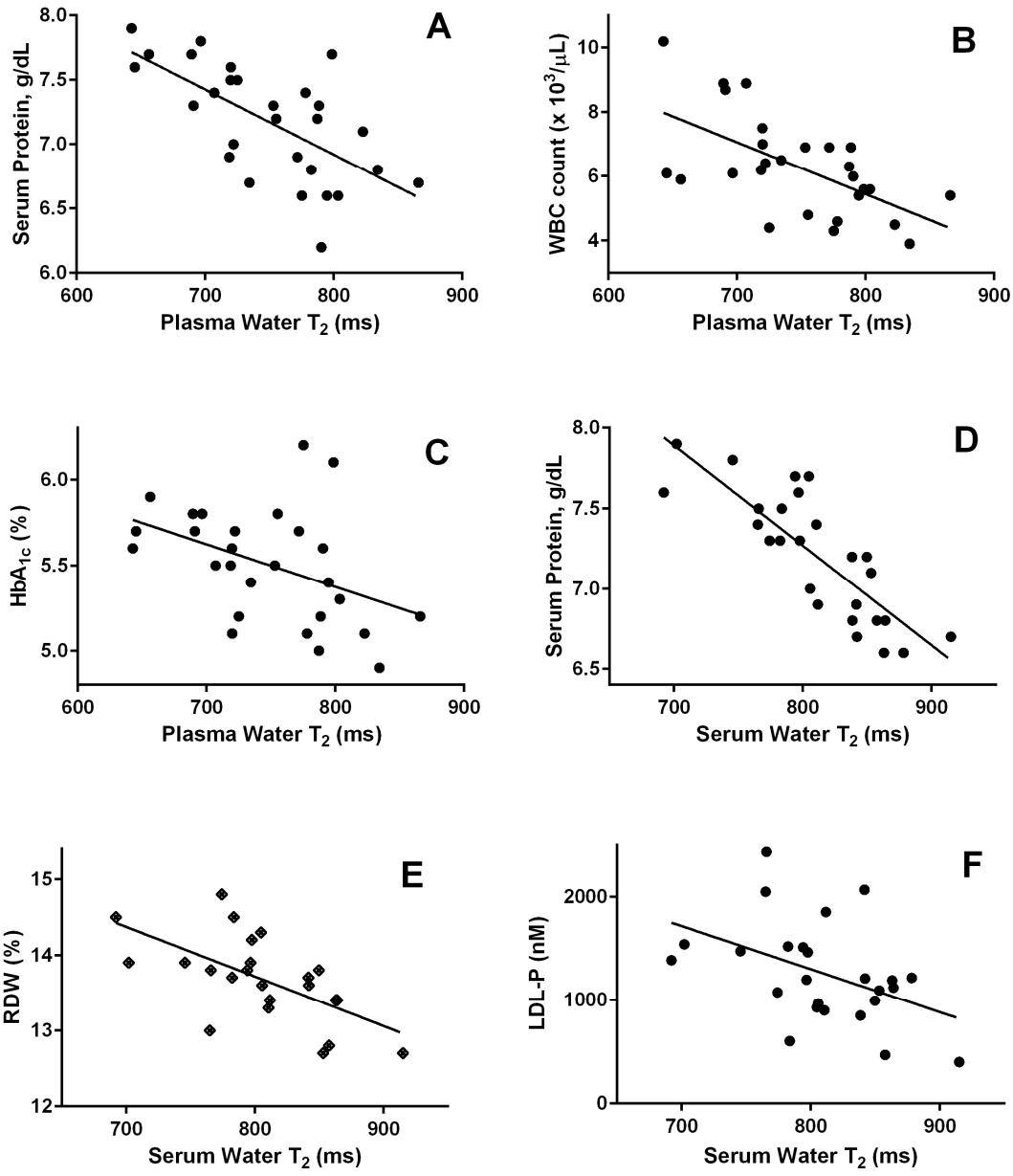

<u>Figure 2</u>. Linear regression plots for plasma or serum water T_2 vs. various blood biomarkers for the human subjects enrolled in this study. (A) Plasma water T_2 *vs.* total serum protein; (B) Plasma water T_2 *vs.* white blood cell count; (C) Plasma water T_2 *vs.* HbA_{1c} ; (D) Serum water T_2 *vs.* total serum protein; (E) Serum water T_2 *vs.* red cell distribution width; (F) Serum water T_2 *vs.* LDL particle number. The correlation statistics are provided in Tables 1 and 2.

Table 1: Whole plasma T_2 values correlated with biomarkers

Biomarker	N	r (Pearson)	R^2	r_S (Spearman)
Total Protein, Serum	28	-0.65***	0.42***	-0.65***
Globulins, Serum	28	-0.52**	0.27**	-0.54**
Viscosity, Serum	24	-0.49*	0.24*	-0.65***
Viscosity, Plasma	9	-0.82**	0.67**	-0.90***
WBC Count	27	-0.60***	0.36***	-0.60***
Neutrophil Count	27	-0.54**	0.29**	-0.47*
Platelet Count	27	-0.38	0.14	-0.39*
C-reactive Protein	27	-0.57**	0.33**	-0.54**
HbA_{1c}	27	-0.43*	0.19*	-0.44*
Insulin C-peptide	28	-0.42*	0.18*	-0.41*
HOMA2-IR	28	-0.39*	0.16*	-0.39*
HOMA2-%B	28	-0.40*	0.16*	-0.36
HOMA2-%S	28	+0.44*	0.20*	+0.40*
Triglycerides	28	-0.30	0.09	-0.43*
Asparagine	26	+0.41*	0.17*	+0.23

*p<0.05 **p<0.01 ***p<0.001

Table 1. Correlation coefficients for plasma water T_2 with biomarkers for protein concentration and viscosity (yellow), inflammation (red), insulin resistance (green) and other processes (unshaded). Biomarkers were included in the table if they demonstrated at least one correlation coefficient with a p value < 0.05. The null hypothesis is defined as no correlation between plasma water T_2 and a particular biomarker in the overall population.

The plasma and serum water T_2 values from TD-NMR vary considerably across the study population (Fig. 1C and Table S1). To identify the factors governing the variation, we measured over 70 blood biomarkers and correlated them with plasma and serum water T_2 values (Table S2). The correlation coefficients are listed in Tables 1 and 2, and selected linear regression plots are shown in Figure 2. Strong inverse correlations are observed between plasma water T_2 total serum protein concentration and viscosity (Table 1, yellow). Of the main protein fractions, the concentration of serum globulins, but not serum albumin, correlates with plasma water T_2. Among the strongest correlations with plasma water T_2 are several inflammatory markers: white blood cell, neutrophil and platelet counts, and C-reactive protein (Table 1, red). In addition, plasma water T_2 correlates with markers of insulin resistance: HbA_{1c}, insulin C-peptide, HOMA2-IR, -%B, -%S and triglycerides (Table 1, green). Plasma water T_2 measurements did not correlate with body-mass index or age.

Serum water T_2 values reveal a somewhat different set of correlations as compared with plasma. Serum water T_2 does not correlate with markers of insulin resistance. Rather, it correlates with a number of LDL-related cholesterol markers (Table 2, blue). However, serum water T_2 does show significant correlations with total serum protein, globulin and albumin concentrations as well as serum viscosity (Table 2, yellow). Like plasma, serum water T_2 correlates with white blood cell and neutrophil counts, as well as C-reactive protein (Table 2, red). The correlations from this observational study led us to consider the factors that may contribute directly to the variation in plasma and serum water T_2, as well as those that may be indirectly linked through another variable or a network of variables. Human blood plasma and serum are complex mixtures containing hundreds of different proteins and lipoproteins as well as numerous small molecule metabolites. At first thought, de-convoluting these myriad variables

would seem to be hopelessly complex. However, the ten most abundant proteins in plasma (albumin, IgG, transferrin, fibrinogen, IgA, α2-macroglobulin, IgM, α_1-antitrypsin, C3 complement and haptoglobin) account for over 90% of total protein mass and the top two, nearly 80% [273]. So identifying the primary contributors to water T_2 may be feasible.

We used two approaches to tease apart the factors giving rise to variations in plasma and serum water T_2. The first approach was reductionist, utilizing controlled experiments on simplified model systems that mimic one or more components of human serum or plasma. The second was statistical and involved eliminating the influence of one variable and analyzing the correlations with those that remain.

Figure 3A displays the variation of water T_2 with protein concentration in a sample containing only human serum albumin in buffer (▲). As protein concentration increases, the water T_2 decreases, and the viscosity of the sample increases. Similar results are observed for lipoprotein-deficient serum (■) and whole serum (●). The influence of viscosity on water T_2 can be eliminated by analyzing the regression residuals [271], yielding the parameter T_{2v}. The water T_{2v} values for albumin solutions, like uncorrected T_2, are inversely correlated with protein concentration. Likewise, water T_{2v} values for serum samples from the human study group are inversely correlated with total serum protein concentration (Table S3). Therefore, the water T_2 value must be influenced not only by viscosity, but other factors such as the binding of water to protein molecules [275,276]. The ^{1}H T_2 values for water and other small molecules in solution are inversely proportional to the correlation time for rotational diffusion, *i.e.*, the time it takes for reorientation of the ^{1}H magnetic dipoles of water molecules in the static magnetic field of the NMR instrument[32].

Table 2: Whole serum T_2 values correlated with biomarkers

Biomarker	N	r (Pearson)	R^2	rs (Spearman)
Total Protein, Serum	26	-0.82****	0.67****	-0.86****
Albumin, Serum	26	-0.39*	0.15*	-0.39*
Globulins, Serum	26	-0.49*	0.24*	-0.57**
Viscosity, Serum	25	-0.52*	0.27*	-0.76****
WBC Count	25	-0.54**	0.29**	-0.51**
Neutrophil Count	25	-0.52**	0.27**	-0.52**
Eosinophil Count	25	-0.32	0.10	-0.45*
C-reactive Protein	25	-0.37	0.14	-0.49*
RDW	23	-0.61**	0.38**	-0.66***
Total Cholesterol	26	-0.47*	0.23*	-0.52**
Non-HDL-C	26	-0.42*	0.18*	-0.49*
LDL-C	26	-0.42*	0.18*	-0.44*
LDL-P	25	-0.45*	0.20*	-0.47*
Apo B	26	-0.39*	0.15*	-0.42
3-Methyl-Histidine§	24	+0.39	0.15	+0.50**
Phenylalanine	24	-0.42*	0.17*	-0.33
Anion Gap	26	-0.39*	0.15*	-0.41*

***p<0.05 **p<0.01 ***p<0.001 ****p<0.0001**

Table 2. Correlation coefficients for serum water T_2 values with biomarkers for protein concentration and viscosity (yellow), inflammation (red), dyslipidemia (blue) and other metabolic processes (unshaded). Biomarkers were included in this table if they demonstrated at least one correlation coefficient with a p value < 0.05. §Numbering is based on current IUPAC nomenclature, as explained elsewhere[274]. Defined with this convention, 3-methyl-histidine refers to the amino acid found in anserine, a dipeptide not produced in human tissues, but derived from dietary ingestion of poultry and fish.

Table S3: Water T_{2v} Correlations, Human Serum

Biomarker	N	r (Pearson)	R^2	r_S (Spearman)
Total Protein, Serum	**24**	**-0.47***	**0.22***	**-0.41***
Viscosity, Serum	**24**	**0.00**	**0.00**	**-0.01**
Insulin	**24**	**-0.42***	**0.18***	**-0.46***
Total Cholesterol	**24**	**-0.50***	**0.25***	**-0.46***
Non-HDL-C	**24**	**-0.40***	**0.16***	**-0.41***
LDL-C (VAP)	**24**	**-0.43***	**0.18***	**-0.40**
LDL-P	**24**	**-0.46***	**0.21***	**-0.54****

Table S3. Correlation coefficients for serum water T_{2v} values with biomarkers for protein concentration and viscosity (yellow), insulin resistance (green) and dyslipidemia (blue). Serum water T_{2v} values represent the regression residuals obtained from a linear fit of serum water T_2 *vs*. serum viscosity. This analysis removes the influence of viscosity on serum water T_2 and highlights the concentration-dependent binding of water to proteins and lipoproteins. One subject with an extremely high serum viscosity level, a statistical outlier, was excluded from this analysis. See Table S1 legend for further information about this subject.

In turn, the rotational correlation time depends on temperature and viscosity, as defined by the Stokes-Einstein-Debye equation [201,277,278]. Water molecules bound to proteins sense the slower rotational tumbling of the protein; thus, the observed water T_2 is lower than that of unbound water [275]. In addition, the protein-bound water molecules undergo exchange with unbound water, and the hydrogen atoms on ionizable groups of the proteins exchange with those of unbound water. Both exchange processes further decrease the observed ^{1}H T_2 for water [276]. Overall, water T_2 is influenced by sample viscosity as well as the binding and exchange of water molecules on and off protein binding sites.

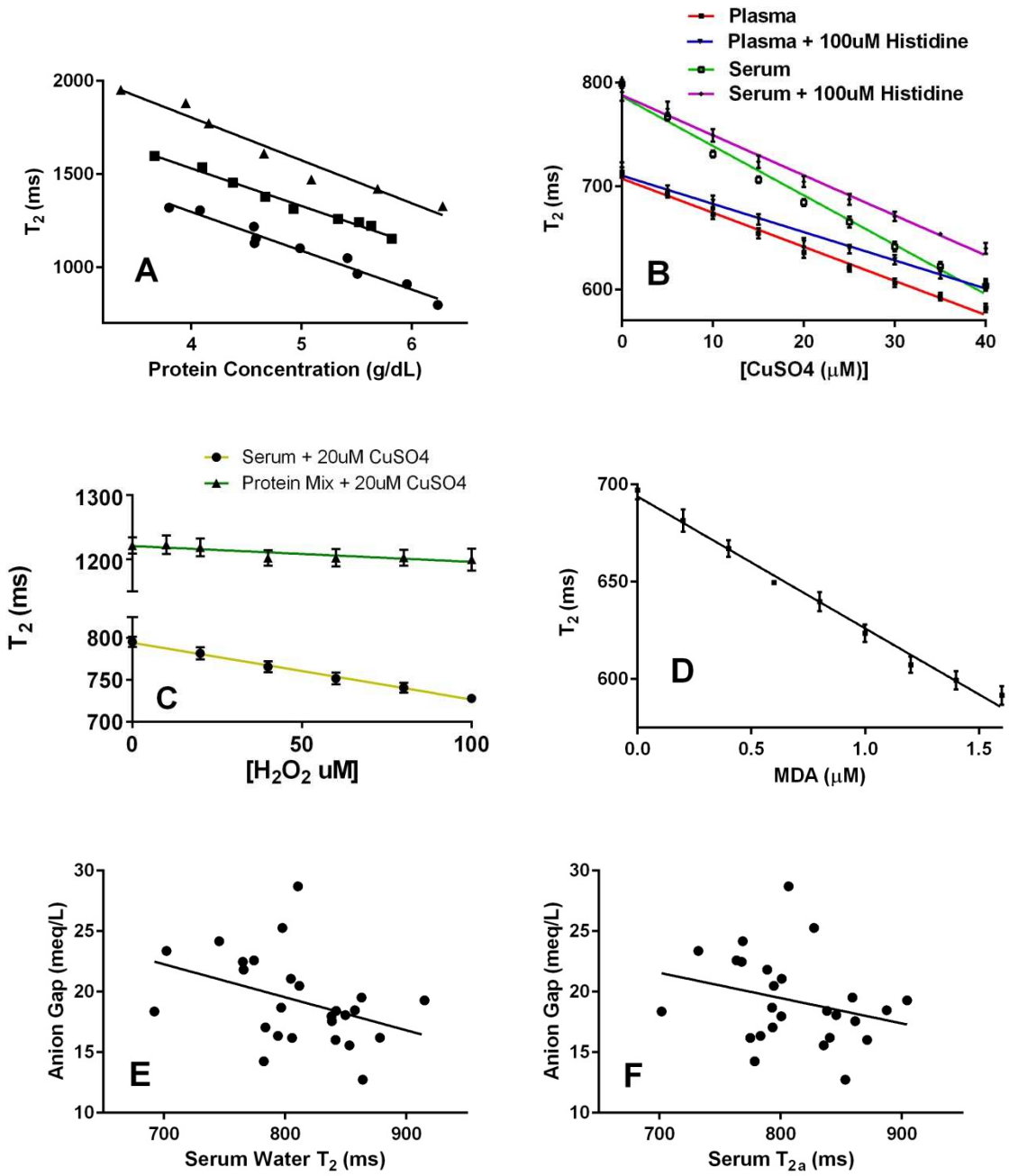

Figure 3. Protein concentration and oxidation affect water T_2 values. (A) Water T_2 values vs. protein concentration for human serum albumin (▲), lipoprotein-depleted human serum (■) and whole human serum (●); the serum samples were progressively diluted with buffer to change protein concentration; (B) and (C) Metal-catalyzed oxidation of proteins. In (B), whole serum or plasma was titrated with $CuSO_4$ in the presence or absence of added histidine. In (C), 20uM of $CuSO_4$ was added to either human serum or a protein mixture containing human serum albumin and γ-globulin, after which the samples was titrated H_2O_2. (D) Whole human serum (C) was titrated with malondialdehyde tetrabutylammonium salt, which reacts with protein side chains to form carbonyl derivatives. (E) Linear regression of serum water T_2 with the anion gap; (F) Linear regression of serum water T_{2a} with the anion gap.

Insulin Resistance and Water T_2. We sought to identify the factors that underlie the correlation of plasma, but not serum, water T_2 with markers of insulin resistance. The primary difference between plasma and serum is the presence of clotting factors I, II, V, VIII and XIII in plasma [273]. All have negligible concentrations except factor I (fibrinogen), which constitutes ~4% of total plasma protein. Fibrinogen levels increase in insulin resistance and diabetes, and increased fibrinogen is an established risk factor for cardiovascular disease[279-281] . Correction of plasma water T_2 values by removing the influence of *serum* protein concentration highlights the influence of fibrinogen. Like uncorrected T_2, plasma water T_{2p} values display an inverse correlation with insulin resistance biomarkers (Table S4). Thus, plasma water T_2 appears to be sensing insulin resistance, in part, through variations in fibrinogen concentration.

Although fibrinogen level is a significant contributor, it is not the only factor linking T_2 and insulin resistance. Plasma water T_{2a} lacks the influence of albumin and emphasizes both fibrinogen and globulin concentrations. Among all of the water T_2 variants, plasma water T_{2a} exhibits the strongest correlations with insulin resistance markers (Table S5). Conversely, plasma water T_{2g}, which eliminates the influence of serum globulin concentration, shows weaker correlations (Table S6). *Serum* water T_{2a}, which highlights the influence of globulins in the absence of fibrinogen, also correlates with insulin resistance markers (Table S9). The most abundant proteins present in the serum globulin fraction include IgG, IgA and IgM. Immunoglobulin concentrations, especially IgA, increase in metabolic disorders including metabolic syndrome, obesity and hyperglycemia [282]. Thus, plasma water T_2 appears to be sensing insulin resistance through variations in both fibrinogen and immunoglobulin concentrations.

Table S4: Water T_{2p} Correlations, Human Plasma

Biomarker	N	r (Pearson)	R^2	r_S (Spearman)
Total Protein, Serum	28	0.00	0.00	-0.04
Albumin, Serum	28	0.09	0.01	0.05
Globulins, Serum	28	-0.07	0.01	-0.08
Viscosity, Serum	24	-0.27	0.07	-0.32
Viscosity, Plasma	9	-0.90***	0.81***	-0.93***
WBC Count	27	-0.43*	0.18*	-0.40*
Neutrophil Count	27	-0.39*	0.15*	-0.44*
C-reactive Protein	27	-0.48*	0.23*	-0.41*
HbA_{1c}	27	-0.41*	0.17*	-0.45*
Insulin C-peptide	28	-0.43	0.19*	-0.47*
HOMA2-IR	28	-0.41*	0.17*	-0.45*
HOMA2-%B	28	-0.41*	0.16*	-0.36
HOMA2-%S	28	+0.48**	0.23**	+0.46*
Triglycerides	28	-0.28	0.08	-0.38*
Alanine	26	-0.42*	0.18*	-0.43*
Citrulline	26	-0.36	0.13	-0.41*
TSH	28	-0.33	0.11	-0.39*

*p<0.05 **p<0.01 ***p<0.001

Table S4. Correlation coefficients for plasma water T_{2p} with biomarkers for protein concentration and viscosity (yellow), inflammation (red), insulin resistance (green) and other processes (unshaded). The plasma water T_{2p} values represent the regression residuals obtained from a linear fit of plasma water T_2 vs. total serum protein. This analysis removes the influence of total *serum* protein concentration on plasma water T_2 values, emphasizing the influence of fibrinogen concentration.

Table S5: Water T_{2a} Correlations, Human Plasma

Biomarker	N	r (Pearson)	R^2	r_S (Spearman)
Total protein, serum	28	-0.52**	0.27**	-0.50**
Albumin, Serum	28	0.00	0.00	0.03
Globulins, Serum	28	-0.60***	0.36***	-0.62***
Viscosity, Plasma	9	-0.83**	0.68**	-0.90**
WBC Count	27	-0.53**	0.28**	-0.49**
Neutrophil Count	27	-0.51**	0.26**	-0.49**
C-reactive Protein	27	-0.61**	0.37**	-0.63**
HbA_{1c}	27	-0.46*	0.21*	-0.48*
Insulin C-peptide	28	-0.50**	0.25**	-0.51**
HOMA2-IR	28	-0.47*	0.22*	-0.48**
HOMA2-%B	28	-0.46*	0.21*	-0.48**
HOMA2-%S	28	+0.49**	0.24**	-0.50**
Triglycerides	28	-0.37	0.14	-0.47*
TG/cholesterol ratio	28	-0.32	0.10	-0.40*
Asparagine	26	+0.47*	0.22*	+0.29
Bicarbonate ion	28	+0.31	0.10	+0.41*

*p<0.05 **p<0.01 ***p<0.001

Table S5. Correlation coefficients for plasma water T_{2a} with biomarkers for protein concentration and viscosity (yellow), inflammation (red), insulin resistance (green) and other processes (unshaded). Plasma water T_{2a} values represent the regression residuals obtained from a linear fit of plasma T_2 *vs*. serum albumin concentration. This analysis removes the influence of albumin concentration on plasma T_2 and emphasizes the influence of globulins and fibrinogen concentration.

Table S6: Water T_{2g} Correlations, Human Plasma

Biomarker	N	r (Pearson)	R^2	r_S (Spearman)
Albumin, Serum	28	-0.46*	0.21*	-0.44*
Globulins, Serum	28	0.00	0.00	-0.05
Viscosity, Plasma	9	-0.82**	0.67**	-0.87**
C-reactive Protein	27	-0.43*	0.18*	-0.40*
WBC Count	27	-0.59**	0.35**	-0.54**
Neutrophil Count	27	-0.46*	0.21*	-0.41*
Platelet Count	27	-0.44*	0.19*	-0.42*
Monocyte Count	27	-0.44*	0.19*	-0.54**
HbA_{1c}	27	-0.37	0.14	-0.38*
HOMA2-%S	28	+0.38*	0.15*	+0.34
IR Score (LipoScience)	17	-0.31	0.09	-0.49*
LDL-P	27	-0.39*	0.15*	-0.42*
Small LDL-P/HDL-P	17	-0.36	0.13	-0.52*
Alanine	26	-0.44*	0.20*	-0.44*
Homocysteine	27	-0.30	0.09	-0.41*
Ethanolamine	26	-0.37	0.14	-0.43*
MCV	27	+0.34	0.12	+0.38*
Chloride ion	28	+0.43*	0.18*	+0.49**

*p<0.05 **p<0.01 ***p<0.001

Table S6. Correlation coefficients for plasma water T_{2g} with biomarkers for protein concentration and viscosity (yellow), inflammation (red), insulin resistance (green), dyslipidemia (blue) and other processes (unshaded). Plasma water T_{2g} values represent the regression residuals obtained from a linear fit of plasma T_2 *vs*. serum globulin concentration. This analysis removes the influence of serum globulin concentration on plasma water T_2 and highlights the influence of albumin and fibrinogen.

Table S7: Water T_{2c} Correlations, Human Plasma

Biomarker	N	r (Pearson)	R^2	rs (Spearman)
Total protein, serum	28	-0.64***	0.41***	-0.65***
Albumin, Serum	28	-0.25	0.06	-0.29
Globulins, Serum	28	-0.54**	0.30**	-0.57**
Viscosity, Plasma	9	-0.81**	0.65**	-0.90**
WBC Count	27	-0.64***	0.41***	-0.59**
Neutrophil Count	27	-0.58**	0.34**	-0.47*
Platelet Count	27	-0.36	0.13	-0.39*
C-reactive Protein	27	-0.60***	0.36***	-0.51**
HbA_{1c}	27	-0.45*	-0.20*	-0.49**
Insulin C-peptide	28	-0.42*	0.18*	-0.47*
HOMA2-IR	28	-0.39*	0.15*	-0.45*
HOMA2-%B	28	-0.40*	0.16*	-0.40*
HOMA2-%S	28	+0.42*	0.18*	+0.49
Triglycerides	28	-0.30	0.09	-0.40*
Asparagine	26	+0.39*	0.15*	+0.29

*p<0.05 **p<0.01 ***p<0.001

Table S7. Correlation coefficients for plasma water T_{2c} with biomarkers for protein concentration and viscosity (yellow), inflammation (red), insulin resistance (green) and other processes (unshaded). Plasma water T_{2c} values represent the regression residuals obtained from a linear fit of plasma water T_2 *vs*. total cholesterol concentration. This analysis removes the influence of total cholesterol concentration on plasma water T_2 and emphasizes the influence of plasma proteins other than lipoproteins.

Table S8: Water T_{2v} Correlations, Human Plasma

Biomarker	N*	r (Pearson)	R^2	rs (Spearman)
Total protein, serum	**9**	**-0.79***	**0.63***	**-0.73***
Viscosity, Plasma	**9**	**0.00**	**0.00**	**-0.25**
RDW	**9**	**-0.53**	**0.28**	**-0.73***
Omega 3 Index	**9**	**-0.71***	**0.50***	**-0.85****
DHA	**9**	**-0.70***	**0.48***	**-0.77***
3-Methyl-Histidine	**9**	**+0.70***	**0.48***	**+0.54**
Hydroxy-Proline	**9**	**-0.54**	**0.29**	**-0.76***

***p<0.05 **p<0.01 ***p<0.001**

Table S8. Correlation coefficients for plasma water T_{2v} values with biomarkers for protein concentration and viscosity (yellow) and other processes (unshaded). Plasma water T_{2v} values represent the regression residuals obtained from a linear fit of plasma water T_2 *vs*. plasma viscosity. This analysis removes the influence of plasma viscosity on plasma water T_2 and emphasizes the influence of water binding to proteins and lipoproteins. *For some subjects, there was not enough blood available to measure both serum and plasma viscosity, so the number of subjects with plasma viscosity data is smaller.

Table S9: Water T_{2a} Correlations, Human Serum

Biomarker	N	r (Pearson)	R^2	r_S (Spearman)
Total Protein, Serum	26	-0.75****	0.56****	-0.74****
Albumin, Serum	26	0.00	0.00	-0.01
Globulins, Serum	26	-0.72****	0.52****	-0.72****
Viscosity, Serum	25	-0.44*	0.19*	-0.62***
WBC Count	25	-0.43*	0.19*	-0.40*
Neutrophil Count	25	-0.47*	0.22*	-0.44*
Eosinophil Count	25	-0.30	0.09	-0.41*
Basophil Count	25	-0.36	0.13	-0.44*
RDW	25	-0.14	0.02	-0.41*
RDW (see caption)§	23	-0.59**	0.34**	-0.55**
C-reactive Protein	25	-0.42*	0.18*	-0.57**
Total Cholesterol	26	-0.43*	0.19*	-0.48*
Non-HDL-C	26	-0.38	0.15	-0.48*
LDL-C (VAP)	26	-0.36	0.13	-0.41*
LDL-P	25	-0.40*	0.16*	-0.43*
Apo B	26	-0.35	0.13	-0.44*
Remnant-C	26	-0.35	0.13	-0.41*
Insulin	26	-0.46*	0.21*	-0.47*
Insulin C-peptide	26	-0.39*	0.15*	-0.42*
HOMA2-IR	26	-0.38	0.14	-0.40*
HOMA2-%S	26	+0.33	0.11	+0.42*

- Table S9 continued on next page –

Table S9: Water T_{2a} Correlations, Human Serum (continued)

Biomarker	N	r (Pearson)	R^2	r_S (Spearman)
Bicarbonate ion	**26**	**+0.45***	**0.20***	**+0.46***
3-methyl histidine	**24**	**+0.35**	**0.12**	**+0.43***

***p<0.05 **p<0.01 ***p<0.001 ****p<0.0001**

Table S9. Correlation coefficients for serum water T_{2a} values with biomarkers for protein concentration and viscosity (yellow), inflammation (red), dyslipidemia (blue), insulin resistance (green) and other processes (unshaded). Serum water T_{2a} values represent the regression residuals obtained from a linear fit of serum water T_2 *vs*. serum albumin concentration. This analysis removes the influence of serum albumin concentration on serum water T_2 and emphasizes the influence of globulin and lipoproteins concentrations.

Dyslipidemia and Water T_2. Serum, but not plasma, water T_2 is inversely correlated with a number of LDL-related biomarkers. Similar correlations of T_2 and LDL markers are observed with serum water T_{2p}, T_{2g}, T_{2a} and T_{2v} (Tables S9-11, 3). This pattern suggests that serum water T_2 is sensing elevated LDL cholesterol and particle number concentration primarily through the direct binding of water molecules to lipoprotein particles. Although most of the plasma water T_2 variants do not track with LDL, an exception is plasma T_{2g} (Table S6), which correlates with LDL-P, as well as the ratio of small LDL-P to HDL-P and the lipoprotein-derived insulin resistance score [98].

Table S10: Water T_{2p} Correlations, Human Serum

Biomarker	N	r (Pearson)	R^2	r_S (Spearman)
Total Protein, Serum	**26**	**0.00**	**0.00**	**0.00**
Total Cholesterol	**26**	**-0.42***	**0.18***	**-0.40***
LDL-P	**25**	**-0.40***	**0.16***	**-0.45***
HDL-P	**15**	**+0.52***	**0.27***	**0.46**
small-LDL-P/HDL-P	**15**	**-0.45**	**0.20**	**-0.53***
Platelet Count	**25**	**-0.30**	**0.09**	**-0.43***
Phenylalanine	**24**	**-0.53****	**0.29****	**-0.57****
Alanine	**24**	**-0.49***	**0.24***	**-0.57****
Tyrosine	**24**	**-0.41***	**0.17***	**-0.45***
1-Methyl-Histidine[§]	**24**	**-0.39**	**0.15**	**-0.42***

***p<0.05 **p<0.01 ***p<0.001 ****p<0.0001**

Table S10. Correlation coefficients for serum water T_{2p} values with biomarkers for protein concentration and viscosity (yellow), inflammation (red), dyslipidemia (blue) and other processes (unshaded). Serum water T_{2p} values represent the regression residuals obtained from a linear fit of serum water T_2 *vs*. total serum protein concentration. This analysis removes the influence of albumin, globulins and viscosity on serum water T_2 and emphasizes the influence of serum lipoproteins.

[§]This numbering is based on current IUPAC nomenclature, as explained elsewhere [274]. As defined with this convention, 1-methyl-histidine refers to the amino acid found in carnosine, a dipeptide present in human muscle tissue. Elevated 1-methyl-histidine in the circulation is consistent with protein breakdown in muscle, as seen in insulin resistance and diabetes, or with strenuous exercise. Concurrent elevations of phenylalanine, alanine and tyrosine support that interpretation.

Table S11: Water T_{2g} Correlations, Human Serum

Biomarker	N	r (Pearson)	R^2	r_S (Spearman)
Total Protein, Serum	26	-0.53**	0.28**	-0.49*
Albumin, Serum	26	-0.70****	0.49****	-0.72****
Globulins, Serum	26	0.00	0.00	0.01
Viscosity, Serum	25	-0.41*	0.16*	-0.48*
WBC Count	25	-0.51**	0.26**	-0.49*
Neutrophil Count	25	-0.45*	0.20*	-0.48*
Monocyte Count	25	-0.38	0.14	-0.44*
Total Cholesterol	26	-0.47*	0.22*	-0.49*
Non-HDL-C	26	-0.41*	0.17*	-0.44*
LDL-C (VAP)	26	-0.43*	0.19*	-0.44*
LDL-P	25	-0.47*	0.22*	-0.48*
Apo B	26	-0.37	0.14	-0.41*
IR Score (LipoScience)	15	-0.37	0.14	-0.53*
Phenylalanine	24	-0.57**	0.33**	-0.60**
Tyrosine	24	-0.54**	0.29**	-0.62**
Alanine	24	-0.44*	0.19*	-0.47*
Ethanolamine	24	-0.40	0.16	-0.50*
α-amino-butyric acid	24	-0.40	0.16	-0.50*
Chloride Ion	26	+0.40*	0.16*	+0.51**
Anion Gap	26	-0.37	0.13	-0.41*

Table S11. Correlation coefficients for serum water T_{2g} values with biomarkers for protein concentration and viscosity (yellow), inflammation (red), dyslipidemia (blue) and other processes (unshaded). Serum water T_{2g} values represent the regression residuals obtained from a linear fit of serum water T_2 *vs.* serum globulin concentration. This analysis removes the influence of serum globulins on serum water T_2 and emphasizes the influence of albumin and lipoproteins.

Inflammation and Water T_2. Both plasma and serum water T_2 correlate inversely with inflammatory markers, namely white blood cell and neutrophil counts, and C-reactive protein. Serum water T_2 shows a strong inverse correlation with red cell distribution width, which is also linked with inflammation [283]. For white blood cell counts, the strongest correlations are observed for plasma water T_2 (Table 1) and serum water T_{2c}, which removes the influence of cholesterol concentration (Table S12), whereas no detectable correlations were observed for plasma water T_{2v} and serum water T_{2p}. Overall, it appears that water T_2 is sensing white blood cell counts via changes in fibrinogen, albumin and globulins (plasma) or just albumin and globulins (serum). Neutrophils, which comprise three fourths of the white blood cell population and are linked with both inflammation and insulin resistance [284], show a similar pattern. For C-reactive protein, the pattern is different. The strongest correlation is observed with plasma water T_{2a}, whereas no correlations with $p<0.05$ are observed for plasma water T_{2v}, serum water T_{2v}, T_{2g}, or T_{2p}. Taken together, it appears that water T_2 is sensing C-reactive protein levels via fluctuations in fibrinogen and globulins (plasma) or just globulins (serum).

Both plasma and serum water T_{2g}, but not other T_2 variants, correlate with monocyte count, another marker of inflammation [285]. Similarly, plasma water T_{2g} correlates with platelets, which have dual roles in thrombosis and inflammation [286]. Although preliminary, correlations are observed with other inflammatory markers (Table S2). The inverse correlation of TNFα with plasma water T_2 and T_{2a} is particularly intriguing and warrants further study.

Table S12: Water T_{2c} Correlations, Human Serum

Biomarker	N	r (Pearson)	R^2	r_S (Spearman)
Total Protein, Serum	26	-0.78****	0.61****	-0.82****
Globulins, Serum	26	-0.49*	0.24*	-0.65***
Viscosity, Serum	25	-0.30	0.09	-0.62**
WBC Count	25	-0.64***	-0.40***	-0.57**
Neutrophil Count	25	-0.65***	-0.43***	-0.62**
C-reactive Protein	25	-0.41*	0.17*	-0.49*
3-Methyl-Histidine	24	+0.47*	0.22*	+0.57*

Table S12. Correlation coefficients for serum water T_{2c} values with biomarkers for protein concentration and viscosity (yellow), inflammation (red), and other metabolic states (unshaded). Serum water T_{2c} values represent the regression residuals obtained from a linear fit of serum water T_2 *vs*. total cholesterol concentration. This analysis removes the influence of cholesterol and lipoprotein levels on serum water T_2 and highlights the influence of albumin and globulins.

Metabolite Levels and Water T_2. To assess the possible contribution of small metabolites to variations in water T_2, we conducted a series of controlled experiments. The samples contained fixed physiological concentrations of human albumin and γ-globulins, and varying amounts of metabolites, either an amino acid mixture (0.05 - 5.0 mg/ml), glucose (50 - 400 mg/dl), ATP (0.5 - 2.5 mg/ml), uric acid (2.5 - 8.6 mg/dl), urea (1 - 5 mg/dl), or glyceraldehyde (1.2 - 4.3 mg/dl). No significant changes in water T_2 are observed across these physiological ranges of metabolites. Only glucose at 400 mg/dl, a level found in severe uncontrolled diabetes, causes a significant decrease in T_2. Although water can bind to small molecules, the effect on its rotational correlation time and T_2 is negligible compared to that for water bound to protein and lipoprotein assemblies.

Proteolysis, Oxidation and Water T_2. The measurement of water T_2 requires only six minute experiments, but we also acquire data for longer periods of time in order to track the much smaller lipid and protein peaks. The T_2 value of the water peak (not the lipid/protein peaks) slowly decreased over a 3 to 18 hour period of incubation at 37°C. Initially, we hypothesized that the slow, gradual decrease in water T_2 may be resulting from *ex vivo* proteolysis. To assess the effect of proteolysis, we incubated whole human serum with exogenous trypsin and monitored T_2 over time. This incubation did not lead to a decrease in water T_2. Similar incubations of simple protein mixtures and trypsin did not result in a decrease in T_2, but rather a small increase. The lack of sensitivity of water T_2 to proteolysis could arise from two factors. Water binding to smaller protein fragments would cause less of a decrease in T_2 compared to water binding to larger, intact proteins. If substantial proteolysis occurs, it may cause T_2 to increase, not decrease. Another consideration is that human blood has evolved to resist proteolysis, especially through the activity of α_1-antitrypsin. It is notable that across our human subject population, the concentration of α_1-antitrysin does not correlate with any of the water T_2 markers.

Another possible cause of slow decrease in serum water T_2 is *ex vivo* protein oxidation. Hydrogen peroxide is ubiquitous in the human body [287] and can serve as a substrate for metal-catalyzed oxidation involving albumin-bound copper [288]. The product is hydroxyl radical, a highly reactive oxygen species that can non-enzymatically hydroxylate proline and lysine side chains [289] and cause a range of other protein modifications including carbonylation [290]. Such modifications increase the polarity of protein side chains and create additional binding sites for water.

Figure 3B illustrates the decrease in water T_2 for human serum and plasma samples incubated with increasing amounts of copper (II) sulfate. The effect was lessened when histidine, a copper chelator, was included in the buffer. A similar decrease in water $T_2$was observed when 20um of $CuSO_4$ was added to whole human serum is titrated with hydrogen peroxide. Interestingly, the same phenomena were not observed when the experiment was repeated with a protein solution indicating a variable found in whole human serum, but not the protein mixture, was driving the reaction(Fig. 3C). Also, malondialdehyde causes a concentration-dependent decrease in water T_2 (Fig. 3D); this agent modifies protein side chains, generating carbonyl derivatives [290]. Albumin, by sequestering copper and preventing metal catalyzed oxidation of other proteins, is thought to be the most abundant anti-oxidant in human blood [291]. Some of the hydrogen peroxide needed for this reaction may come from neutrophils activated during inflammation [292,293].

Is water T_2 able to sense metal-catalyzed protein oxidation that occurs *in vivo*? One of the consequences of albumin oxidation *in vivo* is a change in the protein's net charge, with an anionic shift to lower isoelectric point [294]. Similarly, glycation of albumin lowers its isoelectric point [295]. Therefore, we searched for evidence of an anionic shift in the blood samples from our study population.

Serum water T_2 and T_{2g} are inversely correlated with the anion gap, and T_{2g} is positively correlated with chloride ion concentration (Fig. 3E; Tables 2 and S10). The anion gap is used in clinical medicine to help diagnose different types of acid-base abnormalities . The body maintains charge neutrality in the circulation, but the concentration of measured cations nearly always exceeds that of measured anions. The anion gap is defined as $[UA] - [UC] = [Na^+] + [K^+] - ([Cl^-] + [HCO_3^-])$, where UA and UC represent unmeasured anions and cations,

respectively. The gap results primarily from albumin, an anionic protein with an isoelectric point of ~4.9. As the albumin concentration increases *in vivo*, the body decreases the chloride ion concentration to maintain charge balance, resulting in an increase in the anion gap. Across this human study population, serum water T_2 and T_{2g} are sensing differences in chloride ion and anion gap, in part, through variation in albumin concentration.

Another factor that modulates the anion gap is the net charge of albumin molecules. Correcting serum water T_2 values for albumin concentration does not eliminate the dependence of T_2 on anion gap (Fig. 3F). This observation indicates that serum water T_2 is sensing changes in albumin net charge, as well as concentration, likely as a result of glyco-oxidation linked to inflammation. In support of this conclusion, the anion gap corrected for albumin concentration correlates positively with levels of C-reactive protein, a marker of inflammation.

Correlations of other biomarkers with water T_2. Alanine concentration is noteworthy for its inverse correlations with water T_2 values, specifically serum and plasma water T_{2p} and T_{2g}. One of the most abundant free amino acids in the blood, alanine levels correlate with HbA_{1c}, triglycerides, small LDL and LDL particle number, and the levels of other amino acids in our database. This pattern is consistent with insulin resistance, protein mobilization from muscle and abnormalities in LDL metabolism.. Phenylalanine concentration correlates inversely with serum water T_2, T_{2p}, T_{2g} and T_{2v}, but not T_{2c}, T_{2a} or any of the plasma water T_2 markers. It correlates positively with markers of abnormal LDL metabolism. Thus, serum water T_2 appears to be sensing variation in phenylalanine levels primarily via changes in LDL-C and LDL-P, whereas it is sensing variation in alanine through both insulin resistance and LDL markers. Homocysteine, a known marker of cardiovascular risk, correlates with plasma water T_{2g}.

Two amino acids show positive correlations with water T_2: asparagine and 3-methyl-histidine. For the latter, serum water T_2 appears to be sensing its levels via changes in globulin levels. Of note, 3-methyl-histidine is not synthesized by humans, but is a breakdown product of anserine, a dipeptide derived from the dietary ingestion of poultry and fish. Both anserine and 3-methylhistidine are chelators of divalent cations and may inhibit copper-catalyzed oxidation, as well as glycation and lipoxidation[274].

Inverse Proteomics for Health Assessment and Promotion. Conventional proteomics uses mass spectrometry to measure a large number of protein biomarkers and establish phenotypic profiles [296]. Here we generated protein-based phenotypic profiles by measuring just one biomarker: water T_2. Also, conventional proteomics focuses on the less abundant proteins in blood after removing the most abundant proteins during pre-treatment [297,298]. In contrast, the current approach involves no pre-treatment or sample manipulation and leverages the information content of all plasma and serum proteins, especially the most abundant ones. For these reasons, we refer to this approach as inverse proteomics.

Lower values of water T_2 in serum and plasma are indicative of increasing degrees of metabolic dysfunction, even in apparently healthy human subjects. The unique value of inverse proteomics is that health status with respect to insulin resistance, low-grade inflammation, dyslipidemia and oxidative stress can be assessed simultaneously in one measurement without having to order a panel of clinical lab tests or biomarkers. One could envision the development of a T_2 Health Score, a practical screening tool for the early identification of hidden abnormalities in healthy subjects. This is contrast with conventional diagnostic tests, which are designed to rule in or rule out existing disease, typically in individuals who are already symptomatic. Early detection and correction of subclinical abnormalities in healthy individuals

could prevent the progression to serious diseases like diabetes, coronary artery disease, and possibly Alzheimer's disease [299]. These disorders account for much of the morbidity and mortality in modern societies. Effective screening tools that can be implemented practically, inexpensively and broadly across the population will have a place in P4 medicine: personal, predictive, preventative and participatory [300].

Although this study focused on the analysis of blood plasma and serum, it is conceivable that similar information could be extracted from whole blood, after correcting for hematocrit. Conversely, information could be gleaned about blood cells after correcting for plasma protein levels. Given the intensity of the water NMR signal, it should be feasible to monitor the mobility of water in blood from outside of the body using a TD-NMR-enabled finger clip, earlobe clip or a wristwatch-like device linked to a smart phone. This concept is not farfetched, as portable NMR devices are already in use in industry [9].

Chapter 6: Methods Development for the Analysis of Biological Samples using Benchtop Time-Domain Nuclear Magnetic Resonance

Introduction

The high-resolution analysis of biological samples using nuclear magnetic resonance spectroscopy (NMR) typically demands the use of instruments with mid-to-high-field superconducting magnets and sophisticated electronic consoles. Proper operation of these complex instruments usually requires the skill set of a NMR specialist, and they can be expensive to purchase and maintain. Recently, a number of low-field benchtop NMR instruments with permanent magnets have been developed that overcome some of the operational and economic barriers of high-field NMR [26]. While they sacrifice some degree of sensitivity and resolution, the low price, small footprint and simplified user interface has increased the accessibility of NMR to non-NMR specialists. Some low-field benchtop instruments are designed to function as miniature NMR spectrometers, generating conventional NMR spectra, sometimes with heteronuclear 2D capabilities.

A different class of benchtop system is designed for relaxometry rather than spectroscopy. Known as benchtop time-domain NMR (TD-NMR), these instruments analyze the raw free-induction decay (FID) or perform relaxation experiments in the time domain, without the use of Fourier transforms. A key practical advantage is that the magnetic field need not be high or homogeneous. While TD-NMR sacrifices the chemical shift and is no substitute for spectroscopy, useful information can often be extracted directly from the FID or from relaxation

decay curves without chemical shift resolution. Benchtop TD-NMR is particularly useful for analyzing oil-fat-protein content or the phase behavior of complex samples. Thus, applications of TD-NMR have been developed for manufacturing and process control in industrial settings [9,27,28]. Some of the most common applications include: evaluation of the relaxation properties of contrast agents used for magnetic resonance imaging (MRI) [1-4], petrophysical applications in oil and gas companies [5-11], food processing and quality[12-20] and the conservation and characterization of building materials in chemical engineering [12,21-25]. Thus, relaxometry offers great potential for the characterization and quantification of components in complex mixtures [301].

Our lab set out to evaluate benchtop TD-NMR as a tool for clinical diagnostic purposes, especially for the analysis of human blood samples. We have successfully characterized the lipid, protein and water components in whole human serum, an especially complex aqueous biological sample. Our approach is to generate multi-exponential T_2 decay curves from CPMG experiments and employ inverse Laplace transforms to resolve the individual exponential parameters. In particular, we have focused on extracting data for the slower relaxing components in whole human serum, including water and the mobile lipid domains of serum lipoproteins. Here we describe the experimental considerations important for generating and analyzing T_2 data for whole human serum using benchtop TD-NMR.

Experimental Procedures

Serum and plasma preparation and analysis

Human subject volunteers were recruited with informed consent through two protocols approved by the Institutional Review Board of the University of North Texas Health Science Center (UNTHSC). One protocol recruited seemingly healthy subjects from the student and staff

population at UNTHSC. The second protocol recruited members enrolled in the Health and Aging Brain Study at UNTHSC.

Blood samples were collected in the morning after an overnight fast. Serum was collected into plain glass red-top tubes, which lack a clot activator and gel separator (BD model 366441). The samples were processed immediately after each blood draw, centrifuged to remove blood cells, followed by a second low speed spin of the supernatant to remove any residual blood cells.

Benchtop TD-NMR relaxometry

Most of the TD-NMR measurements of T_2 and T_1 were performed on Bruker mq20 Minispec instrument equipped with a 10 mm variable temperature probe (Model H20-10-25-AVGX) and operating at 20MHz. Some experiments were performed with a similarly equipped mq40 operating at 40 MHz. The 10 mm NMR tube was filled to a sample height of 1 cm, corresponding to a sample volume of ~680 uL. All measurements were performed at 37°C. Samples were equilibrated inside the instrument at for at least 30 minutes before analysis. The T_2 is measured using a modified CPMG pulse sequence, as shown in Figure 2A.

Materials

Relaxation agents Fe-R_{ex} (MR-7200) and Gadolinium DTPA (MR-00P10) were purchased from Biopal. D_2O was 99.9% pure and purchased from Cambridge Isotope Labs (7789-20-0).

Results and Discussion

Radiation damping and optimizing solvent suppression for aqueous samples

Our first attempts to analyze ^1H T_2 relaxation curves at 40 MHz for whole human serum and other aqueous biological samples failed to provide useful data. The Bruker

mq40/Hyperquant TD-NMR instrument used for these experiments is equipped with a 10mm probe which holds approximately 700 µL of sample. Under these conditions, the CPMG decay curves were not purely exponential, but exhibited oscillatory distortions.

Radiation damping is a common occurrence for ^{1}H NMR of aqueous samples. The strong rf signal induces a current in the receiver coil, which in turn generates a weak RF field that exerts a torque on the nuclear spins [30,302]. This phenomenon leads to a deviation from the intended response of the pulse sequence, resulting in premature relaxation and an oscillatory decay curve. Figure 1 demonstrates how radiation damping manifests itself within the data.

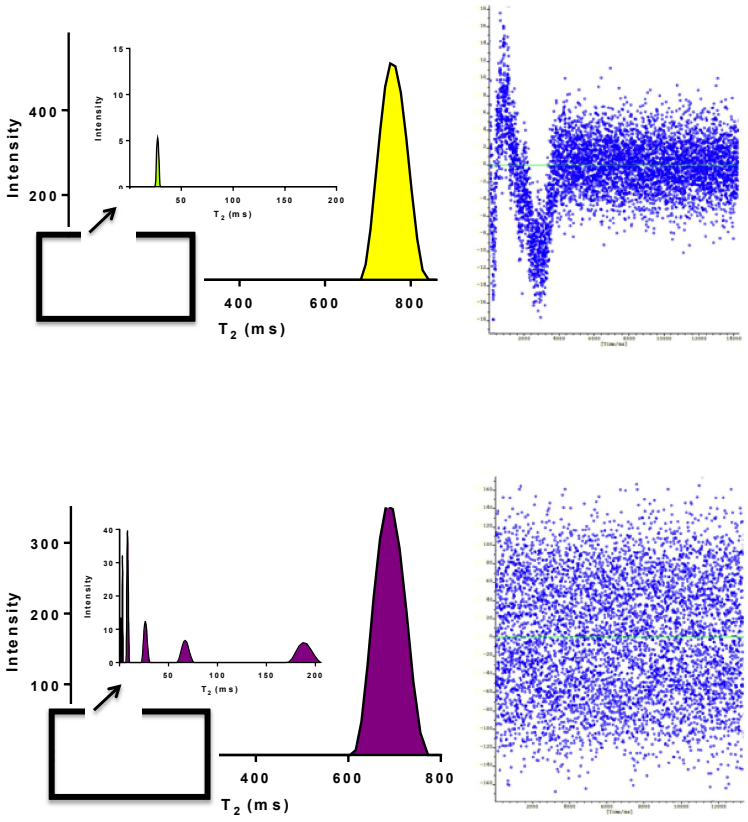

Figure 1: Effect of radiation damping on whole human serum. (A) The T_2 profile of human serum shows only two peaks when radiation damping is present, as the T_2 decay curve is distorted by non-exponential components. Those components manifest themselves as osciallatory artifacts in the residuals comparing the experimental and calculated decay curves (right panel). (B) In the absence of radiation damping, the T_2 profile of human serum reveals up to seven peaks and the residuals appear random, without an oscillatory distortion.

The T_2 profiles following inverse Laplace transform of the CPMG decay curve using CONTIN contains one intense water peak, which overshadows other T_2 components (Figure 1A). This can be attributed to a systematic oscillatory component within the raw decay curve, observable with the residual analysis, which displays the point-by-point differences between the raw decay curve and that calculated from the inverse Laplace analysis.

We investigated multiple solvent suppression techniques to eliminate the radiation damping artifact. First we tested the efficacy of MRI relaxation agents, whose paramagnetic properties drastically shorten the relaxation times of water [276,303]. The two relaxation agents tested were Fe-Rex, an iron oxide-based T_2 relaxation agent [304], and Gadolinium-DTPA, a T_1 relaxation agent [305]. We reasoned that these MRI agents would suppress the water signal to prevent radiation damping and shift the water T_2 value from ~700 ms to a much lower value, possibly unveiling useful lipid and protein T_2 peaks. While both agents were successful in reducing water relaxation times and partially suppressing the water, they created other undesirable artifacts. Fe-Rex is coated with a proton-rich polymer, which gave rise to additional T_2 peaks, interfering with the analysis whole human serum. Gadolinium-DTPA seemed promising but distorted the T_2 values for non-water peaks in a concentration dependent fashion. Even if the relaxation agents had the desired NMR response, the addition of compounds not native human serum raises the possibility of other chemical artifacts and adds an additional layer of complexity to a blood serum analysis protocol that should be as simple as possible.

Another approach was to replace a portion of the H_2O in human serum with varying amounts of isotonic D_2O using pressure dialysis. Empirically, we determined that optimal water suppression occurred when the D_2O content was between 70-80%, leaving 20-30 % of the proton signal intact. In this range, there was no evidence of oscillatory artifacts and radiation damping.

The T_2 profile in 70% D_2O revealed 3-5 additional non-water peaks that were eventually assigned to lipid and protein components in human serum. Although the D_2O exchange approach was successful and useful for preliminary proof-of-concept experiments, solvent exchange is not practical for a clinical diagnostics protocol. The buffer exchange process is labor and time-intensive, and D_2O is somewhat expensive in that context.

A better approach is to incorporate water suppression into the pulse sequence so that no sample manipulations are necessary. Although the 20MHz Bruker mq20 TD-NMR instrument that we currently use for serum analysis is equipped with a pulsed field gradient accessory, our aim was to use the simplest, most practical water suppression scheme that would be suitable for simpler instruments that lacked gradients. The best approach was a WEFT-like sequence, although no Fourier transform is employed in this case [306]. Spin population inversion is achieved at the beginning of the pulse sequence, prior to the CPMG, using a composite 180-degree pulse (90x-180y-90x) followed by a delay τ to allow partial longitudinal relaxation of the water (Figure 2). This takes advantage the fact that the non-water lipid and protein components in the sample have much shorter T_1 relaxation times than water and relax fully during the delay. The delay can be tuned to achieve the desired degree of water suppression. Unlike NMR spectroscopy, where essentially complete water suppression is desirable, some residual water is advantageous in TD-NMR as it increases the overall signal-to-noise ratio of the CPMG decay curve. The increased information content from the improved signal-to-noise stabilizes the inverse Laplace calculation and improves the precision of the measurement.

We determined empirically that a delta delay of $0.95*T_1$ for water (leading to a water signal that is ~23% of its full intensity) provides a level of suppression sufficient to avoid radiation damping, while still maximizing the overall signal-to-noise of the CPMG decay curve.

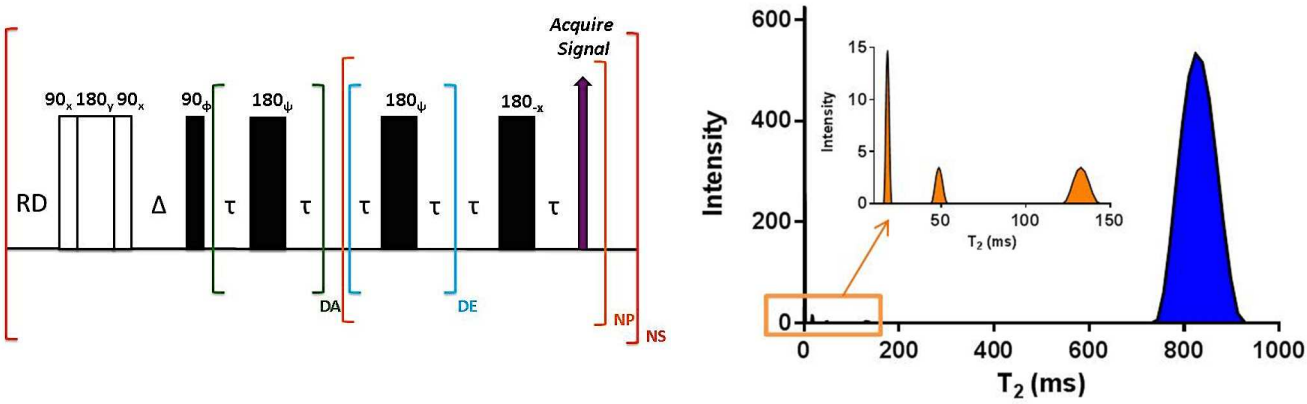

Figure 2: Modified CPMG pulse sequence successfully eliminates radiation damping in whole human serum. Panel A displays the pulse sequence. Panel B shows an example of a T_2 profile and residuals after implementing the solvent suppression scheme.

This level of residual water is consistent with our empirical findings from the D_2O exchange experiments, which gave optimal results at 70-80% D_2O. Figure 2B shows a T_2 profile of human serum that does not suffer from radiation damping.

CPMG parameter optimization

Selecting the right combination of CPMG parameters was critically important for obtaining reproducible data and eliminating artifacts. A short tau (0.19ms) was selected to prevent translational diffusion from complicating the T_2 analysis, as TD-NMR instruments have somewhat inhomogeneous fields with fixed field gradients across the sample. Using a tau significantly less than 0.19 ms can cause sample heating and data oversampling. The dummy echo and acquisition time were set to ensure that the decay curve reached baseline as to not truncate the signal. This was achieved by using a CPMG acquisition time ≥ 5 times the longest T_2. The acquisition time was adjusted by varying the number of data points. The 90° and 180° degree pulses were calibrated for each sample, typically 8.22 and 16.44 µs, respectively, and showed little sample-to-sample variation.

Other modifications were made to the original CPMG pulse sequence program obtained from Bruker. The phase of the 180° pulse in the CPMG loop is alternated to mimimize pulse imperfections, which can introduce oscillatory artifacts into the CPMG decay curve. In addition, the pulse sequence incorporates an 8-step phase cycle, alternating the 90° pulse along with the receiver to eliminate artifacts [307,308].

The acquisition parameters for the CPMG pulse sequence are summarized in Table 1.

Table 1: CPMG acquisition parameters

Parameter	Input
Tau Delay	0.19 ms
Dummy Echo	5
Recycle Delay	5* Longest T_1
Acquisition Time	5* Longest T_2
Delta Delay	0.95 * Longest T_1
Minimum # of scans	16 scans – water analysis only 256 scans – lipid/protein analysis
Number of points	5600 – Serum 8000 – Fractionated Lipoproteins

Data analysis: choosing the right algorithm

The Inverse Laplace transform (ILT) algorithm employed in the program CONTIN is provided in the Bruker software to extract T_2 components from a multiexponential decay curve. While CONTIN calculations are robust when the solute of interest has high signal-to-noise (and hence high information content), the analysis of weaker signals suffer from poor reproducibility and instability in the calculations. Mathematically, the conversion of the relaxation decay into a continuous distribution of relaxation components using an ILT calculation can be an ill-posed problem. An ill-posed problem is defined as having one of three properties: (A) does not have a solution (B) the solution is NOT unique, or (C) a small perturbation of the problem may cause a

large change in the solution. Even small amounts of noise may lead to an invalid solution [301], leading to irreproducible results. Figure 3 demonstrates the variability within a single sample between four runs of human serum using the ILT algorithm implemented in CONTIN.

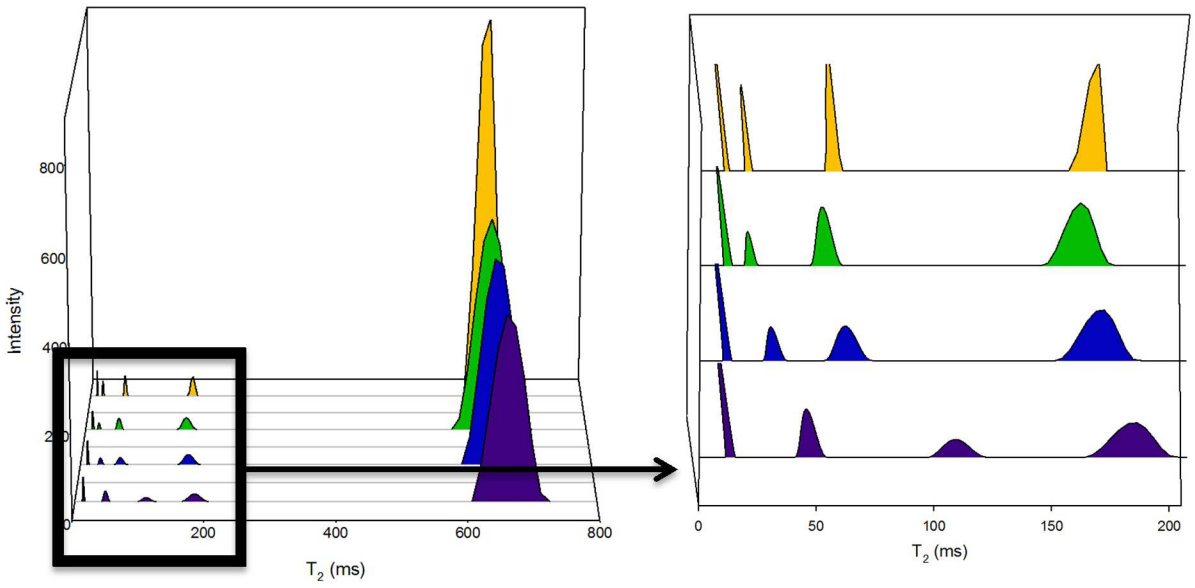

Figure 3: Four identical repeat CPMG experiments on a single human serum sample, showing the variable and inconsistent solutions obtained using the CONTIN ILT algorithm.

To circumvent these issues, we implemented two critical improvements. First, we delayed the data acquisition for 19 ms after the beginning of the CPMG scheme to minimize the number of exponential terms for data processing. Figure 4A shows an example of a fully sampled T_2 relaxation decay curve. In the first 19 ms, there is a fast decaying component (blue box), which results in 3-4 T_2 components from 0-50ms (Figure 4B). By not recording the data points for the first 19ms, the very fast relaxation processes at the beginning of the decay curve are deemphasized, and the slower processes of interest are emphasized (Fig. 4C, D). This modification reduces the number of exponential terms, simplifying and stabilizing the inverse Laplace transform calculation.

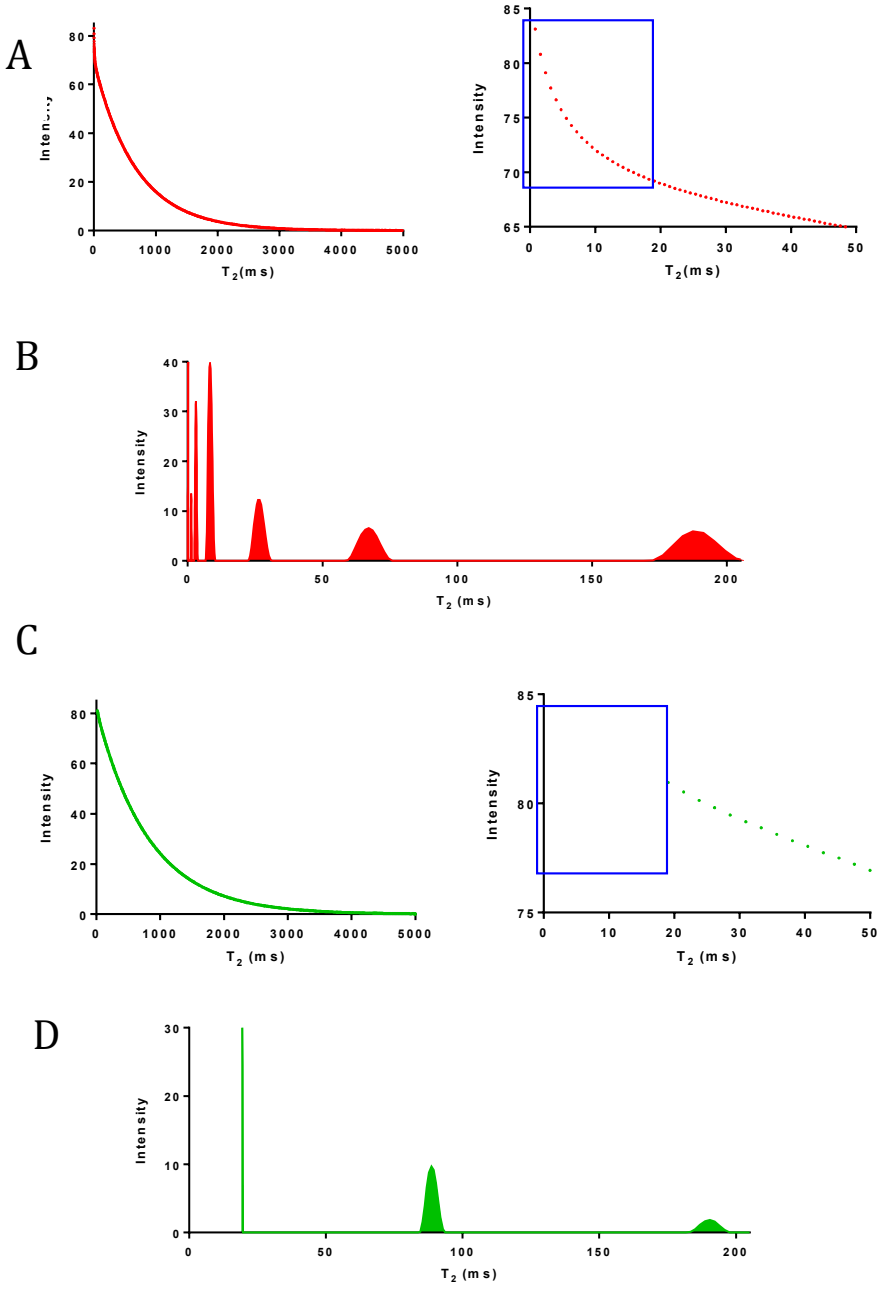

Figure 4: Effect of delayed acquisition on T_2 profile. (A-B) Full decay curve and T_2 profile. (C-D) Delayed acquisition (19ms) T_2 profile and decay curve without the first 19ms.

The second improvement was utilizing a different ILT algorithm as implemented in XPfit (http://www.softscientific.com/science/xpfit.html). This program permits the user to constrain the number of exponential terms. For subject-to-subject comparisons of human serum samples,

it is essential to restrain the number of exponential terms to a consistent number, up to four. The XPFit program employs a non-negative truncated single value decomposition algorithm, which stabilizes the calculation.

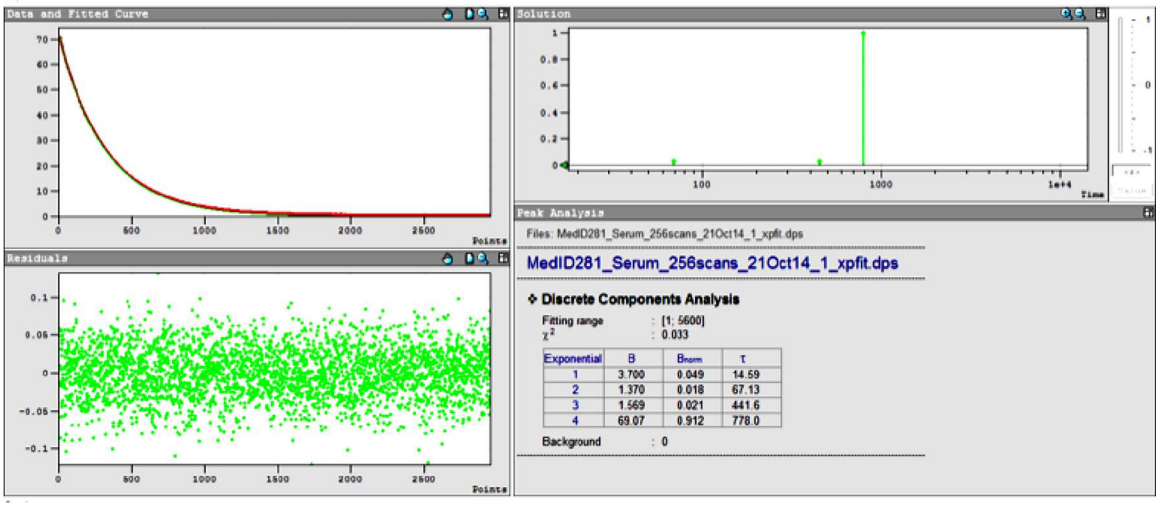

Figure 5: XPFit data analysis output

Figure 5 shows an example of the XPfit data output screen. Initial input of reasonable starting value estimates for the amplitude and T_2 is important for obtaining consistent results. For the data to converge in whole human serum, the starting amplitude of the solvent peak must be at least two magnitudes greater than the lipid and protein peaks. We found that starting amplitude of 85 for the solvent and 0.5 for the remaining peaks was sufficient for the algorithm.

Conclusions

This study identified the conditions necessary to obtain robust, reproducible multi-exponential T_2 profiles of human serum using benchtop TD-NMR. High-quality, artifact-free CPMG decay curves were obtained using a modified CPMG pulse sequence. This pulse scheme was tuned to achieve partial suppression of the strong water signal sufficient to eliminate

radiation damping while optiminzing the signal-to-noise ratio of the decay curve. Delayed acquisition was employed to deemphasize the first 19ms, which reduced the number of exponentials and emphasized the slower relaxing lipid and water components. Finally, the ILT algorithm in XPfit was utilized to analyze the multiexponential decay curve, as it provided more stable and reproducible results compared with the CONTIN algorithm, which does not permit user control over the number of exponentials.

These methods can be extrapolated from human serum into other aqueous biological samples. For example, we have used this protocol to analyze fractionated lipoproteins, pure proteins and complex protein mixtures, and multilamellar phospholipid bilayer systems. Similar applications may be envisioned that would benefit the experimental approach used here.

Chapter 7: Discussion and Conclusions

Overview

Low-field NMR is a fast developing field due to recent advancements in hardware and data processing. The novel ^{1}H benchtop TD-NMR methods presented here demonstrate that the molecular dynamics of water, lipoproteins and proteins in whole human serum correlate with a large number of clinical biomarkers for insulin resistance, oxidative stress, dyslipidemia and inflammation. This was accomplished by implementing a modified CPMG pulse sequence, which achieved partial water suppression to overcome the radiation damping artifact. Another crucial development was the utilization of the data analysis software XPfit, which allowed us to constrain the number of components to obtain run-to-run reproducibility.

Aside from aqueous liquids, we also developed a novel method for analyzing oil-phase lipid fluidity. We found that the NMR T_2 directly monitors hydrocarbon chain packing, which is proportional to the polyunsaturated fatty acid content, omega-3's in particular. Together, these novel applications demonstrate the potential for opportunity and expansion of low-field NMR beyond its conventional scope.

Future Exploration and Development

Optimization of Human Serum and Plasma Collection and Analysis

Upon completion of the first phase, it is necessary to review and update the protocol to ensure an efficient secondary phase. Three major improvements will be investigated before the next round of specimen collection will begin. We have analyzed only freshly draw blood products in this study, which limits our analysis to 1 sample/day because of processing demands and subject recruitment. Through a network of collaborators at UNTHSC, we have access to a

large number of human serum and plasma samples stored at -80°C. Utilizing these samples would quickly increase our patient sample size, and enhance the statistical power. Therefore the first study would assess human serum and plasma integrity after they have been thawed. It is well documented that triglyceride-rich samples cannot withstand multiple freeze-thaw cycles [309], which may or may not impact our TD-NMR analysis.

The second improvement to explore is the sample volume. Currently the experiment requires ~700ul of serum or plasma for analysis. Realistically, this volume would be difficult to obtain in the clinical setting. Therefore we will investigate a variety of methods to decrease the required sample size. Previously we demonstrated that decreasing the NMR tube size from 10mm to 7.5mm eliminated a radiation damping effect in oil-phase lipids [201]. We hypothesize the same will hold true for the aqueous water samples, whereby reducing the sample volume will eliminate the need for water suppression, hence decreasing total acquisition time.

Finally, it is necessary to revise the list of biomarkers collected now that a hypothesis concerning the mechanism and disease risk has been developed. Tailoring the data collection will enhance or disprove our theories. Biomarkers that should be included are adipokines, inflammatory cytokines, kidney function markers, and various cognitive function markers such as MMSE. After this is complete the lab will begin the next round of patient sample collection to increase the sample size and further explore the capability of this instrument.

Oil-phase lipids – Oxidation

Polyunsaturated fatty acids (PUFAs), commonly found in edible food oils and dietary supplements, are highly susceptible to peroxidation due to the numerous *cis*-double bonds they contain. Auto-oxidation and photo-oxidation can occur during processing and storage which results in rancidity and the production of toxic compounds [310]. Peroxidation by-products are

subject to crosslinking reactions, resulting in a polymeric network of hydrocarbon chains.[311] Current methods currently to detect lipid peroxidation include infared or mass spectroscopy, high-resolution NMR, scanning calorimetry and size exclusion chromatography [312].

Benchtop TD-NMR may be a simpler less expensive method for the detection of peroxidation in oil-phase lipids. Previously we demonstrated the sensitivity of TD-NMR to omega-3 content, on the basis of monitoring hydrocarbon molecular motions. An increased number of double bonds disrupt tight packing rendering the oil more fluid. The same theory can be applied to monitor lipid peroxidation. The crosslinking induced by lipid peroxidation will decrease sample fluidity, which we hypothesize will be detectable by TD-NMR. Correlating the TD-NMR values of suspected oxidize lipids with conventional peroxidation markers, such as HNE and MDA, will aid in validating the method.

Adipose Tissue Fluidity

In addition to oil-phase lipids, benchtop TD-NMR may be able to probe the fluidity of adipose tissue. Body fat distribution (visceral vs subcutaneous) and fatty acid adipose tissue composition (saturated vs monounsaturated vs polyunsaturated lipids) are both associated with a number of disorders such at metabolic syndrome, insulin resistance and cardiovascular disease[313-316]. Preliminary experiments of canine adipose tissue display a T_2 profile similar to that of an oil-phase lipid. Therefore, adipose tissue fluidity may be a useful marker for characterizing metabolic dysfunction. Statistical correlations between adipose tissue T_2 and adipokines, inflammatory, insulin resistance and cholesterol markers should be tested in the future to assess the utility of this potential method.

Protein Modification – Oxidation and Glycation

We have previously shown how dramatically the concentration of protein in solution can affect the water peak in an aqueous sample. As the protein concentration increases, so does the number of binding sites for water to associate with. Certain protein modification processes may also lead to increased protein water binding sites. For example, once albumin becomes oxidized, its overall surface charge is altered leading to increased water binding[288,290,291]. Therefor it becomes plausible that benchtop TD-NMR can monitor protein modification by studying the differential water binding in a solution. TD-NMR values should be correlated against known protein modification indicators such as carbonylation, glycation and electrophoretic mobility.

Potential for commercialization and biomarker development

Human Serum Analysis

Benchtop TD-NMR relaxation times T_1 and T_2 have the ability to survey a range of metabolic abnormalities such as insulin resistance, oxidative stress, dyslipidemia and inflammation in whole human serum or plasma. The participants in the study were seemingly healthy, with normal conventional clinical values and displayed no signs of illness. Yet we observed within this group that lower water T_2 values are characteristic of increasing metabolic dysfunction. Therefore this would suggest evidence of hidden abnormalities, that could lead to diseases in the future such as diabetes and cardiovascular disease.

The purpose of this study was not to diagnose an already sick individual, but rather assess the overall health status to identify those at risk for developing metabolic abnormalities. Early detection of such may correct or delay the development of disease if the appropriate lifestyle changes and interventions are taken. Advancements in biotechnology are paving the way to make this possible, especially through the implementation of P4 Medicine (personalized, predicative,

preventative and participatory) in healthcare systems, which aims to anticipate and manage health status instead of reacting to a disease [300,317]. In the future is may be feasible to obtain a benchtop TD-NMR T_2 value for serum, which will provide the user with an overall health score based on a library of patient data collected in a large cohort study.

Oil-phase lipid analysis

The omega-3 concentration in fish-oil supplements could be accurately quantified using benchtop TD-NMR. Unlike other commonly used methods, TD-NMR is simple, inexpensive and does not suffer from complications due to chemometircs or complex algorithms. This method holds similar implications for determination of omega 3's in flax seed and other edible oils. In addition, several instruments are capable of on-line real time monitoring, which would allow this method to be implemented during the purification and production process not just at the end for quality control.

References

References

1. Gordon, R. E.; Hanley, P. E.; Shaw, D. Topical magnetic resonance. *Progress in Nuclear Magnetic Resonance Spectroscopy* **1982***, 15*, 1-47.

2. Neuringer, L. J. Nuclear magnetic resonance spectroscopy and imaging of humans. *Phys. B: Cond. Matter.* **1990***, 164*, 193-199.

3. Wehrli, F. W. From NMR diffraction and zeugmatography to modern imaging and beyond. *Progress in Nuclear Magnetic Resonance Spectroscopy* **1995***, 28*, 87-135.

4. Haacke, E. M.; Brown, R. W.; Thompson, M. R.; Venkattesan, R. *Magnetic Resonance Imaging: Physical Principles and Sequence Design;* John Wiley & Sons Inc: 1999; .

5. Allen, D. F.; Flaum, C.; Ramakrishnan, T. S.; Bedford, J.; Castelijns, K.; Fairhurst, D.; Gubelin, G.; Heaton, N. J.; Minh, C. C.; Norville, M. A.; Seri, M. R.; Pritchard, T.; Ramamoorthy, R. Trends in NMR logging. *Schlumberger Oilfield Review* **2000***, 12*, 2-19.

6. Allen, D. F.; Crary, S.; Freedman, R.; Andreani, M.; Klopf, W.; Badry, R.; Flaum, C.; Kenyon, W. E.; Kleinberg, R. L.; Gossenberg, R.; Horkowirz, D.; Logan, P.; Singer, J.; White, J. How to use a borehole nuclear magnetic resonance. *Schlumberger Oilfield Review* **1997***, 9*, 34-57.

7. Coates, G. R.; Xiao, L.; Prammer, M. G. *NMR Logging: Principles and Applications;* Gulf Publication Company: Houston, Texas, USA, 1999; .

8. Mitchell, J.; Staniland, J.; Chassagne, R.; Fordham, E. J. Quantitative in-situ enhanced oil recovery monitoring using magnetic resonance. *Trans. Porous Med.* **2012***, 94*, 683-706.

9. Mitchell, J.; Gladden, L. F.; Chandrasekera, T. C.; Fordham, E. J. Low-field permanent magnets for industrial process and quality control. *Progress in Nuclear Magnetic Resonance Spectroscopy* **2014***, 76*, 1-60.

10. Mitchell, J.; Edwards, J.; Fordham, E. J.; Staniland, J.; Chassagne, R.; Cherukipalli, P.; Wilson, O.; Faber, R.; Bouwmeester, R. Quantitative remaining oil interpretation using magnetic resonance: from the laboratory to the pilot. *EOR Conference at Oil and Gas West Asia* **2012**, 16-18.

11. Brown, J. A.; Brown, L. F.; Jackson, J. A.; Milewski, J. V.; Travis, B. J. NMR logging tool development: laboratory studies of tight gas sands and artificial porous material. *Unconventional Gas Symposium* **1982**, 203-208.

12. Song, Y. Q. A 2D NMR method to charactarize granlar structure of dairy products. *Progress in Nuclear Magnetic Resonance Spectroscopy* **2009***, 55*, 324-334.

13. Pearce, K. L.; Rosenvold, K.; Andrsen, H. J.; Hopkins, D. L. Water distribution and mobility in meat during the conversion of muscle to meat and age and the impact on fresh meat quality attributes-a review. *Meat Science* **2011***, 89*, 111-124.

14. Bertram, H. C.; Andersen, H. J.; Karlsson, A. H. Comparative study of low-field NMR relaxation measurements and two traditional methods in the determination of water holding capacity of pork. *Meat Science* **2001***, 57*, 125-132.

15. Bertram, H. D. Field gradient CPMG applied on postmortem muscles. *Magnetic resonance imaging* **2004***, 22*, 557-563.

16. Veliyulin, E.; van der Zwagg, C. H.; Burk, W.; Erikson, U. In vitro determination of fat content in Atlantic salmon with a mobile NMR spectrometer. *Journal of Food Agriculture* **2005***, 85*, 1299-1304.

17. Hurlimann, M. D.; Burcaw, L.; Song, Y. Q. Quantitative charactarization of food products by two-dimensional D-T2 and T1-T2 distribution functions in a static gradient. *J. Colloil Interface* **2006***, 297*, 303-311.

18. Erikson, U.; Standal, I. B.; Aursand, I. G.; Veliyulin, E.; Aursand, M. Use of NMR is fish processing optimization: a review of recent progress. *Magnetic Resonance Chemistry* **2012***, 50*, 471-480.

19. Mariette, F. Investigations of food colloids by NMR and MRI. *Current opinion Colloid Interface Sci.* **2009***, 14*, 203-211.

20. Voda, M. A.; van Duynhoven, J. P. M. Charactarization of food emulsions by PFG NMR. *Trend. Food Sci. Technol.* **2009***, 29*, 533-543.

21. Blumich, B.; Anferova, S.; Kremer, K.; Sharma, S.; Herrmann, V.; Sefre, A. Unilateral NMR for quality control: the NMR-MOUSE. *Spectroscopy* **2003***, 18*, 18-34.

22. Davenal, A.; Pouvreau, S.; Cambert, M.; Suquet, M.; Mariette NMR relaxometry as a potential non-invasive routine sensor for characterization of phenotype in Crassostrea gigas. *Aquaculture* **2009***, 291*, 74-77.

23. Neville, A. M. Properties of concrete. *Longman Scientific & Technical , 1991*.

24. Muller, A. C. A.; Scrivener, K. L.; Gajewicz, A. M.; McDonald, P. J. Use of bench-top NMR to measure the density, composition and desorption isotherm of C-S-H in cement paste. *Microporous Mesoporous Mater* **2013***, 178*, 99-103.

25. Tulio, V. D.; Proietti, N.; Gobbino, M.; Capitani, D.; Olmi, R.; Priori, S.; Riminesi, C.; Giani, E. Non-destructive mapping of dampness and salts in degraded wall paintings in hypogenous buildings: the case of St. Clement as mass fresco in St. Clement Basilica, Rome. *Anal. Bioanal. Chem.* **2010**, *396*, 1885-1896.

26. Blumich, B.; Casanova, F.; Appelt, S. NMR at Low Magnetic Fields. *Chemical Physical Letters* **2009**, *477*, 231-240.

27. Malet-Martino, M.; Holzgrabe, U. NMR techniques in biomedical and pharmaceutical analysis. *J. Pharm. Biomed. Anal.* **2011**, *55*, 1-15.

28. Metz, H.; Mader, K. Benchtop-NMR and MRI--a new analytical tool in drug delivery research. *Int. J. Pharm.* **2008**, *364*, 170-175.

29. Levitt, M. *Spin Dynamics: basics of nuclear magnetic resonance;* John Wiley & Sons, Ltd: New York, NY, 2001; .

30. Freeman, R. *A Handbook of Nuclear Magnetic Resonance;* Longman Group: United Kingdom, 1997; .

31. Bloch, F. The Principle of Nuclear Induction. *Science* **1953**, *118*, 425-430.

32. James, T. L. In *Fundamentals of NMR;* Selected Topics in Biophysics, http://www.biophysics.org/portals/1/PDFs/Education/james.pdf; Biophysical Society: Rockville, MD, 1998; pp 1-31.

33. Leftin, A.; Brown, M. F. An NMR database for simulations of membrane dynamics. *Biochim. Biophys. Acta* **2011**, *1808*, 818-839.

34. Matsubara, T.; Matsuda, H. A lattice model of liquid helium. *Prog. Theor. Phys.* **1956**, *16*, 569-582.

35. Levitt, M. *Spin Dynamics: basics of nuclear magnetic resonance;* John Wiley & Sons, Ltd: New York, NY, 2001; .

36. Reddy, T.; Rainey, J. K. Interpretation of biomolecular NMR spin relaxation parameters. *Biochem. Cell Biol.* **2010**, *88*, 131-142.

37. Void, R. L.; Waugh, J. S.; Klein, M. P.; and Phelps, D. E. Measurement of Spin Relaxation in Complex Systems. *Chem. Phys.* **1968**, *48*, 3831-3832.

38. Chavhan, G. B.; Babyn, P. S.; Haacke, E. M. Principles, Techniques, and Applications of T2*-based MR Imaging and Its Special Applications. *Radiographics* **2009**, *25*, 1443-1449.

39. Carr, H. Y.; Purcell, E. M. Effects of Diffusion on Free Precession in Nuclear Magnetic Resonance Experiments. *Phys.Rev.* **1954**, *94*, 630-638.

40. Hahn, E. L. Spin Echos. *Phys. Rev.* **1950***, 80*, 580.

41. Bloch, F. Nuclear Induction. *Phys.Rev.* **1946***, 70*, 460-474.

42. Torrey, H. C. Bloch Equations with Diffusion Terms. *Phys.Rev.* **1956***, 104*, 563-565.

43. Levitt, M. *Spin Dynamics: basics of nuclear magnetic resonance;* John Wiley & Sons, Ltd: New York, NY, 2001; .

44. Leftin, A.; Brown, M. F. An NMR database for simulations of membrane dynamics. *Biochim. Biophys. Acta* **2011***, 1808*, 818-839.

45. Case, D. A. Molecular dynamics and NMR spin relaxation in proteins. *Acc. Chem. Res.* **2002***, 35*, 325-331.

46. Leftin, A.; Brown, M. F. An NMR database for simulations of membrane dynamics. *Biochim. Biophys. Acta* **2011***, 1808*, 818-839.

47. Prompers, J. J.; Bruschweiler, R. General framework for studying the dynamics of folded and nonfolded proteins by NMR relaxation spectroscopy and MD simulation. *J. Am. Chem. Soc.* **2002***, 124*, 4522-4534.

48. Reddy, T.; Rainey, J. K. Interpretation of biomolecular NMR spin relaxation parameters. *Biochem. Cell Biol.* **2010***, 88*, 131-142.

49. Bloch, F.; Hansen, W. W.; Packard, M. The nuclear induction experiment. *Phys. Rev.* **1946***, 70*, 474.

50. Purcell, E. M.; Torrey, H. C.; Pound, R. V. Resonance absorption by nuclear magnetic moments in a solid. *Phys. Rev.* **1946***, 69*, 37.

51. Rigden, J. S. Quantum states and precession: The two discoveries of NMR. *Reviews of Modern Physics* **1986***, 58*, 433-449.

52. Freeman, R. A short history of NMR. *Chemistry of heterocyclic compounds* **1995***, 31*, 1004-1005.

53. Brennan, L. NMR-based metabolomics: From sample preparation to applications in nutrition research. *Progress in Nuclear Magnetic Resonance Spectroscopy* **2014***, 83*, 42-49.

54. Malet-Martino, M.; Holzgrabe, U. NMR techniques in biomedical and pharmaceutical analysis. *J. Pharm. Biomed. Anal.* **2011***, 55*, 1-15.

55. Otvos, J. D. Why Cholesterol Measurements May be Misleading about Lipoprotein Levels and Cardiovascular Disease Risk ? Clinical Implications of Lipoprotein Quantification Using NMR Spectroscopy. *Laboratoriums Medizin* **2002***, 26*, 544-550.

56. Otvos, J. D.; Jeyarajah, E. J.; Cromwell, W. C. Measurement issues related to lipoprotein heterogeneity. *Am. J. Cardiol.* **2002***, 90*, 22i-29i.

57. Otvos, J. D.; Mora, S.; Shalaurova, I.; Greenland, P.; Mackey, R. H.; Goff, D. C.,Jr Clinical implications of discordance between low-density lipoprotein cholesterol and particle number. *J. Clin. Lipidol.* **2011***, 5*, 105-113.

58. Otvos, J. Measurement of triglyceride-rich lipoproteins by nuclear magnetic resonance spectroscopy. *Clin. Cardiol.* **1999***, 22*, II21-7.

59. Mayer, B. P.; Valdez, C. A.; Hok, S.; Chinn, S. C.; Hart, B. R. 31P-edited diffusion-ordered 1H NMR spectroscopy for the spectral isolation and identification of organophosphorus compounds related to chemical weapons agents and their degredation products. *Anal. Chem.* **2012***, 84*, 10478-10484.

60. Lankhorst, P. P.; Haasnoot, C. A.; Erkelens, C.; Westerink, H. P.; van der Marel, G. A.; van Boom, J. H.; Altona, C. Carbon-13 NMR in conformation analysis of nucleic acid fragments. *Nucleic Acids Res.* **1985***, 13*, 927-942.

61. Lopez-Cebral, R.; Martin-Pastor, M.; Seijo, B.; Sanchez, A. Progress in the charactarization of bio-functionalized nanoparticles using NMR methods and their applications as MRI contrast agents. *Progress in Nuclear Magnetic Resonance Spectroscopy* **2014***, 79*, 1-13.

62. Coffey, A.; Truong, M.; Chekmenev, E. Low-field MRI can be more sensitive than high-field MRI. *Journal of Magnetic Resonance* **2013***, 237*, 169-174.

63. Ghazinoor, S.; Crues, J. V. Low Field MRI: A Review of the Literature and Our Experience in Upper Extremity Imaging. *Clinics in Sports Medicine* **2006***, 25*, 591-606.

64. Cosmus, T. C.; Parizh, M. Advances in whole body MRI magnets. *Applied Supercond.* **2011***, 21*, 2104-2109.

65. Dalitz, F.; cudaj, M.; Maiwald, M.; Guthausen, G. Process and reaction monitoring by low-field NMR spectroscopy. *Magnetic Resonance Spectroscopy* **2012***, 60*, 52-70.

66. Stejskal, E. D.; Tanner, J. E. Spin diffusion measurements: spin echos in the presence of a time-dependent field gradient. *J. Chem. Phys.* **1965***, 42*, 288-292.

67. Tanner, J. E.; Stejskal, E. D. Restricted self-diffusion of protons in colloidal systems by the pulsed gradient, spin-echo method. *J. Chem. Phys.* **1968***, 49*, 1768-1777.

68. Tanner, J. E. Use of the stimulated echo in NMR diffusion studies. *J. Chem. Phys.* **1970***, 52*, 2523-2526.

69. Karger, J.; Heink, W. The propagator representation of molecular transport in microporous crystallites. *J. Magn. Reson.* **1983***, 51*, 1-7.

70. Hurlimann, M. D.; Venkataramanan, L. Quantitative measurement of two-dimensional distribution functions of diffusion and relaxation in grossly inhomogenous fields. *J. Magn. Reson.* **2002***, 157*, 31-42.

71. Schoengelder, W.; Glaser, H. R.; Mitreiter, I.; Stallmach, F. Two-dimensional NMR relaxometry study of pore space characteristics of carbonate rocks from a Permian aquifer. *J. Appl. Geophys.* **2008***, 65*, 21-29.

72. Song, Y. Q.; Venkataramanan, L.; Hurlimann, M. D.; Flaum, M.; Frulla, P.; Straley, C. T1-T2 correlation spectra obtained using a fast two-dimensional Laplace inversion. *J. Magn. Reson.* **2002***, 154*, 261-268.

73. Dusschoten, D.; Moonen, C. T. W.; Jager, P. A.; Van As, A. Unraveling diffusion constants in biological tissue by combining Carr-Purcell-Meiboom-Gill imaging and pulsed field gradient NMR. *Magn. Reson. Imag.* **1994***, 36*, 907-913.

74. Fordham, E. J.; Gibbs, S. J.; Hall, L. D. Partially restricted diffusion in a permeable sandstone: observations by stimulated echo PFG NMR. *Magn. Reson. Imag.* **1994***, 12*, 279-284.

75. Gibbs, S. J.; Johnson, C. S. A PFG NMR experiment for accurate diffusion and flow studies in the presence of eddy currents. *J. Magn. Reson.* **1991***, 93*, 395-402.

76. Monteihet, L.; Korb, J. P.; Mitchell, J.; McDonald, P. J. Observation of exchange of micropore water in cement pastes by two-dimensional T2-T2 nuclear magnetic resonance relaxometery. *Phys. Rev.* **2006***, 74*, 061404.

77. Washburn, E. W.; Callaghan, P. T. Tracking pore to pore exchange using relaxation exchange spectroscopy. *Phys. Rev. Lett.* **2006***, 97*, 175502.

78. Mitchell, J.; Griffith, J. D.; Collins, J. H. P.; Sederman, A. J.; Gladden, L. F.; Johns, M. L. Validation of NMR relaxation exchange time measurements in porous media. *J. Chem. Phys.* **2007***, 127*, 234701.

79. Laghi, L.; Cremonini, M. A.; Placucci, G.; Sykora, S.; Wright, K.; Hills, B. A proton NMR relaxation study of hen egg quality. *Magn. Reson. Imag.* **2005***, 23*, 501-510.

80. Lucas, T.; Wagner, M.; Barey, P.; Mariette, F. NMR assessment of mix and ice cream. Effect of formation on liquid water and ice. *Int. Dairy J.* **2005***, 15*, 1064-1073.

81. Simpson, A. J.; McNally, D. J.; Simpson, M. J. NMR spectroscopy in environmental research: From molecular interactions to global processes. *Progress in Nuclear Magnetic Resonance Spectroscopy* **2011***, 58*, 97-175.

82. Holzgrabe, U.; Malet-Martino, M. NMR spectroscopy in pharmaceutical and biomedical analysis. *J Pharm Biomed Anal* **2014***, 93*.

83. Jones, M.; Aptaker, P. S.; Cox, J.; Gardiner, B.; McDonald, P. J. A transportable magnetic resonance imaging system for in situ measurements of living trees: the Tree Hugger. *Journal of Magnetic Resonance* **2012***, 218*, 133-140.

84. Crues, J. V.; Shellock, F. G.; Dardashti, S. Identification of wrist and metacarpophalangeal joint erosions using a portable-MR system compared to conventional X-ray. *J Rhuematol* **2004***, 31*, 676-685.

85. Eidmann, R.; Savelsberg, P.; Blümler, B. The NMR MOUSE, a Mobile Universal Surface Explorer. *J. Magn. Reson. A 122* **1996**, 104-109.

86. Blumichm B.; Blumler, P.; Eidmann, G.; Guthausen, A.; Haken, R. l. S., U.; Saito, K.; Zimmer, G. The NMR-mouse: construction, excitation and applications. *Magnetic resonance imaging* **1998***, 16*, 479-484.

87. Aptaker, P. S.; McDonald, P. J.; Mitchell, J. Surface GARField: a novel one-sided NMR magnet and RF probe. *Magnetic Resonance Imaging* **2007***, 25*, 544.

88. Vance, D.; Vance, J. *Biochemistry of Lipids, Lipoproteins and Membranes, Fifth Edition (New Comprehension Biochemistry);* 2008; .

89. Farnier, M.; Perevozskaya, I.; Taggart, W. V.; Kush, D.; Mitchel, Y. B. VAP II analysis of lipoprotein subclasses in mixed hyperlipidemic patients on treatment with ezetimibe/simvastatin and fenofibrate. *J. Lipid Res.* **2008***, 49*, 2641-2647.

90. Kulkarni, K. R. Cholesterol profile measurement by vertical auto profile method. *Clin. Lab. Med.* **2006***, 26*, 787-802.

91. Anderson, D. W.; Nichols, A. V.; Forte, T. M.; Lindgren, F. T. Particle distribution of human serum high density lipoproteins. *Biochim. Biophys. Acta* **1977***, 493*, 55-68.

92. Holmquist, L.; Carlson, L. A. Subfractionation and characterization of native and incubation enlarged human plasma high density lipoprotein particles by high performance gel filtration. *Lipids* **1985***, 20*, 378-388.

93. Nichols, A. V.; Krauss, R. M.; Musliner, T. A. Nondenaturing polyacrylamide gradient gel electrophoresis. *Methods Enzymol.* **1986***, 128*, 417-431.

94. Warnick, G. R.; McNamara, J. R.; Boggess, C. N.; Clendenen, F.; Williams, P. T.; Landolt, C. C. Polyacrylamide gradient gel electrophoresis of lipoprotein subclasses. *Clin. Lab. Med.* **2006***, 26*, 803-846.

95. Jeyarajah, E. J.; Cromwell, W. C.; Otvos, J. D. Lipoprotein particle analysis by nuclear magnetic resonance spectroscopy. *Clin. Lab. Med.* **2006***, 26*, 847-870.

96. Kuller, L.; Arnold, A.; Tracy, R.; Otvos, J.; Burke, G.; Psaty, B.; Siscovick, D.; Freedman, D. S.; Kronmal, R. Nuclear magnetic resonance spectroscopy of lipoproteins and risk of coronary heart disease in the cardiovascular health study. *Arterioscler. Thromb. Vasc. Biol.* **2002***, 22*, 1175-1180.

97. Mora, S.; Otvos, J. D.; Rifai, N.; Rosenson, R. S.; Buring, J. E.; Ridker, P. M. Lipoprotein particle profiles by nuclear magnetic resonance compared with standard lipids and apolipoproteins in predicting incident cardiovascular disease in women. *Circulation* **2009***, 119*, 931-939.

98. Shalaurova, I.; Connelly, M. A.; Garvey, W. T.; Otvos, J. D. Lipoprotein insulin resistance index: a lipoprotein particle-derived measure of insulin resistance. *Metab. Syndr. Relat. Disord.* **2014***, 12*, 422-429.

99. Charles, M. A.; Kane, J. P. New molecular insights into CETP structure and function: a review. *J. Lipid Res.* **2012***, 53*, 1451-1458.

100. Krauss, R. M.; Wojnooski, K.; Orr, J.; Geaney, J. C.; Pinto, C. A.; Liu, Y.; Wagner, J. A.; Luk, J. M.; Johnson-Levonas, A. O.; Anderson, M. S.; Dansky, H. M. Changes in lipoprotein subfraction concentration and composition in healthy individuals treated with the CETP inhibitor anacetrapib. *J. Lipid Res.* **2012***, 53*, 540-547.

101. Goldberg, I. J.; Eckel, R. H.; McPherson, R. Triglycerides and heart disease: still a hypothesis? *Arterioscler. Thromb. Vasc. Biol.* **2011***, 31*, 1716-1725.

102. Fuchs, F. D.; Fuchs, S. C.; Moreira, L. B.; Gus, M. Proof of concept in cardiovascular risk: the paradoxical findings in blood pressure and lipid abnormalities. *Vasc. Health. Risk Manag.* **2012***, 8*, 437-442.

103. Krentz, A. J. Lipoprotein abnormalities and their consequences for patients with type 2 diabetes. *Diabetes Obes. Metab.* **2003***, 5 Suppl 1*, S19-27.

104. Adiels, M.; Matikainen, N.; Westerbacka, J.; Soderlund, S.; Larsson, T.; Olofsson, S. O.; Boren, J.; Taskinen, M. R. Postprandial accumulation of chylomicrons and chylomicron remnants is determined by the clearance capacity. *Atherosclerosis* **2012***, 222*, 222-228.

105. Borggreve, S. E.; De Vries, R.; Dullaart, R. P. Alterations in high-density lipoprotein metabolism and reverse cholesterol transport in insulin resistance and type 2 diabetes mellitus: role of lipolytic enzymes, lecithin:cholesterol acyltransferase and lipid transfer proteins. *Eur. J. Clin. Invest.* **2003***, 33*, 1051-1069.

106. Boullart, A. C.; de Graaf, J.; Stalenhoef, A. F. Serum triglycerides and risk of cardiovascular disease. *Biochim. Biophys. Acta* **2012***, 1821*, 867-875.

107. Chan, D. C.; Watts, G. F. Postprandial lipoprotein metabolism in familial hypercholesterolemia: thinking outside the box. *Metabolism* **2012***, 61*, 3-11.

108. Cohn, J. S. Postprandial lipemia and remnant lipoproteins. *Clin. Lab. Med.* **2006***, 26*, 773-786.

109. Hamilton, J. A.; Morrisett, J. D. Nuclear Magnetic Resonance Studies of Lipoproteins. *Meth. Enzymol.* **1986***, 128*, 472-515.

110. Pownall, H.; Shepherd, J.; Mantulin, W.; Sklar, L.; Gotto, A. Effect of saturated and polyunsaturated fat diets on the composition and structure of human low density lipoproteins. *Atherosclerosis* **1980***, 36*, 299-314.

111. Blankenhorn, D. H.; Johnson, R. L.; Mack, W. J.; el Zein, H. A.; Vailas, L. I. The influence of diet on the appearance of new lesions in human coronary arteries. *JAMA* **1990***, 263*, 1646-1652.

112. McNamara, J. R.; Small, D. M.; Li, Z.; Schaefer, E. J. Differences in LDL subspecies involve alterations in lipid composition and conformational changes in apolipoprotein B. *J. Lipid Res.* **1996***, 37*, 1924-1935.

113. Schuster, B.; Prassl, R.; Nigon, F.; Chapman, M. J.; Laggner, P. Core lipid structure is a major determinant of the oxidative resistance of low density lipoprotein. *Proc. Natl. Acad. Sci. U. S. A.* **1995***, 92*, 2509-2513.

114. Liu, Y.; Lou, D.; Atkinson, D. Human LDL core cholesterol ester packing: three-dimensional image reconstruction and SAXS simulation studies. *J. Lipid Res.* **2011***, 52*, 256.

115. Chapman, D. Phase transitions and fluidity characteristics of lipids and cell membranes. *Q. Rev. Biophys.* **1975***, 8*, 185-235.

116. Small, D. M. Lateral Chain Packing in Lipids and Membranes. *J. Lipid Res.* **1984***, 25*, 1490.

117. Small, D. M. *The Physical Chemistry of Lipids: From Alkanes to Phospholipids.* Plenum Press: New York, N.Y., 1986; .

118. Vance, D.; Vance, J. *Biochemistry of Lipids, Lipoproteins and Membranes;* 2008; .

119. Thiam, A. R.; Farese Jr, R. V.; Walther, T. C. The biophysics and cell biology of lipid droplets. *Nat. Rev. Mol. Cell Biol.* **2013***, 14*, 775-786.

120. Deckelbaum, R. J.; Shipley, G. G.; Small, D. M.; Lees, R. S.; George, P. K. Thermal Transtions in Human Plasma LDL. *Science* **1975***, 190*, 392.

121. Atkinson, D.; Deckelbaum, R. J.; Small, D. M.; Shipley, G. G. Structure of human plasma low-density lipoproteins: Molecular organization of the central core. *Proc. Natl. Acad. Sci. USA* **1977***, 74*, 1042.

122. Zechner, R.; Kostner, G. M.; Dieplinger, H.; Degovics, G.; Laggner, P. In vitro modification of the chemical composition of human plasma low density lipoproteins: effects on morphology and thermal properties. *Chem. Phys. Lipids* **1984**, *36*, 111.

123. Pregetter, M.; Prassl, R.; Schuster, B.; Kriechbaum, M.; Nigon, F.; Chapman, J.; Laggner, P. Microphase separation in low density lipoproteins. Evidence for a fluid triglyceride core below the lipid melting transition. *J. Biol. Chem.* **1999**, *274*, 1334-1341.

124. Prassl, R.; Laggner, P. Molecular structure of low density lipoprotein: current status and future challenges. *European Biophysical Journal* **2009**, *38*, 145.

125. Liu, Y.; Lou, D.; Atkinson, D. Human LDL core cholesterol ester packing: three-dimensional image reconstruction and SAXS simulation studies. *J. Lipid Res.* **2011**, *52*, 256-262.

126. Schuster, B.; Prassl, R.; Nigon, F.; Chapman, M. J.; Laggner, P. Core lipid structure is a major determinant of the oxidative resistance of low density lipoprotein. *Proc. Natl. Acad. Sci. U. S. A.* **1995**, *92*, 2509-2513.

127. Morton, R.; Parks, J. S. Plasma cholesteryl ester transfer activity is modulated by the phase transition of the lipoprotein core. *J. Lipid Res.* **1996**, *37*, 1915.

128. McNamara, J. R.; Small, D. M.; Li, Z.; Schaefer, E. J. Differences in LDL subspecies involve alterations in lipid composition and conformational changes in apolipoprotein B. *J. Lipid Res.* **1996**, *37*, 1924-1935.

129. Melchoir, J.; Sawyer, J.; Kelley, K.; Shah, R.; Wilson, M.; Hantgan, R.; Rudel, L. L. LDL Particle Core Enrichment in Cholesteryl Oleate Increases Proteoglycan Binding and Promotes Atherosclerosis. *J. Lipid Res.* **2013**, *54*, 2495-2503.

130. Kirchhausen, T.; Untracht, S.; Fless, G.; Scanu, A. Atherogenic Diets and Neutral-Lipid Organization in Plasma Low Density Lipoproteins. *Atherosclerosis* **1979**, *33*, 59-70.

131. Pownall, H.; Shepherd, J.; Mantulin, W.; Sklar, L.; Gotto, A. Effect of saturated and polyunsaturated fat diets on the composition and structure of human low density lipoproteins. *Atherosclerosis* **1980**, *36*, 299.

132. Berlin, E.; Judd, J.; Marshall, M.; Kliman, P. Dietary linoleate increases fluidity and influences chemical composition of plasma low density lipoprotein in adult men. *Atherosclerosis* **1987**, *66*, 215-225.

133. Nenseter, M.; Rustan, A.; Lund-Katz, S.; Soyland, E.; Maelandsmo, G.; Phillips, M. C.; Drevon, C. A. Effect of dietary supplementation with n-3 polyunsaturated acids on physical properties and metabolism of low density lipoprotein in humans. *Arterioscler. Thromb. Vasc. Biol.* **1992**, *12*, 369-379.

134. Nordöy, A.; Hatcher, L. F.; Ullmann, D. L.; Connor, W. E. Individual effects of dietary saturated fatty acids and fish oil on plasma lipids and lipoproteins in normal men. *American Journal of Nutrition* **1993***, 57*, 634.

135. Sundram, K.; Ismail, A.; Hayes, K. C.; Jeyamalar, R.; Pathmanathan, R. Trans (elaidic) fatty acids adversely affect the lipoprotein profile relative to specific saturated fatty acids in humans. *J. Nutr.* **1997***, 127*, 514.

136. Callow, J.; Summers, L.; Bradshaw, H.; Frayn, K. Changes in LDL Particle Composition After the Consumption of Meals Containing Different Amounts and Types of Fat. *Am. J. Clin. Nutr.* **2001***, 76*, 345-350.

137. Spector, A.; Yorek, M. Membrane Lipid Composition and Cellular Function. *J. Lipid Res.* **1985***, 26*, 1015-1035.

138. Lenaz, G. Lipid Fluidity and Membrane Protein Dynamics. *Biosci. Rep.* **1987***, 7*.

139. Hollan, S. Membrane Fluidity of Blood Cells. *Haematologia* **1996***, 27*, 109.

140. Clamp, A.; Ladha, S.; Clakc, D.; Grimble, R.; Lund, E. The Influence of Dietary Lipids on the Composition and Membrane Fluidity of Rat Hepatocyte Plasma Membrane. *Lipids* **1997***, 32*, 179-184.

141. Crane, J.; Tamm, L. Role of Cholesterol in the Formation and Nature of Lipid Rafts in Planar and Spherical Model Membranes. *Biophys. J.* **2004***, 86*, 2965-2979.

142. Mansilla, M.; Cybulski, L.; Albanesi, D.; Mendoza, D. Control of Membrane Lipid Fluidity by Molecular Thermosensors. *J. Bacteriol.* **2004***, 186*, 6681-6688.

143. Shaikh, R.; Edidin, M. Polyunsaturated fatty acids, membrane organization, T cells, and antigen presentation. *Journal of Clinical Nutrition* **2006***, 84*, 1277-1289.

144. Sanchez, S.; Tricerri, M.,Ossato, G.; Gratton, E. Lipid packing determines protein-membrane interactions: Challenges for apolipoprotein A-1 and high density lipoproteins. *Biochim. Biophys. Acta* **2010***, 1798*, 1399.

145. Yang, X.; Sheng, W.; Sun, G.; Lee, J. Effects of fatty acid unsaturation numbers of membrane fluidity and alpha-secretase-dependent amyloid precursor protein processing. *Neurochem. Int.* **2011***, 58*, 321-329.

146. Shaikh, R. Biophysical and biochemical mechanisms by which dietary N-3 polyunsaturated fatty acids from fish oil disrupt membrane lipid rafts. *J. Nutr. Biochem.* **2012***, 23*, 101.

147. Calder, P. Fat chance to enhance B cell function. *J. Leukoc. Biol.* **2013***, 93*, 457-459.

148. Nicolson, G. The Fluid—Mosaic Model of Membrane Structure: Still relevant to understanding the structure, function and dynamics of biological membranes after more than 40 years. *Biochim. Biophys. Acta* **2014***, 1838*, 451.

149. Rocket, B. D.; Melton, M.; Harris, M.; Bridges, L. C.; Shaikh, S. R. Fish oil disrupts MHC class II lateral organization on the B-cell side of the immunological synapse, independent of B-T cell adhesion. *J. Nutr. Biochem.* **2013***, 11*, 1810-1816.

150. Vanderkooi, J.; Fishkoff, S.; Chance, B.; Cooper, R. A. Fluotescent probe analysis of the lipids architecture of natural and experimental cholesterol-rich membranes. *Biochemistry (N. Y.)* **1974***, 18*, 1589.

151. Kveder, M.; Pifat, G.; Pecar, S.; Schara, M. TheÂ ESRÂ characterization of molecular mobility in theÂ lipidÂ surface layer of human serumÂ lipoproteins. *Chem. Phys. Lipids* **1994***, 70*, 101-108.

152. Chochina, S. V.; Avdulov, N. A.; Igbavboa, U.; Cleary, J. P.; O'Hare, E. O.; Wood, W. G. Amyloid beta-peptide1-40 increases neuronal membrane fluidity: role of cholesterol and brain region. *J. Lipid Res.* **2001***, 42*, 1292-1297.

153. Kahya, N.; Scherfeld, D.; Bacia, K.; Poolman, B.; Schwille, P. Probing lipid mobility of raft-exhibiting model membranes by fluorescence correlation spectroscopy. *The Journal of Biological Chemistry* **2003***, 278*, 28109.

154. Valeur, B.; Berberan-Santos, M. N. In *Microviscosity, fluidity, molecular mobility. Estimation by means of fluorescent probes.* Molecular Fluorescence: Principles and Applications; John Wiley and Sons: 2013; pp 226-245.

155. Hormel, T. T.; Kurihara, S. Q.; Brennan, M. K.; Wozniak, M. C.; Parthasarathy, R. Measuring Lipid Membrane Viscosity Using Rotational and Translational Probe Diffusion Â. **2014***, 12*, 188101.

156. Johnson, L.; Spence, M. In *Probes for Lipids and Membranes;* Molecular Probes Handbook, A Guide to Fluorescent Probes and Labeling Technologies; 2010; pp 549-579.

157. Fretten, P.; Morris, S. J.; Watts, A.; Marsh, D. Lipid-lipid and lipid-protein interactions in chromaffin granule membranes. A spin label ESR study. *Biochim. Biophys. Acta* **1980***, 598*, 247.

158. Crepeau, R. H.; Saxena, S.; Lee, S.; Patyal, B.; Freed, J. H. Studies on lipid membranes by two-dimensional Fourier transform ESR: Enhancement of resolution to ordering and dynamics. *Biophys. J.* **1994***, 66*, 1489-1504.

159. Jurkiewicz, P.; Olżyńska, A.; Cwiklik, L.; Conte, E.; Jungwirth, P.; Megli, F. M.; Hof, M. Biophysics of lipid bilayers containing oxidatively modified phospholipids: insights from

fluorescence and EPR experiments and from MD simulations. *Biochimica et Biophysica Acta (BBA)-Biomembranes* **2012***, 1818*, 2388-2402.

160. Mainali, L.; Feix, J. B.; Hyde, J. S.; Subczynski, W. K. Membrane fluidity profiles as deduced by saturation-recovery EPR measurements of spin-lattice relaxation times of spin labels. *Journal of Magnetic Resonance* **2011***, 212*, 418-425.

161. Hamilton, J. A.; Morrisett, J. D. Nuclear Magnetic Resonance Studies of Lipoproteins. *Meth. Enzymol.* **1986***, 128*, 472-515.

162. Seelig, A.; Seelig, J. Dynamic structure of fatty acyl chains in a phospholipid bilayer measured by deuterium magnetic resonance. *Biochemistry* **1974***, 13*, 4839-4845.

163. Hakumäki, J. M.; Kauppinen, R. A. 1H NMR-visible lipids in the life and death of cells. *Trends Biochem. Sci.* **2000***, 25*, 357-362.

164. Orädd, G.; Lindblom, G.; Westerman, P. W. Lateral diffusion of cholesterol and dimyristoylphosphatidylcholine in a lipid bilayer measured by pulsed field gradient NMR spectroscopy. *Biophys. J.* **2002***, 83*, 2702-2704.

165. Larijani, B.; Dufourc, E. J. Polyunsaturated phosphatidylinositol and diacylglycerol substantially modify the fluidity and polymorphism of biomembranes: a solid-state deuterium NMR study. *Lipids* **2006***, 41*, 925-932.

166. Brown, M. F.; Chan, S. I. Bilayer Membranes: Deuterium and Carbon-13 NMR. *eMagRes* **2007**.

167. Schafer, T. Nearly Perfect Fluidity. *Physics* **2009***, 88*, 126001-126041.

168. Corti, R.; Fuster, V. Imaging of Athosclerosis: Magnetic Resonance Imaging. *Eur. Heart J.* **2011***, 32*, 1709-1719.

169. Meisamy, S.; Hines, C. G.; Hamilton, G.; Sirlin, C. B.; McKenzie, C. A.; Yu, H.; Brittain, J. H.; Reeder, S. B. Quantification of hepatic steatosis with T1-independent, T2*-corrected MR imaging with spectral modeling of fat: Blinded comparison with MR spectroscopy
. *Radiology* **2011***, 258*, 767-775.

170. Johnson, N. A.; Walton, D. W.; Sachinwalla, T.; Thompson, C. H.; Smith, K.; Ruell, P. A.; Stannard, S. R.; and George, J. Noninvasive assessment of hepatic lipid composition: Advancing understanding and management of fatty liver disorders. *Hepatology* **2008***, 47*, 1523.

171. Gambarota, G.; Tanner, M.; van der Graaf, M.; Mulkern, R.; Newbould, R. 1H-MRS of hepatic fat using short TR at 3T: SNR optimization and fast T2 relaxometry . *Magn. Reson. Mater. Phys. , Biol. Med.* **2011***, 24*, 345.

172. Carr, H. Y.; Purcell, E. M. Effects of Diffusion on Free Precession in Nuclear Magnetic Resonance Experiments. *Phys.Rev.* **1954***, 94*, 630-638.

173. Meiboom, S.; Gill, D. Modified Spin Echo for Measuring Nuclear Relaxation Times. *Rev. Sci. Instrum.* **1958***, 29*, 688-691.

174. Provencher, S. Contin: A general purpose constrained regularization program for inverting noisy linear algebraic and integral equations. *Comput. Phys. Commun.* **1982***, 35*, 229-242.

175. Cistola, D. P.; Hamilton, J. A.; Jackson, D.; Small, D. M. Ionization and phase behavior of fatty acids in water: application of the Gibbs phase rule. *Biochemistry* **1988***, 27*, 1881-1888.

176. Dote, J. L.; Kivelson, D. Hydrodynamic rotational friction coefficients for nonspheroidal particles. *Journal of Physical Chemistry* **1983***, 87*, 3889-3893.

177. Opperman, M.; Benade, S. Analysis of the omega-3 fatty acid content of South African fish oil supplements: a follow-up study. *Cardiovascular Journal of Africa* **2013***, 24*, 297-302.

178. Pipingas, A.; Cockerell, R.; Grima, N.; Sinclair, A.; Stough, C.; Scholey, A.; Myers, S.; Croft, K.; Sali, A.; Pase, M. Randomized Controlled Trial Examining the Effects of Fish Oil and Multivitamin Supplementation on the Incorporation of *n*-3 and *n*-6 Fatty Acids into Red Blood Cells. *Nutrients* **2014***, 6*, 1956-1970.

179. Bekhit, M. Y.; Grung, B.; Mjøs, S. A. Determination of omega-3 fatty acids in fish oil supplements using vibrational spectroscopy and chemometric methods. *Applied Spectroscopy* **2014***, 68*, 1190-1200.

180. Kleiner, A.; Cladis, D. P.; Santerre, C. R. A comparison of actual versus stated label amounts of EPA and DHA in commercial omega-3 dietary supplements in the United States. *Journal of Food Agriculture* **2014**.

181. Mozaffarin, D.; Wu, J. Omega-3 Fatty Acids and Cardiovascular Disease. *Journal of the American College of Cardiology* **2011***, 58*, 2047-2067.

182. Wang, C.; Harris, W. S.; Chung, M.; Lichtenstein, A. H.; Balk, E. M.; Kupelnick, B. n-3 fatty acids from fish or fish-oil supplements, but not alpha-linolenic acid, benefit cardiovascular disease outcomes in primary-and-secondary-prevention studies: a systematic review. *American Journal of Clinical Nutrition* **2006***, 84*, 5-17.

183. Wenstrom, K. D. The FDA's new advice on fish: it's complicated. *American Journal of Obstetrics* **2014***, 211*, 475-478.

184. Molfino, A.; Gioia, G.; Fanelli, F.; Muscaritoli, M. The Role for Dietary Omega-3 Fatty Acids Supplementation in Older Adults. *Nutrients* **2014***, 6*, 4058-4072.

185. Mozaffarin, D.; Rimm, E. B. Fish Intake, Contaminants, and Human Health: Evaluating the Risks and Benefits. *JAMA* **2006**, *296*, 1885-1899.

186. Bradberry, J. C.; Hilleman, D. E. Overview of Omega-3 Fatty Acid Therapies. *Pharmacy and Therapeutics* **2013**, *38*, 681-691.

187. Harris, W. S.; Mozaffarin, D.; Lefevre, M.; et al Towards Establishing Dietary Reference Intakes for Eicosapentaenoic and Docosahexaenoic Acids. *Journal of Nutrition* **2009**, *139*, 804-819.

188. Leon, H.; Shibata, H. C.; Sivakumaran, S.; Dorgan, M.; Chatterley, T.; Tsuyuki, R. T. Effect of Fish Oil on Arrhythmias and Mortality: Systematic Review. *BMJ* **2008**, *337*, 2931.

189. Marik, P. E.; Varon, J. Omega-3 Dietary Supplements and the Risk of Cardiovascular Events: a Systematic Review. *Clinical Cardiology* **2009**, *32*, 365-372.

190. Surette, M. E. The Science Behind Dietary Omega-3 Fatty Acids. *Can Med Assoc* **2008**, *178*, 177-180.

191. Kris-Etherton, P. M.; Harris, W. S.; Appel, L. J. Omega-3 fatty Acids and Cardiovascular Disease: New Recomendations from the American Heart Association. *Arterioscler. Thromb. Vasc. Biol.* **2003**, *23*, 151-152.

192. U.S. Department of Agriculture and U.S. Department of Health and Human Services, Ed.; In *Dietary Guidelines for Americans 2010;* Washington, DC: U.S.: 2010; .

193. U.S. Department of Health and Human Services Using Dietary Supplements Wisely. **2014**.

194. Andlauer, W.; Furst, P. Nutraceuticals: a piece of history, present status and outlook. *Food Research International* **2002**, *35*, 171-176.

195. Warner, J. Some Fish Oil Supplements Fishy on Quality. *http://www.webmd.com/diet/news/20111206/some-fish-oil-supplements-fishy-on-quality* (accessed January/1, 2015).

196. Tatarczyk, T.; Engl, J.; Ciardi, C.; Laimer, M.; Kaser, S.; Salzmann, K.; Lenners, R.; Patsch, J. R.; Ebenbichler, C. F. Analysis of long-chain ω-3 fatty acid content in fish-oil supplements. *The Middle European Journal Of Medicine* **2007**, *119*, 417-422.

197. Kang, J. X.; Wang, J. A simplified method for analysis of polyunsaturated fatty acids. *BMC Biochemistry* **2005**, *6*.

198. Paulson, D. R.; Saranto, J. R. The fatty acid composition of edible oils and fats. *Journal of Chemical Education* **1974**, *51*, 406-408.

199. Schultz, E.; Pugh, M. E. Determination of the fatty content of biological membranes: A highly versatile GC-MS experiment. *Journal of Chemical Education* **2001***, 78*, 944-946.

200. Petrovic, M.; Kezic, N.; Bolanca, V. Optimization of the GC method for routine analysis of the fatty acid profile in several food samples. *Food Chemistry* **2010***, 122*, 285-291.

201. Robinson, M. D.; Cistola, D. P. Nanofluidity of Fatty Acid Hydrocarbon Chains As Monitored by Benchtop Time-Domain Nuclear Magnetic Resonance. *Biochemistry* **2014***, 53*, 7515-7522.

202. Carr, H. Y.; Purcell, E. M. Effects of Diffusion on Free Precession in Nuclear Magnetic Resonance Experiments. *Phys.Rev.* **1954***, 94*, 630-638.

203. Bloch, F. The Principle of Nuclear Induction. *Science* **1953***, 118*, 425-430.

204. Torrey, H. C. Bloch Equations with Diffusion Terms. *Phys.Rev.* **1956***, 104*, 563-565.

205. Meiboom, S.; Gill, D. Modified Spin Echo for Measuring Nuclear Relaxation Times. *Rev. Sci. Instrum.* **1958***, 29*, 688-691.

206. Provencher, S. Contin: A general purpose constrained regularization program for inverting noisy linear algebraic and integral equations. *Comput. Phys. Commun.* **1982***, 35*, 229-242.

207. Kaneko, F.; Yano, J.; Sato, K. Diversity in the fatty-acid conformation and chain packing of cis-unsatruated lipids. *Current opinion in structural biology* **1998***, 8*, 417-425.

208. Small, D. M. *The Physical Chemistry of Lipids: From Alkanes to Phospholipids.* Plenum Press: New York, N.Y., 1986; .

209. Rosetti, C.; Pastorino, C. Polyunsatruated and Saturated Phopholipids in Mixed Bilayers: A Study from the Molecular Scale to the Lateral Lipid Organization. *The Journal of Physical Chemistry* **2010***, 115*, 1002-1013.

210. Salm, P.; Taylor, P. J.; Kostern, K. Simultaneous quantification of total eicosapentaenoic acid, docosahexaenoic acid and arachidonic acid in plasma by high-perfonamce liquid chromatography-tandem mass-spectrometry. *Biomedical chromatography* **2010***, 25*, 652-659.

211. Hellmuth, C.; Weber, M.; Koletzko, B.; Peissner, W. Nonesterfied fatty acid determination for functional lipidomics: Conprehensive ultrahigh performance liquid chromatogrpahy-Tandem mass spectrometry quantitation, qualification and parameter prediction. *Analytical Chemistry* **2012***, 84*, 1483-1490.

212. Lacaze, J. P. C.; Stobo, L. A.; Turrel, E. A.; Quiliam, M. A. Solid-phase extraction and liquid chromatography-mass spectrometry for the determination of free fatty acids in shellfish. *Journal of chromatography* **2007***, 1145*, 51-57.

213. von Schacky, C. Omega-3 index and cardiovascular disease prevention: principle and rationale. *Lipid Technology* **2010***, 22*, 151-154.

214. von Schacky, C. The omega-3 index as a risk factor for cardiovascular diseases. *Prostaglandins and other lipid mediators* **2011***, 96*, 94-98.

215. Albert, B. B.; Derraik, J. G. B.; Brennan, C. M.; Biggs, J. B.; Smith, G. C.; Garg, M. L.; Cameron-Smith, D.; Hofman, P. L.; Cutfield, W. S. Higher omega-3 index is associated with increased insulin sensitivity and more favorable metabolic profile in middle-aged overweight men. *Scientific Reports Nature* **2014**, 1-7.

216. Yi, T.; Li, S. M.; Fan, L. L.; Zhang, Z. F.; Luo, P.; Zhang, X. J.; Wang, J. G.; Zhu, L.; Zhao, Z. Z.; Chen, H. B. Comparative analysis of EPA and DHA in fish oil nutritional capsules by GC-MS. *Lipids in Health and Disease* **2014***, 13*, 190-196.

217. Vongsvivut, J.; Heraud, P.; Zhang, W.; Kralovec, J. A.; McNaughton, D.; Barrow, C. J. Quantitative determination of fatty acid compositions in micro-encapsulated fish-oil supplements using Fourier transform infrared (FTIR) spectroscopy. *Food Chemistry* **2012***, 135*, 603-609.

218. Wu, D.; He, Y. Potential of spectroscopic techniques and chemometric analysis for rapid measurements of docosahexaenoic acid and eicosapentaenoic acid in algal oil. *Food Chemistry* **2014***, 158*, 93-100.

219. Marcone, M. F.; Wang, S.; Albabish, W.; Nie, S.; Xomnarain, D.; Hill, A. Diverse food-based applications of nuclear magnetic resonance (NMR) technology. *Food Research International* **2013***, 51*, 729-747.

220. Barazzoni, R.; Silva, V.; Singer, P. Clinical biomarkers in metabolic syndrome. *Nutrition in clinical practice* **2013***, 29*, 215-221.

221. Alberti, K. G.; Eckel, R. H.; Grundy, S. M. Harmonizing the metabolic syndrome: a joint interim statement of the International Diabetes Federation Task Force on Epidemiology and Prevention. *Circulation* **2009***, 120*, 1640-1645.

222. Arca, M. Alterations of intestinal metabolism in diabetes mellitus and metabolic syndrome. *Atherosclerosis Supplements* **2015***, 17*, 12-16.

223. Ford, E. S.; Giles, W. H.; Dietz, W. H. Prevalence of the metabolic syndrome among U.S. adults: Findings from the third national health and nutrition examination survey. *JAMA* **2002***, 287*, 356-359.

224. Grundy, S. M. Drug therapy of the metabolic syndrome: minimizing the emerging crisis in polypharmacy. *Nat. Rev. Drug Discov.* **2006***, 5*, 295-309.

225. Gupta, A.; Gupta, V. Metabolic syndrome: what are the risks for humans? *Biosci. Trends* **2010***, 4*, 204-212.

226. Falahi, E.; Rad, A. H. K.; Roosta, S. What is the best biomarker for metabolic syndrome diagnosis? *Diabetes and Metabolic Syndrome: Clinical Research and Reviews* **2013**, 1-7.

227. Flachs, P.; Rossmeisl, M.; Kopecky, J. The effect of n-3 fatty acids on glucose homeostasis and insulin sensitivity. *Physiol. Res.* **2014***, 63*, 93-118.

228. Warensjo, E.; Riserus, U.; Vessby, B. Fatty acid composition of serum lipids predicts the development of metabolic syndrome in men. *Diabetologia* **2005***, 48*, 1999-2005.

229. Duncan, B. B.; Schmidt, M. I.; Pankow, J. S.; et al Low-grade systematic inflammation and the development of type-2 diabetes: the atherosclerosis risk in communities study. *Diabetes* **2003***, 52*, 1799-1805.

230. Pradhan, A. D.; Manson, J. E.; Rifai, N.; Buring, J. E.; Ridker, P. M. C-reactive protein, interleukin 6, and risk of developing type 2 diabetes mellitus. *JAMA* **2001***, 286*, 327-334.

231. Goldstein, B. J.; Mahadev, K.; Wu, X. Redox paradox: insulin action is facilitated by insulin-stimulated reactive oxygen species with multiple potential signaling targets. *Diabetes* **2005***, 54*, 311-321.

232. Furukawa, S.; Fujita, T.; Shimabukuro, M. Increased oxidative stress in obesity and its impact on metabolic syndrome. *Journal of Clinical Investigation* **2004***, 114*, 1752-1761.

233. Urakawa, H.; Katsuki, A.; Sumida, Y. Oxidative stress is associated with adiposity and insulin resistance in men. *J Clin Endocrinal Metab* **2003***, 88*, 4673-4676.

234. Kumar, M.; Sarin, S. Biomarkers of disease in medicine. *Current Trends in Science* **2009**, 403-417.

235. Mayeux, R. Biomarkers: Potential Uses and Limitations. *The journal of the American society of experimental neurotherapeutics* **2004***, 1*, 182-188.

236. Drucker, E.; Krapfenbauer, K. Pitfalls and limitation in translation from biomarker discovery to clinical utility in predictive and personalized medicine. *The EPMA Journal* **2013***, 4*, 7-17.

237. Shibusawa, Y. Lipoproteins: comparison of different separation strategies. *J. Chromatogr. B Biomed. Sci. Appl.* **1997***, 699*, 419-437.

238. Daykin, C. A.; Corcoran, O.; Hansen, S. H.; Bjornsdottir, I.; Cornett, C.; Connor, S. C.; Lindon, J. C.; Nicholson, J. K. Application of directly coupled HPLC NMR to separation and characterization of lipoproteins from human serum. *Anal. Chem.* **2001***, 73*, 1084-1090.

239. Chung, B. H.; Segrest, J. P.; Ray, M. J.; Brunzell, J. D.; Hokanson, J. E.; Krauss, R. M.; Beaudrie, K.; Cone, J. T. Single vertical spin density gradient ultracentrifugation. *Methods Enzymol.* **1986**, *128*, 181-209.

240. Terpstra, A. H. M.; Pels, A. E. Isolation of plasma lipoproteins by a combination of differential and density gradient ultracentrifugation. *Fresenius' Zeitschrift für analytische Chemie* **1988**, *330*, 149-151.

241. Chapman, M. J.; Goldstein, S.; Lagrange, D.; Laplaud, P. M. A density gradient ultracentrifugal procedure for the isolation of the major lipoprotein classes from human serum. *J. Lipid Res* **1981**, *22*, 339-358.

242. Redgrave, T. G.; Roberts, D. C. K.; Westa, C. E. Separation of plasma lipoproteins by density-gradient ultracentrifugation. *Analytical Biochemistry* **1975**, *65*, 42-49.

243. Bricarello, D. A.; Smilowitz, J. T.; Zivkovic, A. M.; German, J. B.; Parikh, A. N. Reconstituted lipoprotein: a versatile class of biologically-inspired nanostructures. *ACS Nano* **2011**, *5*, 42-57.

244. Jonas, A.; Wald, J. H.; Toohill, K. L.; Krul, E. S.; Kezdy, K. E. Apolipoprotein A-I structure and lipid properties in homogeneous, reconstituted spherical and discoidal high density lipoproteins. *J. Biol. Chem.* **1990**, *265*, 22123-22129.

245. Atkinson, D.; Small, D. M. Recombinant lipoproteins: implications for structure and assembly of native lipoproteins. *Annu. Rev. Biophys. Biophys. Chem.* **1986**, *15*, 403-456.

246. Atkinson, D.; Deckelbaum, R. J.; Small, D. M.; Shipley, G. G. Structure of human plasma low-density lipoproteins: Molecular organization of the central core. *Proc. Natl. Acad. Sci. USA* **1977**, *74*, 1042-1046.

247. Ginsburg, G. S.; Small, D. M.; Atkinson, D. Microemulsions of phospholipids and cholesterol esters. Protein-free models of low density lipoprotein. *J. Biol. Chem.* **1982**, *257*, 8216-8227.

248. Shahzad, M. M.; Mangala, L. S.; Han, H. D.; Lu, C.; Bottsford-Miller, J.; Nishimura, M.; Mora, E. M.; Lee, J. W.; Stone, R. L.; Pecot, C. V.; Thanapprapasr, D.; Roh, J. W.; Gaur, P.; Nair, M. P.; Park, Y. Y.; Sabnis, N.; Deavers, M. T.; Lee, J. S.; Ellis, L. M.; Lopez-Berestein, G.; McConathy, W. J.; Prokai, L.; Lacko, A. G.; Sood, A. K. Targeted Delivery of Small Interfering RNA Using Reconstituted High-Density Lipoprotein Nanoparticles. *Neoplasia* **2011**, *13*, 309-319.

249. Motulsky, H. *Intuitive Biostatistics: A Nonmathematical Guide to Statistical Thinking;* Oxford University Press: New York, 2010; .

250. McMillan, D. E. Disturbance of serum viscosity in diabetes mellitus. *J. Clin. Invest.* **1974**, *53*, 1071-1079.

251. Rosenson, R. S.; McCormick, A.; Uretz, E. F. Distribution of blood viscosity values and biochemical correlates in healthy adults. *Clin. Chem.* **1996***, 42*, 1189-1195.

252. American Diabetes Association, National Institute of Diabetes, Digestive and Kidney Disorders The prevention or delay of type 2 diabetes. *Diabetes Care* **2002***, 25*, 742-749.

253. genuth, S.; Kahn, R. A step backward-or is it forward? *Diabetes Care* **2008***, 31*, 1093-1096.

254. Richard A. McPherson, Matthew R. Pincus,John Bernard Henry, Ed.; In *Henry's clinical diagnosis and management by laboratory methods;* Saunders Elsevier: Chicago, IL, 2007; , pp 1450.

255. Barbieri, M.; Ragno, E.; Benvenuti, E.; Zito, G. A.; Corsi, A.; Ferrucci, L.; Paolisso, G. New aspects of the insulin resistance syndrome: impact on hematological parameters. *Diabetologia* **2001***, 44*, 1232-1237.

256. kim, J. A.; Choi, Y. S.; Hong, J. I.; Kim, S. H.; Jung, H. H.; Kim, S. M. Assocation of metabolic syndrome with white blood cell subtypes and red blood cells. *Endocrine Journal* **2006***, 53*, 133-139.

257. Akahane, K.; Tojo, A.; Urabe, A.; Takaku, F. Pure erythropoietic colony and burst formations in serum-free culture and their enhancement by insulin like growth factor 1. *Exp Hematol* **1987***, 15*, 797-802.

258. Boyer, S. H.; Bishop, T. R.; Rogers, C. O.; Noyes, A. N.; Frelin, L. P.; Hobbs, S. Roles of erythropoietin, insulin-like growth factor 1 and unidentified serum factors in promoting maturation of purified murine erythroid colony-forming units. *Blood* **1992***, 80*, 2503-2512.

259. Ratajczak, M. Z.; Light, B.; Ratajczak, J.; Kuczysnki, W.; Gewirta, A. M. Human erythropoiesis *in vitro*: definition and clinical implications of optimal stimulatory conditions. *Cancer Res Ther Cont* **1993***, 94*, 1806-1810.

260. Lowe, G. D. O.; Lee, A. J.; Rumley, A.; Price, J. F.; Fowkes, F. G. R. Blood viscosity and risk of cardiovascular events: the Edinburgh artery study. *British Journal of Haematology* **1997***, 96*, 168-173.

261. Sandstrom, C. S.; Ohlsson, B.; Melander, O.; Westin, U.; Mahadeva, R.; Janciauskiene, S. An association between type 2 diabetes and alpha 1-antitrypsin deficiency. *Diabetic Medicine* **2008***, 25*, 1370-1373.

262. Xue, G. B.; Zheng, W. L.; Wang, L. H.; Lu, L. Y. Alpha 1-antitrypsin A novel biomarker for obesity in humans. *Saudi Med J* **2013***, 34*, 34-39.

263. Chapman, M. J.; Ginsberg, H. N.; Amarenco, P.; Andreotti, F.; Boren, J.; Catapano, A. L.; Descamps, O. S.; Fisher, E. l.; Kovanen, P. T.; Kuivenhoven, J. A.; Lesnik, P.; Masana, L.; Nordestgaard, B. G.; Ray, K. K.; Reiner, Z.; Taskinen, M. R.; Tokgozoglu, L.; Tybjaerg-

Hansen, A.; Watts, G. F. Triglyceride-rich lipoproteins and high-density lipoprotein cholesterol in patients at high risk of cardiovascular disease: evidence and guidance for management. *European Heart Journal* **2011**, 1-23.

264. Adiels, M.; Matikainen, N.; Westerbacka, J.; Soderlund, S.; Larsson, T.; Olofsson, S. O.; Boren, J.; Taskinen, M. R. Postprandial accumulation of chylomicrons and chylomicron remnants is determined by the clearance capacity. *Atherosclerosis* **2012**, *222*, 222-228.

265. Havel, R. J. Postprandial hyperlipidemia and remnant lipoproteins. *Curr. Opin. Lipidol.* **1994**, *5*, 102-109.

266. Jones, A. L.; Hradek, G. T.; Hornick, C.; Renaud, G.; Windler, E. E.; Havel, R. J. Uptake and processing of remnants of chylomicrons and very low density lipoproteins by rat liver. *J. Lipid Res.* **1984**, *25*, 1151-1158.

267. Nakajima, K.; Nakano, T.; Tokita, Y.; Nagamine, T.; Yatsuzuka, S.; Shimomura, Y.; Tanaka, A.; Sumino, H.; Nara, M.; Machida, T.; Murakami, M. The characteristics of remnant lipoproteins in the fasting and postprandial plasma. *Clin. Chim. Acta* **2012**, *413*, 1077-1086.

268. Rohlff, C. Protemoics in neuropsychiatric disorders. *Int J Neuropsychopharmacol* **2001**, *4*, 93-102.

269. O'Bryant, S. E.; Johnson, L.; Reisch, J.; Edwards, M.; Hall, J.; Barber, R.; Devous MD, S.; Royall, D.; Singh, M. Risk factors for mild cognitive impairment among Mexican Americans. *Alzheimers Dement.* **2013**, *9*, 622-631.e1.

270. Rosenson, R. S.; Brewer, H. B.,Jr; Chapman, M. J.; Fazio, S.; Hussain, M. M.; Kontush, A.; Krauss, R. M.; Otvos, J. D.; Remaley, A. T.; Schaefer, E. J. HDL measures, particle heterogeneity, proposed nomenclature, and relation to atherosclerotic cardiovascular events. *Clin. Chem.* **2011**, *57*, 392-410.

271. Klingenberg, C. P. MorphoJ: an integrated software package for geometric morphometrics (see also http://www.flywings.org.uk/MorphoJ_guide/frameset.htm?covariation/regression.htm). *Mol. Ecol. Resour.* **2011**, *11*, 353-357.

272. Klingenberg, C. P. Regression. MorphoJ User's Guide. 2014).

273. Lundblad, R. Considerations for the Use of Blood Plasma and Serum for Proteomic Analysis. *The Internet Journal of Genomics and Proteomics* **2003**, *1(2)*.

274. Boldyrev, A. A.; Aldini, G.; Derave, W. Physiology and pathophysiology of carnosine. *Physiol. Rev.* **2013**, *93*, 1803-1845.

275. Venu, K.; Denisov, V. P.; Halle, B. Water ^{1}H Magnetic Relaxation Dispersion in Protein Solutions. A Quantitative Assessment of Internal Hydration, Proton Exchange, and Cross-Relaxation. *J. Am. Chem. Soc.* **1997***, 119*, 3122-3134.

276. Chen, E.; Kim, R. J. Magnetic Resonance Water Proton Relaxation in Protein Solutions and Tissue: $T_{1(rho)}$ Dispersion Characterization. *PLoS ONE* **2010***, 5*, e8565.

277. Einstein, A. *Investigations on the Theory of the Brownian Movement;* Dover Publications: Mineola, New York, 1956 (re-publication of the original translation from 1926); .

278. Debye, P. J. W. *Polar molecules;* The Chemical Catalog Company, Inc.: New York, 1929; .

279. Fuller, J. H.; Keen, H.; Jarrett, R. J.; Omer, T.; Meade, T. W.; Chakrabarti, R.; North, W. R.; Stirling, Y. Haemostatic variables associated with diabetes and its complications. *Br. Med. J.* **1979***, 2*, 964-966.

280. Kannel, W. B.; D'Agostino, R. B.; Wilson, P. W.; Belanger, A. J.; Gagnon, D. R. Diabetes, fibrinogen, and risk of cardiovascular disease: the Framingham experience. *Am. Heart J.* **1990***, 120*, 672-676.

281. Raynaud, E.; Perez-Martin, A.; Brun, J.; Aissa-Benhaddad, A.; Fedou, C.; Mercier, J. Relationships between fibrinogen and insulin resistance. *Atherosclerosis* **2000***, 150*, 365-370.

282. Gonzalez-Quintela, A.; Alende, R.; Gude, F.; Campos, J.; Rey, J.; Meijide, L. M.; Fernandez-Merino, C.; Vidal, C. Serum levels of immunoglobulins (IgG, IgA, IgM) in a general adult population and their relationship with alcohol consumption, smoking and common metabolic abnormalities. *Clinical & Experimental Immunology* **2008***, 151*, 42-50.

283. Lippi, G.; Targher, G.; Montagnana, M.; Salvagno, G. L.; Zoppini, G.; Guidi, G. C. Relation between red blood cell distribution width and inflammatory biomarkers in a large cohort of unselected outpatients. *Arch. Pathol. Lab. Med.* **2009***, 133*, 628-632.

284. Talukdar, S.; Oh da, Y.; Bandyopadhyay, G.; Li, D.; Xu, J.; McNelis, J.; Lu, M.; Li, P.; Yan, Q.; Zhu, Y.; Ofrecio, J.; Lin, M.; Brenner, M. B.; Olefsky, J. M. Neutrophils mediate insulin resistance in mice fed a high-fat diet through secreted elastase. *Nat. Med.* **2012***, 18*, 1407-1412.

285. Shi, C.; Pamer, E. G. Monocyte recruitment during infection and inflammation. *Nat Rev Immunol* **2011***, 11*, 762-774.

286. von Hundelshausen, P.; Weber, C. Platelets as Immune Cells: Bridging Inflammation and Cardiovascular Disease. *Circulation Research* **2007***, 100*, 27-40.

287. Halliwell, B.; Clement, M. V.; Long, L. H. Hydrogen peroxide in the human body. *FEBS Lett.* **2000***, 486*, 10-13.

288. Halliwell, B.; Gutteridge, J. M. Role of free radicals and catalytic metal ions in human disease: an overview. *Methods Enzymol.* **1990***, 186*, 1-85.

289. Trelstad, R. L.; Lawley, K. R.; Holmes, L. B. Nonenzymatic hydroxylations of proline and lysine by reduced oxygen derivatives. *Nature* **1981***, 289*, 310-312.

290. Stadtman, E. R. Oxidation of free amino acids and amino acid residues in proteins by radiolysis and by metal-catalyzed reactions. *Annu. Rev. Biochem.* **1993***, 62*, 797-821.

291. Anraku, M.; Chuang, V. T.; Maruyama, T.; Otagiri, M. Redox properties of serum albumin. *Biochim. Biophys. Acta* **2013***, 1830*, 5465-5472.

292. Hampton, M. B.; Kettle, A. J.; Winterbourn, C. C. Inside the neutrophil phagosome: oxidants, myeloperoxidase, and bacterial killing. *Blood* **1998***, 92*, 3007-3017.

293. Kolaczkowska, E.; Kubes, P. Neutrophil recruitment and function in health and inflammation. *Nat. Rev. Immunol.* **2013***, 13*, 159-175.

294. Bruschi, M.; Candiano, G.; Santucci, L.; Ghiggeri, G. M. Oxidized albumin. The long way of a protein of uncertain function. *Biochim. Biophys. Acta* **2013***, 1830*, 5473-5479.

295. Vidal, P.; Deckert, T.; Hansen, B.; Welinder, B. S. High-performance liquid chromatofocusing and column affinity chromatography of in vitro ^{14}C-glycated human serum albumin. Demonstration of a glycation-induced anionic heterogeneity. *J. Chromatogr.* **1989***, 476*, 467-475.

296. Savaryn, J. P.; Catherman, A. D.; Thomas, P. M.; Abecassis, M. M.; Kelleher, N. L. The emergence of top-down proteomics in clinical research. *Genome Med.* **2013***, 5*, 53.

297. Apweiler, R.; Aslanidis, C.; Deufel, T.; Gerstner, A.; Hansen, J.; Hochstrasser, D.; Kellner, R.; Kubicek, M.; Lottspeich, F.; Maser, E.; Mewes, H. W.; Meyer, H. E.; Mullner, S.; Mutter, W.; Neumaier, M.; Nollau, P.; Nothwang, H. G.; Ponten, F.; Radbruch, A.; Reinert, K.; Rothe, G.; Stockinger, H.; Tarnok, A.; Taussig, M. J.; Thiel, A.; Thiery, J.; Ueffing, M.; Valet, G.; Vandekerckhove, J.; Verhuven, W.; Wagener, C.; Wagner, O.; Schmitz, G. Approaching clinical proteomics: current state and future fields of application in fluid proteomics. *Clin. Chem. Lab. Med.* **2009***, 47*, 724-744.

298. Hansson, G. K. Inflammation, atherosclerosis, and coronary artery disease. *N. Engl. J. Med.* **2005***, 352*, 1685-1695.

299. De Felice, F. G.; Ferreira, S. T. Inflammation, Defective Insulin Signaling, and Mitochondrial Dysfunction as Common Molecular Denominators Connecting Type 2 Diabetes to Alzheimer Disease. *Diabetes* **2014***, 63*, 2262-2272.

300. Flores, M.; Glusman, G.; Brogaard, K.; Price, N. D.; Hood, L. P4 medicine: how systems medicine will transform the healthcare sector and society. *Per Med.* **2013***, 10*, 565-576.

301. Berman, P.; Leshem, A.; Etziony, O.; Levi, O.; Parmet, Y.; Saunders, M.; Wiesman, Z. Novel ^{1}H low field nuclear magnetic resonance applications for the field of biodiesel. *Biotechnology for Biofuels* **2013***, 6*, 55.

302. Krishnan, V. V.; Murali, N. Radiation damping in modern NMR experiments: Progress and challenges. *Progress in Nuclear Magnetic Resonance Spectroscopy* **2013***, 68*, 41-57.

303. Raymond, K. N.; Pierre, V. C. Next generation, high relaxivity gadolinium MRI agents. *Bioconjug. Chem.* **2005***, 16*, 3-8.

304. Yilmaz, A.; Chu, S. C.; Osmanoglu, S. Dependence of the solvent proton 1/T1 on the iron content in normal human serum. *Magn. Reson. Med.* **1988***, 7*, 337-339.

305. Weinmann, H. J.; Brasch, R. C.; Press, W. R.; Wesbey, G. E. Characteristics of gadolinium-DTPA complex: a potential NMR contrast agent. *AJR Am. J. Roentgenol.* **1984***, 142*, 619-624.

306. Patt, S. L.; Sykes, B. D. Water eliminated Fourier transform NMR spectroscopy. *Journal of Chem. Physics* **1972***, 52*, 3192.

307. Cavanagh, J.; Fairbrother, W. J.; Palmer III, W. G.; Rance, M.; Skelton, N. J. *Protein NMR Spectroscopy;* Elsevier: 2007; .

308. Yip, G. N.; Zuiderweg, E. R. A phase cycle scheme that significantly suppresses offsset-dependant artifacts in the R2-CPMG 15N relaxation experiment. *Journal of Magnetic Resonance* **2004***, 171*, 25-36.

309. McPherson, R.; Pincus, M. *Henry's Clinical Diagnosis and Management by Laboratory Methods (Clinical Diagnosis & Management by Laboratory Methods);* Saunders elsevier: 2006; .

310. Halvorsen, B. L.; Blomhoff, R. Determination of lipid oxidation products in vegetable oils and marine omega-3 supplements. *Food and Nutrition Research* **2011***, 55*, 5792.

311. Reiter, R. J.; Tan, D. X.; Galano, A. Melatonin reduces lipid peroxidation and membrane viscosity. *Frontiers in Physiology* **2014***, 5*, 377.

312. Muizebelt, W. J.; Nielen, M. W. F. Oxidative Crosslinking of Unsaturated Fatty Acids Studied with Mass Spectrometry. *Journal of Mass Spectrometry* **1998***, 31*, 454-554.

313. Garaulet, M.; Pérez-Llamas, F.; Pérez-Ayala, M.; Martínez, P.; Sánchez de Medina, F.; Tebar, F. J.; Zamora, S. Site-specific differences in the fatty acid composition of abdominal adipose tissue in an obese population from a Mediterranean area: relation with dietary fatty acids, plasma lipid profile, serum insulin, and central obesity. *American Society for Clinical Nutrition* **2001***, 74*, 585-591.

314. Cespedes, E.; Baylin, A.; Campos, H. Adipose tissue n-3 fatty acids and metabolic syndrome. *European Journal of Clinical Nutrition* **2015***, 69*, 114-120.

315. Gustafson, B.; Hedjazifar, S.; Gogg, S.; Hammarstedt, A.; Smith, U. Insulin Resistance and Impaired Adipogenesis. *Trends in Endocrinology and Metabolism* **2015**.

316. Kihara, S.; Matsuzawa, Y. Fat Distribution and Cardiovascular Disease Risk. *Curr Cardiovasc Risk Rep* **2015***, 9*, 8.

317. Sobradillo, P.; Pozo, F.; Agusti, A. P4 Medicine: the Future Around the Corner. *Arch Bronconeumol* **2011***, 47*, 35-40.

Appendix A: IRB Protocol Novel Methods for Analyzing Human Serum Lipoproteins (Protocol 2013-205; first approved 10/11/13) Protocol Synopsis

Novel Methods for Characterizing Human Serum Lipoprotein Particles
PI: David P. Cistola, M.D., Ph.D.

Protocol Synopsis

PURPOSE OF THE STUDY

The overall, long-term objective is to develop novel diagnostic and screening methods for human blood, including serum and plasma, focusing primarily on lipoprotein particles as biomarkers. The overall approach is to correlate these biomarkers with metabolic abnormalities and disease risk. We hypothesize that benchtop time-domain NMR (TD-NMR), dynamic light scattering, flow cytometry, high-pressure liquid chromatography (HPLC) and related methods can be used to observe the properties of lipoprotein nanoparticles, such as particle core composition, size, number and morphology.

BACKGROUND, SPECIFIC AIMS AND SIGNIFICANCE

Lipoproteins are spherical assemblies of lipids and proteins that circulate in the blood stream transporting triglycerides and cholesterol to and from tissues for metabolic and storage purposes. Lipoprotein abnormalities are strongly associated with cardiovascular disease events as well as metabolic disorders such as insulin resistance and diabetes. These particle abnormalities include lipoprotein particle cholesterol concentration, particle size and number. While generally useful, many of the current scientific and clinical methods for monitoring these abnormalities are either insufficient for detecting disease risk across the entire population, or too expensive and complex for routine use in a clinical diagnostic or community setting.

The specific aims of this pilot project are:

(1) Monitor variability in lipoprotein *core composition* in human subjects using benchtop TD-domain NMR and related methods; assess the resolution of individual lipoprotein classes in unfractionated or partially fractionated serum or plasma samples.

(2) Monitor variability in lipoprotein *particle size and size distributions* in human subjects using dynamic light scattering, HPLC and related methods; assess the resolution of individual lipoprotein classes in unfractionated and partially fractionated serum samples

(3) Monitor changes in lipoprotein *particle number* using a modified flow cytometry and related methods; assess the resolution of lipoprotein classes in unfractionated and partially fractionated serum samples.

The ability to determine lipoprotein core composition, particle size and particle number using these novel techniques may improve early risk detection for a number of diseases, and may aid in patient diagnosis and management.

PRELIMINARY STUDIES

Benchtop Time-domain NMR

We have developed and parameterized a method to detect several resolvable components in unfractionated whole human serum using the NMR relaxation time constant, T_2. Unlike high-resolution frequency-domain NMR, benchtop TD- NMR can characterize and resolve mobility domains of macromolecules using much simpler instrumentation and techniques. Comparison of the TD-NMR T_2 profiles for whole serum and fractionated lipoproteins revealed that LDL and HDL particles have unique T_2 values that can be resolved in whole human serum. The T_2 components appear to originate from mobility domains within the lipid acyl chains of the LDL particle. Variations in T_2 primarily reflect changes in the triglyceride/cholesteryl ester ratio in the lipid core of LDL and HDL particles. During an oral triglyceride tolerance test in one human subject, benchtop TD-NMR was able to monitor the remodeling of the lipid core of LDL and HDL during post-prandial metabolism. A US Patent on this method was filed in March 2013.

A key issue to be addressed in the current study is the degree of subject-to-subject variation in human serum T_2 and the possible correlation of T_2 with metabolic and cardiovascular biomarkers.

Dynamic Light Scattering

We have been developing dynamic light scattering as a method for examining lipoprotein particle size distributions in whole human serum. So far we have collected and analyzed data from whole serum and from ultracentrifuge fractions of human plasma and compared our findings with data from transmission electron microscopy.

INVESTIGATOR EXPERIENCE

Dr. David P. Cistola:
Completed all necessary training necessary for UNTHSC including but not limited to; BSL 2 training, ethics, blood borne pathogens, and laboratory safety.

Dr. Cistola holds the M.D. and Ph.D. (Biochemistry) degrees from Boston University School of Medicine. After graduation in 1985, he held a NIH Post-doctoral Fellowship in the Cardiovascular and Biophysics Institutes for two years and the Andrew Costello Fellowship of the Juvenile Diabetes Foundation International for an additional two years. In 1989, he joined the faculty of the Washington University School of Medicine, where he served as a faculty member in the Department of Biochemistry & Molecular Biophysics for 18 years. In 2007, he joined East Carolina University as an Associate Dean for Research and a faculty member in Clinical Laboratory Science and in Biochemistry & Molecular Biology in the Brody School of Medicine. In 2012, he became Vice President for Research and Professor at the UNT Health

Science Center. He has 35 years of research and teaching experience in the application of NMR and biophysical methods to the study of lipid and proteins.

Michelle D. Robinson:
Completed all necessary training necessary for UNTHSC including but not limited to; BSL 2 training, ethics, blood borne pathogens, and laboratory safety.

Ms. Robinson has been working in the laboratory since 2006, starting at Edinboro University, where she earned a Bachelor degree. She started graduate school in 2009 and has worked alongside Dr. Cistola to collect most of the preliminary data since the summer of 2010 as his graduate student at East Carolina University. Currently, she is a full-time employee at UNTHSC, serving as Senior Research Assistant. Her specialized areas of knowledge and expertise include lipoprotein metabolism, lipoprotein remnants, cardiovascular disease, time-domain NMR, protein quantitation, serum cholesterol and triglyceride quantitation, western blotting and obtaining, handling and processing blood samples from the clinical laboratory.

Sneha Deodhar:
Completed all necessary training necessary for UNTHSC including but not limited to; BSL 2 training, ethics, blood borne pathogens, and laboratory safety.

Ms. Deodhar joined the laboratory in December 2013 and serves as our Chief Technician and Lab Manager. She has a MS in Biotechology from Louisiana Tech University and has several years of research experience working with nanoparticles. She has developed and tested several of the liquid chromatography techniques used on our laboratory. She was added to the protocol during the past year.

Ina Mishra and Vipulkumar Patel:
Completed all necessary training necessary for UNTHSC including but not limited to; BSL 2 training, ethics, blood borne pathogens, and laboratory safety.

Ina and Vipul are second-year PhD students in the Biochemistry & Cancer Program, Graduate School of Biomedical Sciences, UNTHSC. They were added to the protocol this past year.

Stephen Atkinson:
Completed all necessary training necessary for UNTHSC including but not limited to; BSL 2 training, ethics, blood borne pathogens, and laboratory safety.

Stephen joined the lab in summer 2014 as a TCOM Summer Fellow. He is currently a second-year medical student in TCOM and continues to be engaged in this research on an intermittent basis, as his educational schedule permits. He was added to this protocol during the past year.

Katrina Gordon, Ph.D.:
Katrina is Core Facility Manager of the UNTHSC Discovery Center. She has significant biomedical research experience as a staff scientist, and previously as a postdoctoral fellow and

PhD student. She is collaborating with us on this protocol and has completed all necessary training. She was added to the protocol in May 2014.

DESCRIPTION OF ASSOCIATED RESEARCH PROJECTS

Metabolic Remodeling of Human Serum Lipoprotein Particles: IRB 2013-018.
This protocol received full board review and approval in February 2013 and was renewed in 2014. Unlike the current protocol, 2013-018 involves multiple blood draws in a single individual in one day.

DESCRIPTION OF BIOSPECIMENS AND BEHAVIORAL/HEALTH DATA THAT WIL BE USED I N THE STUDY

The plasma and serum samples will be submitted for routine clinical testing (lipid panel, serum glucose, A1C, serum protein, etc.) as well as project-specific analyses. Analyses of the unfractionated and fractionated serum or plasma samples by dynamic light scattering, benchtop time-domain NMR, transmission electron microscopy, flow cytometry and related methods will be ongoing for several weeks following the blood draw in the UNTHSC lab. All specimens will be handled according to BSL 2 protocol.

In most cases, there will only be one blood draw per subject. In cases where the protocol may be repeated in a given subject, it will occur no sooner than 8 weeks after the prior blood donation. If the subject's health status changes, no donation will occur without prior permission from the subject's primary care physician.

The identification of subjects associated with a particular blood sample does not place them at risk of criminal or civil liability. This research is not classified. A Waiver of Documentation of Informed Consent (Form A) will be obtained, signed and filed for each participating subject. If the subject has any questions they are to be directed towards the research personnel in charge.

To prevent the sample identification each specimen will be given a special research code number that is intended to protect the subjects' identity. The blood specimens will be labeled with a unique research number (URN) that will be known only to research personnel, which includes Dr. David P. Cistola, Michelle D. Robinson and other key personnel, on a strict need to know basis. A portion of the samples will be kept in storage and may be used for future research or by other researchers. We will keep the list of samples donors in a secure location and only authorized study personnel will have access to it.

PROSPECTIVE (FUTURE) COLLECTION OF BIOSPECIMENS FROM HUMAN SUBJECTS

Blood Draw Protocol

The blood tubes will be drawn by a nurse or trained phlebotomist at the University of North Texas Health Science Center, possibly including those employed by Quest or Labcorp. The blood samples will be transported to the laboratory according to BSL 2 procedure.

(1.) Fasting blood draw (option 1 – used with most subjects):

- The subject will undergo a fast of at least 12 hours (typically overnight) by not consuming any food or calories (water only). Following the blood draw (typically in the early morning), the subject is free to consume food, beverages and medications immediately after.

(2.) Fasting and post prandial blood draw (option 2) :

- The subject will undergo a fast of at least 12 hours (typically overnight) by not consuming any food or calories (water only). Immediately after the first blood draw, the patient will consume an over-the-counter beverage containing the following nutritional content.

Boost Glucose Control (Nestle Healthcare Nutrition, Inc)
56 fluid ounces containing:
1330 calories (approximately half of the recommended daily caloric intake for an adult male/female)
49 g fat, including 70 mg cholesterol
112 g carbohydrates (28g as sugars)
112 g protein

- Following the liquid meal in the morning, the donor drinks only water throughout the blood collection period. At a specific post prandial time point (1-9 hours after the meal has been ingested) a second blood draw will be performed. Normal eating is resumed immediately after the final blood draw.

Total blood volume drawn **Less than 550cc**

Description of human subjects:

Up to 45 human subjects, male or female, of all races, between the ages of 18 and 70 will be accepted for participation. The subjects will be recruited by word-of-mouth by lab personnel without impact on employee position or student status. A medical history questionnaire will be completed by each subject before enrollment (copy attached). The rationale for the medical history questionnaire is that particular blood test values are more meaningfully interpreted in the context of the subject's history. For example, a serum cholesterol value of 200 mg/dl has a different significance in an individual taking a statin drug vs. someone not on cholesterol lowering therapy. The patient must be over 110 pounds, not pregnant or planning on becoming pregnant or currently breast feeding. HIV positive subjects will not be eligible. If the subject has a history of anemia, problems with blood clotting, bleeding disorders or other blood

diseases, they will be excluded. Informed Consent will be obtained, signed and filed for each participating subject. If the subject has any questions they are to be directed towards the research personnel in charge.

TRANSFER OF THE BIOSPECIMENS AND RELATED DATA

The blood samples will be transported to the laboratory according to BSL 2 procedure and handled with care by qualified research personnel at UNTHSC, where the blood draws will take place. The serum and plasma samples that are sent off for clinical testing will be carefully sealed and picked up by Labcorp, Quest or shipped to other offsite laboratories. Key lab personnel will be responsible for the safe and effective transportation or shipping of the samples to their appropriate destination. Some of the serum and plasma clinical samples will be analyzed at Labcorp, Quest and other outside companies contracted for this research. The data (without patient identifiers) will be available to key lab personnel, for which you need a user name and password to gain entry. Only key research personnel know this username and password.

The ultracentrifugation fractions will be processed at UNTHSC, were all of the experiments and analysis will take place. All other testing will be performed in Dr. Cistola's laboratory.

ANALYSIS OF THE BIOSPECIMENS AND RELATED DATA

Once the data has been collected from outside contract labs, it will be analyzed in the laboratory, CBH 303. The specimens that have been kept at UNTHSC for research purposes will also be analyzed in CBH 303 and in several other sites on the UNTHSC campus

The blood samples will be typically be converted to either plasma or serum for future analysis. Whole plasma or serum will be used on the benchtop TD-NMR, dynamic light scatter and with flow cytometry to develop the new diagnostics. The whole plasma and serum samples will then be fractionated using various methods, including density-gradient ultracentrifugation, high-performance liquid chromatography and chemical precipitation.

The fractionated samples will be analyzed on the NMR, DLS and Flow cytometer as well. In addition they will be subjected to enzymatic assays to determine the chemical composition. The fractions and whole plasma and serum will be imaged using negative stain electron microscopy at UNTHSC. The lipoprotein classes will further be characterized by their size and electric charge by gradient gel electrophoresis and related methods in our laboratory.

This work conducted in Dr. Cistola's lab will be performed by key personnel listed on this protocol.

STORAGE OF THE BIOSPECIMENS AND RELATED DATA

In the short term, the samples will be stored in a 4°C refrigerator located in the laboratory in CBH 303. Some samples may be frozen and stored in the -80 degree freezer in the Cistola lab.

The biospecimens will not contaminate the storage area and will be stored according the BLS 2 procedure, where other biological samples are currently being held.

RISK/BENEFIT ASSESSMENT

The probability of harm to any participating individual is extremely low. This is a routine blood draw done by a professional. There will be minor discomfort during the blood draw (when the needle is inserted into the vein) but no more than is experienced in any clinical setting during routine phlebotomy and blood testing.

The identification of subjects associated with a particular blood sample does not place them at risk of criminal or civil liability. This research is not classified. The samples obtained will be de-identified; therefore any information that happens to be exposed will not be linked to any particular individual. The information we get from the study is stored on UNTHSC computers which are highly secure. A user name and password are needed to obtain any of this information and can only be accessed by key personnel of laboratory. In addition, key access is necessary to get into the lab itself.

The subject will not directly benefit from this study other than the opportunity to obtain test results that can be shared with their clinical care provider. Society will benefit from this if the diagnostics become developed into useful clinical tools. If our hypothesis is correct then these instruments may be used in the future to earlier diagnose a metabolic disturbance and treatment can begin sooner preventing future cardiovascular or metabolic events.

SPECIAL PRECAUTIONS

The specimens and related health information will be devoid of personal identifiers, and a numerical code will be assigned to all samples and data sets. The master list and code key will be kept secure in facilities controlled by the principal investigator.

SUBJECT COMPENSATION/SUBJECT COSTS

There will be no cost or compensation to the subject.

OWNERSHIP OF BIOSPECIMENS

After the blood is drawn it will be the property of UNTHSC.

KEY PERSONNEL

Dr. David P. Cistola Michelle D. Robinson
Sneha Deodhar
Ina Mishra
Vipulkumar Patel
Steven Atkinson
Dr. Katrina Gordon

Consent Form

University of North Texas Health Science Center

PERMISSION TO PARTICIPATE IN RESEARCH AND USE OR DISCLOSE YOUR PROTECTED HEALTH INFORMATION

TITLE: Novel Methods for Characterizing Human Serum Lipoprotein Particles

PRINCIPAL INVESTIGATOR: David P. Cistola, M.D., Ph.D.

CO-INVESTIGATOR(S): Sneha Deodhar, Michelle Robinson, Ina Mishra, Vipulkumar Patel, Katrina Gordon, Stephen Atkinson

INSTITUTION: University of North Texas Health Science Center at Fort Worth

SUBJECT NAME: (please print):_____

I. STUDY PURPOSE

Lipoproteins are spherical particles of lipids and proteins that circulate in the blood. They transport triglycerides and cholesterol to and from tissues for metabolic and energy storage purposes. Lipoprotein abnormalities are strongly associated with cardiovascular and metabolic diseases. These abnormalities include increased lipoprotein cholesterol concentration, decreased particle size and increased particle number. While generally useful, some of the current scientific and clinical methods for monitoring these abnormalities are either insufficient for detecting disease risk across the population, or too expensive and complex for routine use in the clinical diagnostic setting.

The overall, long-term objective of this research is to develop novel, simple and inexpensive diagnostic and screening methods for lipoproteins that improve the assessment of a patient's disease risk. In particular, we are investigating the application of benchtop time-domain NMR for assessing variation in the lipoprotein particle's lipid core, and dynamic light scattering for assessing particle size distributions.

In addition to the project-specific analyses, the human plasma and serum samples will be submitted for conventional clinical testing (lipid panel, serum glucose, A1C, serum protein, etc.). Analysis of the unfractionated and fractionated serum or plasma samples by dynamic light scattering, benchtop time-domain NMR, transmission electron microscopy and flow cytometry will be ongoing for several weeks following the blood draw.

II. STUDY PROCEDURES

If you, as a healthy individual between the ages of 18 and 70, agree to participate in this study, we will collect:

Blood samples: we would like you to donate blood as follows:

A maximum of 550 ml (or about 36.7 tablespoons) in a total of 2 or less visits will be collected. In these visits, we will collect blood using a needle inserted into a vein in your arm. Your blood will then be analyzed to understand the physical properties of lipoproteins. We may also keep some samples for future studies and look at them for other biomarkers that may be related to various health and disease factors such as: cardiovascular diseases, type-II diabetes, insulin resistance, and other various metabolic disorders.

At each of these blood draw visits, spaced at least 8 weeks apart, we will collect at the most 550 ml or approximately 36.7 tablespoons of blood. There will be a maximum of 2 blood draws in a week, if needed for an overall total of 550 ml (about 36.7 tablespoons).

Before obtaining blood samples, we will ask you to fill out a medical history questionnaire similar to that in a doctor's office. This questionnaire will not include your name or any other personally identifiable information. The purpose of the questionnaire is to obtain information that assists in the proper interpretation of your blood test values. Please note that if you are pregnant, you will not be allowed in this study. If you are planning to become pregnant or are breast-feeding, you may not participate in the study. If you know you are HIV positive you will be excluded from the study. If you are taking any medications, you should disclose the name of those medications, frequency and dosage to the investigators prior to participating in the study. For example, you should mention any cholesterol or lipid-lowering agents or any agents used to treat high blood pressure. Depending on the type and nature of the medications you are taking, you may be excluded from the study at the discretion of the Principal Investigator. If you have a history of anemia, problems with blood clotting or blood diseases, you should not be in this study and will be excluded.

Sample Storage and Use

Once we collect the samples from you, they will be given a special research code number that is intended to protect your identity. Your blood specimen tube(s) will be labeled with a unique research number (URN) that will be known only to research personnel. A portion of the samples will be kept in storage and may be used for future research or by other researchers. We will keep the list of samples donors in a secure location and only authorized study personnel will have access to it. We may send your de-identified samples along with your de-identified research clinical information to other researchers at UNTHSC or other research institutions. These samples will be stored indefinitely. It is important that you understand that once your blood samples are collected and stored for this study; there will not be a way to withdraw them. These

samples will be de-identified. As a result, we will not be able to locate your specific sample and destroy it.

As a precaution and to manage and minimize risk, please know that any future research use of your samples must be reviewed and approved by an independent scientific ethics committee, often called an IRB (Institutional Review Board) at UNTHSC. This IRB will be responsible for making sure that your de-identified samples are used for legitimate research purposes.

III. RISKS AND DISCOMFORTS OF THE STUDY

There are two different kinds of risk from being in this study: procedural risks associated with the blood draw itself, and informational risk associated with the information we obtain from your samples.

The Procedural Risk for the blood draw involves potential side effects such as pain and tenderness in the area from which the blood is drawn. A small amount of bruising at the area from which the blood is drawn may occur. There is a small risk of any prolonged bleeding and/or infection at the injection site. We plan to manage this risk by using standard clinical procedures for taking blood, similar to when you go to a clinic or lab to have blood work done.

The Informational Risk associated with being in this study is the possibility that information from your blood (blood levels of biomarkers, genetic information, etc.) may fall into the wrong hands. We manage this risk by having strict confidentiality controls over the information, and restrict who has access to your blood values or genetic information. In this way, we hope to manage and minimize the risk of breach of confidentiality.

IV. BENEFITS

You will receive no direct benefit by participating in this study, but we hope that the samples and information you provide may give scientists a better understanding of lipoprotein physiochemical properties related to disease risk as monitored by benchtop time-domain NMR, dynamic light scattering and related methods.

V. ARE THERE ALTERNATIVES TO BEING IN THIS STUDY?

You may choose not to take part in this study. Whether you choose to take part or not, your treatment and/or medical care will stay the same.

VI. WHAT ABOUT COSTS?

Taking part in this research study will not require any additional costs for you or your insurance company. There are no plans to compensate you should any new products be developed using the samples that you donated for this study.

The University of North Texas Health Science Center (UNTHSC) has not set aside any funds to compensate (pay) you in case you are injured as a result of taking part in this research study.

VII. WILL I BE PAID TO BE IN THIS STUDY?

No. Only one visit is anticipated, although we may call you back for additional visits with at least 8 weeks in between.

VIII. WILL MY RECORDS BE KEPT CONFIDENTIAL?

Efforts will be made to keep your personal information private. Unfortunately, complete privacy cannot be assured. Information about you may be disclosed as allowed by law. Published results of this research will not identify you as a participant in any way.

The Health Information Portability and Accountability Act (HIPAA) was written to make sure that the privacy of patients and their families is respected by the people that use your Protected Health Information (PHI). Protected Health Information includes any information that relates to your past, present, or future physical or mental health or condition; the health care being provided to you; or the past, present, or future payment for the health care that was, is or will be provided to you. UNTHSC is dedicated to the protection of your personal, medical, and financial information. However, if you are enrolled in research, it may be necessary to submit your PHI to fulfill the objectives of the research as is outlined above.

What else should I know?

- The choice to give permission (authorization) for UNTHSC researchers to use or share (disclose) your protected health information (PHI) is voluntary. No one can force you to give permission. However, you must give permission if you want to be in the research. Sharing the information includes sending it to the sponsor.

- UNTHSC will keep all patient information private in accordance with federal law. However, once your information has been shared, UNTHSC cannot guarantee that it will remain protected.

- By signing this document, you are allowing UNTHSC, and the research team led by the Principal Investigator, Dr. David P. Cistola, to use and/or disclose your PHI for the purpose of participating in this research.

How long can my information be used or shared?

- Unless you withdraw your permission in writing to Dr. Dr. David P. Cistola, UNTHSC researchers can continue to use or share your information indefinitely, or until the study is totally closed and the researchers no longer need additional information about the research participant population for this study.

- If you choose to withdraw your permission, the information that was used or disclosed prior to your withdrawal will continue to be used by the researchers.

- At the time of withdrawal of your permission/participation in the research, your PHI will no longer be submitted for use to the researchers.

What are my rights as a research participant?

You have the right to know about the release of your PHI. You have the right to withdraw your participation at any and all levels of participation at any time. You have the right to have all your questions and concerns addressed and answered to the best of our ability.

Note that your information and records will be kept as confidential as possible under current local, state, and federal laws. However, personnel from federal regulatory agencies and members of the Institutional Review Board may examine your records and study data. In case the final data should be prepared for publication, your name will not appear in any published material.

IX. COMPENSATION FOR INJURY

We at the University of North Texas Health Science Center at Fort Worth have not set aside any funds for financial compensation or for costs of medical treatment should you be injured as a result of your participation in this research. If required, medical care will be made available to you in the case of such injury, but you (or your private insurer, Medicare, Medicaid or other governmental healthcare program) will be responsible for the expense of any medical care, including hospitalization that is needed.

You should know that by signing this form you are neither waiving any of your legal rights against nor releasing Dr. Dr. David P. Cistola, the University of North Texas Health Science Center at Fort Worth or any of their respective agents from liability for negligence with respect to the conduct of this study. If you are injured and feel that your injury justifies pursuing a legal remedy, you have the right to do so.

X. LEAVING THE STUDY

You can choose not to be in the study or to leave the study at any time without penalty or loss of benefits that you are otherwise entitled.

XI. CONTACTS

If a study related problem should occur, or if you have any questions at any time about the study, you may contact David P. Cistola, M.D., PhD (817) 735-2634. If you have any questions about your rights as a participant in this study, you may contact the Chairman, Institutional Review Board, and University of North Texas Health Science Center at Fort Worth at (817) 735-0409 for more information.

XII. CONSENT

I voluntarily agree to participate in this study. I have had the chance to ask any questions I have regarding the study. If I am a student or employee of the University of North Texas Health Science Center at Fort Worth, I have been told that my participation (or non-participation) will in no way affect my academic status or employment status.

I WILL RECEIVE A COPY OF THIS SIGNED INFORMED CONSENT AGREEMENT.

_____ _____

Signature of Subject or
Legal Representative of the Subject

Date

_____

Printed Name of Subject or
Legal Representative of the Subject

_____ _____

Signature of the Person obtaining consent

Date

_____

Printed Name of the Person obtaining consent

Medical History Form

MEDICAL HISTORY

GENERAL INFORMATION

UIN (Unique Research Identifier Number _____

Age _____

Sex:

☐ Male ☐ Female

My current weight is: _____

My current height is: _____

List any prescription medications you are now taking: _____

_____

_____

List any self-prescribed medications, dietary supplements, or vitamins you are now taking: _____

_____

_____

List any current medical conditions: _____

_____

_____

List hospitalizations, including dates of and reasons for hospitalization: _____

_____

_____

IRB APPROVED

OCT 10 2014

University of North Texas
Health Science Center

Past Medical History

Check those questions to which your answer is yes (leave others blank).

- ☐ Heart attack - If so, how many years ago? _____
- ☐ Dementia
- ☐ Seizures or Epilepsy
- ☐ Diseases of the arteries
- ☐ Head Injury (concussion, etc)
- ☐ Hypertension
- ☐ Diabetes or abnormal blood-sugar tests
- ☐ Phlebitis (inflammation of a vein)
- ☐ Dizziness or fainting spells
- ☐ Irregular heart beat or Arrhythmia
- ☐ Stroke
- ☐ High cholesterol
- ☐ High triglycerides
- ☐ Cancer
- ☐ Nervous or emotional problems
- ☐ Anemia
- ☐ Thyroid problems
- ☐ Hepatitis
- ☐ Bleeding disorders
- ☐ Asthma
- ☐ Abnormal chest X-ray
- ☐ Other lung disease
- ☐ Injuries to back, arms, legs or joint
- ☐ Jaundice or gall bladder problems
- ☐ Other (please specify in comments below)

Comments: _____

_____

_____

_____

History/problems donating or giving blood? Please describe _____

_____

_____

Family Medical History

Father:

☐ Alive Current age _____

☐ Deceased ☐ Age at death and cause _____

My father's general health is:

☐ Excellent ☐ Good ☐ Fair ☐ Poor

Reason for poor health: _____

Mother:

☐ Alive Current age _____

☐ Deceased ☐ Age at death and cause _____

My mother's general health is:

☐ Excellent ☐ Good ☐ Fair ☐ Poor

Reason for poor health: _____

Siblings:

Number of brothers _____ Number of sisters _____ Age range _____

Health problems _____

Familial Diseases

Have you or your blood relatives had any of the following (include grandparents)?

Check those to which the answer is yes and list relation (leave other blank).

- ☐ Heart attacks under age 50 _____
- ☐ Strokes under age 50 _____
- ☐ High blood pressure _____
- ☐ Elevated cholesterol _____
- ☐ Diabetes _____
- ☐ Asthma or hay fever _____
- ☐ Congenital heart disease (existing at birth but not hereditary) _____
- ☐ Heart operations _____
- ☐ Thyroid Disease _____
- ☐ Obesity (20 or more pounds overweight) _____
- ☐ Leukemia or cancer under age 60 _____

Comments: _____

_____

_____

_____

Other Heart Disease Risk Factors

Smoking

Do you currently smoke cigarettes, cigars or a pipe?

☐ Yes ☐ No

Diet

How would you describe your eating habits?

☐ Excellent ☐Good ☐Fair ☐Poor

Do you ever drink alcoholic beverages?

☐ Yes ☐ No

If yes, what is your approximate intake of these beverages?

☐ None ☐ Occasional ☐ Often

Appendix B: Methods for monitoring changes in the core of lipoprotein particles in metabolism and disease

US 20140273247A1

(19) **United States**

(12) **Patent Application Publication**

Cistola et al.

(10) **Pub. No.: US 2014/0273247 A1**

(43) **Pub. Date: Sep. 18, 2014**

(54) **METHODS FOR MONITORING CHANGES IN THE CORE OF LIPOPROTEIN PARTICLES IN METABOLISM AND DISEASE**

(71) Applicant: **EAST CAROLINA UNIVERSITY**, Greenville, NC (US)

(72) Inventors: **David P. Cistola**, Fort Worth, TX (US); **Michelle Robinson**, Greenville, NC (US)

(73) Assignee: **EAST CAROLINA UNIVERSITY**, Greenville, NC (US)

(21) Appl. No.: **13/839,420**

(22) Filed: **Mar. 15, 2013**

Publication Classification

(51) **Int. Cl.**
G01N 24/08 (2006.01)

(52) **U.S. Cl.**
CPC ***G01N 24/087*** (2013.01)
USPC **436/63**; 436/71; 422/68.1

(57) **ABSTRACT**

A method is disclosed for measuring the properties of protein and lipoprotein elements in a sample. The method includes the of placing a small volume of a sample into a NMR instrument tuned to measure a particular nucleus, applying a series of radiofrequency pulses with intermittent delays in order to measure spin-spin and/or spin-lattice relaxation time constants from the time-domain decay of the signal, without the use of chemical shifts and without converting data into the frequency domain by Fourier transform or other means, at least partially suppressing the water signal prior to the beginning of a sequence used to record relaxation time constants in the time domain, optionally utilizing relaxation contrast agents or other chemical additives to perturb the solvent water or other elements of the sample, analyzing the exponentially decaying NMR signal in the time domain using multi-exponential analysis, and comparing differences in the relaxation time constants for lipoprotein- or protein-specific elements within a single human subject, or between subjects, to assess normal and abnormal metabolism reflective of increased disease risk or active disease.

BACKGROUND

The present invention relates to the analysis of blood to identify and measure properties that correlate with cardiovascular disease.

Cardiovascular disease—primarily in the form of heart attack or stroke—is the leading cause of death in the United States and other developed countries. Cardiovascular disease is likewise becoming an increasing cause of death in developing countries as the risk of death from infectious diseases decreases in such countries.

Some of the main risk factors associated with cardiovascular disease are generally well understood. They include an elevated amount of low density lipoprotein (LDL), high blood pressure, cigarette smoking, diabetes mellitus ("diabetes"), family history, and a less physically

active, more sedentary lifestyle.

Serum LDL cholesterol levels are positively correlated with cardiovascular disease risk. However, approximately half of patients who suffer from symptomatic coronary artery disease have normal LDL-cholesterol concentrations. Therefore, there appears to be a hidden risk not detected by conventional clinical laboratory measurements of cholesterol.

As currently best understood, cholesterol deposited in arteries represents a main factor in cardiovascular disease. Cholesterol is effectively insoluble in water and blood and thus the body carries cholesterol using particles called lipoproteins. The body uses several lipid transporting particles present in blood and these lipoprotein particles are typically referred to as chylomicrons, very low density lipoproteins (VLDL), intermediate density lipoproteins (IDL) and high density lipoproteins (HDL). Density increases when less cholesterol is present and density decreases when more cholesterol is present. Thus, the layman often refers to LDL cholesterol as "bad" cholesterol and HDL cholesterol as "good" cholesterol.

Low density lipoprotein particles tends to deposit in artery walls to form atherosclerotic plaques in the artery. In turn, the deposition of LDL to form the atherosclerotic plaques is promoted by an increased LDL concentration (or remnants that can form LDL particles) and a decreased LDL particle size.

In order to help predict and potentially moderate or avoid cardiovascular disease in individuals, conventional clinical tests are carried out to measure certain of the known risk factors. Currently, the most common test is the basic lipid panel which measures total cholesterol, HDL cholesterol ("HDL-C"), and triglycerides. The LDL cholesterol ("LDL-C") is calculated as the difference between total cholesterol and HDL cholesterol.

Currently, approximately 250,000,000 such tests are carried out in the United States every year, and on a worldwide basis 540 million tests are carried out each year. Current costs are between about $26 and $56 per test.

As an additional factor, LDL can be present in different LDL particle sizes. In turn, smaller LDL particle sizes are associated with an increased risk of cardiovascular disease. Because of the size relationship, information about the size of the LDL particles is valuable in combination with information about the concentration of LDL particles.
Currently, the common tests for measuring LDL particle size include vertical autoprofile (VAP®), gradient gel electrophoresis, and NMR lipoprofiles.

VAP is also referred to as a vertical spin density gradient ultracentrifugation and an exemplary version ("The VAP Cholesterol Test"®) is provided by Atherotech, Inc. of Birmingham, Ala. (USA).

Gradient gel electrophoresis distinguishes particle size in a otherwise conventional electrophoresis (i.e. chromatography) process with an exemplary test offered by Berkeley HeartLab Inc. of (South San Francisco Calif. (USA).

In one commercial embodiment, NMR lipoprofile testing is based upon the chemical shift of the resonant frequencies. LipoScience Inc. (Raleigh, N.C. USA) is an exemplary provider of such tests, a number of which are based on U.S. Pat. No. 5,343,389 (and others) to James D. Otvos ("the Otvos patents"). The Otvos patents employ frequency-domain FT-NMR to study lipoprotein particle properties, such as particle size and particle number, in order to perform clinical diagnostic testing and disease risk assessment. In order to provide accurate data, however, chemical shift NMR is typically carried out in large (e.g., 400 megahertz or higher) high resolution Fourier-transform NMR instruments. Many such instruments incorporate a superconducting magnet cooled by a surrounding environment of liquid helium which in turn is

surrounded by liquid nitrogen. As a result, the device is large and expensive and the testing is carried out in a small number of central laboratories at a cost of between about 100 and $200 per test.

Such tests also require a frequency-domain analysis, typically performed by a Fourier transform of the data. The key measurable is the chemical shift, a measure of relative frequency and atomic environment. Differences in chemical shifts are used to distinguish and resolve different lipoprotein classes and permit the detection of particle size and number.
In evaluating an individual's lipid profile, core mobility or fluidity of the lipids is a reflection of the relative ratio of different cholesteryl ester and triglyceride molecules in the particle core, which in turn, is a reflection of normal or abnormal lipid metabolism.

Lipoproteins are the body's nanoparticle delivery systems that carry water-insoluble cholesterol and triglyceride molecules through the blood and target them to particular tissues for metabolism. Lipoprotein particles can be distinguished by their density, size, chemical composition and charge. They can also be distinguished by the relative lipid content of the particle's oily core compartment. For example, the cores of LDL and HDL are relatively rich in cholesteryl ester (a highly water-insoluble form of cholesterol), whereas VLDL and chylomicrons are relatively rich in triglycerides. Triglyceride molecules are more flexible than cholesteryl esters, so oil phases rich in triglycerides will appear more fluid and mobile, less viscous. Also, the ratio of these components and thus, the core mobility, changes with metabolism and disease.

On a broad basis, the use of NMR techniques for medical purposes is not new, and the term “NMR” typically can refer to a variety of diagnostic methods. There are many types of NMR methods and instruments and thousands of distinct NMR experiments. A vivid example of this is magnetic resonance imaging (“MRI”), which was originally called NMR Imaging. MRI is a variation of NMR that yields anatomical images rather than chemical signatures. Although MRI is based on the same fundamental physics, it involves different instrumentation, methods and derived measurable from other NMR techniques. Thus, different kinds of NMR are used in somewhat related but distinct areas of medical diagnosis, imaging, and treatment.
U.S. Pat. No. 7,550,971 B2) to Carpenter and Benson describe a method of determining analyte concentrations in body fluids such as blood plasma or serum, examples given in the claims are the concentrations of glucose, cholesterol, triglycerides, albumin, blood urea nitrogen, alkaline phosphatase and creatinine. The method is restricted to the use of low-field, bench-top TD-NMR instruments, but the measurements and derived quantities are analyte concentration rather than lipoprotein core mobility. These contrasting measurables provide completely different types of diagnostic information.

Arguably, the Carpenter and Benson methods are thinly justified and lack any preliminary data that demonstrates the feasibility of their method for measuring analyte concentrations, and bench-top TD-NMR may not be as suitable for measuring the analyte concentrations as Carpenter and Benson imply. Serum is a complex mixture, and U.S. Pat. No. 7,550,971 lacks any explanation as to how the different analytes in serum can be resolved from one another. Instead, much of the content in U.S. Pat. No. 7,550,971 reflects the known operation of the TD-NMR instrument rather than a technique for resolving analytes from TD-NMR data.

As a result of these various factors, vertical autoprofile, gradient gel electrophoresis, and NMR lipoprofiles can be impractical for routine clinical use; i.e., they are too expensive and too cumbersome to be carried out on-site in a practitioner's office or a hospital laboratory.

As another factor, various lipid tests (e.g., for HDL-C and LDL-C) can be inaccurate in certain circumstances. For example, calculated LDL-C values from a conventional lipid panel are not accurate when determined from non-fasting blood samples or in patients who have elevated triglyceride levels, as is common in diabetes. Likewise, some advanced lipid tests like the NMR LipoProfile require fasting blood samples and thus, cannot monitor changes in lipoprotein particles during metabolism following a meal.

Furthermore, evidence is beginning to emerge that characteristics of lipid-carrying particles other than size and density will correlate with an increased risk of cardiovascular disease.

As yet another factor, when any particular test is difficult to carry out, or must be carried out off-site, or will take significant time to complete, or any combination of these factors, the use of that test will tend to be less frequent than the use of tests that can be carried out quickly and easily at a location—a physician's office, small clinic, or hospital—where patients are typically located and their blood samples taken.

Thus, tests that identify cardiovascular risk and that can be carried out more quickly, more easily, less expensively, and on site would tend to be used more frequently and thus provide greater benefits to individual patients and to the relevant patient population.

Therefore, a need exists for faster, similar and localized techniques that will identify and measure relevant characteristics that correlate to an expected degree of risk of cardiovascular disease.

SUMMARY

This invention describes non-perturbing methods for monitoring changes in the core mobility and core composition of lipoprotein particles in intact, unfractionated body fluids such as blood serum or plasma.

In one aspect, the method includes the of placing a small volume of a sample into a NMR instrument tuned to measure a particular nucleus, applying a series of radiofrequency pulses with intermittent delays in order to measure spin-spin ("T_2") and/or spin-lattice ("T_1") relaxation time constants from the time-domain decay of the signal, without the use of chemical shifts and without converting data into the frequency domain by Fourier transform or other means, at least partially suppressing the water signal prior to the beginning of a sequence used to record relaxation time constants in the time domain, optionally utilizing relaxation contrast agents or other chemical additives to perturb the solvent water or other elements of the sample, analyzing the exponentially decaying NMR signal in the time domain using multi-exponential analysis, and comparing differences in the relaxation time constants for lipoprotein- or protein-specific elements within a single human subject, or between subjects, to assess normal and abnormal metabolism reflective of increased disease risk or active disease.

In another aspect, the method comprises measuring the pulsed time domain NMR spin-spin relaxation time for a plurality of LDL samples, normalizing the viscosity of the same LDL samples, plotting the product of spin-spin relaxation time and viscosity for the samples against an axis defined by spin-spin relaxation time to thereby develop a database of T_2 or T_2V statistics (or T_1 or T_1V statistics or some combination of T_2, T_2V, T_1, or T_1V) for the original LDL samples, measuring the classic lipoprotein profile for the same LDL samples, and correlating known risks of cardiovascular disease based upon the classic lipoprotein testing with the results as determined by the T_2 or T_2V statistics to thereby correlate the T_2 or T_2V statistics with the known risks of cardiovascular disease in a statistically acceptable manner. As used herein, the

term “normalizing” the viscosity of the sample comprises either using samples at the same viscosity by physically manipulating the samples to obtain the viscosity; or mathematically modeling the resulting data so that the results are comparable across viscosities. Persons skilled in the art are familiar with both techniques and they are not otherwise described in detail herein. Without being bound by theory, the possibility exists that the relevant interpretation of the NMR data can be obtained regardless of normalization; i.e., the viscosity normalization may be option or unnecessary. Thus, where appropriate the phrase “T_2 or T_2V” reflects this.

In another aspect, the invention is a diagnostic kit that includes a pulse time domain NMR instrument, a sample selected from the group consisting of serum and plasma, and a database of T_2 or T_2V data that correlates with known cardiovascular risk statistics.

In another aspect, the invention is a combinatorial library that includes a plurality of patient samples selected from the group consisting of whole or partially fractionated serum or plasma, and a T_2 or T_2V measurement for each sample.

In another aspect, the invention is a method of determining cardiac risk factors based upon blood samples. The method includes the steps of measuring the pulse time domain NMR spin-spin or spin-lattice relaxation time of a sample selected from the group consisting of serum and plasma, measuring the lipid profile of the same sample, optionally combining the spin-spin relaxation time and viscosity of the sample to produce a T_2 or T_2V value for the blood sample, and comparing the T_2 or T_2V value to the lipid profile of the sample to identify the cardiac risk measured by the T_2 or T_2V value based upon the cardiac risk measured by the lipid profile.

BRIEF DESCRIPTION OF THE DRAWINGS

FIG. 1 is a very general schematic diagram of an LDL particle and its internal oil phase.

FIG. 2 is a TD-NMR T_2 profile for purified human low-density lipoprotein at 25° C.

FIG. 3 is a plot of metabolic remodeling of LDL core lipids during metabolism following a meal.

FIGS. 4-6 are CONTIN profiles for pure triolein and for two lipid cores.

FIG. 7 is a plot of T_2V values for albumin, LDL plus albumin, and VLDL plus albumin.

FIG. 8 is a plot of T_2V values for three samples of whole human serum.

FIG. 9 is a plot of T_2V values for lipoprotein particles at various times after a meal.

DETAILED DESCRIPTION

The methods of the invention resolve individual lipoprotein particle classes (e.g., low-density lipoprotein or LDL) by detecting differences in core lipid mobility, which is influenced by the relative amount of cholesteryl ester to triglyceride molecules within each particle's core. Variability in core mobility and core composition within a particle class, such as LDL, can result from patient-to-patient differences, or from particle remodeling within an individual subject as occurs during metabolism following a meal. Changes in lipoprotein particle core mobility and core composition are monitored using a time-domain nuclear magnetic resonance (TD-NMR)

analysis. A hallmark of this approach is that the analysis is performed without Fourier transformation and without the use of frequency-domain information such as chemical shifts. Unlike frequency-domain Fourier-transform NMR, this time-domain NMR analysis can be performed at low magnetic fields (≦60 MHz for hydrogen) in a low-cost, bench-top instrument configuration, although it can also be performed in conventional high-field NMR spectrometers. The general principles of time domain pulse NMR are generally well understood and familiar to persons of ordinary skill in the art and need not be discussed in detail. In brief, however, a sample is positioned in an external magnetic field provided by a permanent magnet. This aligns the magnetic moments of the hydrogen atoms with (or against) the permanent magnetic field. Then, a radio frequency pulse is applied in a direction that provides a secondary (temporary) magnetic field perpendicular to the permanent magnetic field. This moves the magnetic moments of the hydrogen atoms away from their equilibrium state. The time duration of the pulse determines how far the magnetic moments move. The combined movement of many spins (many hydrogen atoms) generates a small but detectable oscillating magnetic field that in turn induces an alternating voltage that is measured as the NMR signal by a detection coil.

At the end of the pulse, the protons in the sample give up excess energy to their surroundings and relax back to the equilibrium state with respect to the permanent magnetic field. This relaxation takes a certain amount of time, so that the NMR signal remains detectable for a period of time that can range from several milliseconds to several seconds.

Furthermore, the relaxing component of the NMR signal will be characteristic of individual mobility domains, which in turn, help identify the molecules involved in the motions. For example, cholesterol molecules are more internally rigid than triglyceride molecules and will tend to give lower T_2 and T_1 values.

Additionally, the data resolution of the pulse time domain NMR technique of the invention is on the order of particle size. In comparison, Fourier transfer NMR resolves data on an atomic scale. As a result, the time domain technique makes fewer technical demands (so to speak) on the instrument and can provide useful data at the available resolution.

According to the invention, it is been determined that time decay constants are sensitive to both particle size and particle mobility.

The method is also tolerant of multiple phases or mixed phases; i.e., solids and liquids in many circumstances.

As part of the correlation discoveries of the invention, it is now been determined that LDL particles with a higher triglyceride/cholesterol molecular ratio in the core have a longer spin-spin relaxation time (T_2) and particles with a lower triglyceride/cholesterol ratio have a shorter T_2.

Although the inventors do not wish to be bound by a particular theory, it appears that this may result from the characteristics of an LDL particle as not being solid in the same sense as a solid homogeneous composition would be. Instead, the LDL particle has an internal oil phase (FIG. 1). In turn, the oil phase moves (tumbles) differently—and typically faster—than the remainder of the particle. This faster internal tumbling increases the spin-spin relaxation time.

In one embodiment, the hydrogen spin-spin relaxation rate constants (or time constants) are measured using a low-field bench-top time-domain NMR analyzer, and the relaxation rate constants for individual lipoprotein classes are resolved through a multi-exponential deconvolution algorithm. Another key feature of this analysis is that measurements can be made directly on intact body fluids (e.g., serum, plasma or blood) without the need for separation or fractionation of individual lipoprotein classes by ultracentrifugation, electrophoresis,

chromatography or other time-consuming, sample-perturbing methods. Because of the relative simplicity and low cost, this method has potential application to clinical testing for the detection of unique dyslipidemias and for the early detection and risk assessment of cardiovascular disease, diabetes and cancer.

The measurements can, of course, be made in conventional high-field NMR spectrometers, but as set forth herein, the use of Benchtop instruments offers a number of clinical advantages.

In the invention, time-domain NMR resolves individual lipoprotein classes by measuring mobility differences in the oil phases within the core compartment of lipoprotein particles. The invention is also based on the discovery that TD-NMR is sensitive to changes in the particle core within a lipoprotein class. For example, the LDL particles in diabetic subjects tend to be richer in triglyceride, which makes the particle core more mobile.

The mobility differences are monitored by measuring relaxation rate constants (or time constants) without chemical shifts. Chemical shifts are the centerpiece of conventional high-field, frequency-domain NMR. By contrast, time-domain NMR does not require chemical shifts for frequency domain resolution and does not require high magnetic field strength or field homogeneity. This approach is fundamentally different from conventional NMR spectroscopy in both methodology and instrumentation requirements.

In one embodiment, the invention is a process for measuring the spin-spin or transverse relaxation time constants (T_2) for the lipid core compartments in unfractionated human serum. The human serum is obtained in a conventional manner from a low-speed centrifugation of human blood after clotting. Approximately 0.6 mL of unmodified serum is pipetted into a 10 mm NMR tube, and the tube is placed into the bore of the magnet of a bench-top TD-NMR analyzer, typically operating at 10, 20, 40 or 60 MHz resonance frequency for hydrogen. In the examples described here, 20 MHz and 40 MHz data were collected using Bruker benchtop mq20 and mq40 TD-NMR instruments (Bruker BioSpin Corporation, Billerica, Mass., USA).

A Carr-Purcell-Meiboom-Gill (CPMG) pulse sequence is used to measure the exponential time-decay curve. This pulse sequence effectively eliminates chemical shifts and magnetic field inhomogeneity, permitting the measurement of T_2 values. Although T_2 measurements can be linked with chemical shifts and measured in the frequency domain, the present TD-NMR method measures T_2 in the time domain without chemical shifts. This provides a distinct advantage with respect to instrument simplicity and cost.

The resulting T_2 decay curve for human serum is multi-exponential, so the individual exponential terms are deconvoluted and resolved with the use of an inverse Laplacian transform. An implementation of this mathematical calculation is provided in the public domain software CONTIN, authored by Steven Provencher (http://s-provencher.com/pages/contin.shtml; accessed Mar. 11, 2013). Under the proper experimental conditions with excellent signal-to-noise, the CONTIN calculation can resolve up to 8 different exponential terms in TD-NMR T2 profiles of human serum. Because human serum has abundant quantities of lipoprotein core lipids and soluble proteins, and because these assemblies are relatively large, the protein and lipoprotein components dominate the T_2 profile.

One experimental issue involves solvent suppression, because an intense water signal can overshadow the contributions of lipoprotein components and lead to artifacts such as radiation damping. The solvent water can be partially suppressed using a number of NMR schemes. In this embodiment, a 180-degree pulse and delay is inserted prior to the CPMG sequence. This achieves partial relaxation (and partial suppression) of the water with full recovery of the

lipoprotein components by the start of the CPMG pulse scheme. Although there are many sophisticated NMR methods for suppressing water, the goal of this invention was to develop the simplest, most inexpensive method for measuring lipoprotein core properties in unmodified human serum.

This embodiment is further illustrated using the figures and tables. FIG. 2 shows a time-domain T_2 NMR profile of normal fasting human serum, and FIG. 3 is the TD-NMR T_2 profile for purified human low-density lipoprotein at 25° C.

The profile of FIG. 2 (not to be confused with a conventional NMR spectrum) was obtained by performing an inverse Laplacian transform of the T_2 decay curve. In turn, the T_2 curve was measured using a modified CPMG experiment on a Bruker 40 MHz TD-NMR analyzer. The profile resolves 7 distinct T_2 components, here represented as peaks in the profile. Higher T_2 values represent more mobile elements. The solvent water peak in serum, not shown in this plot, is observed at T_2 values of approximately 600 ms. The peaks at approximately 200 and 70 ms represent two distinct mobility domains in LDL, as assigned from control samples containing only LDL.

These two peaks are not observed in the other control samples containing fractionated serum proteins or lipoproteins and appear to provide a unique signature for the core lipid mobility of LDL. The peaks at lower T_2 values have contributions from both serum proteins and lipoproteins.

FIG. 9 illustrates the variation in T_2 measurements in response to metabolic changes following a meal. Shown are T_2 profiles for whole human serum at fasting, 2 hours, 4 hours and 6 hours post-prandial. The T_2 values for the LDL-specific peaks increase and peak at 4 hours, reflecting the remodeling of the LDL core as the content of triglyceride increases relative to cholesteryl ester.

These preliminary results demonstrate the feasibility of obtaining particle-specific measurements of the core mobility of LDL in whole human serum. The data also demonstrate that T_2 measurements obtained from TD-NMR are sensitive to metabolic remodeling and patient-to-patient variability.

Furthermore, the invention requires neither high magnetic field instrumentation nor a frequency-domain analysis. Instead, it uses a time-domain analysis. Unlike (for example) the Otvos approach, the methods of the invention can be performed on inexpensive low-field bench-top instruments, because high field strength and field homogeneity is not required. The key measurables are relaxation rate constants rather than chemical shifts. Differences in relaxation rate constants are used to resolve lipoprotein classes (not chemical shifts, as in Otvos and Kremer). Also, the derived parameter in our invention is lipoprotein particle core mobility or fluidity, rather than particle number or particle size. In summary, the instrumentation, data processing, measurables and derived parameters of our invention are different from those of Otvos.

In contrast to (for example) U.S. Pat. No. 7,550,971, the present invention does not measure analyte concentrations. Rather it measures lipoprotein particle properties, specifically the mobility or fluidity ("squishiness") of the oily lipid core found within lipoprotein particles. Also, the invention is not restricted to low-field, bench-top NMR instruments, but can also be performed on conventional high-resolution NMR instruments as well.

Overall, the method of the invention is much simpler and can be performed on inexpensive low-field benchtop NMR analyzers, and the particle core mobility provides diagnostic information different from particle size and concentration distribution.

Additional Examples

In the following Examples, all aqueous samples are prepared in a 9.1 D2O/H2O saline buffer, concentrated to a viscosity of 1.20cP at 37° C. The raw data are in the form of a multi exponential decay curve. The individual relaxation time constants are deconvoluted using an inverse Laplacian transform calculation as implemented in the public domain program CONTIN.

Lipoprotein Lipid Core Mixtures

A CONTIN profile of triolein, the most abundant TG in lipoproteins, is shown in FIG. 4. Each T_2 (or T_2V) corresponds to a mobility domain of the triglyceride molecule. A VLDL like lipid core with 80% TG and 20% CE shows a similar profile (FIG. 5) but is shifted slightly to the left, indicating a less mobile, more vicious environment. The LDL like lipid core (FIG. 6) composed of 80% CE and 20% TG exhibited lower T_2 or T_2V values indicating reduced mobility. This trend resembles that observed with physiological lipoprotein particles with differences in TG/CE ratios. T_2V values for lipid mixtures are summarized in Table 1.

TABLE 1				
	(T_2V times in ms)			
	Fast	**Medium**	**Slow**	**Other**
100% TO	347	155	79	8
80% to 20% CL	303	141	70	25, 5
(VLDL Core)				
20% to 80% CL	183	92	45	19, 9, 4
(LDL Core)				

Fractionated Lipoproteins and Serum Proteins

FIG. 7 shows the T_2V profiles for albumin ("HSA"), LDL plus albumin and VLDL plus albumin. Although all of the profiles display fast decaying components in the range of 2-50 ms, there are T_2V values above 50 ms that are unique to individual lipoprotein classes

Whole Human Serum

De-identified samples of whole human serum, representing various metabolic and disease states were obtained from Pitt County Memorial Hospital (Greenville, N.C., USA). As seen in FIG. 8 variability was observed in lipoprotein T_2V values. Patient samples with a higher HbAlc, indicative of poorly managed Type 2 Diabetes Mellitus, have increased T_2 or T_2V values suggesting that the lipoprotein particles have increasingly mobile, TG-rich lipid cores versus non-diabetic patients.

Results: FIG. 9 shows the remodeling healthy non-diabetic subject ingested a liquid meal that contained 50 grams of lipid following a 16 hour fast, after which blood was drawn every hour for 8 hours. The NMR data are shown in FIG. 4 *b* at 0 hour (fasting) and other time points after the meal. As lipoprotein remodeling occurs and the particles become TG rich, the T_2V peak shifts to the right indicating an increase in lipid core mobility. Table 2 shows standard lipid analysis for these samples.

TABLE 2								
	0 Hr.	**2 Hr.**	**3 Hr.**	**4 Hr.**	**5 Hr.**	**6 Hr.**	**7 Hr.**	**8 Hr.**
Triglycerides	87	184	181	194	197	231	188	169
Cholesterol	197	204	200	199	193	187	184	187
HDL-C	54	55	52	52	49	47	47	48
Non-HDL-C	148	149	148	147	144	140	137	139
LDL-C	125	112	112	108	105	94	99	105

Benchtop TD-NMR appears to provide unique information about LDL and VLDL particle properties reflective of different states of normal and abnormal metabolism. This approach holds promise for translation from the research lab into the clinical setting as the measurements are performed on whole human serum and are relatively simple, inexpensive and non-invasive.

In the drawings and specification there has been set forth a preferred embodiment of the invention, and although specific terms have been employed, they are used in a generic and descriptive sense only and not for purposes of limitation, the scope of the invention being defined in the claims.

CLAIMS

1. A method for measuring the properties of protein and lipoprotein elements in a sample, the method comprising the steps of:
placing a small volume of a sample into a NMR instrument tuned to measure a particular nucleus;
applying a series of radiofrequency pulses with intermittent delays in order to measure spin-spin and/or spin-lattice relaxation time constants from the time-domain decay of the signal, without the use of chemical shifts and without converting data into the frequency domain by Fourier transform or other means;
at least partially suppressing the water signal prior to the beginning of a sequence used to record relaxation time constants in the time domain;
analyzing the exponentially decaying NMR signal in the time domain using multi-exponential analysis; and
comparing differences in the relaxation time constants for lipoprotein- or protein-specific elements within a single human subject, or between subjects, to assess normal and abnormal metabolism reflective of increased disease risk or active disease.

2. A method according to claim 1 comprising using between about 0.2 and −0.6 mL of the sample.

3. A method according to claim 1 comprising tuning the NMR instrument to measure a nucleus selected from the group consisting of hydrogen-1, carbon-13, nitrogen-15, fluorine-19, and

phosphorous-31.

4. A method according to claim 1 wherein the step of suppressing the water signal comprises a 180-degree inversion pulse followed by a delay to partially relax the water signal.

5. A method according to claim 1 wherein the step of analyzing the exponentially decaying NMR signal in the time domain is selected from the group consisting of an inverse Laplacian transform and a multi-exponential analysis.

6. A method according to claim 1 wherein the step of analyzing the exponentially decaying NMR signal in the time domain comprises a chemometric analysis.

7. A method according to claim 1 wherein the step of comparing differences in the relaxation time constants includes an assessment of the remodeling of the core lipid compartment of particles selected from the group consisting of LDL, HDL, VLDL, other lipoprotein particles and remnants during metabolism and in disease.

8. A method according to claim 1 further comprising normalizing the viscosity of the sample.

9. A method for measuring the dynamical, mobility and/or fluidity properties of protein and lipoprotein elements in a sample, including but not limited to lipoprotein particle core mobility and relative core composition, the method comprising:
placing between about 0.2 and 0.6 mL of a sample into a NMR instrument tuned to measure a nucleus selected from the group consisting of hydrogen-1, carbon-13, nitrogen-15, fluorine-19, and phosphorous-31;
applying a series of radiofrequency pulses with intermittent delays in order to measure spin-spin and/or spin-lattice relaxation time constants from the time-domain decay of the signal, without the use of chemical shifts and without converting data into the frequency domain by Fourier transform or other means.
partially suppressing the water signal by including a 180-degree inversion pulse followed by a delay to partially relax the water signal prior to the beginning of a sequence used to record relaxation time constants in the time domain;
utilizing a relaxation contrast agents to perturb the solvent water or other elements of the sample;
analyzing the exponentially decaying NMR signal in the time domain using multi-exponential analysis, including an inverse Laplacian transform; and
comparing differences in the relaxation time constants for lipoprotein- or protein-specific elements within a single human subject, or between subjects, to assess normal and abnormal metabolism reflective of increased disease risk or active disease.

10. The method of claim 9 comprising measuring the properties of a body fluid.

11. The method of claim 9 comprising measuring the properties of whole blood.

12. The method of claim 9 comprising measuring the properties of blood serum.

13. The method of claim 9 comprising measuring the properties of blood plasma.

14. The method of claim 9 comprising measuring the properties of lymph fluid.

15. The method of claim 9 comprising measuring the properties of ascites fluid.

16. The method of claim 9 where the sample is partially fractionated body fluid, including but not limited to human blood serum following selective precipitation or column fractionation.

17. A method according to claim 9 comprising taking a specimen of whole blood from a patient and thereafter extracting a blood plasma sample from the specimen.

18. A method according to claim 9 comprising taking a specimen of whole blood from a patient and thereafter extracting a blood serum sample from the specimen.

19. A method of identifying the cardiovascular risk factors in patients comprising:
measuring the pulsed time domain NMR spin-spin relaxation time for a plurality of LDL samples selected from the group consisting of LDL and other individually fractionated lipoprotein or lipoprotein remnant samples;
normalizing the viscosity of the same samples;
plotting the product of spin-spin relaxation time and viscosity for the samples against an axis defined by spin-spin relaxation time to thereby develop a database of T_2V statistics for the original samples;
measuring the classic lipoprotein profile for the same samples; and
correlating known risks of cardiovascular disease based upon the classic lipoprotein testing with the results as determined by the T_2V statistics to thereby correlate the T_2V statistics with the known risks of cardiovascular disease in a statistically acceptable manner.

20. A method according to claim 19 comprising obtaining the LDL samples from the group consisting of serum or plasma

21. A method according to claim 19 further comprising
taking a blood specimen from a patient;
preparing a sample selected from the group consisting of plasma and serum from the blood specimen;
measuring the spin-spin relaxation time and the viscosity of the plurality of the sample;
calculating a parameter selected from the group consisting of T_2, T_2V, T_1 and T_1V the for the sample; and
determining the risk of cardiovascular disease in the patient sample based upon the correlation between the calculated parameter and the known risks of cardiovascular disease.

22. A method according to claim 19 comprising normalizing the samples by concentrating the samples to a substantially similar viscosity.

23. A method according to claim 19 comprising normalizing the samples by normalizing the viscosity component of the time domain data.

24. A diagnostic kit comprising:
a pulse time domain NMR instrument;
a sample selected from the group consisting of serum and plasma; and
a database of T_2V data that correlates with known cardiovascular risk statistics.

25. A combinatorial library comprising:
a plurality of patient samples selected from the group consisting of plasma and serum; and
a T_2 measurement for each sample.

26. A method of determining cardiac risk factors based upon blood samples, the method comprising:
measuring the pulse time domain NMR spin-spin relaxation time of a sample selected from the group consisting of serum and plasma;
measuring the lipid profile of the same sample;
combining the spin-spin relaxation time and viscosity of the sample to produce a T_2V value for the blood sample;
comparing the T_2V value to the lipid profile of the sample to identify the cardiac risk measured by the T_2V value based upon the cardiac risk measured by the lipid profile.

27. A method according to claim 26 comprising separating a whole blood specimen into a sample selected from the group consisting of plasma and serum prior to the step of measuring the pulse time domain NMR spin-spin relaxation time of the sample.

28. A method according to claim 26 wherein the step of measuring the lipid profile of the sample comprises measuring a profile selected from the group consisting of total cholesterol, HDL-C and LDL-C.

29. A method according to claim 26 comprising carrying out the measuring, combining and comparing steps for a plurality of samples.

30. A method according to claim 26 comprising normalizing the viscosity of the samples.

FIGURES

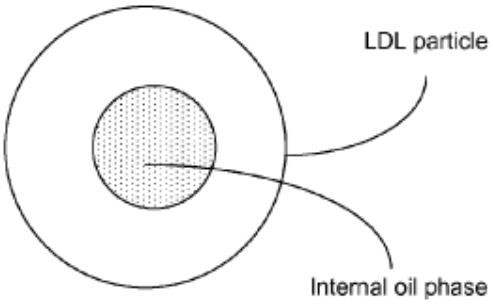

Fig. 1

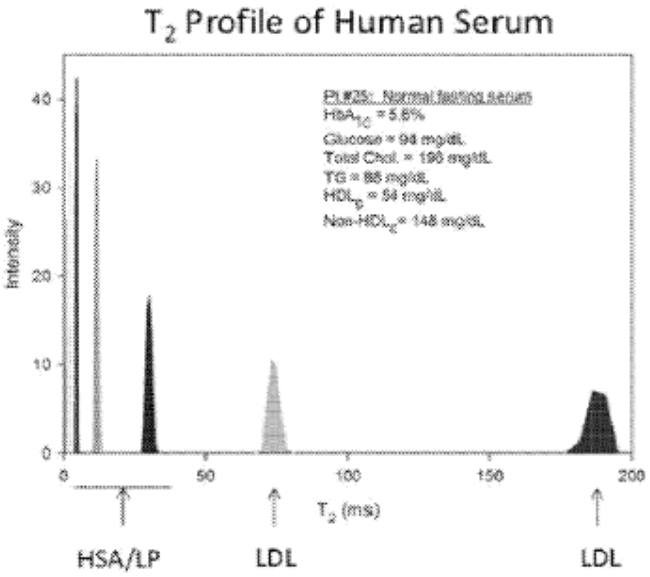

Fig. 2

Fig. 3

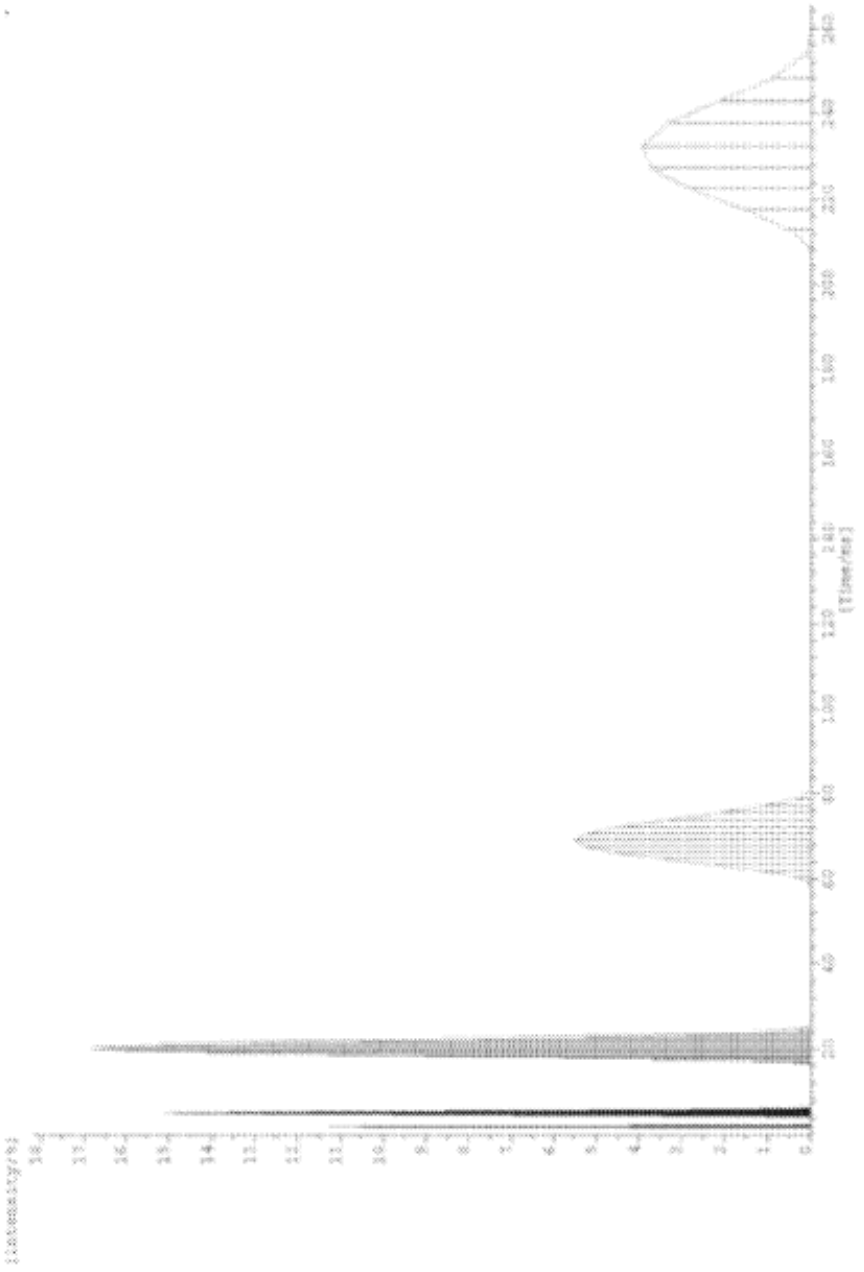

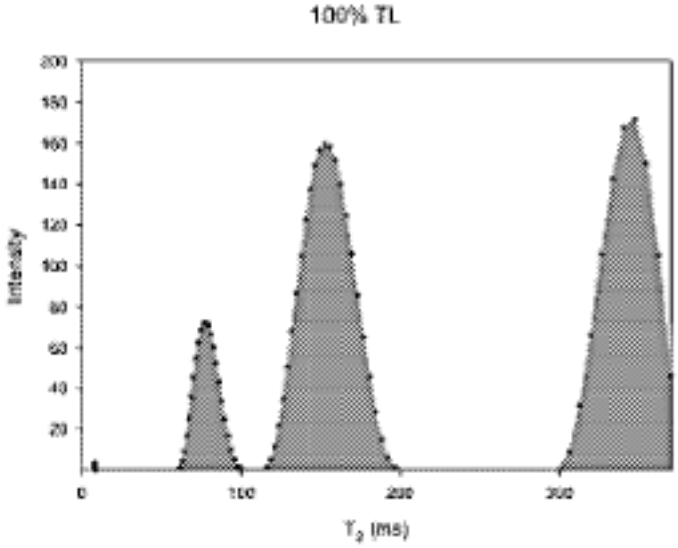

Fig. 4

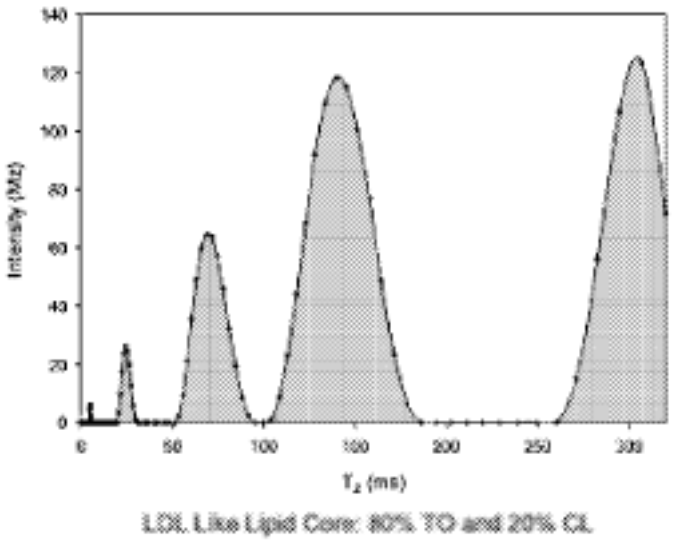

Fig. 5

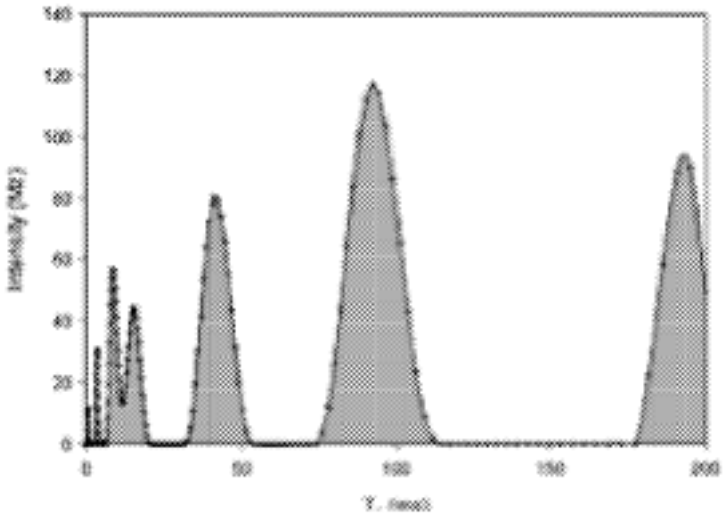

Fig. 6

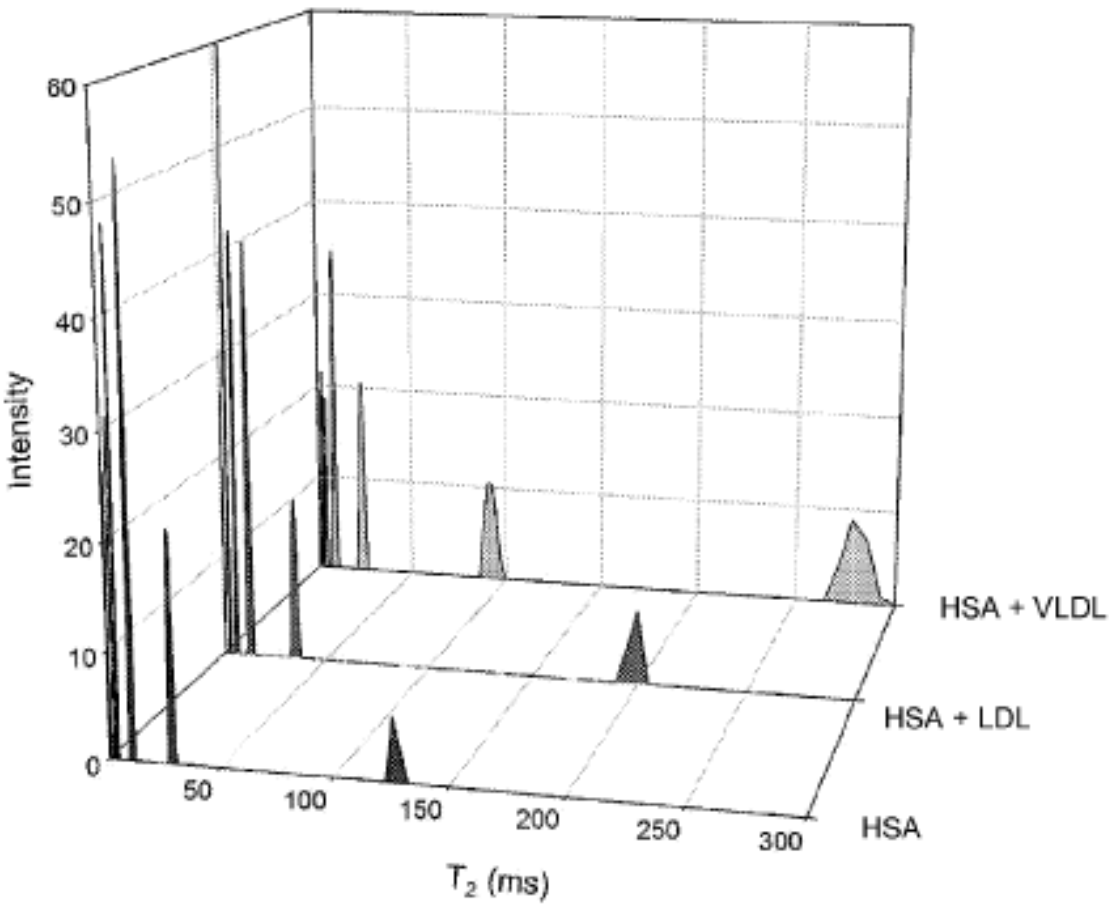
60
50
40
30
20
10
0
Intensity
50
100
150
200
250
300
T_2 (ms)
HSA + VLDL
HSA + LDL
HSA

Fig. 7

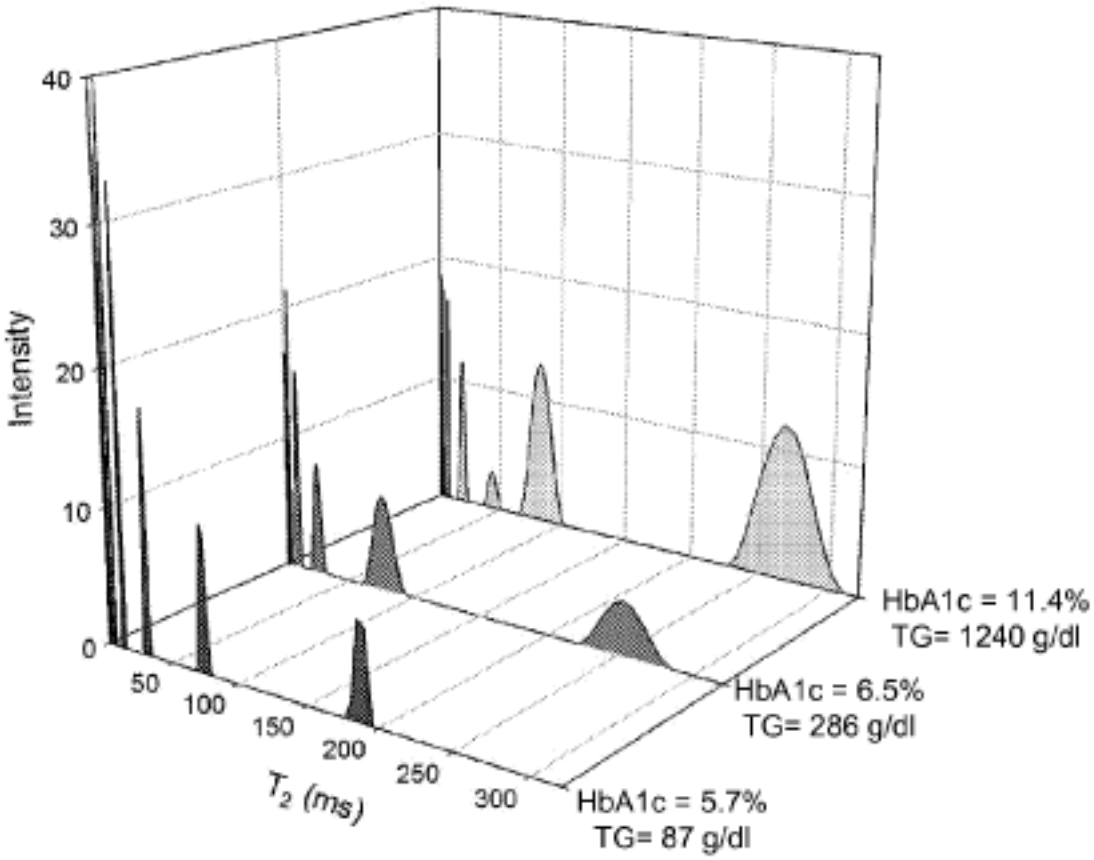
40
30
20
10
0
Intensity
50
100
150
200
250
300
T_2 (ms)
HbA1c = 11.4%
TG= 1240 g/dl
HbA1c = 6.5%
TG= 286 g/dl
HbA1c = 5.7%
TG= 87 g/dl

Fig. 8

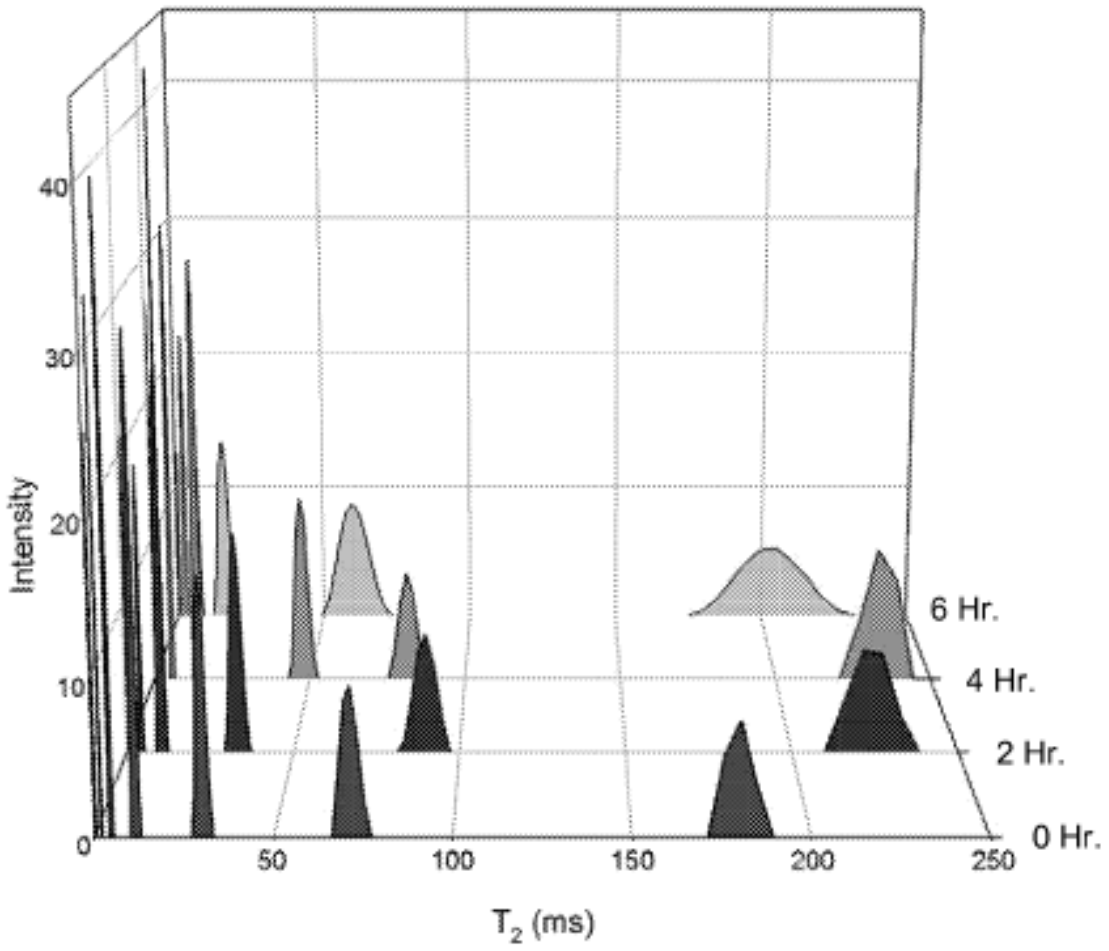

Fig. 9

Appendix C:

Method and Tools for Assessing Health Status Using NMR Relaxation Times for Water

U.S. Provisional Patent Application Docket No. UNT.108P
METHODS AND TOOLS FOR ASSESSING HEALTH STATUS USING NMR RELAXATION TIMES FOR WATER
(Cistola, Robinson)
Serial No. 62/113,112; filed February 6, 2015
Your Ref. No. 2014-021

DESCRIPTION

METHODS AND TOOLS FOR ASSESSING HEALTH STATUS USING NMR RELAXATION TIMES FOR WATER

BACKGROUND OF THE INVENTION

Conventional proteomics uses mass spectrometry to measure a large number of protein biomarkers to establish profiles of health and disease *(2)*. The subject application generates protein profiles by measuring just one biomarker: water T_2. conventional proteomics focuses on the less abundant proteins in blood after removing the most abundant ones during pre-treatment prior to analysis *(2, 3)*. In contrast, the subject application has developed a technique, termed "inverse proteomics" that involves no pre-treatment or sample manipulation and leverages the information content of all plasma and serum proteins, including the most abundant ones.

Brief Summary of the Invention

This application provides a means for developing an inexpensive blood test for front-line health screening and monitoring. The test analyzes the spin relaxation times (T_2 and/or T_1) of water in plasma, serum or whole blood using nuclear magnetic resonance (NMR). The blood samples can be obtained using a conventional needle stick or finger prick. However, given the intensity of the water NMR signal, it should be feasible to monitor the relaxation times of water in blood from outside of the body using a NMR-enabled finger clip, earlobe clip or a wristwatch-like device linked to a smart phone. Portable NMR devices are already available *(1)*. The

NMR T_2 for water reports on the concentration and chemical state of the proteins and lipoproteins in the blood. We refer to this approach as inverse proteomics. The NMR T_2 for water reports on the concentration and chemical state of the proteins and lipoproteins in the blood. We refer to this approach as "inverse proteomics".

The subject application has determined that lower water T_2 and/or T_1 values in serum and plasma are indicative of increasing degrees of metabolic dysfunction, even in an essentially healthy population with clinical lab values that fall in the normal reference ranges. The unique value of time-domain nuclear magnetic resonance (TD-NMR) is that an individual's overall health status with respect to insulin resistance, inflammation, dyslipidemia and possibly oxidative stress can be assessed simultaneously in one measurement without having to survey a large panel of clinical lab tests or biomarkers. Given its simplicity, water T_2 and/or T_1 *(4)* can serve as a screening tool for the early identification of individuals with hidden risk for diseases that are linked with metabolic abnormalities. Non-limiting examples of such diseases include, but are not limited to, diabetes, coronary artery disease, and Alzheimer's disease *(5, 6)*. These disorders account for much of the morbidity and mortality in modern societies. There is a continuing need for effective screening tools that can be implemented practically, inexpensively and broadly across the population. Such tools will have a place in P4 medicine: personal, predictive, preventative and participatory *(7)*. The invention disclosed herein provides a solution to this continuing need.

Brief Description of the Drawings

The patent or application file contains at least one drawing executed in color. Copies of this patent or patent application publication, with color drawing(s), will be provided by the Office upon request and payment of the necessary fee.

Figures 1A-1C. Time-domain NMR relaxometry analysis of water in unmodified human plasma and serum. (Fig. 1A) Raw data for human serum consisting of a multi-exponential decay curve, (Fig. 1B) T_2 profile for human serum derived from an inverse Laplace transform of the multi-exponential decay curve. This profile reveals an intense water peak (blue) and a few small peaks arising from direct detection of lipid and protein components in serum (orange). (Fig. 1C) Expansions of T_2 profiles for 28 human subjects illustrating the wide range of water T_2 values observed in this study population.

Figures 2A-2F. Linear regression plots for plasma or serum water T_2 vs. various blood biomarkers for the human subjects enrolled in this study. (Fig. 2A) Plasma water T_2 *vs.* total serum protein; (Fig. 2B) Plasma water T_2 *vs*. white blood cell count; (Fig. 2C) Plasma water T_2 *vs.* HbA_{1c}; (Fig. 2D) Serum water T_2 *vs.* total serum protein; (Fig. 2E) Serum water T_2 *vs.* red cell distribution width; (Fig. 2F) Serum water T_2 *vs.* LDL particle number. The correlation coefficients are provided in Tables 1 and 2.

Figures 3A-3F. Protein concentration and oxidation affect water T_2 values. (Fig. 3A) Water T_2 values vs. protein concentration for human serum albumin (triangles), lipoprotein-depleted human serum (squares) and whole human serum (circles); (Fig. 3B) and (Fig. 3C) Metal-catalyzed oxidation of proteins. In Fig. 3B, whole serum or plasma was titrated with $CuSO_4$, in the presence or absence of added histidine. In Fig. 3C, a protein solution containing

human serum albumin and γ-globulin was titrated with $CuSO_4$, in the presence or absence of added histidine. (Fig. 3D) The same protein solution as in Fig. 3C was titrated with malondialdehyde, which reacts with protein side chains to form carbonyl derivatives. (Fig. 3E) Linear regression of serum water T_2 with the anion gap; (Fig. 3F) Linear regression of serum water T_2 (corrected for albumin concentration) with the anion gap.

Figure 4. Modified Carr-Purcell-Meiboom-Gill (CPMG) pulse sequence for measuring water T_2 in human serum or plasma using benchtop time-domain NMR. In contrast to NMR spectroscopy, the time points for the exponential decay curve are acquired directly during the CPMG pulse scheme, during the middle of the τ delay between successive 180° pulses, as designated by the purple arrow. For the current study, the first 180˚ pulse and Δ delay were added prior to the CPMG scheme to achieve partial water suppression and eliminate radiation damping. The Δ delay was tuned to $0.95*T_1$ for each sample, which corresponds to suppression of the water to 23% of its full intensity. The τ delay was kept short (0.19 ms) to eliminate any possible impact of translational diffusion on T_2 in an inhomogeneous B_o field. For all experiments, RD was set to $5* T_1$, which corresponds to ~ 8 sec for serum or plasma; DE=5, NP=5600 and NS=16. The total experiment time was 6.4 minutes. Analysis of the resulting exponential decay curves is discussed in Materials and Methods. Abbreviations: RD, relaxation delay; DE, dummy echoes; NP, number of decay points acquired; NS, number of scans.

Figure 5 illustrates an example system architecture in which an implementation of techniques for health screening using T_1 and/or T_2 values for water may be carried out.

Figure 6 shows a block diagram illustrating components of a computing device or system used in some implementations of an apparatus for health screening using T_1 and/or T_2 values for water.

Brief Description of the Tables

Table 1: Correlation coefficients for plasma water T_2 with biomarkers for protein concentration and viscosity , inflammation , insulin resistance and other metabolic processes. Biomarkers were included in the table if they demonstrated at least one correlation coefficient with a p value < 0.05.

Table 2: Correlation coefficients for serum water T_2 values with biomarkers for protein concentration and viscosity, inflammation, dyslipidemia and other metabolic processes.

Table 3: Characteristics of the Human Subject Population.

Table 4: Biomarkers Measured in this Study.

Tables 5-9: Correlation Coefficients for Water T_2 Variants in Human Plasma.

Tables 10-14: Correlation Coefficients for Water T_2 Variants in Human Serum.

DETAILED DISCLOSURE OF THE INVENTION

The term “about” is used in this patent application to describe some quantitative aspects of the invention, for example, time. It should be understood that absolute accuracy is not required with respect to those aspects for the invention to operate. When the term “about” is used to describe a quantitative aspect of the invention, the relevant aspect may be varied by up to ±10%. As used herein, the term “subject” refers to a human or non-human animal, such as a rat, mouse, pig, dog, cat, horse or any other animal, including animal models of human diseases.

The subject application discloses a method that involves at least three steps: (1) acquisition of a NMR relaxation decay curve for plasma, serum or whole blood samples, or for tissues monitored from outside the body, (2) analysis of the relaxation decay or recovery curve to extract the T_2 and/or T_1 relaxation times for water, and (3) conversion of the water T_2 and/or T_1 values into a measure of someone's health status (referred to as a T_2 or T_1 health score depending on the value (T_1 or T_2 or both T_1 and T_2) associated with the score). The T_1 and/or T_2 health score utilizes a statistical database derived from previous studies of subjects having varying degrees of metabolic abnormalities, such as inflammation, insulin resistance, lipid abnormalities (dyslipidemia), oxidative stress, brain abnormalities or other disorders, and provides a measure of a subject's overall metabolic and brain health status. Specifically, the disclosed method detects or rules out hidden problems such as inflammation, insulin resistance, lipid abnormalities (dyslipidemia), oxidative stress, brain abnormalities or other disorders. The disclosed invention has value as a front-line health screening test and provides a subject with a T_2 and/or T_1 Health Score that provides individuals with an overall assessment of their metabolic and brain health. The T_2 and/or T_1 Health Score provides evidence of hidden abnormalities that could lead to disease in the future. Non-limiting examples of these abnormalities include, but are not limited to, inflammation, insulin resistance, neurological abnormalities, oxidative stress and lipid abnormalities. Early detection and subsequent intervention can remedy or delay the manifestation of disease arising from the abnormalities disclosed herein (e.g., atherosclerosis, etc.) Thus, if an apparently healthy subject has a moderately low T_2 and/or T_1 Health Score, the subject can choose an intervention, such as an exercise program, and check the score 4-8 weeks later to see if the health score has improved. Alternatively, the subject can alter its diet, take low dose aspirin or add a nutritional supplement, such as an antioxidant or a fish oil and assess the

impact of this change in diet on the T_2 and/or T_1 Health Score. Subjects with the lowest scores would be advised to visit their physician for a more complete workup to rule out a disease diagnosis and/or subjects can be treated with an appropriate therapeutic intervention. With respect to the overall assessment of metabolic and brain health, subjects can be separated into at least three categories. In some embodiments, the subjects can be separated as follows on the basis of the T_2 and/or T_1 Health Score (based on plasma T_2 values): >800: lowest likelihood of metabolic abnormalities; 700-800 or between 720 to 800: medium likelihood of metabolic abnormalities; <700 or <720: highest likelihood of metabolic abnormalities. Thus, subjects with a T_2 and/or T_1 Health Score of 800 or less can be treated according to the methods disclosed herein, subjected to heightened monitoring for the development of metabolic abnormalities or referred to a health provider for further evaluation for a hidden metabolic abnormality, such as inflammation, insulin resistance, lipid abnormalities (dyslipidemia), oxidative stress, brain abnormalities or other disorders.

As discussed above, the subject application has determined that lower water T_2 and/or T_1 values in serum and plasma are indicative of increasing degrees of metabolic dysfunction, even in an essentially healthy population with clinical lab values that fall in the normal reference ranges. The unique value of TD-NMR is that an individual's overall health status with respect to insulin resistance, inflammation, dyslipidemia and possibly oxidative stress can be assessed simultaneously in one measurement without having to survey a large panel of clinical lab tests or biomarkers. Given its simplicity, water T_2 and/or T_1 *(4)* can serve as a screening tool for the early identification of individuals with hidden risk for diseases that are linked with metabolic abnormalities. Non-limiting examples of such diseases include, but are not limited to, diabetes, coronary artery disease, and Alzheimer's disease *(5, 6)*. These disorders account for much of the

morbidity and mortality in modern societies. There is a continuing need for effective screening tools that can be implemented practically, inexpensively and broadly across the population will have a place in P4 medicine: personal, predictive, preventative and participatory *(7)*. The invention disclosed herein provides a solution to this continuing need. This subject application describes methods for determining an individual's overall health status with respect to insulin resistance, inflammation, dyslipidemia, oxidative stress and brain abnormalities can be assessed simultaneously in one measurement without having to survey a large panel of clinical lab tests or biomarkers by measuring water T_2 and/or T_1 values in samples obtained from a subject. In various embodiments, the samples are subjected to no pre-treatment or other sample manipulation. The method leverages the information content of all plasma and serum proteins, including the most abundant ones, in developing T_2 and/or T_1 Health Scores.

In one aspect, the method includes the of placing a small volume of a sample comprising water into a NMR instrument tuned to measure a particular nucleus, such as ^{1}H, ^{2}H or ^{17}O, by applying a series of radiofrequency pulses with intermittent delays in order to measure spin-spin ("T_2") and/or spin-lattice ("T_1") relaxation time constants from the time-domain decay or recovery of the signal. The delay from pulse to data acquisition can range from about 1 to about 50 milliseconds after the start of pulse scheme that acquires the relaxation decay curve; about 16 to about 20 milliseconds after the start of the pulse scheme; or about 19 milliseconds after the start of the pulse scheme. In some embodiments, the signal is used in a raw form, without the use of chemical shifts and without converting data into the frequency domain by Fourier transform or other means. The method can also be performed by, at least, partially suppressing the water signal prior to the beginning of a sequence used to record relaxation time constants in the time domain, analyzing the exponentially decaying NMR signal in the time domain using

multi-exponential analysis, and comparing differences in the relaxation time constants for water within a single human subject, or between subjects, to assess normal and abnormal water T_2 and/or T_1 values that are reflective of increased disease risk or active disease. In another aspect, the method comprises application of the disclosed method to a plurality of samples obtained from a plurality of subjects and developing a database of T_2 and/or T_1 values for water in said samples. The database can be used to provide a range of values for individuals having, or at risk of developing, a disorder such as insulin resistance, inflammation, dyslipidemia, oxidative stress and brain abnormalities (e.g., lower cognitive scores or mild cognitive impairment that often precedes Alzheimer's disease or Parkinson's disease).

In some embodiments, the database can provide further guidance in the development of T_2 and/or T_1 Health Score (based on T_2 and/or T_1 values). For example, plasma T_2 and/or T_1 Health Scores >800 are indicative of the lowest likelihood of metabolic abnormalities; T_2 and/or T_1 Health Score values of between 700-800 or 720 to 800 indicate a medium likelihood of metabolic abnormalities; and T_2 and/or T_1 Health Score values of <700 or <720 are indicative of the highest likelihood of metabolic abnormalities.

In another aspect, the invention is a diagnostic kit that includes a pulse time domain NMR instrument, a sample selected from the group consisting of serum and plasma, and a database of T_2 and/or T_1 data for water that correlates with a disorder such as insulin resistance, inflammation, dyslipidemia, oxidative stress and brain abnormalities (e.g., low cognitive scores or mild cognitive impairment).

The general principles of time domain pulse NMR are generally well understood and familiar to persons of ordinary skill in the art and need not be discussed in detail. In brief, however, a sample is positioned in an external magnetic field provided by a permanent magnet.

This aligns the magnetic moments of the hydrogen atoms with (or against) the permanent magnetic field. Then, a radio frequency pulse is applied in a direction that provides a secondary (temporary) magnetic field perpendicular to the permanent magnetic field. This moves the magnetic moments of the hydrogen atoms away from their equilibrium state. The time duration of the pulse determines how far the magnetic moments move. The combined movement of many spins (many hydrogen atoms) generates a small but detectable oscillating magnetic field that in turn induces an alternating voltage that is measured as the NMR signal by a detection coil.

At the end of the pulse, the protons in the sample give up excess energy to their surroundings and relax back to the equilibrium state with respect to the permanent magnetic field. This relaxation takes a certain amount of time, so that the NMR signal remains detectable for a period of time that can range from several milliseconds to several seconds. Furthermore, the relaxing component of the NMR signal will be characteristic of individual mobility domains, which in turn, help identify the molecules involved in the motions and the rate of the motions. Samples can be scanned and the NMR signal acquired multiple times, such as between 1 and 256 times or up to 10 to 50 times.

In one embodiment, the hydrogen spin-spin relaxation rate constants (or time constants) are measured using a low-field bench-top time-domain NMR analyzer, and the relaxation rate constant for water is resolved through a multi-exponential deconvolution algorithm. The analysis can be made directly on serum, plasma, whole blood or intact tissue. Because of the relative simplicity and low cost, this method has potential application to clinical testing for the detection of a disorder such as insulin resistance, inflammation, dyslipidemia, oxidative stress and brain abnormalities (e.g., low cognitive scores or mild cognitive impairment). Alternatively, the measurements can be made in conventional high-field NMR spectrometers or a portable,

wearable NMR device. In one embodiment, a tube containing a sample is placed into the bore of the magnet of a bench-top TD-NMR analyzer. Typically, the analyzer can be operated at 5,10, 20, 40 or 60 MHz resonance frequency for hydrogen.

A Car-Purcell-Miniboom-Gill (CPMG) pulse sequence can, in some embodiments, be used to measure the exponential T_2 time-decay curve for water. This pulse sequence effectively eliminates chemical shifts and magnetic field inhomogeneity, permitting the measurement of T_2 values. Of course, any pulse sequence capable of measuring T_2 and, if necessary, partially suppressing the water signal can be used in the disclosed method. Although T_2 measurements can be linked with chemical shifts and measured in the frequency domain, the present TD-NMR method measures T_2 in the time domain without chemical shifts. The resulting T_2 decay curve for human serum is multi-exponential, so the individual exponential terms can be deconvoluted and resolved with the use of an inverse Laplacian transform. The mathematical calculation can be implemented using Xpfit, a public domain program, among other open-source or commercially available solutions. While the use of an inverse Laplace transform is exemplified in this application for the exponential analysis algorithm, any other suitable exponential analysis algorithm can be used for the analysis of the exponential data acquired by the practice of the disclosed methods. With respect to the exponential analysis of the acquired data, at least one exponential term is analyzed. In various embodiments, between one and 10 terms are analyzed. Other embodiments provide for the analysis of up to 6 terms or up to three exponential terms.

Plasma and serum water T_2 values from TD-NMR have been correlated with over 70 blood tests (Table 4). Strong correlations exist between plasma water T_2, plasma viscosity and total serum protein concentration, particularly serum globulins (Table 1). Inflammatory markers also correlated with plasma water T_2. These include the inflammatory markers: C-reactive

protein, white blood cell counts and neutrophil counts. Plasma water T_2 also correlated with the following markers of insulin resistance: insulin C-peptide, HOMA2-IR, -%B, -%S, triglycerides and HbA_{1c}.

Serum water T_2 values (Table 2) reveal a slightly different set of correlations as compared with plasma. Serum water T_2 correlates with a number of LDL-related cholesterol markers. Serum water T_2 also shows significant correlations with serum protein, globulin and albumin concentrations as well as serum viscosity. Additionally, serum water T_2 also correlates with white blood cell counts, neutrophil counts and C-reactive protein (inflammatory markers). Thus, serum water T_2 values can be used to assess the risk or presence of disorders such as inflammation or dyslipidemia (lipid disorders in a subject).

The disclosed methods can also be coupled with treatments (under the supervision of a physician or appropriate licensed health care provider) for the disorders discussed herein for subjects identified to be at risk for the development of diabetes, coronary artery disease, Alzheimer's disease, etc. For example, subjects with evidence of inflammation can be treated with a variety of anti-inflammatory agents. Non-limiting examples of such agents include: non-steroidal anti-inflammatory agents such as ibuprofen, naproxen, aspirin, celecoxib, sulindac, oxaprozin, salsalate, diflunisal, piroxicam, indomethacin, etodolac, meloxicam, nambumetone, ketorolac tromethamine, and diclofenac; corticosteroids, such as beclomethasone, beclometasone, budesonide, flunisolide, fluticasone, tramcinolone, methylprednisone, prenisolone or prednisone. For patients showing evidence of insulin resistance, the patients can be treated by altering diet, initiating a diabetic treatment, increasing exercise or otherwise modifying behavior so as to reduce the likelihood of developing diabetes arising from insulin resistance. For subjects showing evidence of a dyslipidemia, the subject can be treated with low

dose aspirin and/or statins (such as atorvastatin, fluvastatin, lovastatin, pitavastatin, pravastatin, rosuvastatin or simcastatin), or another suitable lipid-lowering therapy.

Figure 5 illustrates an example system architecture in which an implementation of techniques for health screening using T_1 and/or T_2 values for water may be carried out. In the example illustrated in Figure 5, a health screening service **200** may receive information from an NMR **210**, used to process a subject **205** sample. Health screening service **200** may output results, such as a health score or treatment information to subject **205**.

A device appropriate for a health screening service **200** may be implemented as software or hardware (or a combination thereof) on a device which may be an instantiation of system **300**. Such a device may be or include computing systems or devices such as a laptop, desktop, tablet, reader, mobile phone, wearable device, "Internet of things" device, and the like.

An NMR device **210** may be laboratory device, bench-top device, or even a portable device. A portable NMR device **210** may be capable of being worn (e.g., wearable), connected to a subject's skin through a biosensor. In such cases the NMR device **210** may communicate with the health screening service over a wireless communications network, such as Bluetooth®.

Health screening service **200** may interact with a data store **220**, which can store biomarkers and their associated T_1 and/or T_2 reference values and/or ranges for different sample types. Data store **220** may also store additional information, for example, treatment information and data sets derived from samples gathered from other subjects. All or part of data store **220** may be instantiated on the same system as health screening service, or may be instantiated on multiple systems, connected by a network.

Communications and interchanges of data between components in the environment may take place over a network (not shown). The network can include, but is not limited to, a cellular

network (e.g., wireless phone), a point-to-point dial up connection, a satellite network, the Internet, a local area network (LAN), a wide area network (WAN), a Wi-Fi network, an ad hoc network, an intranet, an extranet, or a combination thereof. The network may include one or more connected networks (e.g., a multi-network environment) including public networks, such as the Internet, and/or private networks such as a secure enterprise private network.

Figure 6 shows a block diagram illustrating components of a computing device or system used in some implementations of an apparatus for health screening using T_1 and/or T_2 values for water. For example, any computing device operative to run a health screening service **200** or intermediate devices facilitating interaction between other devices in the environment may each be implemented as described with respect to system **300,** which can itself include one or more computing devices. The system **300** can include one or more blade server devices, standalone server devices, personal computers, routers, hubs, switches, bridges, firewall devices, intrusion detection devices, mainframe computers, network-attached storage devices, and other types of computing devices. The hardware can be configured according to any suitable computer architectures such as a Symmetric Multi-Processing (SMP) architecture or a Non-Uniform Memory Access (NUMA) architecture.

The system **300** can include a processing system **301**, which may include a processing device such as a central processing unit (CPU) or microprocessor and other circuitry that retrieves and executes software **302** from storage system **303**. Processing system **301** may be implemented within a single processing device but may also be distributed across multiple processing devices or sub-systems that cooperate in executing program instructions.

Examples of processing system **301** include general purpose central processing units, application specific processors, and logic devices, as well as any other type of processing device,

combinations, or variations thereof. The one or more processing devices may include multiprocessors or multi-core processors and may operate according to one or more suitable instruction sets including, but not limited to, a Reduced Instruction Set Computing (RISC) instruction set, a Complex Instruction Set Computing (CISC) instruction set, or a combination thereof. In certain embodiments, one or more digital signal processors (DSPs) may be included as part of the computer hardware of the system in place of or in addition to a general purpose CPU.

Storage system **303** may comprise any computer readable storage media readable by processing system **301** and capable of storing software **302** including health screening service **200** and/or data store **220**. Storage system **303** may include volatile and nonvolatile, removable and non-removable media implemented in any method or technology for storage of information, such as computer readable instructions, data structures, program modules, or other data.

Examples of storage media include random access memory (RAM), read only memory (ROM), magnetic disks, optical disks, CDs, DVDs, flash memory, solid state memory, phase change memory, or any other suitable storage media. Certain implementations may involve either or both virtual memory and non-virtual memory. In no case do storage media consist of a propagated signal. In addition to storage media, in some implementations, storage system **303** may also include communication media over which software **302** may be communicated internally or externally.

Storage system **303** may be implemented as a single storage device but may also be implemented across multiple storage devices or sub-systems co-located or distributed relative to each other. Storage system **303** may include additional elements, such as a controller, capable of communicating with processing system **301**.

Software **302** may be implemented in program instructions and among other functions may, when executed by system **300** in general or processing system **301** in particular, direct system **300** or processing system **301** to operate as described herein for enabling health screening with T_2 and/or T_1 values. Software **302** may provide program instructions **304** that implement a health screening service **200** or subcomponents thereof. Software **302** may implement on system **300** components, programs, agents, or layers that implement in machine-readable processing instructions the methods described herein as performed by health screening service **200** (as instructions **304**).

Software **302** may also include additional processes, programs, or components, such as operating system software, database management software, or other application software. Software **302** may also include firmware or some other form of machine-readable processing instructions executable by processing system **301**.

In general, software **302** may, when loaded into processing system **301** and executed, transform system **300** overall from a general-purpose computing system into a special-purpose computing system customized to facilitate health screening with T_2 and/or T_1 values. Indeed, encoding software **302** on storage system **303** may transform the physical structure of storage system **303**. The specific transformation of the physical structure may depend on various factors in different implementations of this description. Examples of such factors may include, but are not limited to, the technology used to implement the storage media of storage system **303** and whether the computer-storage media are characterized as primary or secondary storage.

System **300** may represent any computing system on which software **302** may be staged and from where software **302** may be distributed, transported, downloaded, or otherwise

provided to yet another computing system for deployment and execution, or yet additional distribution.

In embodiments where the system **300** includes multiple computing devices, one or more communications networks may be used to facilitate communication among the computing devices. For example, the one or more communications networks can include a local, wide area, or ad hoc network that facilitates communication among the computing devices. One or more direct communication links can be included between the computing devices. In addition, in some cases, the computing devices can be installed at geographically distributed locations. In other cases, the multiple computing devices can be installed at a single geographic location, such as a server farm or an office.

A communication interface **305** may be included, providing communication connections and devices that allow for communication between system **300** and other computing systems (not shown) over a communication network or collection of networks (not shown) or the air. Examples of connections and devices that together allow for inter-system communication may include network interface cards, antennas, power amplifiers, RF circuitry, transceivers, and other communication circuitry. The connections and devices may communicate over communication media to exchange communications with other computing systems or networks of systems, such as metal, glass, air, or any other suitable communication media. The aforementioned communication media, network, connections, and devices are well known and need not be discussed at length here.

It should be noted that many elements of system **300** may be included in a system-on-a-chip (SoC) device. These elements may include, but are not limited to, the processing system

301, a communications interface **305**, and even elements of the storage system **303** and software **302**.

Alternatively, or in addition, the functionality, methods and processes described herein can be implemented, at least in part, by one or more hardware modules (or logic components). For example, the hardware modules can include, but are not limited to, application-specific integrated circuit (ASIC) chips, field programmable gate arrays (FPGAs), system-on-a-chip (SoC) systems, complex programmable logic devices (CPLDs) and other programmable logic devices now known or later developed. When the hardware modules are activated, the hardware modules perform the functionality, methods and processes included within the hardware modules.

MATERIALS AND METHODS

Materials and Methods

Subject recruitment. Human subject volunteers were recruited with informed consent into two protocols approved by the Institutional Review Board of the University of North Texas Health Science Center in Fort Worth (UNTHSC). One protocol recruited healthy adult subjects from the student and staff population of UNTHSC, including some spouses and significant others. The second protocol recruited subjects from the community who are participating in the Health and Aging Brain Study at UNTHSC *(8)*. Exclusion criteria for the current study included diabetes ($HbA_{1C} > 6.4$), acute/chronic infection or illness (C-reactive protein > 10), or not fasting for at least 12 hours. Characteristics of the human study group are summarized in Table 3.

Plasma and serum preparation. Blood samples were drawn in the morning by a trained nurse or phlebotomist after a ≥12 hour overnight fast. For plasma preparation, blood was drawn

into lavender-top tubes containing EDTA as the anticoagulant. For serum, blood was drawn into plain glass red-top tubes lacking any gel separator or clot activators (BD model 366441) in order to avoid potential interference with TD-NMR or viscosity testing. Blood obtained for NMR LipoProfile analysis (LipoScience/LabCorp) were drawn into black-top tubes specialized for that purpose. Every effort was made to collect enough blood from each subject to perform all 70+ planned measurements. However, there were situations where the amount of blood collected from a given subject was not sufficient or samples were rejected by the testing lab. That variability accounts for the test-to-test differences in sample size (n) in the statistical analyses.

Blood Sample analysis and banking. The plasma and serum samples were processed immediately after each blood draw. The samples were centrifuged to remove pelleted blood cells, followed by a second low speed spin of the supernatant to remove residual blood cells. The TD-NMR water T_2 measurements were performed five times on fresh plasma followed immediately by 5 repeats on serum such that all water T_2 measurements were completed within ~2 hours after the blood draw. Likewise, viscosity was measured in house on fresh serum and plasma samples within a few hours of the blood draw using methods described elsewhere *(9)*. Aliquots of fresh serum were sent on ice to Atherotech for the Vertical Autoprofile advanced lipoprotein testing, as well as to determine LDL-P, hs-CRP, GGT, homocysteine, and Lp(a). Assays for apolipoprotein E, total antioxidant capacity, protein carbonylation, HNE and free fatty acids were performed in house using kits. All other testing of serum and plasma samples was performed by LabCorp, Quest Diagnostics and their affiliates including LipoScience and OmegaQuant. Sample aliquots for amino acid analysis were frozen immediately and stored prior to shipment.

Benchtop Time-domain NMR Relaxometry. Measurements of T_2 and T_1 were performed at 37°C on unmodified whole serum or plasma using methods and instrumentation described elsewhere *(9)*, with significant modifications noted below. The pulse sequence for T_2 measurement included a Carr-Purcell-Meiboom-Gill refocusing scheme *(10, 11)* with a prior 180° pulse and delta delay incorporated for partial water suppression (Figure 4). In our experience, a critical factor in obtaining high quality TD-NMR data with aqueous samples is carefully tuning the delta delay to avoid radiation damping. This artifact occurs when the additional magnetic field created by the intense oscillating water signal distorts the performance of CPMG pulse scheme *(12)*. Radiation damping readily manifests itself by a non-random oscillatory artifact observed in the residuals of the fit of the data after inverse Laplace transform. We determined empirically that a delta delay of $0.95*T_1$ (leading to a water signal that is ~23% of its full intensity) provides a level of suppression of the water sufficient to avoid radiation damping, while still maximizing the overall signal intensity of the water and the other lipid/protein peaks for analysis. Even after partial suppression, the intensity of the water signal was still sufficiently intense to measure water T_2 with high precision after only 16 scans. In this regard, the goals of water suppression in TD-NMR are different from that of frequency-domain NMR spectroscopy, where essentially complete suppression of the water is normally desired. Another unique aspect to this TD-NMR pulse scheme was the delayed acquisition of the data points, which began 19 ms after the beginning of the CPMG scheme. This strategy was a deliberate attempt to de-emphasize the very fast decay processes at the beginning of the decay curve in order to reduce the number of exponential terms and simplify the multi-exponential profile for analysis.

The raw decay curves were analyzed using an inverse Laplace transform as implemented in Xpfit, a public domain program. A key to obtaining stable, reproducible results with this data was to restrain the number of exponential terms to a consistent number, in this case to three. Less than three terms was not adequate to fit the data and gave poor residuals, and more than three rendered the calculations to be increasingly ill posed. Given the high signal-to-noise of the water peak, it was not difficult to obtain stable solutions for serum or plasma data recorded with 16 scans.

The correlation, linear regression and statistical analyses were performed using GraphPad Prism v. 6.05 (GraphPad Software, Inc.). The guiding principles for the statistical analyses used in this study are discussed in the book by Motulsky *(13)*.

EXAMPLE 1

Time-domain NMR relaxometry, in contrast with conventional frequency-domain NMR spectroscopy, involves the analysis of single- or multi-exponential decay curves to extract relaxation time constants (Fig. 1). As acquired with this experimental protocol *(14)*, the T_2 profiles for human serum are comprised of three tiny peaks with T_2 values <200 ms (Fig. 1B, orange) and a much more intense water peak with a T_2 value >600 ms (Fig. 1B, blue). When trying to monitor the tiny peaks,, the intense water signal is considered a nuisance, as it can lead to radiation damping and obscure the detection and analysis of the much smaller lipid/protein peaks. We assessed the variability of serum and plasma T_2 values in a human subject population and modified the protocol to include fast, six-minute analyses of the water in samples obtained

from the test population. The water T_2 values for serum and plasma exhibit high precision, with standard errors less than 0.5%.

The characteristics of the human subjects analyzed in this study are summarized in Table 3. Overall, this is an apparently healthy group of adults spanning a wide age range, with approximately equal numbers of males and females of diverse race and ethnicity. Exclusion criteria were diabetes (HbA_{1c} >6.4) or acute/chronic illness (C-reactive protein >10). The mean values for various blood biomarkers fall within the normal reference ranges, although the values for some individual subjects are outside of those ranges. For example, the mean HbA_{1c} value is 5.5 ± 0.3, and 19 of the 29 subjects are non-diabetic by HbA_{1C} criteria. Of the remaining 9, seven have HbA_{1C} values of 5.7 or 5.8, near the borderline between non-diabetic and pre-diabetic. By fasting glucose criteria, only 3 of the 29 show evidence of pre-diabetes. Similarly, some individual subjects have lipid levels outside the reference ranges, even though the mean values are not. However, for white blood cell counts, insulin C-peptide, total protein and albumin concentrations, all 29 subjects are within normal reference ranges.

The plasma and serum water T_2 values from TD-NMR vary considerably across the study population (Fig. 1C and Table 3). To identify the factors governing the variation in T_2, we measured over 70 blood tests and correlated those values with the plasma and serum T_2 values for water (Table 4). The correlation coefficients for plasma water T_2 are listed in Table 1 and sample linear regression plots are provided in Figure 2. Not surprisingly, strong correlations exist between water T_2, plasma viscosity and total serum protein concentration. Of the main protein fractions, the concentration of serum globulins, but not serum albumin, met the threshold of $p<0.05$. Among the strongest correlations with plasma water T_2 were several inflammatory markers: C-reactive protein, white blood cell and neutrophil counts. In addition, plasma water

T_2 correlated with markers of insulin resistance: insulin C-peptide, HOMA2-IR, -%B, -%S, triglycerides and HbA_{1c}.

Serum water T_2 values (Table 2) reveal a somewhat different set of correlations as compared with plasma. Serum water T_2 does not correlate with markers of insulin resistance. Rather, it correlates with a number of LDL-related cholesterol markers. However, serum water T_2 does show significant correlations with serum protein, globulin and albumin concentrations as well as serum viscosity. Like plasma, serum water T_2 also correlates with white blood cell and neutrophil counts, as well as C-reactive protein.

The correlations from this observational study led us to consider the factors that may contribute directly to the variation in plasma and serum water T_2, as well as those that may be indirectly linked through another variable or a network of variables. Human blood plasma and serum are complex mixtures containing hundreds of different proteins and lipoproteins as well as numerous small molecule metabolites. At first thought, de-convoluting these myriad variables would seem to be hopelessly complex. However, the five most abundant proteins in serum (albumin, IgG, transferrin, α1-antitrypsin and IgA) account for nearly 90% of total serum protein mass and the top two, nearly 80%. So identifying the primary contributors to water T_2 may not be impossible.

We used two approaches to tease apart the factors giving rise to variations in plasma and serum T_2. The first approach was reductionist, utilizing controlled experiments on simplified model systems that mimic one or more components of human serum or plasma. The second was statistical and involved correcting for the influence of one variable and analyzing the correlations with those that remain.

Figure 3A displays the variation of water T_2 with protein concentration in a sample containing only human serum albumin in buffer (triangles). As protein concentration increases, the water T_2 decreases linearly, while the viscosity of the sample increases. Similar results are observed for lipoprotein-deficient serum (Fig. 3A, squares) and whole serum (circles), progressively diluted to change protein concentration. The influence of viscosity on T_2 can removed by analyzing the regression residuals *(15)*, yielding the parameter T_{2v}. The T_{2v} values for albumin solutions, like uncorrected T_2, are negatively correlated with protein concentration. Likewise, T_{2v} values for whole human serum are negatively correlated with total serum protein concentration (Table 14). Therefore, the water T_2 value must be influenced not only by viscosity, but other factors such as the binding of water to protein molecules *(16, 17)*.

The ^1H T_2 values for water and other small molecules in solution are inversely proportional to the correlation time for rotational diffusion, *i.e.*, the time it takes for reorientation of the ^1H magnetic dipoles of water molecules in the static magnetic field of the NMR instrument *(18, 19)*. In turn, the rotational correlation time depends on temperature and viscosity, as defined by the Stokes-Einstein-Debye equation *(9)*. Water molecules bound to proteins sense the slower rotational tumbling of the protein, and thus the observed water T_2 is lower than that of unbound water *(16)*. In addition, the protein-bound water molecules undergo exchange with unbound water, and the hydrogen atoms on ionizable groups of the proteins exchange with those of unbound water. Both exchange processes further decrease the observed ^1H T_2 for water *(17)*. In summary, T_2 is influenced by sample viscosity as well as the binding and exchange of water molecules on and off protein binding sites.

Insulin Resistance and T_2. We sought to identify the factors that underlie the correlation of plasma water T_2, but not serum T_2, with markers of insulin resistance. The principal

difference between plasma and serum is the presence of clotting factors III, VIII and XIII and I (fibrinogen) *(20)*. Three of these four factors have negligible concentrations in plasma, but fibrinogen is abundant, representing ~4% of total plasma protein. Fibrinogen levels increase in insulin resistance and diabetes *(21-23)*, and increased fibrinogen is an established risk factor for cardiovascular disease. Correction of plasma T_2 values by removing the influence of serum protein concentration highlights the influence of fibrinogen. Like uncorrected plasma T_2, plasma T_{2p} values display an inverse correlation with insulin resistance biomarkers (Table 5). Thus, plasma T_2 appears to be sensing insulin resistance, in part, through variations in fibrinogen concentration.

Although fibrinogen level is a significant contributor, it is not the only factor linking T_2 and insulin resistance. Plasma T_{2a} removes the influence of albumin and highlights both fibrinogen and globulin concentrations. Among all of the T_2 variants, plasma T_{2a} it exhibited the strongest correlations with insulin resistance markers (Table 6). Conversely, plasma T_{2g} showed weaker correlations (Table 7). *Serum* T_{2a}, which highlights the influence of globulins in the absence of fibrinogen, also correlates with insulin resistance markers (Table 11). The most abundant proteins present in the serum globulin fraction are IgG, transferrin, α1-antitrysin, IgA, IgM and haptoglobin. Immunoglobulin concentrations, especially IgA, increase in metabolic disorders including metabolic syndrome, obesity, hyperglycemia *(24)*. Thus, plasma T_2 appears to be sensing insulin resistance through variations in both fibrinogen and immunoglobulin concentrations.

Dyslipidemia and T_2. Serum water T_2, but not plasma T_2, is inversely correlated with a number of LDL-related biomarkers. This result parallels previous observations by Rosenson *et al.* that LDL-C correlates with serum, but not plasma viscosity *(25)*. Similar correlations of T_2

and LDL markers are observed with serum T_{2p}, T_{2g}, T_{2a} and T_{2v} (Tables 10-12, 14). This pattern suggests that serum water T_2 is sensing elevated LDL cholesterol and particle number concentration through the direct binding of water to lipoprotein particles.

Inflammation and T_2. Both plasma and serum water T_2 values correlate inversely with inflammatory markers, namely white blood cell and neutrophil counts, C-reactive protein and red cell distribution width *(26)*. For white cell counts, the strongest correlations were observed for plasma T_2 and serum T_{2c}, whereas no detectable correlations were observed for plasma T_{2v}, serum T_{2a} and serum T_{2p}. Overall, it appears that T_2 is sensing white blood cell counts via changes in fibrinogen and albumin (plasma) or just albumin (serum). Neutrophils, which comprise three fourths of the white blood cell population and are linked with both inflammation and insulin resistance *(27)*, show a pattern similar to that of white blood cells. For C-reactive protein, the pattern was different. The strongest correlation was observed with plasma T_{2a}, whereas no correlations with $p<0.05$ were observed for plasma T_{2v}, serum T_{2v}, serum T_{2g} and serum T_{2p}. Taken together, it appears that T_2 is sensing C-reactive protein levels via fluctuations in fibrinogen and globulins (plasma) or just globulins (serum).

Both plasma and serum T_{2g}, but not other T_2 variants, correlate with monocyte count, another marker of inflammation *(28)*. Similarly, plasma T_{2g} correlates with platelets, which have dual roles in thrombosis and inflammation *(29)*.

Metabolite Levels and T_2. To assess the possible contribution of small metabolites to variations in water T_2, we conducted a series of controlled experiments. The samples contained fixed physiological concentrations of human albumin and □-globulins, and varying amounts of metabolites, either an amino acid mixture (0.05 - 5.0 mg/ml), glucose (50 - 400 mg/dl), ATP (0.5 - 2.5mg/ml), uric acid (2.5 - 8.6 mg/dl), urea (1 - 5mg/dl), or glyceraldehyde (1.2 - 4.3 mg/dl).

No significant changes in water T_2 were observed across these physiological ranges of metabolites. Only glucose at 400 mg/dl, a level found in severe uncontrolled diabetes, caused a small but significant decrease in T_2. Although water can bind to small molecules, the effect on its rotational correlation time and T_2 is negligible compared to that for water bound to much larger assemblies like proteins and lipoproteins.

Proteolysis, Oxidation and T_2. The measurement of water T_2 required only six minute experiments, but we also acquired data for longer periods of time in order to track the much smaller lipid and protein peaks. The T_2 value of the water peak (not the lipid/protein peaks) slowly decreased over a 3 to 18 hour period of incubation at 37°C. Initially, we hypothesized that the slow, gradual decrease in water T_2 may be resulting from *ex vivo* proteolysis. To assess the effect of proteolysis, we incubated whole human serum with exogenous trypsin and monitored T_2 over time. This incubation did not lead to a decrease in T_2. Similar experiments with simple protein mixtures and trypsin in buffer did not result in a decrease in T_2, but rather a small increase. The lack of sensitivity of T_2 to proteolysis could arise from two factors. Water binding to smaller protein fragments would cause less of a decrease in T_2 compared to water binding to larger, intact proteins. If significant proteolysis occurs, it may cause T_2 to increase, not decrease. Another consideration is that human blood has evolved to resist proteolysis, especially through the activity of α_1-antitrysin. It is notable that across our human subject population, the concentration of α_1-antitrysin did not correlate with any of the T_2 markers.

Another possible cause of slow gradual *ex vivo* decrease in water T_2 is protein oxidation. Hydrogen peroxide is ubiquitous in the human body *(30)* and can serve as a substrate for metal-catalyzed oxidation involving albumin-bound copper *(31)*. The product is hydroxyl radical, a highly reactive oxygen species that can non-enzymatically hydroxylate proline and lysine side

chains *(32)* and cause a range of other protein modifications including carbonylation *(33)*. Such modifications increase the polarity of protein side chains and provide additional binding sites for water.

Figure 3B illustrates the decrease in T_2 for human serum and plasma samples incubated with increasing amounts of copper (II) sulfate. The effect is lessened when histidine, a copper chelator, is included in the buffer. Similar results were observed in protein solutions containing only albumin and □-globulin in buffer (Fig. 3C). By sequestering copper and preventing metal catalyzed oxidation of other proteins, albumin is thought to be the most abundant anti-oxidant in human blood *(34)*. Some of the hydrogen peroxide needed for this reaction may be derived from neutrophils activated during inflammation *(35, 36)*.

Is T_2 able to sense metal-catalyzed protein oxidation in blood samples from human subjects? One of the consequences of albumin oxidation *(37)*, as well as glycation *(38)*, is a change in the protein's net charge, with an anionic shift to lower isoelectric point. Therefore, we searched for evidence of this anionic shift in the blood samples from our study population. Serum T_2 and T_{2g} are positively correlated with chloride ion concentration and the anion gap (Fig. 3E; Tables 2 and 12). The anion gap is used in clinical medicine to help diagnose different types of acid-base abnormalities *(39)*. The body maintains charge neutrality in the circulation, but the concentration of measured cations nearly always exceeds that of measured anions. The anion gap is defined as $[UA] - [UC] = [Na^+] + [K^+] - ([Cl^-] + [HCO_3^-])$, where UA and UC represent unmeasured anions and cations, respectively. The gap results primarily from albumin, an anionic protein with an isoelectric point of ~4.9. As the albumin concentration increases *in vivo*, the body decreases the chloride ion concentration to maintain charge balance, resulting in

an increase in the anion gap. Across this human study population, serum T_2 and T_{2g} are sensing differences in anion gap, in part, through variation in albumin concentration.

Another factor that modulates the anion gap is the net charge of albumin molecules. Correcting serum T_2 values for albumin concentration partially, but not completely, eliminates the dependence of T_2 on anion gap (Fig. 3F). This observation indicates that T_2 is sensing changes in albumin net charge, as well as concentration, likely as a result of glyco-oxidation linked to inflammation. In support of this conclusion, the anion gap corrected for albumin concentration correlates with levels of C-reactive protein in our subject population.

Correlations of other biomarkers with T_2. Alanine concentration is noteworthy for its inverse correlations with water T_2 values, specifically serum and plasma water T_{2p} and T_{2g}. One of the most abundant free amino acids in the blood, alanine levels increase with HbA_{1c}, triglycerides, small LDL and LDL particle number, and the levels of other amino acids. This pattern is consistent with insulin resistance, protein mobilization from muscle and abnormalities in LDL metabolism. Phenylalanine concentration correlates inversely with serum T_2, T_{2p}, T_{2g} and T_{2v}, but not T_{2c} and T_{2a} or any of the plasma T_2 markers. It correlates positively with markers of abnormal LDL metabolism. Serum water T_2 appears to be sensing variation in phenylalanine levels primarily via changes in LDL-C and LDL-P, whereas it is sensing variation in alanine through both insulin resistance and LDL markers. Homocysteine, a known marker of cardiovascular risk, correlates with plasma T_{2g}.

Two amino acids show positive correlations with T_2: asparagine and 3-methyl-histidine *(40)*. For the latter, serum T_2 appears to be sensing its levels via changes in globulin levels. Of note, 3-methyl-histidine is not synthesized by humans, but is a breakdown product of anserine, a dipeptide derived from the dietary ingestion of poultry and fish. Both anserine and 3-

methylhistidine are chelators of divalent cations and may inhibit copper-catalyzed oxidation, as well as glycation and lipoxidation *(41)*.

It should be understood that the examples and embodiments described herein are for illustrative purposes only and that various modifications or changes in light thereof will be suggested to persons skilled in the art and are to be included within the spirit and purview of this application and the scope of the appended claims. In addition, any elements or limitations of any invention or embodiment thereof disclosed herein can be combined with any and/or all other elements or limitations (individually or in any combination) or any other invention or embodiment thereof disclosed herein, and all such combinations are contemplated with the scope of the invention without limitation thereto.

Biomarker	N	r (Pearson)	R^2	r_S (Spearman)
Total Protein, Serum[1]	28	-0.65***	0.42***	-0.65***
Globulins, Serum[1]	28	-0.52**	0.27**	-0.54**
Viscosity, Serum[1]	24	-0.49*	0.24*	-0.65***
Viscosity, Plasma[1]	9	-0.82**	0.67**	-0.90***
WBC Count[2]	27	-0.60***	0.36***	-0.60***
Neutrophil Count[2]	27	-0.54**	0.29**	-0.47*
Platelet Count[2]	27	-0.38	0.14	-0.39*
C-reactive Protein[2]	27	-0.57**	0.33**	-0.54**
HbA_{1c}[3]	27	-0.43*	0.19*	-0.44*
Insulin C-peptide[3]	28	-0.42*	0.18*	-0.41*
HOMA2-IR[3]	28	-0.39*	0.16*	-0.39*
HOMA2-%B[3]	28	-0.40*	0.16*	-0.36
HOMA2-%S[3]	28	+0.44*	0.20*	+0.40*
Triglycerides[3]	28	-0.30	0.09	-0.43*
Asparagine[4]	26	+0.41*	0.17*	+0.23

*p<0.05 **p<0.01 ***p<0.001

Table 1. Correlation coefficients for plasma water T_2 with biomarkers for protein concentration and viscosity ([1]), inflammation ([2]), insulin resistance ([3]) and other processes ([4]). Biomarkers were included in the table if they demonstrated at least one correlation coefficient with a p value < 0.05. The null hypothesis is defined as no correlation between plasma water T_2 and a particular biomarker in the overall population.

Biomarker	N	r (Pearson)	R^2	r_S (Spearman)
Total Protein, Serum[1]	26	-0.82****	0.67****	-0.86****
Albumin, Serum[1]	26	-0.39*	0.15*	-0.39*
Globulins, Serum[1]	26	-0.49*	0.24*	-0.57**
Viscosity, Serum[1]	25	-0.52*	0.27*	-0.76****
WBC Count[2]	25	-0.54**	0.29**	-0.51**
Neutrophil Count[2]	25	-0.52**	0.27**	-0.52**
Eosinophil Count[2]	25	-0.32	0.10	-0.45*
C-reactive Protein[2]	25	-0.37	0.14	-0.49*
RDW[2]	23	-0.61**	0.38**	-0.66***
Total Cholesterol[3]	26	-0.47*	0.23*	-0.52**
Non-HDL-C[3]	26	-0.42*	0.18*	-0.49*
LDL-C[3]	26	-0.42*	0.18*	-0.44*
LDL-P[3]	25	-0.45*	0.20*	-0.47*
Apo B[3]	26	-0.39*	0.15*	-0.42
3-Methyl-Histidine[4§]	24	+0.39	0.15	+0.50**
Phenylalanine[4]	24	-0.42*	0.17*	-0.33
Anion Gap[4]	26	-0.39*	0.15*	-0.41*

*p<0.05 **p<0.01 ***p<0.001 ****p<0.0001

Table 2. Correlation coefficients for serum water T_2 values with biomarkers for protein concentration and viscosity ([1]), inflammation ([2]), dyslipidemia ([3]) and other metabolic processes ([4]). Biomarkers were included in this table if they demonstrated at least one correlation coefficient with a p value < 0.05. The null hypothesis is defined as no correlation between serum water T_2 and a particular biomarker in the overall population. [§]Numbering is based on current IUPAC nomenclature, as explained elsewhere *(30)*. Defined with this convention, 3-methyl-histidine refers to the amino acid found in anserine, a dipeptide not produced in human tissues, but derived from dietary ingestion of poultry and fish.

Table 3: Human Study Group

Parameter	Mean ± SD	Range, This Study	Reference Values[1]
Age	43 ± 18	24 - 80	n/a
Plasma T_2 (ms)	748.8 ± 57.1	642.8 - 865.9	n.d.
Serum T_2 (ms)	810.5 ± 52.1	692.1 - 915.0	n.d.
Total serum protein (g/dL)[3]	7.2 ± 0.4	6.2 - 7.9	6.1 - 8.1
Serum albumin (g/dL)[3]	4.5 ± 0.3	4.0 - 5.0	3.6 - 5.1
α_1-antitrypsin (mg/dL)[3]	130 ± 19	102 - 177	90 - 200
Serum viscosity (cP)[3]	1.17 ± 0.10	1.04 - 1.54[2]	1.27 ± 0.06
Plasma viscosity (cP)[3]	1.27 ± 0.17	1.07 - 1.46	1.39 ± 0.08
WBC count (x $10^3/\mu L$)[4]	6.3 ± 1.5	3.9 - 10.2	3.4 - 10.8
Neutrophil count (x $10^3/\mu L$)[4]	3.6 ± 1.4	1.8 - 7.3	1.4 - 7.0
hs-CRP (mg/L)[4]	1.9 ± 1.6	0.1 - 5.1	< 1.0 (low risk) 1.0 – 3.0 (average risk) > 3.0 (high risk)
Glucose (mg/dL)[5]	91 ± 8	78 - 115	<100 non-diabetic 100-125 (pre-diabetic)
HbA_{1c} (%)[5]	5.5 ± 0.3	4.9 - 6.2	<5.7 (non-diabetic) 5.7-6.4 (pre-diabetic)
Insulin C-peptide (ng/mL)[5]	2.4 ± 0.8	1.1 - 4.3	1.1 - 4.4
Triglycerides (mg/dL)[5]	111 ± 57	42 - 245	< 150 mg/dL
Total cholesterol (mg/dL)[6]	196 ± 44	111 - 329[2]	< 200 mg/dL
HDL-C (mg/dL)[6]	55 ± 12	32 - 85	> 40 mg/dL
LDL-C (mg/dL)[6]	119 ± 43	42 - 257[2]	< 130 mg/dL
TSH (µIU/mL)[7]	2.2 ± 1.1	0.6 - 5.3	0.5 - 4.5
Free T4, direct (ng/dL)[7]	1.2 ± 0.2	0.9 - 1.5	1.0 - 1.5

Table 3: Characteristics of the human study group (n=29). This sample size provided sufficient statistical power to identify correlations using conventional p-value thresholds. There were 15 females and 14 males, with an ethnic/racial distribution of 15 white, 6 Asian/Indian, 5 Hispanic and 3 African American/Caribbean. The mean BMI is 25.6 ± 4.2. [1]Reference values are from Quest, Labcorp and Atherotech; viscosity reference values were obtained from *(40)*; use of a different method may explain why the measured viscosity range is approximately 0.1 cP lower than the reference range. [2]One subject had a serum viscosity of 1.54 cP, a statistical outlier; the next highest was 1.30. This subject had the highest total cholesterol (329 mg/dL) and LDL-C (257 mg/dL), as well as a family history of type II hypercholesterolemia (father). **Correlation coefficients for plasma water T_2 with biomarkers for protein concentration and viscosity ([3]), inflammation ([4]), insulin resistance ([5]), dyslipidemia ([6]) and other metabolic processes ([7]).**

Table 4: Biomarkers Measured in this Study

TD-NMR Markers: plasma water T_2, T_{2p}, T_{2a}, T_{2g}, T_{2c}, T_{2v} serum water T_2, T_{2p}, T_{2a}, T_{2g}, T_{2c}, T_{2v}

Category	Correlated with T_2[†]	Did not correlate with T_2[†]
Protein, viscosity, liver function markers	total serum protein, serum albumin, serum globulins (calc), serum viscosity, plasma viscosity	α1-antitrypsin, AST, ALT, GGT
Inflammation, blood cell and oxidative stress markers	hs-CRP, WBC, neutrophils, monocytes, eosinophils, basophils, platelets, RDW, anion gap corrected for albumin concentration, TNFα, sICAM[*], I-309[*], factor VII[*]	RBC, hematocrit, hemoglobin, MCV, MCH, MCHC, lymphocytes, HNE, ORAC antioxidant capacity
Cholesterol/lipid markers	Total cholesterol, HDL-C, non-HDL-C, LDL-C, LDL-P, LDL size, small LDL-P, HDL-P, VLDL-C, remnant-C, apoB, DHA, omega-3 index	Lp(a), EPA, AA, apoAI, phospholipids, apoE
Insulin resistance & diabetes markers	insulin, insulin C-peptide, HbA_{1c}, HOMA2-IR, -%B, -%S, triglycerides, IR Score (LipoScience)	glucose, free fatty acids, body-mass index
Electrolyte markers	chloride, bicarbonate, anion gap	sodium, potassium, calcium
Kidney function markers	blood urea nitrogen (BUN)[*], estimated glomerular filtration rate (eGFR)[*]	creatinine
Thyroid function markers	thyroid stimulating hormone (TSH)	free T4

Table 4. Biomarkers measured in this study. [†]In this table, a correlation is defined as one where $p<0.05$ for the Pearson correlation, non-parametric Spearman correlation or both for at least one variant of serum or plasma water T_2. The null hypothesis states that there is no correlation between a plasma or serum water T_2 measure and a particular biomarker. The individual correlation coefficients and statistics are provided in Tables 1, 2 and 5-14. [*]These particular biomarkers were measured for only five-to-eight subjects; although they met the p-value threshold, the correlations are considered preliminary. The most compelling of these preliminary correlations was plasma T_{2a} with TNFα: $r = -0.93$, $R^2 = 0.87$, $r_S = -0.97$, with p values <0.05, <0.05 and <0.001, respectively.

Table 5: Water T_{2p} Correlations, Human Plasma

Biomarker	N	r (Pearson)	R^2	r_S (Spearman)
Total Protein, Serum[1]	28	0.00	0.00	-0.04
Albumin, Serum[1]	28	0.09	0.01	0.05
Globulins, Serum[1]	28	-0.07	0.01	-0.08
Viscosity, Serum[1]	24	-0.27	0.07	-0.32
Viscosity, Plasma[1]	9	-0.90***	0.81***	-0.93***
WBC Count[2]	27	-0.43*	0.18*	-0.40*
Neutrophil Count[2]	27	-0.39*	0.15*	-0.44*
C-reactive Protein[2]	27	-0.48*	0.23*	-0.41*
HbA_{1c}[3]	27	-0.41*	0.17*	-0.45*
Insulin C-peptide[3]	28	-0.43	0.19*	-0.47*
HOMA2-IR[3]	28	-0.41*	0.17*	-0.45*
HOMA2-%B[3]	28	-0.41*	0.16*	-0.36
HOMA2-%S[3]	28	+0.48**	0.23**	+0.46*
Triglycerides[3]	28	-0.28	0.08	-0.38*
Alanine[4]	26	-0.42*	0.18*	-0.43*
Citrulline[4]	26	-0.36	0.13	-0.41*
TSH[4]	28	-0.33	0.11	-0.39*

*p<0.05 **p<0.01 ***p<0.001

Table 5. Correlation coefficients for plasma water T_{2p} with biomarkers for protein concentration and viscosity ([1]), inflammation ([2]), insulin resistance ([3]) and other processes ([4]). The plasma water T_{2p} values represent the regression residuals obtained from a linear fit of plasma water T_2 vs. total serum protein. This analysis removes the influence of total *serum* protein concentration on plasma water T_2 values, emphasizing the influence of fibrinogen concentration.

Table 6: Water T_{2a} Correlations, Human Plasma

Biomarker	N	r (Pearson)	R^2	r_S (Spearman)
Total protein, serum[1]	28	-0.52**	0.27**	-0.50**
Albumin, Serum[1]	28	0.00	0.00	0.03
Globulins, Serum[1]	28	-0.60***	0.36***	-0.62***
Viscosity, Plasma[1]	9	-0.83**	0.68**	-0.90**
WBC Count[2]	27	-0.53**	0.28**	-0.49**
Neutrophil Count[2]	27	-0.51**	0.26**	-0.49**
C-reactive Protein[2]	27	-0.61**	0.37**	-0.63**
HbA_{1c}[3]	27	-0.46*	0.21*	-0.48*
Insulin C-peptide[3]	28	-0.50**	0.25**	-0.51**
HOMA2-IR[3]	28	-0.47*	0.22*	-0.48**
HOMA2-%B[3]	28	-0.46*	0.21*	-0.48**
HOMA2-%S[3]	28	+0.49**	0.24**	-0.50**
Triglycerides[3]	28	-0.37	0.14	-0.47*
TG/cholesterol ratio[3]	28	-0.32	0.10	-0.40*
Asparagine[4]	26	+0.47*	0.22*	+0.29
Bicarbonate ion[4]	28	+0.31	0.10	+0.41*

*p<0.05 **p<0.01 ***p<0.001

Table 6. Correlation coefficients for plasma water T_{2a} with biomarkers for protein concentration and viscosity ([1]), inflammation ([2]), insulin resistance ([3]) and other processes ([4]). Plasma water T_{2a} values represent the regression residuals obtained from a linear fit of plasma T_2 *vs*. serum albumin concentration. This analysis removes the influence of albumin concentration on plasma T_2 and emphasizes the influence of globulins and fibrinogen concentration.

Table 7: Water T_{2g} Correlations, Human Plasma

Biomarker	N	r (Pearson)	R^2	r_S (Spearman)
Albumin, Serum[1]	28	-0.46*	0.21*	-0.44*
Globulins, Serum[1]	28	0.00	0.00	-0.05
Viscosity, Plasma[1]	9	-0.82**	0.67**	-0.87**
C-reactive Protein[2]	27	-0.43*	0.18*	-0.40*
WBC Count[2]	27	-0.59**	0.35**	-0.54**
Neutrophil Count[2]	27	-0.46*	0.21*	-0.41*
Platelet Count[2]	27	-0.44*	0.19*	-0.42*
Monocyte Count[2]	27	-0.44*	0.19*	-0.54**
HbA_{1c}[3]	27	-0.37	0.14	-0.38*
HOMA2-%S[3]	28	+0.38*	0.15*	+0.34
IR Score (LipoScience)[4]	17	-0.31	0.09	-0.49*
LDL-P[4]	27	-0.39*	0.15*	-0.42*
Small LDL-P/HDL-P[4]	17	-0.36	0.13	-0.52*
Alanine[5]	26	-0.44*	0.20*	-0.44*
Homocysteine[5]	27	-0.30	0.09	-0.41*
Ethanolamine[5]	26	-0.37	0.14	-0.43*
MCV[5]	27	+0.34	0.12	+0.38*
Chloride ion[5]	28	+0.43*	0.18*	+0.49**

***p<0.05 **p<0.01 ***p<0.001**

Table 7. Correlation coefficients for plasma water T_{2g} with biomarkers for protein concentration and viscosity ([1]), inflammation ([2]), insulin resistance ([3]), dyslipidemia ([4]) and other processes ([5]). Plasma water T_{2g} values represent the regression residuals obtained from a linear fit of plasma T_2 *vs.* serum globulin concentration. This analysis removes the influence of serum globulin concentration on plasma water T_2 and highlights the influence of albumin and fibrinogen.

Table 8: Water T_{2c} Correlations, Human Plasma

Biomarker	N	r (Pearson)	R^2	r_S (Spearman)
Total protein, serum[1]	28	-0.64***	0.41***	-0.65***
Albumin, Serum[1]	28	-0.25	0.06	-0.29
Globulins, Serum[1]	28	-0.54**	0.30**	-0.57**
Viscosity, Plasma[1]	9	-0.81**	0.65**	-0.90**
WBC Count[2]	27	-0.64***	0.41***	-0.59**
Neutrophil Count[2]	27	-0.58**	0.34**	-0.47*
Platelet Count[2]	27	-0.36	0.13	-0.39*
C-reactive Protein[2]	27	-0.60***	0.36***	-0.51**
HbA_{1c}[3]	27	-0.45*	-0.20*	-0.49**
Insulin C-peptide[3]	28	-0.42*	0.18*	-0.47*
HOMA2-IR[3]	28	-0.39*	0.15*	-0.45*
HOMA2-%B[3]	28	-0.40*	0.16*	-0.40*
HOMA2-%S[3]	28	+0.42*	0.18*	+0.49
Triglycerides[3]	28	-0.30	0.09	-0.40*
Asparagine[4]	26	+0.39*	0.15*	+0.29

*p<0.05 **p<0.01 ***p<0.001

Table 8. Correlation coefficients for plasma water T_{2c} with biomarkers for protein concentration and viscosity ([1]), inflammation ([2]), insulin resistance ([3]) and other processes ([4]). Plasma water T_{2c} values represent the regression residuals obtained from a linear fit of plasma water T_2 *vs*. total cholesterol concentration. This analysis removes the influence of total cholesterol concentration on plasma water T_2 and emphasizes the influence of plasma proteins other than lipoproteins.

Table 9: Water T_{2v} Correlations, Human Plasma

Biomarker	N*	r (Pearson)	R^2	r_S (Spearman)
Total protein, serum[1]	9	-0.79*	0.63*	-0.73*
Viscosity, Plasma[1]	9	0.00	0.00	-0.25
RDW[2]	9	-0.53	0.28	-0.73*
Omega 3 Index[3]	9	-0.71*	0.50*	-0.85**
DHA[3]	9	-0.70*	0.48*	-0.77*
3-Methyl-Histidine[3]	9	+0.70*	0.48*	+0.54
Hydroxy-Proline[3]	9	-0.54	0.29	-0.76*

***p<0.05 **p<0.01 ***p<0.001**

Table 9. Correlation coefficients for plasma water T_{2v} values with biomarkers for protein concentration and viscosity ([1]), inflammation ([2]) and other processes ([3]). Plasma water T_{2v} values represent the regression residuals obtained from a linear fit of plasma water T_2 *vs*. plasma viscosity. This analysis removes the influence of plasma viscosity on plasma water T_2 and emphasizes the influence of water binding to proteins and lipoproteins. *For some subjects, there was not enough blood available to measure both serum and plasma viscosity, so the number of subjects with plasma viscosity data is smaller.

Table 10: Water T_{2p} Correlations, Human Serum

Biomarker	N	r (Pearson)	R^2	r_S (Spearman)
Total Protein, Serum[1]	26	0.00	0.00	0.00
Total Cholesterol[2]	26	-0.42*	0.18*	-0.40*
LDL-P[2]	25	-0.40*	0.16*	-0.45*
HDL-P[2]	15	+0.52*	0.27*	0.46
small-LDL-P/HDL-P[2]	15	-0.45	0.20	-0.53*
Platelet Count[3]	25	-0.30	0.09	-0.43*
Phenylalanine[4]	24	-0.53**	0.29**	-0.57**
Alanine[4]	24	-0.49*	0.24*	-0.57**
Tyrosine[4]	24	-0.41*	0.17*	-0.45*
1-Methyl-Histidine[4§]	24	-0.39	0.15	-0.42*

*p<0.05 **p<0.01 ***p<0.001 ****p<0.0001

Table 10. Correlation coefficients for serum water T_{2p} values with biomarkers for protein concentration and viscosity ([1]), dyslipidemia ([2]), inflammation ([3]), and other processes ([4]). Serum water T_{2p} values represent the regression residuals obtained from a linear fit of serum water T_2 *vs*. total serum protein concentration. This analysis removes the influence of albumin, globulins and viscosity on serum water T_2 and emphasizes the influence of serum lipoproteins.

[§]This numbering is based on current IUPAC nomenclature, as explained elsewhere *(30)*. As defined with this convention, 1-methyl-histidine refers to the amino acid found in carnosine, a dipeptide present in human muscle tissue. Elevated 1-methyl-histidine in the circulation is consistent with protein breakdown in muscle, as seen in insulin resistance and diabetes, or with strenuous exercise. Concurrent elevations of phenylalanine, alanine and tyrosine support that interpretation.

Table 11: Water T_{2a} Correlations, Human Serum

Biomarker	N	r (Pearson)	R^2	r_S (Spearman)
Total Protein, Serum[1]	26	-0.75****	0.56****	-0.74****
Albumin, Serum[1]	26	0.00	0.00	-0.01
Globulins, Serum[1]	26	-0.72****	0.52****	-0.72****
Viscosity, Serum[1]	25	-0.44*	0.19*	-0.62***
WBC Count[2]	25	-0.43*	0.19*	-0.40*
Neutrophil Count[2]	25	-0.47*	0.22*	-0.44*
Eosinophil Count[2]	25	-0.30	0.09	-0.41*
Basophil Count[2]	25	-0.36	0.13	-0.44*
RDW[2]	25	-0.14	0.02	-0.41*
RDW (see caption)[2§]	23	-0.59**	0.34**	-0.55**
C-reactive Protein[2]	25	-0.42*	0.18*	-0.57**
Total Cholesterol[3]	26	-0.43*	0.19*	-0.48*
Non-HDL-C[3]	26	-0.38	0.15	-0.48*
LDL-C (VAP)[3]	26	-0.36	0.13	-0.41*
LDL-P[3]	25	-0.40*	0.16*	-0.43*
Apo B[3]	26	-0.35	0.13	-0.44*
Remnant-C[3]	26	-0.35	0.13	-0.41*
Insulin[4]	26	-0.46*	0.21*	-0.47*
Insulin C-peptide[4]	26	-0.39*	0.15*	-0.42*
HOMA2-IR[4]	26	-0.38	0.14	-0.40*
HOMA2-%S[4]	26	+0.33	0.11	+0.42*

Table 11: Water T_{2a} Correlations, Human Serum (continued)

Biomarker	N	r (Pearson)	R^2	r_S (Spearman)
Bicarbonate ion[5]	**26**	**+0.45***	**0.20***	**+0.46***
3-methyl histidine[5]	**24**	**+0.35**	**0.12**	**+0.43***

***p<0.05 **p<0.01 ***p<0.001 ****p<0.0001**

Table 11. Correlation coefficients for serum water T_{2a} values with biomarkers for protein concentration and viscosity ([1]), inflammation ([2]), dyslipidemia ([3]), insulin resistance ([4]) and other processes ([5]). Serum water T_{2a} values represent the regression residuals obtained from a linear fit of serum water T_2 *vs*. serum albumin concentration. This analysis removes the influence of serum albumin concentration on serum water T_2 and emphasizes the influence of globulin and lipoproteins concentrations.

Table 12: Water T_{2g} Correlations, Human Serum

Biomarker	N	r (Pearson)	R^2	r_S (Spearman)
Total Protein, Serum[1]	26	-0.53**	0.28**	-0.49*
Albumin, Serum[1]	26	-0.70****	0.49****	-0.72****
Globulins, Serum[1]	26	0.00	0.00	0.01
Viscosity, Serum[1]	25	-0.41*	0.16*	-0.48*
WBC Count[2]	25	-0.51**	0.26**	-0.49*
Neutrophil Count[2]	25	-0.45*	0.20*	-0.48*
Monocyte Count[2]	25	-0.38	0.14	-0.44*
Total Cholesterol[3]	26	-0.47*	0.22*	-0.49*
Non-HDL-C[3]	26	-0.41*	0.17*	-0.44*
LDL-C (VAP)[3]	26	-0.43*	0.19*	-0.44*
LDL-P[3]	25	-0.47*	0.22*	-0.48*
Apo B[3]	26	-0.37	0.14	-0.41*
IR Score (LipoScience)[3]	15	-0.37	0.14	-0.53*
Phenylalanine[4]	24	-0.57**	0.33**	-0.60**
Tyrosine[4]	24	-0.54**	0.29**	-0.62**
Alanine[4]	24	-0.44*	0.19*	-0.47*
Ethanolamine[4]	24	-0.40	0.16	-0.50*
α-amino-butyric acid[4]	24	-0.40	0.16	-0.50*
Chloride Ion[4]	26	+0.40*	0.16*	+0.51**
Anion Gap[4]	26	-0.37	0.13	-0.41*

Table 12. Correlation coefficients for serum water T_{2g} values with biomarkers for protein concentration and viscosity ([1]), inflammation ([2]), dyslipidemia ([3]) and other processes ([4]). Serum water T_{2g} values represent the regression residuals obtained from a linear fit of serum water T_2 *vs*. serum globulin concentration. This analysis removes the influence of serum globulins on serum water T_2 and emphasizes the influence of albumin and lipoproteins.

Table 13: Water T_{2c} Correlations, Human Serum

Biomarker	N	r (Pearson)	R^2	r_S (Spearman)
Total Protein, Serum[1]	**26**	**-0.78******	**0.61******	**-0.82******
Globulins, Serum[1]	**26**	**-0.49***	**0.24***	**-0.65*****
Viscosity, Serum[1]	**25**	**-0.30**	**0.09**	**-0.62****
WBC Count[2]	**25**	**-0.64*****	**-0.40*****	**-0.57****
Neutrophil Count[2]	**25**	**-0.65*****	**-0.43*****	**-0.62****
C-reactive Protein[2]	**25**	**-0.41***	**0.17***	**-0.49***
3-Methyl-Histidine[3]	**24**	**+0.47***	**0.22***	**+0.57***

Table 13. Correlation coefficients for serum water T_{2c} values with biomarkers for protein concentration and viscosity ([1]), inflammation ([2]), and other metabolic states ([3]). Serum water T_{2c} values represent the regression residuals obtained from a linear fit of serum water T_2 *vs*. total cholesterol concentration. This analysis removes the influence of cholesterol and lipoprotein levels on serum water T_2 and highlights the influence of albumin and globulins.

Table 14: Water T_{2v} Correlations, Human Serum

Biomarker	N	r (Pearson)	R^2	r_S (Spearman)
Total Protein, Serum[1]	24	-0.47*	0.22*	-0.41*
Viscosity, Serum[1]	24	0.00	0.00	-0.01
Insulin[2]	24	-0.42*	0.18*	-0.46*
Total Cholesterol[3]	24	-0.50*	0.25*	-0.46*
Non-HDL-C[3]	24	-0.40*	0.16*	-0.41*
LDL-C (VAP) [3]	24	-0.43*	0.18*	-0.40
LDL-P[3]	24	-0.46*	0.21*	-0.54**

Table 14. Correlation coefficients for serum water T_{2v} values with biomarkers for protein concentration and viscosity ([1]), insulin resistance ([2]) and dyslipidemia ([3]). Serum water T_{2v} values represent the regression residuals obtained from a linear fit of serum water T_2 *vs*. serum viscosity. This analysis removes the influence of viscosity on serum water T_2 and highlights the concentration-dependent binding of water to proteins and lipoproteins. One subject with an extremely high serum viscosity level, a statistical outlier, was excluded from this analysis. See Table 3 legend for further information about this subject.

Abbreviations

AA: arachidonic acid

ALT: alanine aminotransferase

AST: aspartate aminotransferase

BMI: body-mass index

BUN: blood urea nitrogen

CPMG: Carr-Purcell-Meiboom-Gill NMR pulse sequence to measure T_2

DHA: Docosahexaenoic Acid

EDTA: ethylene-diamine-tetra-acetic-acid

eGFR: estimated glomerular filtration rate

EPA: eicosapentaenoic Acid

GGT: gamma glutamyl transpeptidase

HABS: Health & Aging Brain Study at the UNT Health Science Center, Fort Worth

HABLE: Health and Aging Brains in Latino Elders, a sub-study of HABS

HbA_{1C}: glycated hemoglobin

HDL-C: high-density lipoprotein cholesterol concentration

HDL-P: high-density lipoprotein particle number concentration

HNE: 4-hydroxynonenal

HOMA2-%B: homeostatic model assessment version 2, % beta cell function

HOMA2-%S: homeostatic model assessment version 2, % insulin sensitivity

HOMA2-IR: homeostatic model assessment version 2, insulin resistance index

(see https://www.dtu.ox.ac.uk/homacalculator for HOMA2 definitions)

hs-CRP: high-sensitivity C-reactive protein

I-309: member of the CC subfamily of chemokines

IR Score: insulin resistance score (from NMR LipoProfile, LipoScience)

LDL-C: low density lipoprotein cholesterol concentration

LDL-P: low density lipoprotein particle number concentration

Lp(a): lipoprotein (a) cholesterol concentration

MCH: mean corpuscular hemoglobin

MCHC: mean corpuscular hemoglobin concentration

MCV: mean corpuscular volume

MDA: malondialdehyde

NMR, nuclear magnetic resonance

T_{2a}: regression residuals from a linear fit of plasma or serum water T_2 *vs.* serum albumin

T_{2c}: regression residuals from a linear fit of plasma or serum water T_2 *vs.* serum cholesterol

T_{2g}: regression residuals from a linear fit of plasma or serum water T_2 *vs.* serum globulins

(globulins = total serum protein – serum albumin)

T_{2p}: regression residuals from a linear fit of plasma or serum water T_2 *vs.* total serum protein

T_{2v}: regression residuals from a linear fit of plasma or serum water T_2 *vs.* viscosity

r: Pearson correlation coefficient

r_S: Spearman correlation coefficient, non-parametric

R^2: square of the Pearson correlation coefficient

RDW: red cell distribution width

Remnant-C: remnant lipoprotein particle cholesterol concentration

sICAM: soluble intercellular adhesion molecule

TD-NMR: time-domain nuclear magnetic resonance

TG: serum triglyceride concentration

TNFα: tumor necrosis factor alpha

TSH: thyroid stimulating hormone

[UA]: unmeasured anion concentration, in meq/L

[UC]: unmeasured cation concentration, in meq/L

VAP: Vertical AutoProfile test, Atherotech

VLDL-C: very low density lipoprotein cholesterol concentration

WBC: white blood cells

REFERENCES

1. J. Mitchell, L. F. Gladden, T. C. Chandrasekera, E. J. Fordham, Low-field permanent magnets for industrial process and quality control. *Prog Nucl Magn Reson Spectrosc.* **76**, 1-60 (2014).

2. J. P. Savaryn, A. D. Catherman, P. M. Thomas, M. M. Abecassis, N. L. Kelleher, The emergence of top-down proteomics in clinical research. *Genome Med.* **5**, 53 (2013).

3. R. Apweiler *et al.*, Approaching clinical proteomics: current state and future fields of application in fluid proteomics. *Clin. Chem. Lab. Med.* **47**, 724-744 (2009).

4. Although the current study emphasizes T_2, we also measured water T_1 (spin-lattice relaxation times) for the blood serum and plasma samples from this study population. The findings for T_1 will be addressed elsewhere.

5. G. K. Hansson, Inflammation, atherosclerosis, and coronary artery disease. *N. Engl. J. Med.* **352**, 1685-1695 (2005).

6. F. G. De Felice, S. T. Ferreira, Inflammation, Defective Insulin Signaling, and Mitochondrial Dysfunction as Common Molecular Denominators Connecting Type 2 Diabetes to Alzheimer Disease. *Diabetes.* **63**, 2262-2272 (2014).

7. M. Flores, G. Glusman, K. Brogaard, N. D. Price, L. Hood, P4 medicine: how systems medicine will transform the healthcare sector and society. *Per Med.* **10**, 565-576 (2013).

8. S. E. O'Bryant *et al.*, Risk factors for mild cognitive impairment among Mexican Americans. *Alzheimers Dement.* **9**, 622-631.e1 (2013).

9. M. D. Robinson, D. P. Cistola, Nanofluidity of Fatty Acid Hydrocarbon Chains As Monitored by Benchtop Time-Domain Nuclear Magnetic Resonance. *Biochemistry.* **53**, 7515-7522 (2014).

10. H. Y. Carr, E. M. Purcell, Effects of Diffusion on Free Precession in Nuclear Magnetic Resonance Experiments. *Phys.Rev.* **94**, 630-638 (1954).

11. S. Meiboom, D. Gill, Modified Spin Echo for Measuring Nuclear Relaxation Times. *Rev. Sci. Instrum.* **29**, 688-691 (1958).

12. R. Freeman, *A Handbook of Nuclear Magnetic Resonance* (Longman Group, United Kingdom, ed. 2nd, 1997).

13. H. Motulsky, *Intuitive Biostatistics: A Nonmathematical Guide to Statistical Thinking* (Oxford University Press, New York, ed. Second, 2010).

14. Materials and methods are detailed within this application.

15. C. P. Klingenberg, MorphoJ: an integrated software package for geometric morphometrics (see also http://www.flywings.org.uk/MorphoJ_guide/frameset.htm?covariation/regression.htm). *Mol. Ecol. Resour.* **11**, 353-357 (2011).

16. K. Venu, V. P. Denisov, B. Halle, Water ^{1}H Magnetic Relaxation Dispersion in Protein Solutions. A Quantitative Assessment of Internal Hydration, Proton Exchange, and Cross-Relaxation. *J. Am. Chem. Soc.* **119**, 3122-3134 (1997).

17. E. Chen, R. J. Kim, Magnetic Resonance Water Proton Relaxation in Protein Solutions and Tissue: $T_{1(rho)}$ Dispersion Characterization. *PLoS ONE.* **5**, e8565 (2010).

18. T. L. James, in Selected Topics in Biophysics, http://www.biophysics.org/portals/1/PDFs/Education/james.pdf (Biophysical Society, Rockville, MD, 1998), pp. 1-31.

19. This argument assumes dipole-dipole interactions are the dominant mechanism for relaxation, which is supported by prior work (see ref. 5). For water bound to proteins, the other significant contribution to relaxation is chemical exchange.

20. R. Lundblad, Considerations for the Use of Blood Plasma and Serum for Proteomic Analysis. *The Internet Journal of Genomics and Proteomics.* **1(2)**(2003).

21. J. H. Fuller *et al.*, Haemostatic variables associated with diabetes and its complications. *Br. Med. J.* **2**, 964-966 (1979).

22. W. B. Kannel, R. B. D'Agostino, P. W. Wilson, A. J. Belanger, D. R. Gagnon, Diabetes, fibrinogen, and risk of cardiovascular disease: the Framingham experience. *Am. Heart J.* **120**, 672-676 (1990).

23. E. Raynaud *et al.*, Relationships between fibrinogen and insulin resistance. *Atherosclerosis.* **150**, 365-370 (2000).

24. A. Gonzalez-Quintela *et al.*, Serum levels of immunoglobulins (IgG, IgA, IgM) in a general adult population and their relationship with alcohol consumption, smoking and common metabolic abnormalities. *Clinical & Experimental Immunology.* **151**, 42-50 (2008).

25. R. S. Rosenson, A. McCormick, E. F. Uretz, Distribution of blood viscosity values and biochemical correlates in healthy adults. *Clin. Chem.* **42**, 1189-1195 (1996).

26. G. Lippi *et al.*, Relation between red blood cell distribution width and inflammatory biomarkers in a large cohort of unselected outpatients. *Arch. Pathol. Lab. Med.* **133**, 628-632 (2009).

27. S. Talukdar *et al.*, Neutrophils mediate insulin resistance in mice fed a high-fat diet through secreted elastase. *Nat. Med.* **18**, 1407-1412 (2012).

28. C. Shi, E. G. Pamer, Monocyte recruitment during infection and inflammation. *Nat Rev Immunol.* **11**, 762-774 (2011).

29. P. von Hundelshausen, C. Weber, Platelets as Immune Cells: Bridging Inflammation and Cardiovascular Disease. *Circulation Research.* **100**, 27-40 (2007).

30. B. Halliwell, M. V. Clement, L. H. Long, Hydrogen peroxide in the human body. *FEBS Lett.* **486**, 10-13 (2000).

31. B. Halliwell, J. M. Gutteridge, Role of free radicals and catalytic metal ions in human disease: an overview. *Methods Enzymol.* **186**, 1-85 (1990).

32. R. L. Trelstad, K. R. Lawley, L. B. Holmes, Nonenzymatic hydroxylations of proline and lysine by reduced oxygen derivatives. *Nature.* **289**, 310-312 (1981).

33. E. R. Stadtman, Oxidation of free amino acids and amino acid residues in proteins by radiolysis and by metal-catalyzed reactions. *Annu. Rev. Biochem.* **62**, 797-821 (1993).

34. M. Anraku, V. T. Chuang, T. Maruyama, M. Otagiri, Redox properties of serum albumin. *Biochim. Biophys. Acta.* **1830**, 5465-5472 (2013).

35. M. B. Hampton, A. J. Kettle, C. C. Winterbourn, Inside the neutrophil phagosome: oxidants, myeloperoxidase, and bacterial killing. *Blood.* **92**, 3007-3017 (1998).

36. E. Kolaczkowska, P. Kubes, Neutrophil recruitment and function in health and inflammation. *Nat. Rev. Immunol.* **13**, 159-175 (2013).

37. M. Bruschi, G. Candiano, L. Santucci, G. M. Ghiggeri, Oxidized albumin. The long way of a protein of uncertain function. *Biochim. Biophys. Acta.* **1830**, 5473-5479 (2013).

38. P. Vidal, T. Deckert, B. Hansen, B. S. Welinder, High-performance liquid chromatofocusing and column affinity chromatography of in vitro ^{14}C-glycated human serum albumin. Demonstration of a glycation-induced anionic heterogeneity. *J. Chromatogr.* **476**, 467-475 (1989).

39. J. A. Kraut, N. E. Madias, Serum anion gap: its uses and limitations in clinical medicine. *Clin. J. Am. Soc. Nephrol.* **2**, 162-174 (2007).

40. We adhere to the IUPAC nomenclature for 1- and 3-methyl histidine, as discussed by Boldyrev et al., reference 30. Much of the older literature reverses the 1- and 3- designations, as do the lab reports obtained from Quest Diagnostics for amino acid analyses of human plasma. The inconsistent nomenclature creates considerable confusion.

41. A. A. Boldyrev, G. Aldini, W. Derave, Physiology and pathophysiology of carnosine. *Physiol. Rev.* **93**, 1803-1845 (2013).

CLAIMS

We claim:

1. A method for determining the T_2 and/or T_1 health score of a subject comprising obtaining a NMR spin relaxation curve for a sample with an NMR instrument tuned to measure a particular nucleus selected from ^{1}H, ^{2}H, ^{3}H or ^{17}O, analyzing the curve to extract T_2 and/or T_1 relaxation times for water and converting the water T_2 and/or T_1 values into a measure of the health status of the subject (the T_2 and/or T_1 health score).

2. The method according to claim 1, wherein the sample is a plasma sample, a serum sample, whole blood sample, a tissue sample or a subject, such as a human being.

3. The method according to claims 1-2, wherein the method comprises a step of partially suppressing the water signal, for example with a 180-degree inversion pulse followed by a delay or any other suitable method for partial suppression of the water signal prior to recording the relaxation curve.

4. The method according to claim 3, wherein the delay time is tuned to eliminate radiation damping while maximizing water signal intensity.

5. A method according to claims 1-4, wherein the step of analyzing the exponentially decaying or recovering NMR signal comprises acquiring the relaxation curve and subjecting the data to exponential analysis, for example transforming the data with an inverse Laplace transformation, or using any other suitable exponential analysis algorithm.

6. The method according to claim 5, wherein said exponential analysis comprises the analysis of one or more exponential terms, for example one to six exponential terms, two to four exponential terms or three exponential terms.

7. The method according to claims 3-6, wherein data acquisition begins about 1 to about 50 milliseconds after the start of pulse scheme that acquires the relaxation decay curve; about 16 to about 20 milliseconds after the start of the pulse scheme; or about 19 milliseconds after the start of the pulse scheme

8. The method according to claims 1-7, wherein said sample is scanned multiple times, such as between 1 and 256 times or up to 10 to 50 times.

9. The method according to claims 1-8, wherein the step of converting the T_2 and/or T_1 values into a measure of the health status of the subject comprises comparing the T_2 and/or T_1 values obtained for the sample from the subject with T_2 and/or T_1 values obtained from a database, said database comprising T_2 and/or T_1 values obtained for a range of subjects, from those who are normal and healthy to those having varying degrees of inflammation, insulin

resistance, lipid abnormalities, oxidative stress, brain or cognitive abnormalities and/or other disorders.

10. The method according to claims 1-9, said method comprising referring an individual subject with a plasma T_2 value less than about 800 to a registered dietician, certified personal trainer, physician or other licensed health provider to improve health and well-being, and prevent the onset of diabetes, coronary artery disease, myocardial infarction, ischemic vascular disease, stroke, cognitive impairment, neurodegenerative diseases and dementia, including Alzheimer's disease, or any other diseases that arise from metabolic abnormalities such as chronic, low-grade inflammation, insulin resistance, lipid/lipoprotein abnormalities and/or oxidative stress and/or treating the subject with an appropriate treatment for inflammation, insulin resistance, lipid abnormalities, oxidative stress, brain or cognitive abnormalities and/or other disorders.

11. A method of creating a database for determining the health status of a subject comprising obtaining a NMR relaxation curve for a sample obtained from a subject with an NMR instrument tuned to measure a particular nucleus selected from ^{1}H, ^{2}H, ^{3}H or ^{17}O, analyzing the relaxation curve to extract T_2 and/or T_1 relaxation times for water and converting the water T_2 and/or T_1 values into a measure of the health status of the subject, associating the health status of the subject with the converted water T_2 and/or T_1 values and creating a database containing the associated water T_2 and/or T_1 values (T_2 and/or T_1 health scores) and the health status of the subject.

12. The method according to claim 11, wherein the sample is a plasma sample, a serum sample, whole blood sample, a tissue sample or a subject, such as a human.

13. The method according to claims 11-12, wherein the method comprises a step of partially suppressing the water signal, for example with a 180-degree inversion pulse followed by a delay or any other suitable method for partial suppression of the water signal prior to recording the relaxation curve.

14. The method according to claim 13, wherein the delay time is tuned to eliminate radiation damping while maximizing water signal intensity.

15. The method according to claims 11-14, wherein the step of analyzing the exponentially decaying or recovering NMR signal comprises acquiring the relaxation curve and subjecting the data to exponential analysis, for example transforming the data with an inverse Laplace transformation, or using any other suitable exponential analysis algorithm.

16. The method according to claim 15, wherein said exponential analysis comprises the analysis of one or more exponential terms for example one to six exponential terms, two to four exponential terms or three exponential terms.

17. The method according to claims 11-16, wherein data acquisition begins about 1 to about 50 milliseconds after the start of pulse scheme that acquires the relaxation curve; about 16

to about 20 milliseconds after the start of the pulse scheme; or about 19 milliseconds after the start of the pulse scheme.

18. The method according to claims 11-17, wherein said sample is scanned multiple times, such as between 1 and 256 times or up to 10 to 50 times

19. The method according to claims 11-18, said method being applied to a plurality of samples obtained from a plurality of subjects to create said database.

20. An apparatus for health-screening a subject comprising:

a NMR instrument or portable device tuned to measure a particular nucleus selected from ^{1}H, ^{2}H, ^{3}H or ^{17}O;

one or more computer readable storage media;

a processing system;

a data store contained on the one or more computer readable storage media comprising:

one or more reference T_2 relaxation times for water and a reference T_1 relaxation times for water, for one or more of a sample type, wherein the reference T_2 and/or reference T_1 values are associated with a health status;

program instructions for a health screening service stored on the one or more computer readable storage media that direct the processing system to:

acquire an NMR relaxation decay or recovery signal, using the NMR instrument, from a sample of a particular sample type from the subject;

analyze the NMR relaxation curve to extract a T_2 relaxation time for water and/or a T_1 relaxation time for water;

identify the reference values for the particular sample type associated with the extracted T_2 and/or T_1 values and determine the health status associated with the reference values; and

display a health score determined from the health status.

21. The apparatus of claim 20, wherein the sample type is a whole blood sample, a serum sample, a plasma sample, a tissue sample or a subject, such as a human being.

22. The apparatus of claim 20, wherein the NMR instrument is a wearable device or is a benchtop or portable time domain NMR instrument or is a NMR spectrometer or magnetic resonance imager.

23. An apparatus comprising:

one or more computer readable storage media;

a processing system;

program instructions stored on the one or more computer readable storage media that direct the processing system to:

obtain an NMR relaxation decay or recovery curve from a sample obtained from a subject, wherein the relaxation curve was obtained using a NMR instrument tuned to measure a particular nucleus selected from ^{1}H, ^{2}H, ^{3}H or ^{17}O;

analyze the NMR relaxation decay curve to extract a T_2 relaxation time for water and/or a T_1 relaxation time for water;

determine a health status value of the subject, wherein the health status is determined from water T_1 and/or T_2 from the sample; and

store the water T_2 and/or T_1 values in association with the health status in a data store contained on the one or more computer readable storage media.

24. The apparatus according to claim 23, wherein the sample is a plasma sample, a serum sample, whole blood sample, a tissue sample or subject, such as a human being.

25. The method according to claims 23-24, wherein the method comprises a step of partially suppressing the water signal, for example with a 180-degree inversion pulse followed by a delay or any other suitable method for partial suppression of the water signal prior to recording the relaxation curve.

26. The method according to claim 25, wherein the delay time is tuned to eliminate radiation damping while maximizing water signal intensity.

27. The method according to claims 23-26, wherein the step of analyzing the exponentially decaying or recovering NMR signal comprises acquiring the relaxation curve and subjecting the data to exponential analysis, for example transforming the data with an inverse Laplace transformation, or using any other suitable exponential analysis algorithm.

28. The method according to claim 27, wherein said exponential analysis comprises the analysis of one or more exponential terms for example one to six exponential terms, two to four exponential terms or three exponential terms.

29. The method according to claims 23-28, wherein data acquisition begins about 1 to about 50 milliseconds after the start of pulse scheme that acquires the relaxation decay curve; about 16 to about 20 milliseconds after the start of the pulse scheme; or about 19 milliseconds after the start of the pulse scheme

30. The method according to claims 23-29, wherein said sample is scanned multiple times, such as between 1 and 256 times or up to 10 to 50 times.

31. The apparatus according to claims 23-30, wherein the data store comprises water T_2 and/or T_1 values in association with the health status obtained from a plurality of samples from a plurality of subjects.

32. A method of treating a subject with a plasma water T_2 value less than about 800 and at risk for the development of hidden metabolic abnormalities selected from inflammation, insulin resistance, lipid abnormalities (dyslipidemia), oxidative stress, brain abnormalities or other disorders comprising obtaining a health score for a subject according to the methods of claims 1-11 and treating a subject having a health score lower than about 800 for said metabolic abnormality and/or referring said subject to a physician for further evaluation.

33. The method according to claim 32, wherein said hidden metabolic abnormality is low grade inflammation and said subject is further evaluated for treatment with one or more anti-inflammatory agents and/or treated with one or more anti-inflammatory agents.

34. The method according to claim 33, wherein said anti-inflammatory agent is selected from ibuprofen, naproxen, aspirin, celecoxib, sulindac, oxaprozin, salsalate, diflunisal, piroxicam, indomethacin, etodolac, meloxicam, nambumetone, ketorolac tromethamine, or corticosteroids selected from as beclomethasone, beclometasone, budesonide, flunisolide, fluticasone, tramcinolone, methylprednisone, prenisolone or prednisone.

35. The method according to claim 32, wherein said metabolic abnormality is insulin resistance and said subject is further evaluated and/or treated to improve insulin sensitivity, said treatment to improve insulin sensitivity being selected from the start or modification of an exercise and physical activity program, alteration of diet, or other modification of behavior so as to improve insulin sensitivity and reduce the likelihood of developing diabetes arising from insulin resistance.

36. The method according to claim 32, wherein the metabolic abnormality is dyslipidemia and said subject is referred to a physician for further diagnostic evaluation and/or treated with low dose aspirin, statins and/or other lipid-lowering agents.

37. The method according to claim 36, wherein the statin is selected from atorvastatin, fluvastatin, lovastatin, pitavastatin, pravastatin, rosuvastatin or simcastatin.

38. The method according to claim 32, wherein the metabolic abnormality is oxidative stress and a subject is referred to a physician and/or registered dietician to receive nutritional advice and/or is evaluated and treated with anti-oxidants such as ascorbic acid (Vitamin C), vitamin E or other nutritional supplements, and/or evaluated and treated for any accompanying inflammation or insulin resistance.

39. A method of referring an individual with a plasma water T_2 value less than about 800 to a registered dietician, certified personal trainer, physician or other licensed health provider, with the goal to improve health and well-being, and prevent the onset of diabetes, coronary artery disease, myocardial infarction, ischemic vascular disease, stroke, cognitive impairment, neurodegenerative disease and dementia, including Alzheimer's disease, or any other diseases that arise from hidden metabolic abnormalities such as chronic, low-grade inflammation, insulin resistance, lipid/lipoprotein abnormalities, oxidative stress and/or brain abnormalities.

40. The method according to claim 39, wherein said hidden metabolic abnormality is low grade inflammation and said subject is further evaluated for treatment with one or more anti-inflammatory agents.

41. The method according to claim 40, wherein said anti-inflammatory agent is selected from ibuprofen, naproxen, aspirin, celecoxib, sulindac, oxaprozin, salsalate, diflunisal, piroxicam, indomethacin, etodolac, meloxicam, nambumetone, ketorolac tromethamine, or

corticosteroids selected from as beclomethasone, beclometasone, budesonide, flunisolide, fluticasone, tramcinolone, methylprednisone, prenisolone or prednisone.

42. The method according to claim 39, wherein said metabolic abnormality is insulin resistance and said subject is further evaluated, advised to start or modifying an exercise and physical activity program, alter diet, or otherwise modify behavior so as to improve insulin sensitivity and reduce the likelihood of developing diabetes arising from insulin resistance.

43. The method according to claim 39, wherein the metabolic abnormality is dyslipidemia and said subject is referred to a physician for further diagnostic evaluation and possibly treated with low dose aspirin, statins and/or other lipid-lowering agents.

44. The method according to claim 43, wherein the statin is selected from atorvastatin, fluvastatin, lovastatin, pitavastatin, pravastatin, rosuvastatin or simcastatin.

45. The method according to claim 39, wherein the metabolic abnormality is oxidative stress and a subject is referred to a physician and/or registered dietician to receive nutritional advice and/or is evaluated and treated with anti-oxidants such as ascorbic acid (Vitamin C), vitamin E or other nutritional supplements, and/or evaluated and treated for any accompanying inflammation or insulin resistance.

ABSTRACT OF THE DISCLOSURE

The subject invention pertains to a method that involves at least three steps: (1) acquisition of a NMR spin relaxation curve for plasma, serum or whole blood samples, or for tissues monitored from outside the body, (2) analysis of the relaxation curve to extract the T_2 and/or T_1 relaxation times for water, and (3) conversion of the water T_2 and/or T_1 values into a measure of someone's health status (referred to as a T_2 or T_1 health score depending on the value (T_1 or T_2 or both T_1 and T_2) associated with the score). The T_1 and/or T_2 health score utilizes a statistical database derived from previous studies of subjects ranging from normal, healthy individuals to those having varying degrees of hidden or non-hidden metabolic abnormalities, such as inflammation, insulin resistance, lipid abnormalities (dyslipidemia), oxidative stress, brain abnormalities, cognitive impairment or other disorders, and provides a measure of a subject's overall metabolic and brain health status.

FIGURES

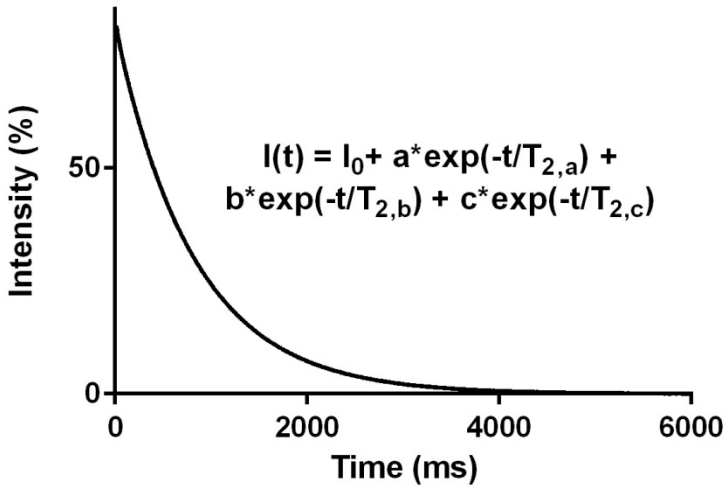

FIG. 1A

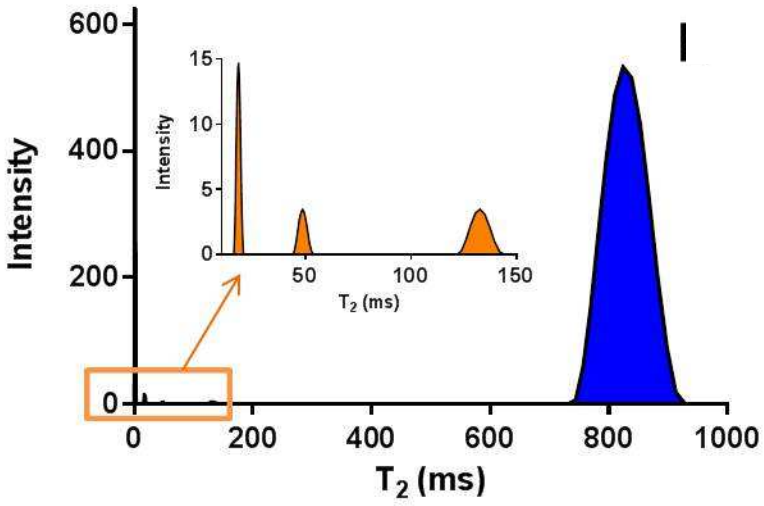

FIG. 1B

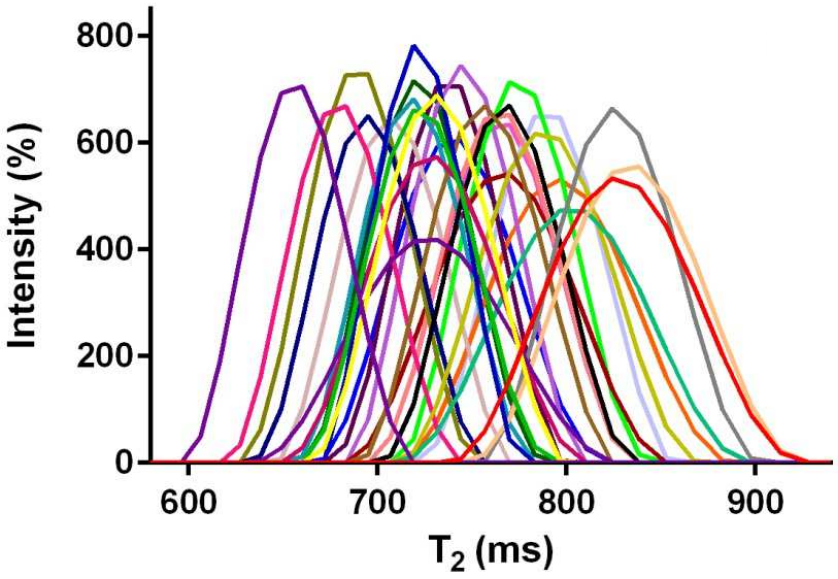
800
600
400
200
0
Intensity (%)
600
700
800
900
T2 (ms)

FIG. 1C

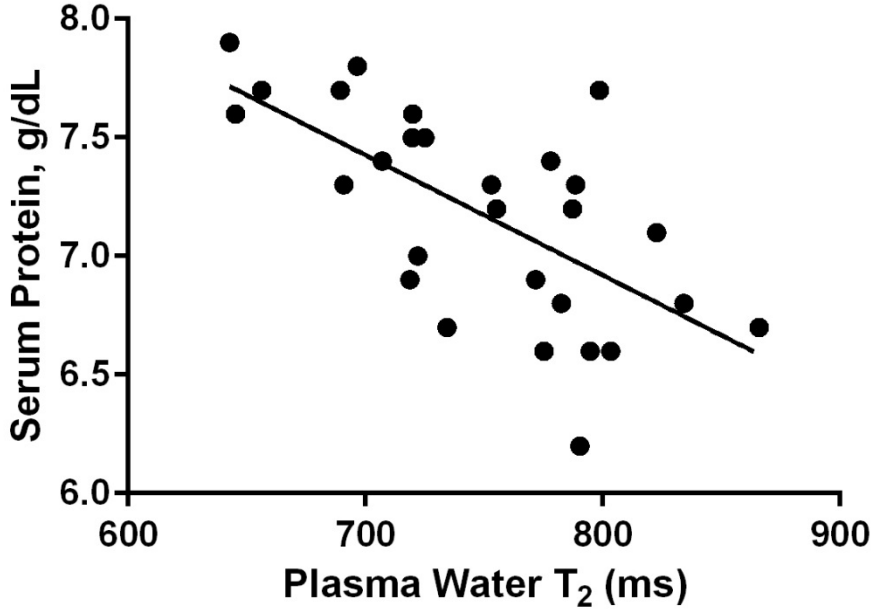
8.0
7.5
7.0
6.5
6.0
Serum Protein, g/dL
600
700
800
900
Plasma Water T2 (ms)

FIG. 2A

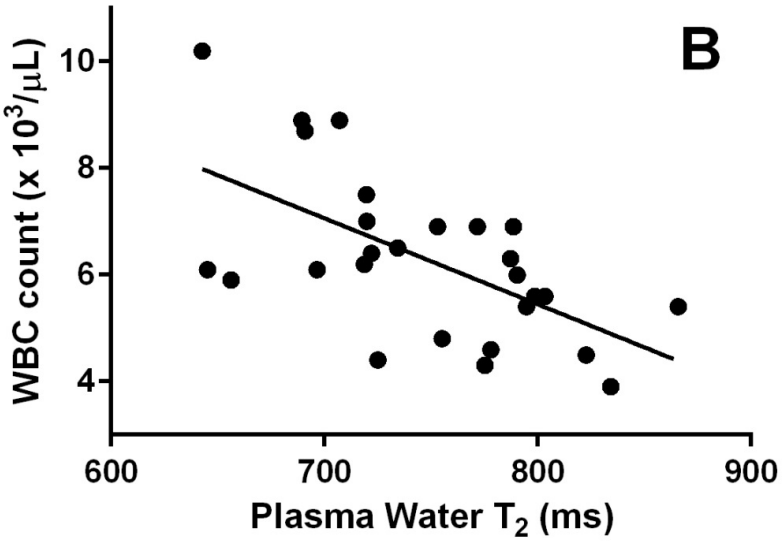
B
WBC count (x $10^3/\mu L$)
10
8
6
4
600
700
800
900
Plasma Water T_2 (ms)

FIG. 2B

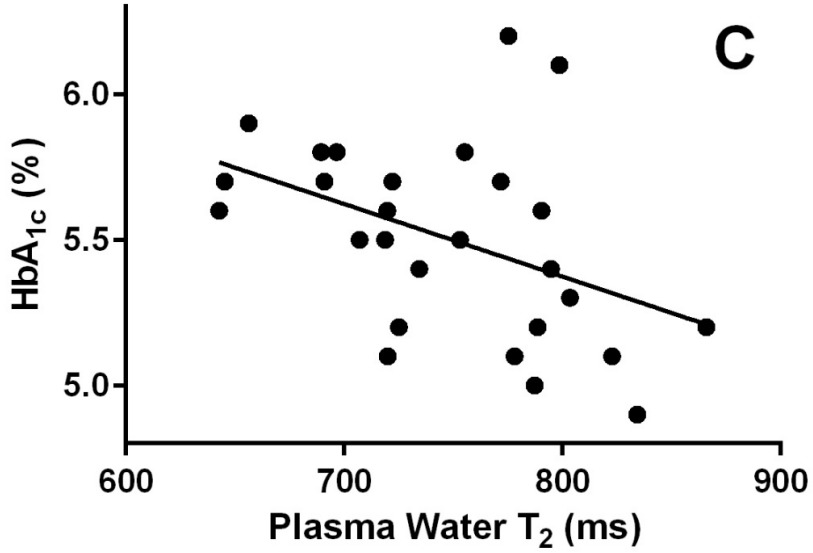
C
HbA_{1c} (%)
6.0
5.5
5.0
600
700
800
900
Plasma Water T_2 (ms)

FIG. 2C

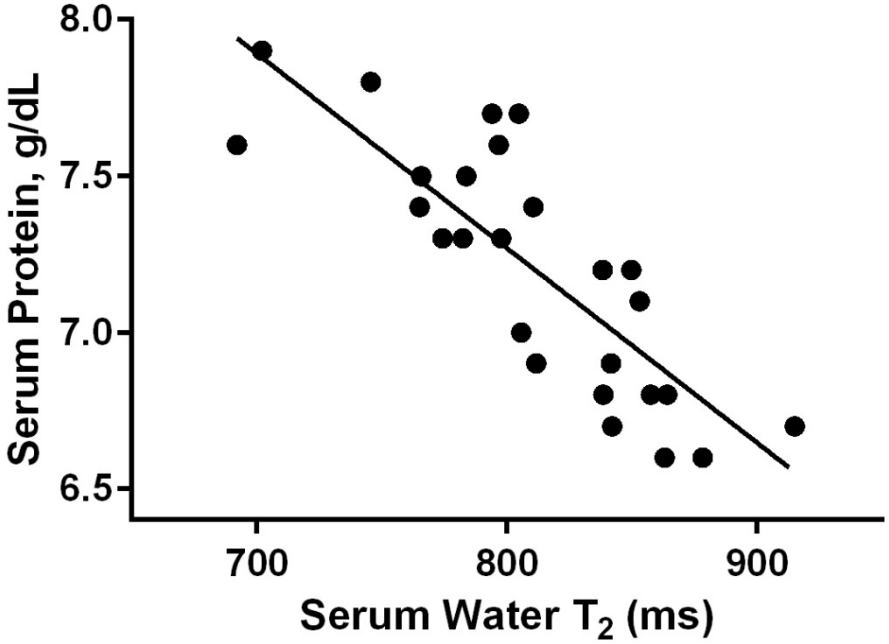
8.0
7.5
7.0
6.5
Serum Protein, g/dL
700
800
900
Serum Water T_2 (ms)

FIG. 2D

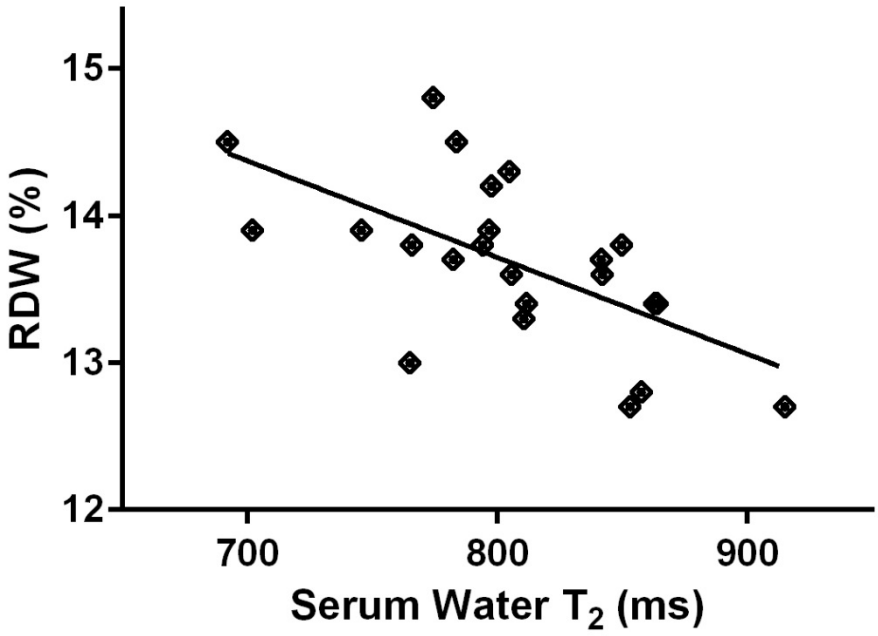
15
14
13
12
RDW (%)
700
800
900
Serum Water T_2 (ms)

FIG. 2E

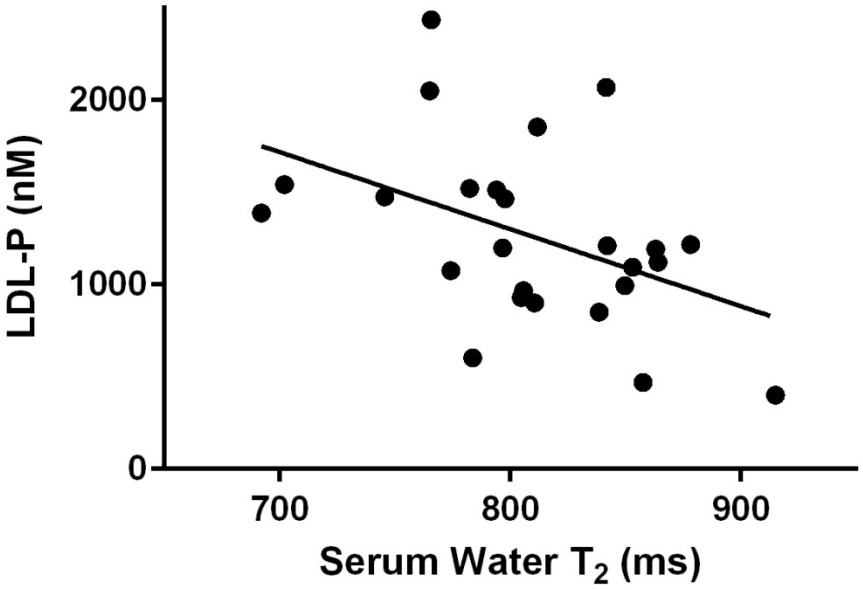
LDL-P (nM)
2000
1000
0
700
800
900
Serum Water T_2 (ms)

FIG. 2F

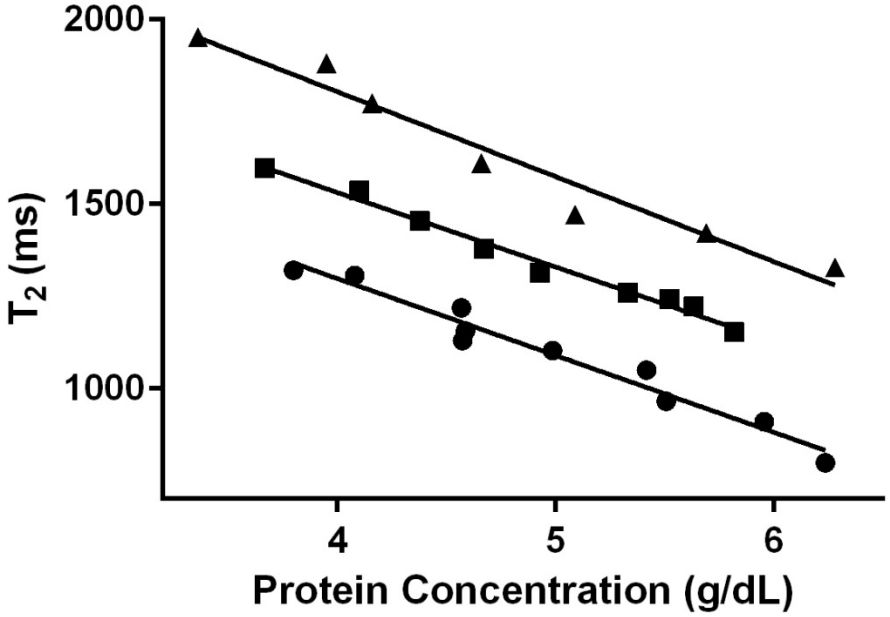
T_2 (ms)
2000
1500
1000
4
5
6
Protein Concentration (g/dL)

FIG. 3A

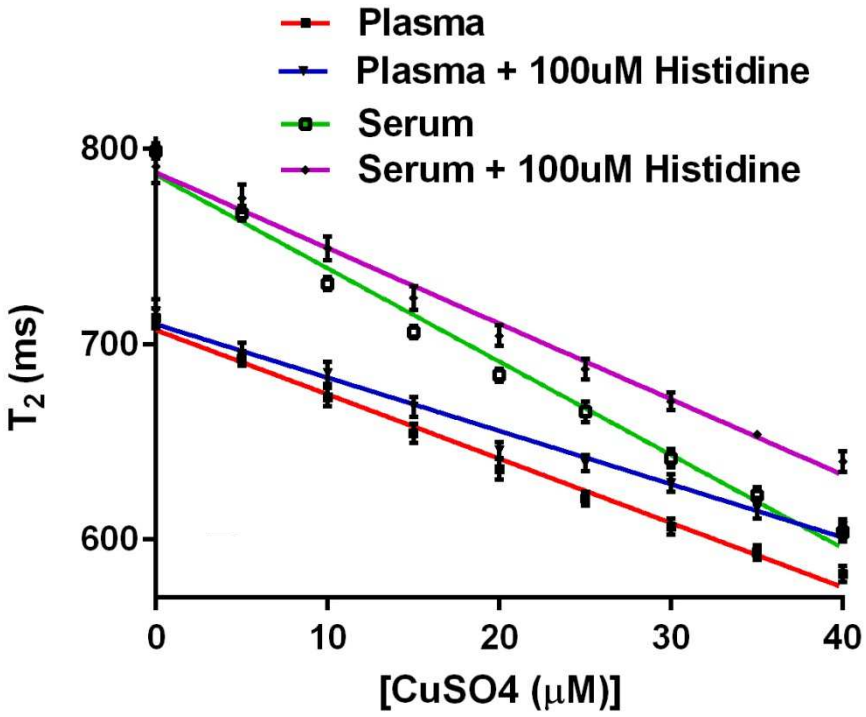
Plasma
Plasma + 100uM Histidine
Serum
Serum + 100uM Histidine
800
700
600
T2 (ms)
0
10
20
30
40
[CuSO4 (μM)]

FIG. 3B

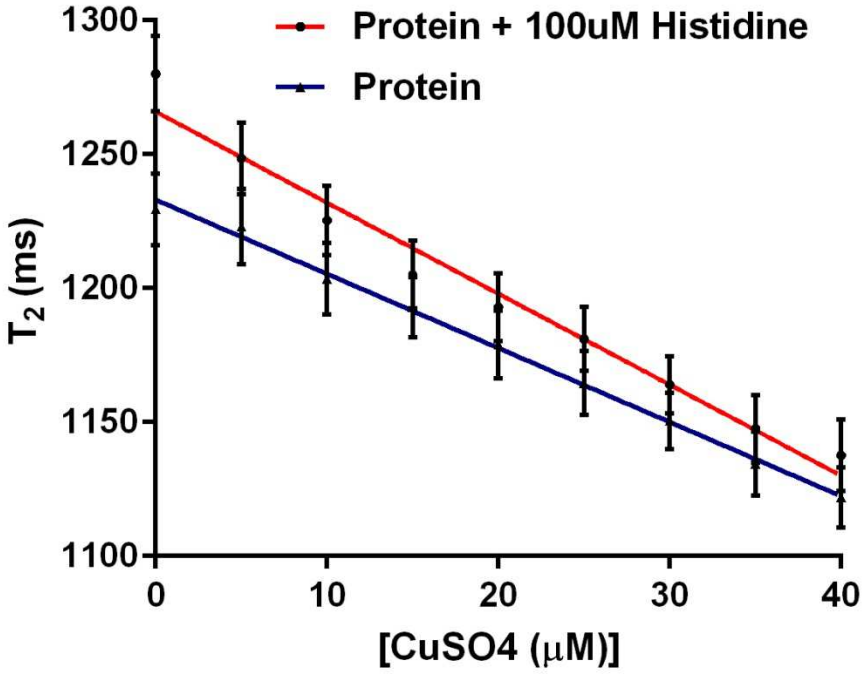
Protein + 100uM Histidine
Protein
1300
1250
1200
1150
1100
T2 (ms)
0
10
20
30
40
[CuSO4 (μM)]

FIG. 3C

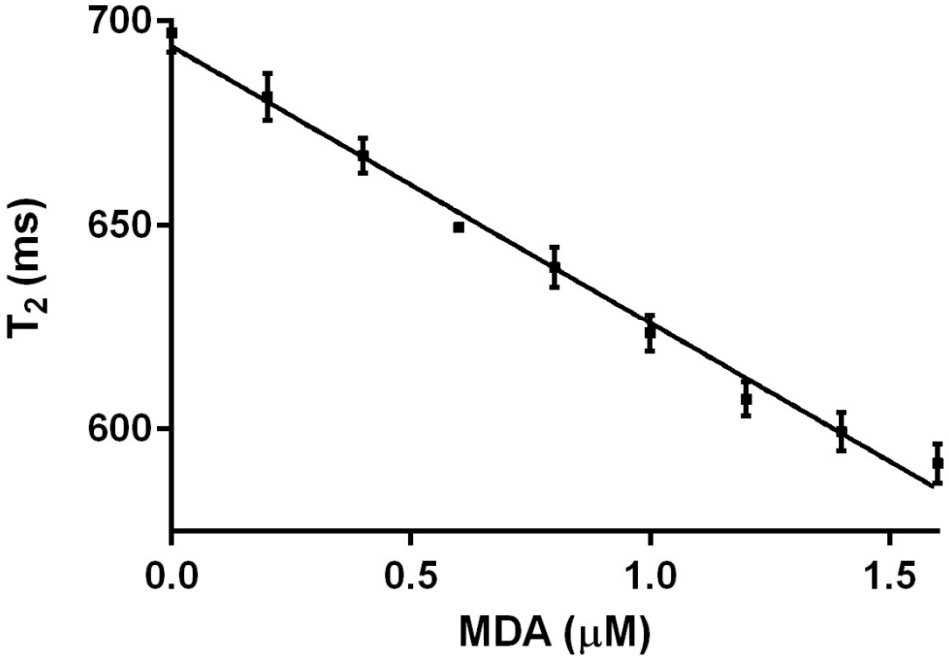
700
650
600
T_2 (ms)
0.0
0.5
1.0
1.5
MDA (μM)

FIG. 3D

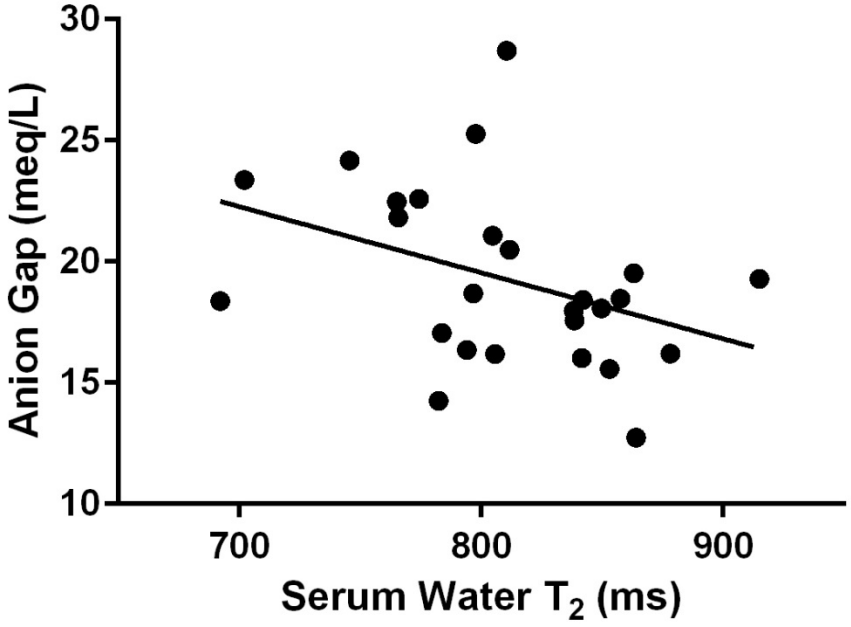
30
25
20
15
10
Anion Gap (meq/L)
700
800
900
Serum Water T_2 (ms)

FIG. 3E

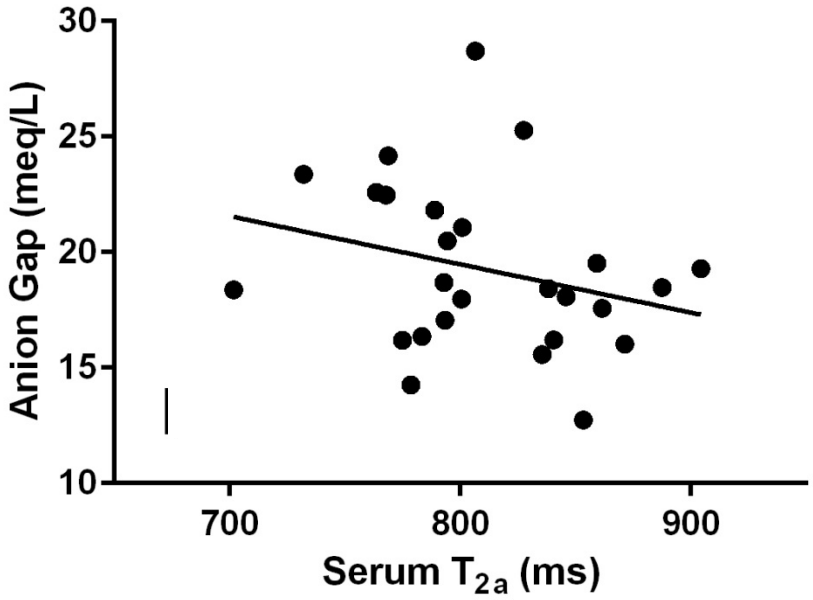
Anion Gap (meq/L)
30
25
20
15
10
700
800
900
Serum T_{2a} (ms)

FIG. 3F

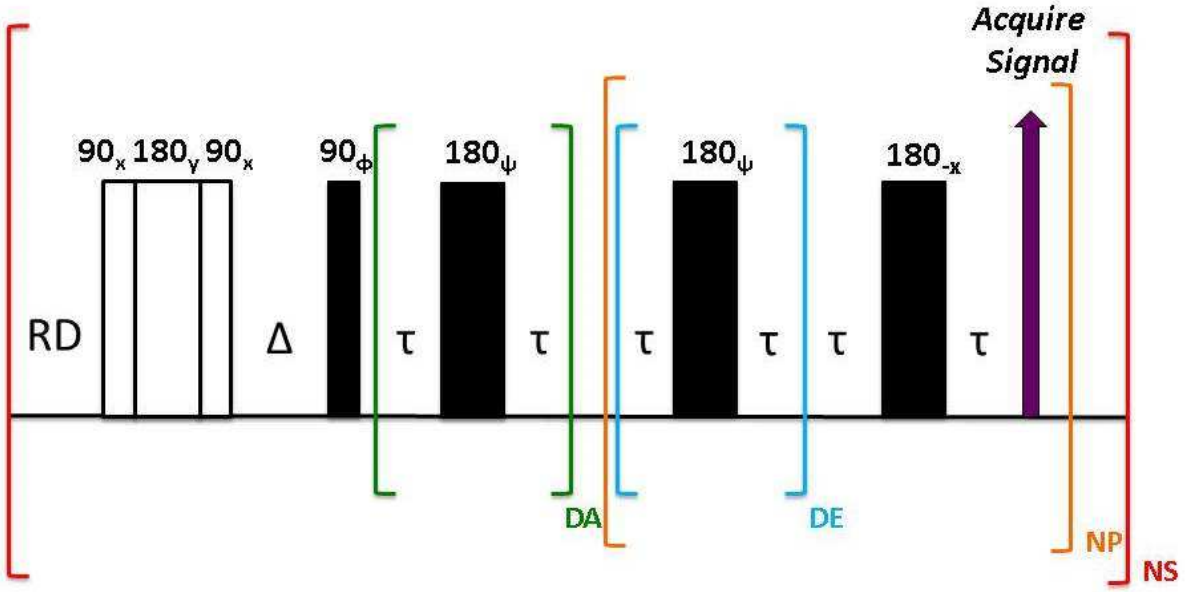
Acquire Signal
90_x 180_y 90_x
90_Φ
180_ψ
180_ψ
180_{-x}
RD
Δ
τ
τ
τ
τ
τ
τ
DA
DE
NP
NS

FIG. 4

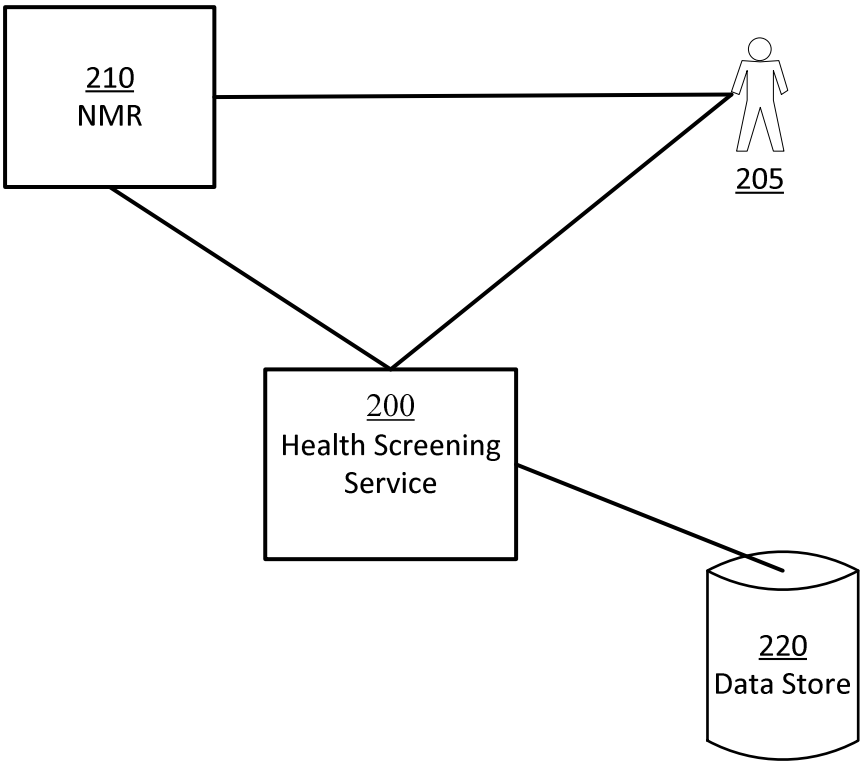
210
NMR
205
200
Health Screening
Service
220
Data Store

FIG. 5

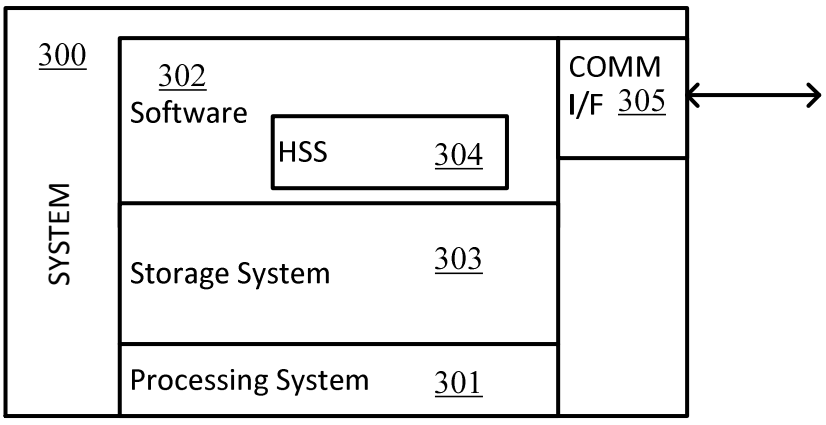
300
SYSTEM
302
Software
HSS
304
COMM
I/F 305
Storage System
303
Processing System
301

FIG. 6